



Regulators of growth plate maturation

Joyce A.M. Emons

Regulators of growth plate maturation

Joyce A.M. Emons

The project was supported by a grant from ZonMW, the Netherlands Organisation for Health Research and Development (grant number 920-03-358)

The printing of this thesis was financially supported by: the department of Pediatrics of the LUMC, the Jurriaanse foundation, the NVCB, Ipsen, Novo Nordisk, Greiner Bio-One, Ferring B.V., Ipsen, Eli Lilly, Pfizer, Nutricia.

Cover : I'm growing up, shutterstock

Design : DTPat - Patrick Mostert

Lay-out : DTPat - Patrick Mostert

Printed by : Vestagraphics B.V.B.A

© J.A.M. Emons, Berkel en Rodenrijs, 2010

All rights reserved. No part of this thesis may be reproduced or transmitted to any form, by any means, electronic or mechanical, without the prior written permission of the author.

Regulators of growth plate maturation

Proefschrift

ter verkrijging van
de graad van Doctor aan de Universiteit van Leiden,
op gezag van de Rector Magnificus Prof. Mr. P.F. van der Heijden,
volgens besluit van het College voor Promoties
te verdedigen op woensdag 14 april 2010
klokke 16.15 uur

door

Joyce Adriana Mathilde Emons

geboren te Berkel en Rodenrijs in 1977

Promotiecommissie

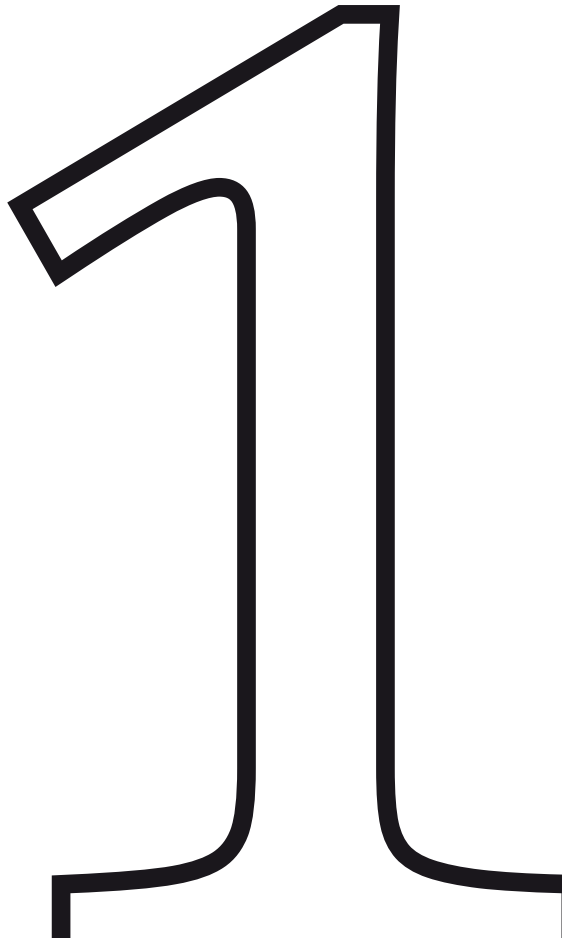
Promotor : Prof. dr. J.M. Wit

Co-promotor : Dr. H.B.J. Karperien, Department of Tissue Regeneration Universiteit van Twente

Overige leden : Prof. dr. H.A. Delemarre-van de Waal
Prof. dr. C.W.G.M. Lowik
Prof. dr. W. Fibbe

Contents

<i>Chapter 1</i>	General introduction	007
<i>Chapter 2</i>	Evidence for genomic and nongenomic actions of estrogen in growth plate regulation in female and male rats at the onset of sexual maturation	029
<i>Chapter 3</i>	Expression of vascular endothelial growth factor (VEGF) in the growth plate is stimulated by estradiol and increases during pubertal development	049
<i>Chapter 4</i>	The role of p27 kip1 in the regulation of growth plate chondrocytes proliferation in mice	067
<i>Chapter 5</i>	Catch-up growth: testing the hypothesis of delayed growth plate senescence in humans	085
<i>Chapter 6</i>	Genome wide screening of human growth plates during early and progressed stage puberty in one patient: evidence for a role of RunX2 in growth plate maturation.	095
<i>Chapter 7</i>	A cross-sectional microarray study of human epiphyseal growth plates during pubertal maturation	119
<i>Chapter 8</i>	Epiphyseal fusion in the human growth plate does not involve classical apoptosis.	133
<i>Chapter 9</i>	Preferential chondrogenic differentiation potential of human bone marrow-derived mesenchymal stem cells	149
<i>Chapter 10</i>	Fetal mesenchymal stem cells differentiating towards chondrocytes display a similar gene expression profile as growth plate cartilage	165
<i>Chapter 11</i>	General discussion	189
<i>Chapter 12</i>	Summary	205
<i>Chapter 13</i>	Samenvatting	211
	Curriculum Vitae	217
	List of publications	221



General introduction

Longitudinal bone growth and the growth plate

Longitudinal growth occurs at the epiphyseal plate or growth plate, a thin layer of cartilage entrapped between epiphyseal and metaphyseal bone, at the distal ends of the long bones. This growth plate is highly organized and consists of chondrocytes in three principal layers: the resting zone, proliferative zone and hypertrophic zone (fig 1). The resting zone is located at the epiphyseal end of the growth plate and contains resting chondrocytes, originating from mesenchymal stem cells, forming a proliferative reservoir for the entire growth plate. Resting chondrocytes enter the proliferative zone in organized columns and undergo cell-divisions in longitudinal direction regulated by a multitude of hormones and growth factors. In this zone chondrocytes start producing significant amounts of extracellular matrix proteins (ECM) essential for the structure of the growth plate. More towards the hypertrophic zone chondrocytes lose their proliferating capacity and begin to increase in size while they differentiate into hypertrophic chondrocytes. In the hypertrophic zone chondrocytes increase their size 6-10 fold and secrete a large amount of matrix proteins. Longitudinal bone growth is the result of proliferation, enlargement of hypertrophic chondrocytes and production of ECM proteins in the proliferative and hypertrophic zone.

From the adjacent metaphyseal bone osteogenic progenitors and osteoclasts are recruited to remodel the newly formed cartilage and deposit trabecular bone at the bottom of the growth plate. During childhood the growth plate matures, its total width decreases and eventually it disappears at the end of puberty with complete replacement by bone along with cessation of longitudinal growth (1).

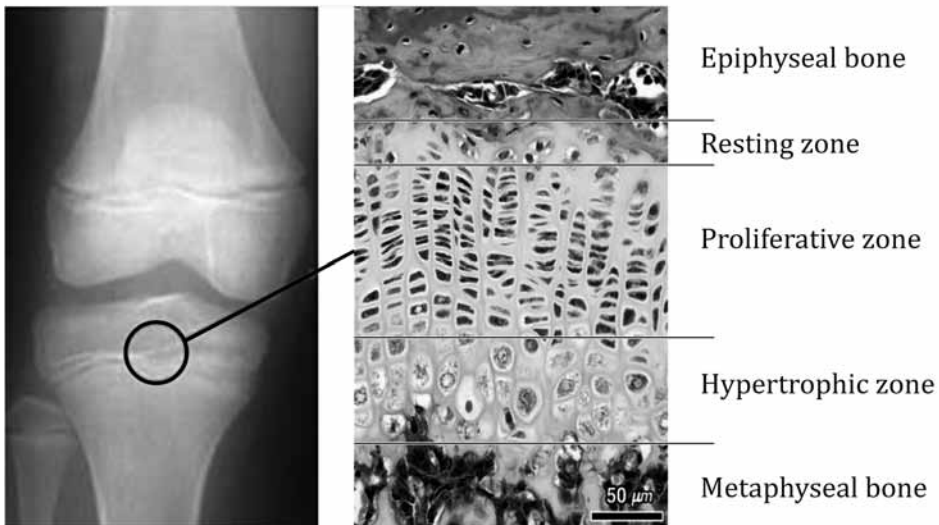


Figure 1: The structure of the growth plate

Extracellular matrix (ECM) proteins

Chondrocytes are embedded in an extracellular matrix consisting of various large and multifunctional molecules. An important group consists of the collagens, of which collagen type II is most abundantly present throughout the proliferative and hypertrophic zone. Another important collagen in the growth plate, often used as a marker for hypertrophic chondrocytes, is collagen type X that is solely expressed in the hypertrophic zone of the growth plate. Dysplasias caused by mutations in these collagens are associated with growth disorders and short stature (2;3). Another group of ECM molecules are the glycosaminoglycans (GAGs), heteropolysaccharide molecules. The majority of GAGs in the body are linked to core proteins, forming large mucopolysaccharide proteoglycans cross-linking the matrix. Members of this proteoglycan group are aggrecan, biglycan, glypican and chondroitin.

Within the ECM there are endopeptidases called Matrix Metalloproteinases (MMPs), remodelling these molecules, and tissue inhibitors of MMPs, preserving the integrity of the ECM (4). In addition the MMPs initiate angiogenesis for vascular invasion of growth plate cartilage together with various growth factors like vascular endothelial growth factor (VEGF) produced by chondrocytes in the growth plate (4-6). Besides controlling angiogenesis, VEGF has also been shown to modulate chondrocyte differentiation and survival, osteoblast differentiation and osteoclasts recruitment (7-9).

The ECM is furthermore a reservoir for various growth factors, hormones and proteins like Transforming growth factor beta (TGF- β), Fibroblast growth factors (FGFs), Indian Hedgehog (Ihh), Parathyroid hormone-related peptide (PTHrP), Wnt signalling factors and Bone Morphogenetic Proteins (BMPs), interacting together to tightly control chondrocyte proliferation and differentiation in the growth plate (1).

Hormones and their influence on the growth plate

Longitudinal bone growth is influenced by a variety of hormones and growth factors acting directly or indirectly on the growth plate. A fine and tight control of several hormone systems is obligatory to control longitudinal bone growth. For example triiodothyronine (T3) and thyroxine (T4) in the hypothalamic-pituitary-thyroid axis are crucial for normal skeletal growth and bone maturation illustrated by cases of congenital or acquired hypothyroidism that show a severe retardation of growth and skeletal maturation, while hyperthyroidism is associated with an increased growth velocity and bone maturation (10-12). Glucocorticoids are strong inhibitors of growth and long-term treatment often leads to growth failure, which might be the result of an inhibiting effect on chondrocyte proliferation and a stimulating effect on apoptosis of growth plate chondrocytes (13;14). In children suffering from chronic inflammatory diseases growth failure is frequently observed. These disorders are associated with increased circulating cytokine levels acting locally in the growth plate or through systemic effects on other growth regulatory mechanisms (15).

Growth hormone and IGF-I are the most well-known hormones involved in longitudinal growth, whereas estrogen is thought to be the most important hormone during pubertal growth and epiphyseal fusion. Both hormonal systems are described in more detail in the following sections and interactions between these systems and the ones described above frequently occur.

Growth hormone and insulin-like growth factor-I (IGF-I)

Growth hormone and IGF-I are important stimulators of longitudinal bone growth. Both GH and IGF-I receptors are expressed in the growth plate (16). Defects in GH and IGF-I pathways result in marked growth disorders (17-20). GH can stimulate skeletal growth directly by local action in the growth plate and indirectly by liver-derived IGF-I (21;22).

The effect of GH on longitudinal growth has been a captivating subject of research through the years. The original hypothesis was the *somatomedin hypothesis* in which it was thought that GH stimulates hepatic production of somatomedin (IGF-I), which in turn stimulates chondrocytes locally in the growth plate (23). In 2001 this hypothesis was questioned by Le Roith et al who found little effect on the growth rate in mice with a selective *igf1* deletion in their liver while their circulating IGF-I was 20-25% of normal (24). The terminal hypertrophic zone in the growth plates of these mice was reduced and therefore it was thought that IGF-1 is responsible for chondrocyte differentiation (24).

The majority of circulating IGF-I is bound to a complex with IGF binding protein 3 (IGFBP-3) and the acid labile subunit (ALS). Knocking out the *als* gene or the *igf1* gene results in just a small effect on longitudinal growth in mice (24;25). On the contrary, a deletion of the *igfbp-3* gene results in an increase in linear growth in mice. A double knock out mouse of *als* and *igf1* as well as a triple knockout of each gene results in significant growth retardation, suggesting that there might be a threshold level of circulating IGF-I to control skeletal growth and that both ALS and IGF-I are crucial participators (26).

Nowadays it is well known that GH not only generates liver produced IGF-1, but also acts locally on chondrocytes in the growth plate. These findings were described in the *dual effector hypothesis*, in which GH acts locally on chondrocytes in the resting zone to enhance the recruitment of resting chondrocytes in the proliferative state and to stimulate local IGF-I production, resulting in an increase in proliferation by both GH and IGF-I stimulation (21;27-29). Several clinical reports and laboratory results have demonstrated the importance of both IGF-I and GH in the regulation of longitudinal bone growth, however the exact contributions and roles of circulating and local effects of these hormones still need to be clarified in more detail.

Estrogen and its effect on longitudinal bone growth

Estrogens are known to play a key role in longitudinal bone growth through growth plate maturation, epiphyseal fusion and augmentation of accrual of bone. The main active form of estrogen is 17 β -estradiol (E₂) that can be synthesized from estrone and testosterone (figure 2). Other estrogen metabolites are less active and have less affinity for the estrogen receptors. The effects of estrogen have been suggested to be mediated mainly through the nuclear receptors ER α and ER β , both expressed in growth plate chondrocytes of several species, including the human (30-33). Expression patterns co-localize throughout the whole growth plate with a more abundant expression in the resting and proliferative zone (32). The two receptors show high conservation in their DNA-binding domain (97%) and share considerable homology (55%) in their ligand-binding domain (34). Recently a new membrane G protein-coupled estrogen receptor was discovered, the GPR30 receptor, which was shown to be expressed in human and mice and was shown to be

functional in the growth plate of mice (35;36). Estrogen receptor gene polymorphism is reported to have an effect on adult height. There are two studies demonstrating that a mutation in a certain region of the estrogen receptor allele can result in an average of 3 cm increase in adult height (37;38).

The important role of estrogen is supported by several clinical observations. Premature estrogen exposure in for example precocious puberty accelerates skeletal maturation, whereas on the contrary hypogonadism results in delay in skeletal maturation. Smith et al in 1994 described a male with an inactivating mutation in the estrogen receptor that showed no pubertal growth spurt and continued to grow into adulthood due to absence of growth plate fusion, resulting in tall stature (210 cm) and osteoporosis (39). A similar phenotype was described in a second report of two boys with a mutation in the aromatase gene (40). Aromatase catalyzes the conversion of androgens into estrogens, thus also in these boys there was a lack of estrogen action. Thirdly, from clinical observations it is known that high levels of estrogen inhibit longitudinal bone growth (41).

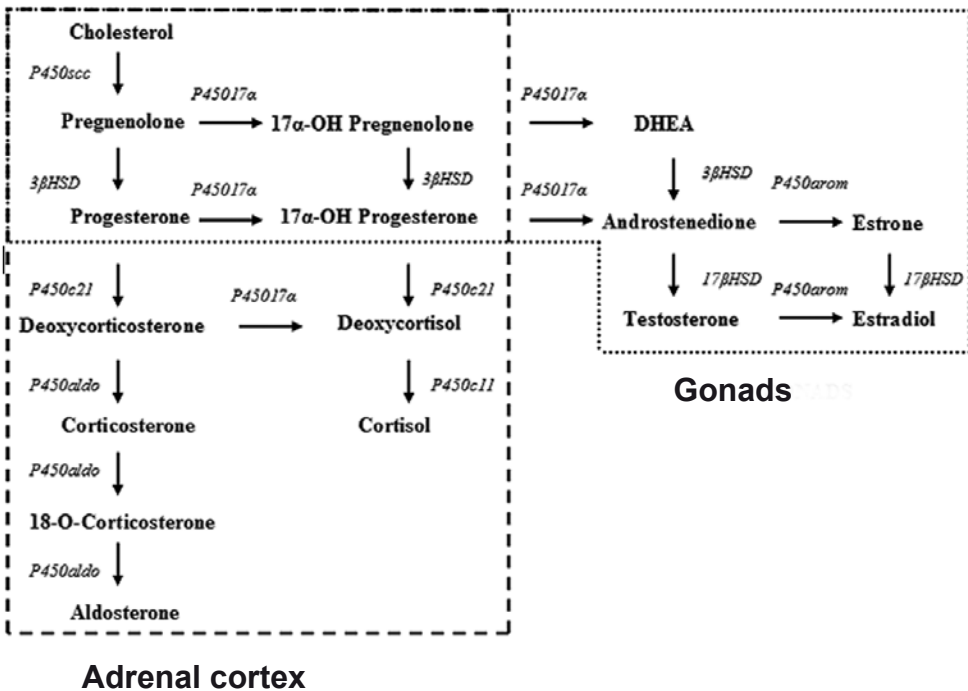


Figure 2: Steroid hormone synthesis pathways.

Reproduced from <http://herkules oulu.fi/isbn951426844X/html/graphic99.png>

Estrogen action

Estrogens can exert their effect through several mechanisms. In the classical way estrogen diffuses through the plasma membrane into the cytosol where it binds cytoplasmic receptors to form hormone-receptor complexes. These complexes dimerize and are translocated into the nucleus where they bind estrogen response elements in or close to a promoter region of a specific gene to activate gene transcription (42).

In a non-classical way estrogen can also act without binding to the DNA. Estrogen receptors can have an effect through interaction with DNA-bound proteins that function as transcription factors or co-regulators like cyclic AMP-response element binding protein (CREB), specificity protein-1 (SP-1) and activator protein-1 (AP-1) (43-45). Alternatively, estrogens act through interaction with membrane-bound receptors, like GPR30 that results in a relatively rapid non-genomic estrogen response through intracellular signaling pathways (46).

Not only do estrogenic ligands regulate ER-dependent gene expression, but the ER can also be phosphorylated and activated by a variety of signaling pathways such as pathways involving IGF-1 and epidermal growth factor (EGF) (47;48). Vice versa estrogens can influence the GH-IGF-I axis, demonstrated by increasing GH but decreasing IGF-1 levels in patients with oral estrogen treatment (49;50). High dose of estrogen treatment decreases IGF-1 levels by 35% (51). However, transdermally administered estrogens increase IGF-1 levels (52). In addition, in puberty an increase in the amplitude of GH-secretion is seen and blocking estrogen signaling results in a drop of GH level (53). It has been suggested that estrogen can act on an AP-1 motif in the promoter site of the IGF-1 gene (54). Another indirect effect of estrogen on longitudinal growth might be through interference with components of the Indian Hedgehog/PTHrP growth restraining feedback loop suggested by experimental data in rats where estrogen increased mRNA expression of PTHrP and its receptor (55).

Senescence

The mechanism by which estrogens exert their effect on longitudinal growth and finally growth plate fusion is not fully understood. One of the postulated hypothesis is that estrogen accelerates the senescent decline (56). Senescence is a term for the structural and functional changes over time in the growth plate, such as a gradual decline in the overall growth plate height, proliferative zone height, hypertrophic zone height, size of hypertrophic chondrocytes and column density (56). Growth plate transplantation experiments showed that the growth rate of a transplanted growth plate depends on the age of the donor and not on the age of the recipient, suggesting that growth velocity in time is regulated by a local mechanism intrinsic to the growth plate besides hormonal regulation in time (57). It is believed that the growth plate fuses when senescence reaches a critical point in the growth plate. Recent evidence indicates that senescence might occur because stem-like cells in the resting zone have a finite proliferative capacity, which is gradually exhausted (58;59). Estrogen is thought to advance growth plate senescence, causing earlier proliferative exhaustion, and thus earlier fusion. This might explain that estrogen treatment does not induce fusion rapidly, but often must act for years before fusion occurs. In addition, the period of estrogen treatment required for growth plate fusion is longer in cases of precocious puberty and shorter in adults with a deficiency in aromatase than for normal individuals.

SERMS

Estrogen is known to be a major regulator of longitudinal growth and growth plate fusion. A low estrogen concentration increases growth velocity, while a high concentration inhibits growth (60;61). A high dose of estrogen is used in the treatment of extremely tall girls to reduce adult height. However, it not only affects longitudinal growth but has also potential side-effects like an increased risk for breast and uterus cancer and decreased fertility (62). These side effects can partially be circumvented by the use of selective estrogen receptor modulators (SERMs), that display both pro- and anti-estrogenic activity in a tissue-specific manner (63).

One of the best-studied SERMs is raloxifen, which prevents postmenopausal bone loss but has minimal effects on breast and uterus tissue (64). In rabbits it induces growth plate fusion without influencing uterus weight (65). Tamoxifen, a SERM widely used in the treatment of breast cancer appears to act as a estrogen antagonist at the growth plate in the treatment of progressive precocious puberty in McCune-Albright patients (66;67). A more detailed understanding of estrogen action and interactions on tissues is needed to enable the use of SERMs in the modulation of longitudinal growth.

Intracrinology

The major source of sex steroids acting on the growth plate is the gonads, which secrete sex steroids into the circulation in a classical endocrine fashion. In addition to this endocrine route, estrogen can also be produced locally. This phenomenon is seen with many other hormones as well and is called intracrinology. Sex steroids can be formed from various precursors by locally expressed enzymes in many tissues like adipose tissue, bone, breast tissue or brain (68;69). Oz et al showed aromatase expression in the human growth plate which was confirmed together with 17 β -estradiol production in rat costochondral chondrocytes (70;71).

A few years later more of these converting enzymes, i.e. 17 β -hydroxysteroid dehydrogenase, steroid sulfatase and type I 5 α -reductase, were detected in the surroundings of the growth plate at time of sexual maturation, suggesting that bone cells possess the capacity to metabolize sex steroids necessary for skeletal growth (72). Van der Eerden et al showed that various enzymes involved in sex steroid metabolism are upregulated with puberty in the rat growth plate, suggesting a role for these enzymes and the steroids they produce during pubertal growth (73).

Catch-up growth

Following a period of growth inhibition, height velocity usually exceeds the normal range. This phenomenon is termed catch-up growth, and was first described by Prader et al. (74). Tanner proposed the hypothesis that catch-up growth is regulated by a neuroendocrine system that compares the individual's actual body size to the target size of the individual. This target size is described as the 'time tally' most likely localized in the brain. The growth rate is adjusted according to the degree of mismatch (75). More recent studies however suggest that catch-up growth is due to intrinsic factors of the growth plate like delayed growth plate senescence (58;76). Growth-inhibiting conditions slow growth plate chondrocyte proliferation, thus conserving the

proliferative capacity of the chondrocytes and consequently decreasing senescence of the growth plate. When growth inhibition conditions are abolished these chondrocytes are less senescent and retain a greater proliferative capacity resulting in a higher growth rate than expected for age, thus in catch-up growth (77). The relationship between catch-up growth and delayed growth plate senescence has only been studied in rabbits and rats so far (77;78). In catch-up growth after food restriction animal studies showed that HIF-1 α protein and mRNA are upregulated in the growth plate together with IGF-1R and GHR protein levels (79;80). Recently Pando et al. reported an additional possible mechanism in nutritional catch-up growth involving microRNAs in the growth plate of rats.

Puberty and epiphyseal fusion

Puberty is a complex biologic process involving sexual development, adrenal maturation, gametogenesis and increase in growth velocity known as pubertal growth spurt which accounts for 15-20% of final height (81). The secretion of gonadotropin-releasing hormone by the hypothalamus represents the first step, initiating release of the gonadotropins (LH and FSH) that in turn stimulates the gonads to secrete sex steroids (estrogen and testosterone). Increase in sex steroids level induces the external signs of puberty (secondary sex characteristics) and the accompanying pubertal growth spurt. Estrogen mediates pubertal bone growth in both males and females. Along with an increase in estrogen also GH secretion increases 1.5 to 3-fold in puberty together with IGF-I levels (82). Peak levels of circulating GH coincide with Tanner stage B3-4 in girls and at Tanner stage G4 in boys (83). Estrogen levels and GH concentration show a positive correlation through puberty in females, demonstrating the relationship in their actions (84). In addition, estrogen has also a direct stimulatory effect on the growth plate chondrocytes, as demonstrated in Laron patients with GH resistance that still undergo a pubertal growth spurt (85). Furthermore, estrogen receptor beta and GPR30 expression is downregulated in the human growth plate during pubertal progression (32;35). Estrogen stimulates differentiation of the chondrocyte rather than proliferation (86) resulting in growth plate maturation and eventually growth plate fusion with cartilage being replaced by bone. Although the exact role of the estrogen receptor beta is still unclear, from mice experiments a crucial role in growth plate fusion was hypothesized (87). However, the male patient with an estrogen receptor alpha mutation had incomplete epiphyseal closure and a history of continued linear growth into adulthood, suggesting a role for estrogen receptor alpha in growth plate fusion. This patient was still able to produce a 46-kDa isoform of the estrogen receptor alpha which is shown to suppress estrogen receptor activation (88;89). Chagin et al speculated that this isoform might as well suppress the estrogen receptor beta and this might be the cause of delay of growth plate fusion in this patient (90).

The final step in epiphyseal fusion is not completely understood up to now. In endochondral ossification, a nowadays generally accepted hypothesis is that terminally hypertrophic chondrocytes die by the process of apoptosis leaving behind a scaffold of cartilage matrix for osteoblasts that invade and lay down bone resulting in growth plate fusion (91-93). More recent studies have questioned that apoptosis is the final mechanism through which chondrocytes die in the terminal hypertrophic zone, since terminal hypertrophic chondrocytes do not display a typical apoptotic appearance (94-96). Apoptotic cells undergo typical morphological changes like cell shrinkage with intact organelles and integrity of membranes, pyknotic nuclei by aggregation of

chromatin, fragmented DNA, partitioning of the cytoplasm and nucleus into membrane bound-vesicles (apoptotic bodies) and absence of an inflammatory response (94;97-99). Roach et al reported autophagic vacuoles in terminal hypertrophic cells suggesting a role for autophagy in the final step of endochondral ossification (94;97;98;100). A third and oldest hypothesis is that terminal hypertrophic chondrocytes can transdifferentiate into osteoblasts (101-103). The mechanism by which terminal hypertrophic chondrocytes disappear at the chondro-osseous junction is believed to be related to the underlying cause of growth plate fusion.

Cell cycle regulators

The process of longitudinal bone growth requires precise regulation of chondrocyte proliferation which is regulated by intracellular and extracellular mechanisms. Extracellular mechanisms involve for example hormonal systems as described in the sections above. An important intracellular mechanism is the cell cycle which is controlled by orderly activation and inactivation of cyclin-dependent kinases (CDKs) and cyclin-dependent kinase inhibitors (CKIs). Cyclin-dependent kinases control specific points of the cell cycle (104). Activation of the CDKs promotes progression of the cell cycle eventually resulting in cell division. CKIs can bind and inactivate these CDKs, thereby maintaining growth arrest. In mammals, two known families of CKIs have been identified, INK4 and the Cip/Kip family. The Cip/Kip family consists of p21Cip1 (p21), p27Kip1 (p27), and p57Kip2 (p57) which can inhibit all G1/S-phase cyclin-CDK complexes and which are all expressed in the growth plate (105-109). Cip/Kip inhibitors appear to mediate the growth inhibiting and differentiation effects of different stimuli. For example a recent study suggests that the effects of PTHrP on both the rate and extent of chondrocyte proliferation are mediated through suppression of p57 expression (110). In addition, p27 expression is up-regulated during thyroid hormone-induced terminal differentiation of rat resting zone chondrocytes (111). Little is known about the exact role of cell cycle regulators in the regulation of skeletal growth.

Growth plate models and species differences

Studies on growth plate regulation and epiphyseal fusion are hampered by the fact that frequently used *in vivo* and *in vitro* animal models poorly represent the human situation. Mouse and rat for example do not fuse their growth plates at the end of puberty like humans (32;33). This indicates that rodents are not perfectly representative for studies on growth plate fusion, excluding the use of transgenic approaches. This is furthermore illustrated by the discrepancy in growth phenotype between ERa knock out mice and a male patient lacking functional ERa receptors (39;112). The patient did not fuse his growth plates and continued growing into adulthood. Gene ablation of the estrogen receptors in mice had only a marginal effect on longitudinal growth, which only became apparent in part of the long bones late in life. Other animal models occasionally used for studies on growth plate regulation are rabbits and piglets, however these are relatively expensive and few molecular biological tools are available for interventions. *In vitro* human models like primary cultures of human chondrocytes or chondrosarcomatous cells are limited in its representation of the *in vivo* situation and have other impairments like a rapid dedifferentiation in primary cultures, a high variability between donors and loss of differentiation capacity. A promising relatively new

human *in vitro* model is a model with Mesenchymal stem cells (MSCs). MSCs are multipotent cells with the ability to differentiate into several mesenchymal lineages including chondrocytes. They can differentiate from stem cells to proliferating chondrocytes to subsequently hypertrophic chondrocytes, in a similar fashion as observed in the human growth plate (113;114). MSCs were originally isolated from bone marrow (115), but they have also been isolated from other tissue sources such as fetal organs, placenta, umbilical blood and adipose tissue (113;116;117). The lack of representative animal models to study processes occurring in the human growth plate, has led to the realization that human based models are required to elucidate the molecular mechanisms involved in growth plate regulation and fusion.

Rationale and outline of this thesis

Estrogen is known to play an important role in longitudinal bone growth and growth plate maturation, but the mechanism by which estrogens exert their effect is not fully understood. In this thesis this role is further explored. **Chapter 1** contains a general introduction to longitudinal bone growth and the regulation of the growth plate in respect to relevant topics further studied in this thesis. Estrogen can act through a genomic or a nongenomic pathway. Both pathways are explored in rats at the onset of maturation in **chapter 2**. Estrogen stimulates VEGF expression in uterus and bone, which is an important growth factor for chondrocyte differentiation and chondrocytes survival in the growth plate. In **chapter 3** the effect of estrogen on VEGF expression in the growth plate was studied in the rat and human growth plate. Another effect of estrogen is that it accelerates growth plate senescence. Senescence is one of the postulated intrinsic mechanisms by which the growth plate matures and finally fuses. In **chapter 4** we investigated senescence in relation to proliferation, by investigating a cell cycle inhibitor p27Kip1. In animal models, catch-up growth is suggested to be caused by delayed growth plate senescence. In **chapter 5** this hypothesis was further tested in humans.

With puberty estrogen levels increase, the growth plate matures and at the end growth ceases with epiphyseal fusion through mechanisms not yet completely understood. In order to further explore growth plate maturation we subjected two growth plate tissues of the same patient, but with one year and one pubertal Tanner stage in between, to microarray analyses. Gene expression patterns and transcription factor binding sites in relation to pubertal maturation were studied in a longitudinal study within this single patient in **chapter 6**. In addition, we collected extra prepubertal and pubertal growth plate tissues and studied these samples with microarray techniques as well in **chapter 7**. In **chapter 8** the process of epiphyseal fusion and apoptosis was studied in human growth plates.

Animal models are frequently used but not fully representative for the human growth plate. Therefore we investigated a promising human *in vitro* model with multipotent mesenchymal stem cells (MSCs) that can differentiate into chondrocytes. MSCs can be isolated from various tissues. In **chapter 9** we investigated the chondrogenic potential of MSCs from different origins and in **chapter 10** we compared this model with the epiphyseal growth plate by analyzing gene expression patterns and pathways with micro-array analyses. **Chapter 11** contains general conclusions and a discussion regarding the results.

References

1. **van der Eerden BC, Karperien M, Wit JM** 2003 Systemic and local regulation of the growth plate. *Endocr Rev* 24:782-801
2. **Spranger J, Winterpacht A, Zabel B** 1994 The type II collagenopathies: a spectrum of chondrodysplasias. *Eur J Pediatr* 153:56-65
3. **Wallis GA, Rash B, Sykes B, Bonaventure J, Maroteaux P, Zabel B, Wynne-Davies R, Grant ME, Boot-Handford RP** 1996 Mutations within the gene encoding the alpha 1 (X) chain of type X collagen (COL10A1) cause metaphyseal chondrodysplasia type Schmid but not several other forms of metaphyseal chondrodysplasia. *J Med Genet* 33:450-457
4. **Engsig MT, Chen QJ, Vu TH, Pedersen AC, Therkildsen B, Lund LR, Henriksen K, Lenhard T, Foged NT, Werb Z, Delaisse JM** 2000 Matrix metalloproteinase 9 and vascular endothelial growth factor are essential for osteoclast recruitment into developing long bones. *J Cell Biol* 151:879-889
5. **Ortega N, Behonick D, Stickens D, Werb Z** 2003 How proteases regulate bone morphogenesis. *Ann N Y Acad Sci* 995:109-116
6. **Ortega N, Behonick DJ, Werb Z** 2004 Matrix remodeling during endochondral ossification. *Trends Cell Biol* 14:86-93
7. **Zelzer E, Mamluk R, Ferrara N, Johnson RS, Schipani E, Olsen BR** 2004 VEGFA is necessary for chondrocyte survival during bone development. *Development* 131:2161-2171
8. **Zelzer E, Olsen BR** 2005 Multiple roles of vascular endothelial growth factor (VEGF) in skeletal development, growth, and repair. *Curr Top Dev Biol* 65:169-187
9. **Dai J, Rabie AB** 2007 VEGF: an essential mediator of both angiogenesis and endochondral ossification. *J Dent Res* 86:937-950
10. **Buckler JM, Willgerodt H, Keller E** 1986 Growth in thyrotoxicosis. *Arch Dis Child* 61:464-471
11. **Leger J, Czernichow P** 1989 Congenital hypothyroidism: decreased growth velocity in the first weeks of life. *Biol Neonate* 55:218-223
12. **Schlesinger S, MacGillivray MH, Munschauer RW** 1973 Acceleration of growth and bone maturation in childhood thyrotoxicosis. *J Pediatr* 83:233-236
13. **Chrysis D, Ritzen EM, Savendahl L** 2003 Growth retardation induced by dexamethasone is associated with increased apoptosis of the growth plate chondrocytes. *J Endocrinol* 176:331-337

14. **Silvestrini G, Ballanti P, Patacchioli FR, Mocetti P, Di Grezia R, Wedard BM, Angelucci L, Bonucci E** 2000 Evaluation of apoptosis and the glucocorticoid receptor in the cartilage growth plate and metaphyseal bone cells of rats after high-dose treatment with corticosterone. *Bone* 26:33-42
15. **MacRae VE, Wong SC, Farquharson C, Ahmed SF** 2006 Cytokine actions in growth disorders associated with pediatric chronic inflammatory diseases (review). *Int J Mol Med* 18:1011-1018
16. **Werther GA, Haynes K, Edmonson S, Oakes S, Buchanan CJ, Herington AC, Waters MJ** 1993 Identification of growth hormone receptors on human growth plate chondrocytes. *Acta Paediatr Suppl* 82 Suppl 391:50-53
17. **Abuzzahab MJ, Schneider A, Goddard A, Grigorescu F, Lautier C, Keller E, Kiess W, Klammt J, Kratzsch J, Osgood D, Pfaffle R, Raile K, Seidel B, Smith RJ, Chernausek SD** 2003 IGF-I receptor mutations resulting in intrauterine and postnatal growth retardation. *N Engl J Med* 349:2211-2222
18. **Kofoed EM, Hwa V, Little B, Woods KA, Buckway CK, Tsubaki J, Pratt KL, Bezrodnik L, Jasper H, Tepper A, Heinrich JJ, Rosenfeld RG** 2003 Growth hormone insensitivity associated with a STAT5b mutation. *N Engl J Med* 349:1139-1147
19. **Rosenfeld RG, Rosenbloom AL, Guevara-Aguirre J** 1994 Growth hormone (GH) insensitivity due to primary GH receptor deficiency. *Endocr Rev* 15:369-390
20. **Woods KA, Camacho-Hubner C, Savage MO, Clark AJ** 1996 Intrauterine growth retardation and postnatal growth failure associated with deletion of the insulin-like growth factor I gene. *N Engl J Med* 335:1363-1367
21. **Isaksson OG, Lindahl A, Nilsson A, Isgaard J** 1987 Mechanism of the stimulatory effect of growth hormone on longitudinal bone growth. *Endocr Rev* 8:426-438
22. **Isgaard J, Nilsson A, Lindahl A, Jansson JO, Isaksson OGP** 1986 Effects of Local-Administration of Gh and Igf-1 on Longitudinal Bone-Growth in Rats. *American Journal of Physiology* 250:E367-E372
23. **Daughaday WH, Hall K, Raben MS, Salmon WD, Jr., van den Brande JL, van Wyk JJ** 1972 Somatomedin: proposed designation for sulphation factor. *Nature* 235:107
24. **Le Roith D, Bondy C, Yakar S, Liu JL, Butler A** 2001 The somatomedin hypothesis: 2001. *Endocr Rev* 22:53-74
25. **Yakar S, Rosen CJ, Beamer WG, Ackert-Bicknell CL, Wu Y, Liu JL, Ooi GT, Setser J, Frystyk J, Boisclair YR, LeRoith D** 2002 Circulating levels of IGF-1 directly regulate bone growth and density. *J Clin Invest* 110:771-781

26. **Yakar S, Rosen CJ, Bouxsein ML, Sun H, Mejia W, Kawashima Y, Wu Y, Emerton K, Williams V, Jepsen K, Schaffler MB, Majeska RJ, Gavrilova O, Gutierrez M, Hwang D, Pennisi P, Frystyk J, Boisclair Y, Pintar J, Jasper H, Domene H, Cohen P, Clemmons D, LeRoith D** 2009 Serum complexes of insulin-like growth factor-1 modulate skeletal integrity and carbohydrate metabolism. *FASEB J* 23:709-719
27. **Hunziker EB, Wagner J, Zapf J** 1994 Differential effects of insulin-like growth factor I and growth hormone on developmental stages of rat growth plate chondrocytes in vivo. *J Clin Invest* 93:1078-1086
28. **Ohlsson C, Nilsson A, Isaksson O, Lindahl A** 1992 Growth hormone induces multiplication of the slowly cycling germinal cells of the rat tibial growth plate. *Proc Natl Acad Sci U S A* 89:9826-9830
29. **Schlechter NL, Russell SM, Spencer EM, Nicoll CS** 1986 Evidence suggesting that the direct growth-promoting effect of growth hormone on cartilage in vivo is mediated by local production of somatomedin. *Proc Natl Acad Sci U S A* 83:7932-7934
30. **Kennedy J, Baris C, Hoyland JA, Selby PL, Freemont AJ, Braidman IP** 1999 Immunofluorescent localization of estrogen receptor-alpha in growth plates of rabbits, but not in rats, at sexual maturity. *Bone* 24:9-16
31. **Kusec V, Viridi AS, Prince R, Triffitt JT** 1998 Localization of estrogen receptor-alpha in human and rabbit skeletal tissues. *J Clin Endocrinol Metab* 83:2421-2428
32. **Nilsson O, Chrysis D, Pajulo O, Boman A, Holst M, Rubinstein J, Martin RE, Savendahl L** 2003 Localization of estrogen receptors-alpha and -beta and androgen receptor in the human growth plate at different pubertal stages. *J Endocrinol* 177:319-326
33. **van der Eerden BC, Gevers EF, Lowik CW, Karperien M, Wit JM** 2002 Expression of estrogen receptor alpha and beta in the epiphyseal plate of the rat. *Bone* 30:478-485
34. **Kuiper GG, Carlsson B, Grandien K, Enmark E, Haggblad J, Nilsson S, Gustafsson JA** 1997 Comparison of the ligand binding specificity and transcript tissue distribution of estrogen receptors alpha and beta. *Endocrinology* 138:863-870
35. **Chagin AS, Savendahl L** 2007 GPR30 estrogen receptor expression in the growth plate declines as puberty progresses. *J Clin Endocrinol Metab* 92:4873-4877
36. **Windahl SH, Andersson N, Chagin AS, Martensson UE, Carlsten H, Olde B, Swanson C, Moverare-Skrtic S, Savendahl L, Lagerquist MK, Leeb-Lundberg LM, Ohlsson C** 2009 The role of the G protein-coupled receptor GPR30 in the effects of estrogen in ovariectomized mice. *Am J Physiol Endocrinol Metab* 296:E490-E496
37. **Lehrer S, Rabin J, Stone J, Berkowitz GS** 1994 Association of an estrogen receptor variant with increased height in women. *Horm Metab Res* 26:486-488

38. **Lorentzon M, Lorentzon R, Backstrom T, Nordstrom P** 1999 Estrogen receptor gene polymorphism, but not estradiol levels, is related to bone density in healthy adolescent boys: a cross-sectional and longitudinal study. *J Clin Endocrinol Metab* 84:4597-4601
39. **Smith EP, Boyd J, Frank GR, Takahashi H, Cohen RM, Specker B, Williams TC, Lubahn DB, Korach KS** 1994 Estrogen resistance caused by a mutation in the estrogen-receptor gene in a man. *N Engl J Med* 331:1056-1061
40. **Morishima A, Grumbach MM, Simpson ER, Fisher C, Qin K** 1995 Aromatase deficiency in male and female siblings caused by a novel mutation and the physiological role of estrogens. *J Clin Endocrinol Metab* 80:3689-3698
41. **Turner RT, Riggs BL, Spelsberg TC** 1994 Skeletal effects of estrogen. *Endocr Rev* 15:275-300
42. **McKenna NJ, O'Malley BW** 2002 Minireview: nuclear receptor coactivators--an update. *Endocrinology* 143:2461-2465
43. **Kushner PJ, Agard DA, Greene GL, Scanlan TS, Shiau AK, Uht RM, Webb P** 2000 Estrogen receptor pathways to AP-1. *J Steroid Biochem Mol Biol* 74:311-317
44. **Sabbah M, Courilleau D, Mester J, Redeuilh G** 1999 Estrogen induction of the cyclin D1 promoter: involvement of a cAMP response-like element. *Proc Natl Acad Sci U S A* 96:11217-11222
45. **Safe S** 2001 Transcriptional activation of genes by 17 beta-estradiol through estrogen receptor-Sp1 interactions. *Vitam Horm* 62:231-252
46. **Coleman KM, Smith CL** 2001 Intracellular signaling pathways: nongenomic actions of estrogens and ligand-independent activation of estrogen receptors. *Front Biosci* 6:D1379-D1391
47. **Aronica SM, Katzenellenbogen BS** 1993 Stimulation of estrogen receptor-mediated transcription and alteration in the phosphorylation state of the rat uterine estrogen receptor by estrogen, cyclic adenosine monophosphate, and insulin-like growth factor-I. *Mol Endocrinol* 7:743-752
48. **Ignar-Trowbridge DM, Nelson KG, Bidwell MC, Curtis SW, Washburn TF, McLachlan JA, Korach KS** 1992 Coupling of dual signaling pathways: epidermal growth factor action involves the estrogen receptor. *Proc Natl Acad Sci U S A* 89:4658-4662
49. **Coutant R, de Casson FB, Rouleau S, Douay O, Mathieu E, Gatelais F, Bouhours-Nouet N, Voinot C, Audran M, Limal JM** 2004 Divergent effect of endogenous and exogenous sex steroids on the insulin-like growth factor I response to growth hormone in short normal adolescents. *J Clin Endocrinol Metab* 89:6185-6192

50. **Veldhuis JD, Keenan DM, Bailey JN, Adeniji A, Miles JM, Paulo R, Cosma M, Soares-Welch C** 2008 Estradiol supplementation in postmenopausal women attenuates suppression of pulsatile growth hormone secretion by recombinant human insulin-like growth factor type I. *J Clin Endocrinol Metab* 93:4471-4478
51. **Rooman RP, De Beeck LO, Martin M, van DJ, Mohan S, Du Caju MV** 2002 IGF-I, IGF-II, 'free' IGF-I and IGF-binding proteins-2 to -6 during high-dose oestrogen treatment in constitutionally tall girls. *Eur J Endocrinol* 146:823-829
52. **Weissberger AJ, Ho KKY, Lazarus L** 1991 Contrasting Effects of Oral and Transdermal Routes of Estrogen Replacement Therapy on 24-Hour Growth-Hormone (Gh) Secretion, Insulin-Like Growth Factor-I, and Gh-Binding Protein in Postmenopausal Women. *Journal of Clinical Endocrinology and Metabolism* 72:374-381
53. **Metzger DL, Kerrigan JR** 1994 Estrogen receptor blockade with tamoxifen diminishes growth hormone secretion in boys: evidence for a stimulatory role of endogenous estrogens during male adolescence. *J Clin Endocrinol Metab* 79:513-518
54. **Umayahara Y, Kawamori R, Watada H, Imano E, Iwama N, Morishima T, Yamasaki Y, Kajimoto Y, Kamada T** 1994 Estrogen Regulation of the Insulin-Like Growth-Factor-I Gene-Transcription Involves An Ap-1 Enhancer. *Journal of Biological Chemistry* 269:16433-16442
55. **Paspaliaris V, Petersen DN, Thiede MA** 1995 Steroid regulation of parathyroid hormone-related protein expression and action in the rat uterus. *J Steroid Biochem Mol Biol* 53:259-265
56. **Weise M, De Levi S, Barnes KM, Gafni RI, Abad V, Baron J** 2001 Effects of estrogen on growth plate senescence and epiphyseal fusion. *Proc Natl Acad Sci U S A* 98:6871-6876
57. **Stevens DG, Boyer MI, Bowen CV** 1999 Transplantation of epiphyseal plate allografts between animals of different ages. *J Pediatr Orthop* 19:398-403
58. **Gafni RI, Weise M, Robrecht DT, Meyers JL, Barnes KM, De Levi S, Baron J** 2001 Catch-up growth is associated with delayed senescence of the growth plate in rabbits. *Pediatr Res* 50:618-623
59. **Schrier L, Ferns SP, Barnes KM, Emons JA, Newman EI, Nilsson O, Baron J** 2006 Depletion of resting zone chondrocytes during growth plate senescence. *J Endocrinol* 189:27-36
60. **Klein KO, Martha PM, Jr, Blizzard RM, Herbst T, Rogol AD** 1996 A longitudinal assessment of hormonal and physical alterations during normal puberty in boys. II. Estrogen levels as determined by an ultrasensitive bioassay. *J Clin Endocrinol Metab* 81:3203-3207
61. **Ross JL, Long LM, Skerda M, Cassorla F, Kurtz D, Loriaux DL, Cutler GB, Jr.** 1986 Effect of low doses of estradiol on 6-month growth rates and predicted height in patients with Turner syndrome. *J Pediatr* 109:950-953

62. **Venn A, Bruinsma F, Werther G, Pyett P, Baird D, Jones P, Rayner J, Lumley J** 2004 Oestrogen treatment to reduce the adult height of tall girls: long-term effects on fertility. *Lancet* 364:1513-1518
63. **McDonnell DP** 1999 The Molecular Pharmacology of SERMs. *Trends Endocrinol Metab* 10:301-311
64. **Cosman F, Lindsay R** 1999 Selective estrogen receptor modulators: clinical spectrum. *Endocr Rev* 20:418-434
65. **Nilsson O, Falk J, Ritzen EM, Baron J, Savendahl L** 2003 Raloxifene acts as an estrogen agonist on the rabbit growth plate. *Endocrinology* 144:1481-1485
66. **Eugster EA, Shankar R, Feezle LK, Pescovitz OH** 1999 Tamoxifen treatment of progressive precocious puberty in a patient with McCune-Albright syndrome. *J Pediatr Endocrinol zetab* 12:681-686
67. **Eugster EA, Rubin SD, Reiter EO, Plourde P, Jou HC, Pescovitz OH** 2003 Tamoxifen treatment for precocious puberty in McCune-Albright syndrome: a multicenter trial. *J Pediatr* 143:60-66
68. **Folkerd EJ, James VH** 1982 Studies on the activity of 17 beta-hydroxysteroid dehydrogenase in human adipose tissue. *J Steroid Biochem* 16:539-543
69. **Labrie F, Luu-The V, Lin SX, Simard J, Labrie C** 2000 Role of 17 beta-hydroxysteroid dehydrogenases in sex steroid formation in peripheral intracrine tissues. *Trends Endocrinol Metab* 11:421-427
70. **Oz OK, Millsaps R, Welch R, Birch J, Zerwekh JE** 2001 Expression of aromatase in the human growth plate. *J Mol Endocrinol* 27:249-253
71. **Sylvia VL, Gay I, Hardin R, Dean DD, Boyan BD, Schwartz Z** 2002 Rat costochondral chondrocytes produce 17beta-estradiol and regulate its production by 1alpha,25(OH)(2) D(3). *Bone* 30:57-63
72. **van der Eerden BC, Lowik CW, Wit JM, Karperien M** 2004 Expression of estrogen receptors and enzymes involved in sex steroid metabolism in the rat tibia during sexual maturation. *J Endocrinol* 180:457-467
73. **van der Eerden BC, Van D, V, Lowik CW, Wit JM, Karperien M** 2002 Sex steroid metabolism in the tibial growth plate of the rat. *Endocrinology* 143:4048-4055
74. **PRADER A, TANNER JM, von HARNACK G** 1963 Catch-up growth following illness or starvation. An example of developmental canalization in man. *J Pediatr* 62:646-659
75. **TANNER JM** 1963 REGULATION OF GROWTH IN SIZE IN MAMMALS. *Nature* 199:845-850

76. **Baron J, Klein KO, Colli MJ, Yanovski JA, Novosad JA, Bacher JD, Cutler GB, Jr.** 1994 Catch-up growth after glucocorticoid excess: a mechanism intrinsic to the growth plate. *Endocrinology* 135:1367-1371
77. **Nilsson O, Baron J** 2005 Impact of growth plate senescence on catch-up growth and epiphyseal fusion. *Pediatr Nephrol* 20:319-322
78. **Marino R, Hegde A, Barnes KM, Schrier L, Emons JA, Nilsson O, Baron J** 2008 Catch-up growth after hypothyroidism is caused by delayed growth plate senescence. *Endocrinology* 149:1820-1828
79. **Gat-Yablonski G, Shtauf B, Abraham E, Phillip M** 2008 Nutrition-induced catch-up growth at the growth plate. *J Pediatr Endocrinol Metab* 21:879-893
80. **Even-Zohar N, Jacob J, Amariglio N, Rechavi G, Potievsky O, Phillip M, Gat-Yablonski G** 2008 Nutrition-induced catch-up growth increases hypoxia inducible factor 1alpha RNA levels in the growth plate. *Bone* 42:505-515
81. **Perry RJ, Farquharson C, Ahmed SF** 2008 The role of sex steroids in controlling pubertal growth. *Clin Endocrinol (Oxf)* 68:4-15
82. **Juul A, Bang P, Hertel NT, Main K, Dalgaard P, Jorgensen K, Muller J, Hall K, Skakkebaek NE** 1994 Serum insulin-like growth factor-I in 1030 healthy children, adolescents, and adults: relation to age, sex, stage of puberty, testicular size, and body mass index. *J Clin Endocrinol Metab* 78:744-752
83. **Albertsson-Wikland K, Rosberg S, Karlberg J, Groth T** 1994 Analysis of 24-hour growth hormone profiles in healthy boys and girls of normal stature: relation to puberty. *J Clin Endocrinol Metab* 78:1195-1201
84. **Wennink JM, Delemarre-van de Waal HA, Schoemaker R, Schoemaker H, Schoemaker J** 1990 Luteinizing hormone and follicle stimulating hormone secretion patterns in girls throughout puberty measured using highly sensitive immunoradiometric assays. *Clin Endocrinol (Oxf)* 33:333-344
85. **Laron Z, Kowadlo-Silbergeld A, Eshet R, Pertzalan A** 1980 Growth hormone resistance. *Ann Clin Res* 12:269-277
86. **Blanchard O, Tsagris L, Rappaport R, Duval-Beaupere G, Corvol M** 1991 Age-dependent responsiveness of rabbit and human cartilage cells to sex steroids in vitro. *J Steroid Biochem Mol Biol* 40:711-716
87. **Chagin AS, Lindberg MK, Andersson N, Moverare S, Gustafsson JA, Savendahl L, Ohlsson C** 2004 Estrogen receptor-beta inhibits skeletal growth and has the capacity to mediate growth plate fusion in female mice. *J Bone Miner Res* 19:72-77

88. **Chagin A, Nilsson M, Wright KD, Savendahl L** 2006 Remaining estrogenic activity in the man with mutated estrogen receptor alpha [ER alpha]. *Hormone Research* 65:28
89. **Flouriort G, Brand H, Denger S, Metivier R, Kos M, Reid G, Sonntag-Buck V, Gannon F** 2000 Identification of a new isoform of the human estrogen receptor-alpha (hER-alpha) that is encoded by distinct transcripts and that is able to repress hER-alpha activation function 1. *EMBO J* 19:4688-4700
90. **Chagin AS, Savendahl L** 2007 Estrogens and growth: review. *Pediatr Endocrinol Rev* 4:329-334
91. **Akiyama H, Chaboissier MC, Martin JF, Schedl A, de Crombrughe B** 2002 The transcription factor Sox9 has essential roles in successive steps of the chondrocyte differentiation pathway and is required for expression of Sox5 and Sox6. *Genes Dev* 16:2813-2828
92. **Hunziker EB** 1994 Mechanism of longitudinal bone growth and its regulation by growth plate chondrocytes. *Microsc Res Tech* 28:505-519
93. **Kronenberg HM** 2003 Developmental regulation of the growth plate. *Nature* 423:332-336
94. **Ahmed YA, Tatarczuch L, Pagel CN, Davies HM, Mirams M, Mackie EJ** 2007 Physiological death of hypertrophic chondrocytes. *Osteoarthritis Cartilage* 15:575-586
95. **Erenpreisa J, Roach HI** 1998 Aberrant death in dark chondrocytes of the avian growth plate. *Cell Death Differ* 5:60-66
96. **Roach HI, Clarke NM** 2000 Physiological cell death of chondrocytes in vivo is not confined to apoptosis. New observations on the mammalian growth plate. *J Bone Joint Surg Br* 82:601-613
97. **Cohen JJ** 1993 Apoptosis. *Immunol Today* 14:126-130
98. **Kroemer G, Martin SJ** 2005 Caspase-independent cell death. *Nat Med* 11:725-730
99. **Zimmermann KC, Green DR** 2001 How cells die: apoptosis pathways. *J Allergy Clin Immunol* 108:S99-103
100. **Roach HI, Aigner T, Kouri JB** 2004 Chondroptosis: a variant of apoptotic cell death in chondrocytes? *Apoptosis* 9:265-277
101. **Adams CS, Shapiro IM** 2002 The fate of the terminally differentiated chondrocyte: evidence for microenvironmental regulation of chondrocyte apoptosis. *Crit Rev Oral Biol Med* 13:465-473
102. **Moskalewski S, Malejczyk J** 1989 Bone formation following intrarenal transplantation of isolated murine chondrocytes: chondrocyte-bone cell transdifferentiation? *Development* 107:473-480

103. **Thesingh CW, Groot CG, Wassenaar AM** 1991 Transdifferentiation of hypertrophic chondrocytes into osteoblasts in murine fetal metatarsal bones, induced by co-cultured cerebrum. *Bone Miner* 12:25-40
104. **Vermeulen K, Van Bockstaele DR, Berneman ZN** 2003 The cell cycle: a review of regulation, deregulation and therapeutic targets in cancer. *Cell Prolif* 36:131-149
105. **Hirata M, Kugimiya F, Fukai A, Ohba S, Kawamura N, Ogasawara T, Kawasaki Y, Saito T, Yano F, Ikeda T, Nakamura K, Chung UI, Kawaguchi H** 2009 C/EBPbeta Promotes transition from proliferation to hypertrophic differentiation of chondrocytes through transactivation of p57. *PLoS One* 4:e4543
106. **Horner A, Shum L, Ayres JA, Nonaka K, Nuckolls GH** 2002 Fibroblast growth factor signaling regulates Dach1 expression during skeletal development. *Dev Dyn* 225:35-45
107. **Stewart MC, Farnum CE, MacLeod JN** 1997 Expression of p21CIP1/WAF1 in chondrocytes. *Calcif Tissue Int* 61:199-204
108. **Sunters A, McCluskey J, Grigoriadis AE** 1998 Control of cell cycle gene expression in bone development and during c-Fos-induced osteosarcoma formation. *Dev Genet* 22:386-397
109. **Zenmyo M, Komiya S, Hamada T, Hiraoka K, Suzuki R, Inoue A** 2000 p21 and parathyroid hormone-related peptide in the growth plate. *Calcif Tissue Int* 67:378-381
110. **MacLean HE, Guo J, Knight MC, Zhang P, Cobrinik D, Kronenberg HM** 2004 The cyclin-dependent kinase inhibitor p57(Kip2) mediates proliferative actions of PTHrP in chondrocytes. *J Clin Invest* 113:1334-1343
111. **Ballock RT, Zhou X, Mink LM, Chen DH, Mita BC, Stewart MC** 2000 Expression of cyclin-dependent kinase inhibitors in epiphyseal chondrocytes induced to terminally differentiate with thyroid hormone. *Endocrinology* 141:4552-4557
112. **Vidal O, Lindberg M, Savendahl L, Lubahn DB, Ritzen EM, Gustafsson JA, Ohlsson C** 1999 Disproportional body growth in female estrogen receptor-alpha-inactivated mice. *Biochem Biophys Res Commun* 265:569-571
113. **in 't Anker PS, Noort WA, Scherjon SA, Kleijburg-van der Keur C, Kruisselbrink AB, van Bezooijen RL, Beekhuizen W, Willemze R, Kanhai HH, Fibbe WE** 2003 Mesenchymal stem cells in human second-trimester bone marrow, liver, lung, and spleen exhibit a similar immunophenotype but a heterogeneous multilineage differentiation potential. *Haematologica* 88:845-852
114. **Prockop DJ** 1997 Marrow stromal cells as stem cells for nonhematopoietic tissues. *Science* 276:71-74
115. **Friedenstein AJ** 1980 Stromal mechanisms of bone marrow: cloning in vitro and retransplantation in vivo. *Haematol Blood Transfus* 25:19-29

116. **in 't Anker PS, Scherjon SA, Kleijburg-van der Keur C, Groot-Swings GM, Claas FH, Fibbe WE, Kanhai HH** 2004 Isolation of mesenchymal stem cells of fetal or maternal origin from human placenta. *Stem Cells* 22:1338-1345
117. **Zuk PA, Zhu M, Mizuno H, Huang J, Futrell JW, Katz AJ, Benhaim P, Lorenz HP, Hedrick MH** 2001 Multilineage cells from human adipose tissue: implications for cell-based therapies. *Tissue Eng* 7:211-228

2

Evidence for genomic and nongenomic actions of estrogen in growth plate regulation in female and male rats at the onset of sexual maturation

**B C J van der Eerden¹, J Emons¹, S Ahmed¹, H W van Essen²,
C W G M Lowik³, J M Wit¹ and M Karperien^{1,3}**

J Endocrinol 2002. 175(2):277-288

¹Department of Pediatrics, Leiden University Medical Center, Building 1, zone J6-S,
PO Box 9600, 2300 RC Leiden, The Netherlands.

²Department of Endocrinology, Academic Hospital Free University, Amsterdam, The Netherlands.

³Department of Endocrinology and Metabolic Diseases, Leiden University Medical Center,
Building 1, zone C4-R, PO Box 9600, 2300 RC Leiden, The Netherlands.

Abstract

Recently, both estrogen receptor (ER) α and β were detected in growth plate chondrocytes of rats before sexual maturation, implying a role for estrogen at this stage.

In this study, therefore, we investigated the effects of ovariectomy (OVX) or estrogen supplementation on parameters of longitudinal growth in 26-day-old rats, which were sexually immature at the start of the experiment. OVX caused an increase in body weight gain, tibial length and growth plate width due to an increased proliferating zone. This increase correlated with an increase in cell number, with a decrease in cell diameter and with increased proliferating cell nuclear antigen (PCNA) immunostaining compared with sham. Interestingly, the increase in proliferation was not caused by an increase in insulin-like growth factor-I (IGF-I) mRNA expression in the growth plate as assessed by real-time PCR. In contrast to OVX, 17 β -estradiol (E2) supplementation (0.5 mg/21 days) of 26-day-old female rats caused a strong decrease in body weight gain, tibial length and growth plate width. The latter was explained by a reduction of the proliferating zone width, which correlated with a reduced number of PCNA-positive cells (not significant) and by a reduction of the hypertrophic zone width. In male rats supplemented with E2, similar effects were observed compared with the females. ER α and β immunostaining was found predominantly in late proliferating and early hypertrophic chondrocytes. OVX did not affect ER expression but E2 supplementation strongly decreased immunostaining for both ER α and β in both sexes. Besides E2, desoxyestrone (DE), an activator of nongenomic estrogen-like signaling (ANGEL) and 2-methoxyestradiol (2-MeO-E2), a tissue-selective naturally occurring metabolite of E2, were administered to female and male rats of the same age. Compared with E2, these compounds had less pronounced, though significant, effects on some parameters of longitudinal growth in both sexes, especially on growth plate characteristics. In conclusion, E2 may exert effects on longitudinal growth before and at the onset of sexual maturation, despite very low endogenous serum levels at these stages. There may be a role for nongenomic signaling in body weight gain, tibial length and growth plate width but genomic signaling prevails.

Introduction

Recent findings in three male patients, one with an inactivating mutation in the estrogen receptor α (ER α) and β (ER β) and two with an aromatase p450 enzyme deficiency, have established that estrogen modulates essential steps regarding growth during puberty, both in boys and girls (1-3). Estrogen can have both direct and indirect effects on the growth plate. It was shown that anti-estrogen lowers growth hormone (GH) secretion, while estrogen augments GH secretion, especially by increasing the secretory pulse mass (4-6). However, patients with Laron syndrome, who are resistant to GH due to a mutation in its receptor, do have a pubertal growth spurt, suggesting GH independent effects of estrogen as well (7). These effects may be mediated in the growth plate itself, since ER α and β have been demonstrated in growth plate chondrocytes of several species, including rabbit, rat and human (8-12).

In various mouse and rat models, effects of 17 β -estradiol (E2) on longitudinal growth have been described. These studies have, however, been mainly performed in animals that were sexually maturing or mature at the start of the experiment and are limited to a few reports. In 7-week-old sexually maturing female rats, ovariectomy (OVX) enhanced longitudinal growth rate (13). In contrast, high-dose E2 (4 mg/kg per day) strongly reduced tibial growth rate of 2-month-old

intact sexually mature male rats (14). In contrast to humans, rats do not fuse their growth plates at the end of sexual maturation, resulting in a continuation of longitudinal growth, albeit at a very low rate. At these stages, E2 still inhibited longitudinal growth as has been observed in 3-month-old intact female rats (15).

Concomitant with longitudinal growth, growth plate thickness was increased after OVX, which was primarily explained by induced chondrocyte proliferation (13). Likewise, OVX enhanced proliferating cell nuclear antigen (PCNA) protein expression, a marker for cell proliferation, in growth plates from 14-week-old sexually immature rabbits (16). In the same study, serum IGF-I levels were elevated in the OVX animals compared with sham, suggesting an involvement of insulin-like growth factor-I (IGF-I) in the observed increase in chondrocyte proliferation (16). No studies had previously been performed in rats before and at the onset of sexual maturation.

Estrogen actions can be exerted through either a genomic (transcription activation) or a nongenomic pathway, which involves putative membrane-bound receptors and activation of the Src/Shc/ERK signal transduction route. Until now, it has been unclear to what extent the two pathways contribute to the regulation of longitudinal growth by E2. Furthermore, specific estrogen receptor modulators (SERMs) have been described which are known for their tissue selectivity. One of the best-studied SERMs is raloxifene, which prevents postmenopausal bone loss but has minor effects on other tissues, like breast and uterus (17).

One example enabling distinction between genomic and nongenomic effects of estrogen is the synthetic compound desoxyestrone (DE), which has less than 1% binding affinity compared with E2 (18) and is believed to act exclusively through the nongenomic pathway. It has anti-apoptotic effects in cultured osteoblasts and osteocytes and is able to increase bone mineral density (BMD) and bone strength in both estrogen-replete and estrogen-deficient mice (19;20).

Turner & Evans have recently described a naturally occurring metabolite of E2, 2-methoxyestradiol (2-MeOE2), which may well act as a SERM in rats. This compound strongly reduced growth plate thickness in 3-month-old intact female rats due to a reduced chondrocytes proliferation and hypertrophy but no effects were observed on various bone parameters, suggesting a tissue-selective effect of 2-MeO-E2 (21).

Recently, we demonstrated both ERs in tibial growth plates of female and male rats well before and during sexual maturation (1, 4 and 7 weeks of age), with no apparent regulation of expression by sexual maturation (12). Since endogenous levels of estrogen are very low before sexual maturation (22;23), we wondered whether the ERs in the growth plate are functional at this stage.

Furthermore, we wanted to know to what extent genomic and nongenomic actions of E2 might contribute to longitudinal growth. To achieve this, 26-day-old rats were either ovariectomized or intact female and male rats of the same age were supplemented with E2 (0.5 mg/21 days), DE or 2-MeO-E2 (both 5 mg/21 days). Three weeks later, halfway to sexual maturation, the effects on longitudinal growth were examined. Moreover, we investigated PCNA and ER α and β and the relative mRNA expression of IGF-I in the growth plate after OVX, using immunohistochemistry and real-time PCR respectively.

Materials and Methods

Animals

Female and male Wistar rats were obtained from Harlan (Broekman Instituut, Someren, The Netherlands). They were kept in a light- and temperature-controlled room (12 h light : 12 h darkness, 20–22 °C) with food and water available *ad libitum*. Experiments were approved by the local ethics committee for animal experiments.

Experiment 1

Twenty-four 26-day-old female Wistar rats were ovariectomized by the dorsal approach ($n=11$) or sham operated ($n=13$). During the experiment, body weight was measured weekly and after 3 weeks the animals were killed using a fatal dose of pentobarbital sodium (Nembutal, Sanofi Sante Animale, Maassluis, Netherlands). Rats enter sexual maturation around day 30, and maturation takes about 4 weeks. This means that at the start of the experiment rats were still sexually immature, whereas at the end of the experiment they were halfway to sexual maturation. Approximately 50% of the animals from each experimental group (OVX: $n=5$; SHAM: $n=6$) were fixed *in vivo* (2% paraformaldehyde in 0.1 M phosphate buffer supplemented with 75 mM lysine monohydrochloride and 10 mM Na periodate) as described previously (24). Tibiae were isolated and fixed in the same fixative for 24 h. Next, they were decalcified in 15% EDTA, including 0.5% paraformaldehyde for 4 weeks and processed for paraffin embedding. Tibiae were cut in halves in a sagittal orientation, processed for paraffin embedding and 5 μm sections were cut mid-sagittally. From the other half ($n=6$), tibiae were collected and the growth plates were carefully excised, avoiding contamination with other cell types. The obtained growth plate material was frozen rapidly and stored at -80 °C until use.

Experiment 2

Twenty-four female and 24 male 26-day-old Wistar rats were implanted with a slow-release pellet (Innovative Research of America, Sarasota, FL, USA) subcutaneously between the scapulae, releasing 0.5 mg of E2 ($n=6$), 5 mg of DE ($n=6$) or 5 mg of 2-MeO-E2 ($n=6$) over a 21-day period. A fourth group received a placebo pellet ($n=6$).

The doses of DE and 2-MeO-E2 were 10 times higher than that for E2, since they have a lower affinity for the receptor (18;25). During the experiment, body weight was measured weekly, and after 3 weeks the animals were killed using a fatal dose of pentobarbital sodium (Nembutal, Sanofi Sante Animale). All animals were fixed *in vivo* and tibiae were processed as mentioned in the first experiment.

Measurements

In both experiments, body weight gain (g), tibial bone length (cm), growth plate width (total, proliferating zone and hypertrophic zone: all in mm), ratio between proliferating and hypertrophic zone width (P/H ratio), the number of chondrocytes and cell diameter (μm) in each zone (except DE and 2-MeO-E2 treated animals), as well as wet weights of thymus (g) were determined. In the second experiment, uterus, testis and liver wet weight (g) were also measured. Values were expressed as means \pm S.D.

PCNA and ER immunohistochemistry

The immunohistochemical protocol performed for both ERs has been published earlier (24). For

the detection of PCNA, growth plate sections were incubated in 10 mM citrate buffer (pH 6.0) at 95 °C for 10 min followed by 30 min of cooling down. After blocking, sections were incubated overnight at 4 °C in 0.5% locking buffer with the mouse monoclonal PCNA antibody (Clone PC-01; Calbiochem, San Diego, CA, USA; 1:5000), the rabbit polyclonal ER α antibody (Clone MC-20; Santa Cruz Technologies, Santa Cruz, CA, USA; 1:50) or the goat polyclonal ER β antibody (Clone Y-19; Santa Cruz; 1:50). After a number of secondary antibody steps, staining was visualized with AEC (0.2 mg/ml in acetate buffer pH 5.2 with 0.04% H₂O₂; Sigma) for 3 min. After counterstaining with hematoxylin, the sections were embedded in aquamount (BDH, Poole, Dorset, UK). Pictures of growth plate sections from rats in two consecutive experiments were taken with a Nikon DXM 1200 digital camera using the same settings and the average number of positive cells in a fixed window was determined using Image-Pro-Plus software (Media Cybernetics Inc., Silver Springs, MD, USA). Next, mean values \pm S.D. were calculated and tested for significance ($P < 0.05$) versus control groups, using the Student *t*-test.

RNA isolation and cDNA synthesis

Total RNA was extracted from growth plate material according to Chomczynski & Sacchi (1987). Subsequently, RNA samples were treated with RNase-free DNase for 15 min at 37 °C to remove residual DNA contamination (Promega, Madison, WI, USA). The concentration of RNA was determined spectrophotometrically.

One microgram of RNA was denatured (10 min at 70 °C followed by 5 min on ice) and reverse transcribed in a 20 μ l reaction containing first strand buffer (75 mM KCl, 3 mM MgCl₂ and 50 mM Tris-HCl, pH 8.3), 5 mM DTT, 0.375 mM dNTPs, 200 ng of random hexanucleotides (all from Life Technologies, Breda, the Netherlands), 1 unit of RNasin (Promega) and 2.5 units of M-MLV reverse transcriptase (Life Technologies) at 37 °C for 60 min and denatured again at 70 °C for 10 min. A second addition of 1 unit of RNasin and 2.5 units of M-MLV reverse transcriptase was performed in each tube and the reaction was allowed to proceed at 37 °C for 30 min followed by inactivation of the enzymes by incubation at 70 °C for 10 min. Samples were diluted and stored until use at -20 °C.

Real-time PCR

Three microliters of cDNA were amplified in a total volume of 25 μ l containing 1* buffer A, 3.5 mM MgCl₂ (Applied Biosystems, Foster City, CA, USA), 0.2 mM dNTPs (Roche, Basel, Switzerland), 50 pmol/ml of the forward and reverse primer (Eurogentec, Seraing, Belgium), 5 pmol/ml probe and 5U/ml AmpliTaq Gold (Applied Biosystems).

The probe sequences for the household gene, rat porphobilinogen deaminase (PBGD; 5'-CCA-GCTGAC- TCT-TCC-GGG-TGC-CCA-C-3') and rat IGF-I (5'-ACA-GGC-TAT-GGC-TCC-AGC-ATTCGG-A-3') were labeled with the reporter dye FAM on the 5' and with the quencher dye TAMRA on the 3' site. The primer sequences for rat PBGD were: forward (5'-ATG-TCC-GGT-AAC-GGC-GGC-3') and reverse (5'-CAA-GGT-TTT-CAG-CAT-CGC-TAC-CA-3'); and for rat IGF-I: forward (5'-TCA-GTT-CGT-GTGTGG- ACC-AAG-3') and reverse (5'-TCA-CAGCTC- CGG-AAG-CAA-C-3'). The amplified products for PBGD and IGF-I were 135 and 117 bp long respectively.

For standardization, both PBGD and IGF-I primer sets were tested with different amounts of cDNA to determine the suitable amount of cDNA to be used in the quantitative analysis. The Taqman reaction included 40 thermal cycles consisting of 15 s at 95 °C and 1 min at 60 °C and was run on an ABI Prism 7700 Sequence Detector (Applied Biosystems). Finally, the Ct value (number of cycles to reach threshold value) was determined for all samples and mean values_S.D. were calculated for each experimental group.

Results

OVX experiment

We performed OVX in 26-day-old female rats and assessed several parameters concerning longitudinal growth 3 weeks later, which are summarized in Table 1.

At the start of the experiment, the rats were still sexually immature and 3 weeks later, they were halfway to sexual maturation. OVX caused significant increases in body weight gain (Fig. 1). When examining longitudinal growth, both tibial length (Fig. 2A) and growth plate width (Fig. 2B) increased significantly compared with sham-operated rats. The wider growth plates in OVX animals were associated with an increased proliferating zone width, while the width of the hypertrophic zone was unaltered. The ratio between the width of the proliferating and the hypertrophic zone (P/H ratio) increased in the OVX animals (Table 1). The increase in the proliferating zone was associated with a significant increase in cell number with a decreased cell diameter compared with sham. Cell number and diameter were unchanged in the hypertrophic zone (Table 1). Representative HE-stained sections (Fig. 2C) from an OVX (b) and sham-operated (a) rat illustrate the results in Fig. 2B. To further address the increased proliferating zone width after OVX, PCNA immunohistochemistry and real-time PCR for IGF-I on cDNA from growth plate preparations were performed. Based on an analysis of two mid-sagittal growth plate sections from the sham ($n=5$) and OVX group ($n=7$), the number of PCNA-positive cells significantly increased after OVX compared with SHAM (Fig. 3A; 266.37 vs 181.49 cells; $P=0.019$). A representative picture of a PCNA-stained growth plate section of a sham-operated and an OVX rat is shown in Fig. 3B (a and b respectively). PCNA immunostaining was primarily found in the proliferating zone, although some positive cells were detected in the hypertrophic zone. Using real-time PCR on cDNAs from dissected growth plates ($n=6$), amounts of cDNA were adjusted for expression of the housekeeping gene PBGD. The difference between the expression levels of IGF-I and PBGD (Ct value) in each rat for the OVX versus SHAM rats did not reach significance (0.62_0.61 vs 0.36_0.79; $P=0.53$), which was underscored by a near identical IGF-I expression level (OVX/SHAM ratio=0.83). Thymus wet weight of OVX rats was significantly increased compared with sham.

Estrogen supplementation experiment

As a mirror experiment, either E2 (0.5 mg/21 days), DE or 2-MeO-E2 (both 5 mg/21 days) was supplemented to 26-day-old female and male rats for 3 weeks ($n=6$). The effects of estrogen supplementation are summarized in Table 1. Compared with placebo rats, administration of E2 via slow-release pellets caused a significant decrease in body weight gain in females and males (Fig. 1). Longitudinal growth was affected by E2, exemplified by a significant decrease in tibial length (Fig. 2A) and growth plate width (Fig. 2B) in both genders. In females, the reduced width of the growth plate was caused by a significant decrease of both the proliferating zone and the hypertrophic zone (Fig. 2B), with an unaltered P/H ratio compared with placebo. In males, however, the reduction of the hypertrophic zone width was more severe than of the proliferating zone, leading to significantly higher P/H ratio compared with controls (Table 1). In both sexes, the decrease in width of the proliferating and hypertrophic zone was associated with a significant decrease in cell number with unchanged cell diameter compared with placebo (Table 1). Representative HE-stained growth plate sections are shown in Fig. 2C (panels c–f). E2 tended to decrease the number of PCNA immunopositive cells in female (Fig. 3A; 40.8 vs 72.5 cells and Fig. 3B; c and d) but not in male (Fig. 3A; 105.2 vs 88.0 cells and Fig. 3B; e and f) rats ($n=6$). In most of the growth plates studied, staining for PCNA seemed to be dominant in pre-hypertrophic and even hypertrophic chondrocytes, especially in the males (Fig. 3B; c–f). Due to large inter-animal

variation in expression levels, the results did not reach significance. Estrogen supplementation decreased thymus wet weight in females and males and increased uterus or decreased testis wet weight respectively. No effect was observed on liver wet weight (Table 1).

Supplementation of DE led to a number of significant effects (Table 1), albeit to a much lesser extent than E2. Body weight gain significantly decreased compared with placebo in both sexes (Fig. 1). Furthermore, in females there was a trend towards significance concerning decrease of tibial length (Fig. 2A). Despite an unaltered total growth plate width, the width of the proliferating zone was significantly reduced leading to a lower P/H ratio compared with placebo. In DE-supplemented males, tibial length was significantly reduced (Fig. 2A), whereas at the level of the growth plate no changes were evident. When 2-MeO-E2 was supplemented, no effects were seen on body weight gain (Fig. 1) and tibia length (Fig. 2A) in females and males. However, at the level of the growth plate, females had a significantly reduced proliferating zone width (Fig. 2B), leading to a reduced P/H ratio (Table 1), whereas in males the significantly reduced total growth plate width seemed to be associated primarily with a decreased width of the hypertrophic zone, which showed a trend towards significance (Fig. 2B). Due to the small changes in growth plate width, we did not determine the number of cells in the different zones in the DE and 2-MeO-E2 supplemented rats. DE and 2-MeO-E2 had no effect on thymus, uterus, testis or liver wet weight compared with placebo controls.

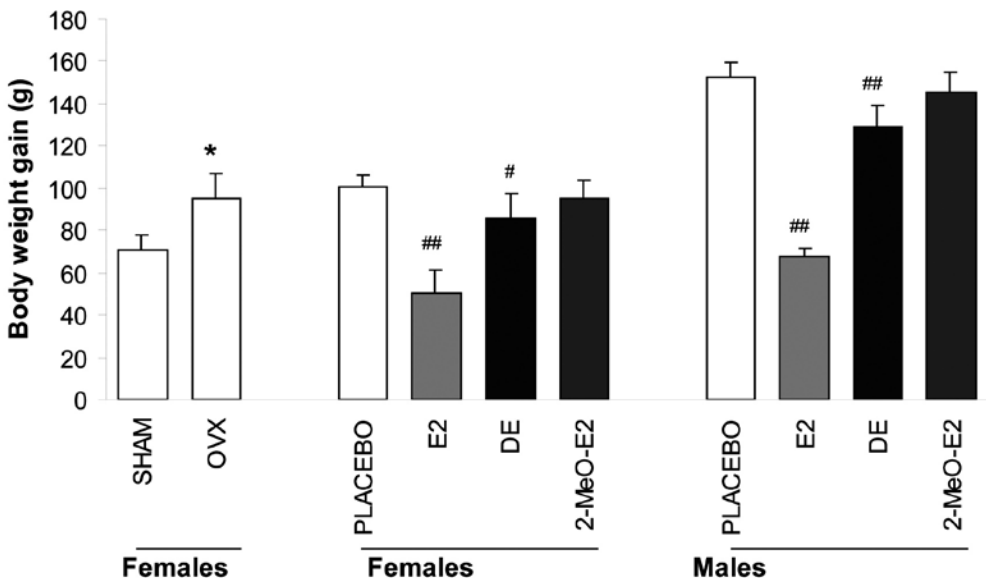


Figure 1

Effects of OVX and estrogen supplementation on body weight gain. Body weight gain was determined 3 weeks after OVX or E2, DE or 2-MeO-E2 supplementation of 26-day-old female and male rats. Values are given as means SD. *P<0.05 compared with sham; #P<0.05 and ##P<0.001 compared with placebo.

Table 1 Effect of OVX or supplementation of E₂, DE or 2-MeO₂ for 3 weeks on parameters of longitudinal growth and other characteristics in 26-day-old rats

Parameter	OVX experiment		E ₂ , DE and 2-MeO ₂ supplementation experiment							
	Females		Females			Males				
	Sham	OVX	Placebo	E ₂	DE	2-MeO-E ₂	Placebo	E ₂	DE	2-MeO-E ₂
Body weight gain (g)	71.0	95.4**	100.4	50.1***	85.8*	94.9	152.8	67.5***	128.6***	145.4
Tibia length (cm)	3.24	3.35***	3.22	3.06***	3.15†	3.23	3.42	3.11***	3.29**	3.41
Total growth plate width (mm)	0.34	0.41**	0.39	0.24***	0.36	0.37	0.50	0.31***	0.48	0.45*
Proliferating zone (P) width (mm)	0.18	0.23**	0.20	0.13***	0.17*	0.16*	0.23	0.15***	0.21	0.20
Hypertrophic zone (H) width (mm)	0.17	0.18	0.19	0.11***	0.20	0.21	0.28	0.16***	0.27	0.25†
P/H ratio	1.04	1.37*	1.08	1.12	0.88*	0.79**	0.82	0.96*	0.80	0.81
Proliferating chondrocyte number	10.47	16.19*	19.72	12.39***	N.D.	N.D.	24.22	14.78***	N.D.	N.D.
Hypertrophic chondrocyte number	6.07	6.56	7.33	4.06***	N.D.	N.D.	9.22	5.61***	N.D.	N.D.
Proliferating chondrocyte diameter (µm)	16.81	13.72*	10.17	10.18	N.D.	N.D.	9.40	10.27	N.D.	N.D.
Hypertrophic chondrocyte diameter (µm)	27.59	28.10	25.54	27.86	N.D.	N.D.	30.42	28.27	N.D.	N.D.
Thymus wet weight (g)	0.51	0.86**	0.61	0.23***	0.56	0.59	0.81	0.33***	0.72	0.83
Uterus/Testis wet weight (g)	N.D.	N.D.	0.16	0.30*	0.18	0.21	0.97	0.45***	0.98	1.01
Liver wet weight (g)	N.D.	N.D.	4.68	4.97	4.88	4.20	4.52	4.47	4.62	4.30

Values are expressed as means. *P<0.05, **P<0.01, ***P<0.001, †trend towards significance (P<0.1) compared with respective control (Student's t-test). N.D. not determined.

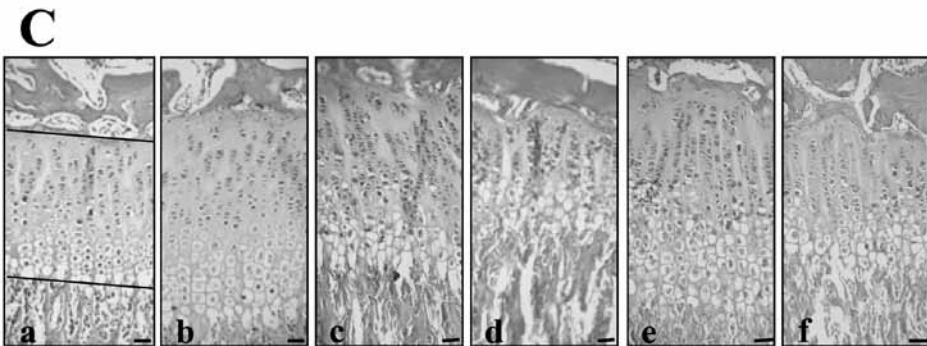
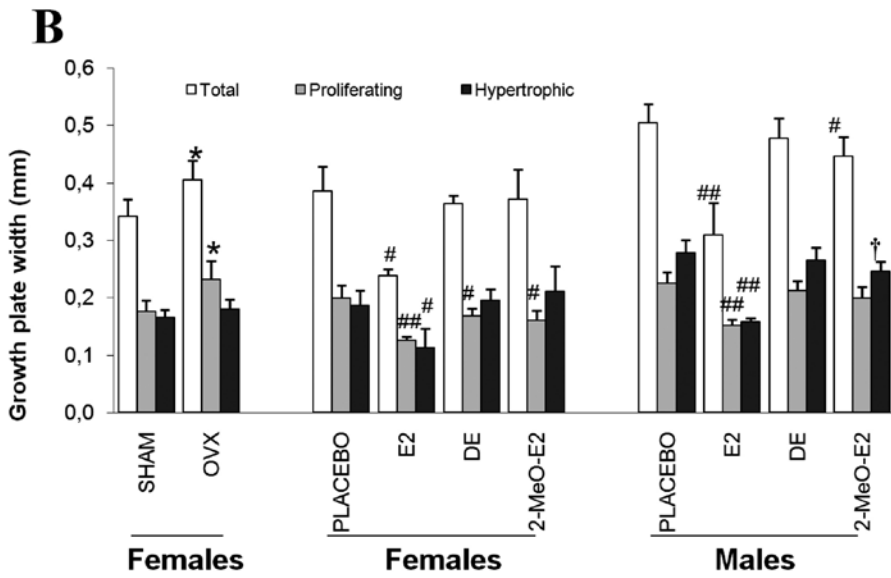
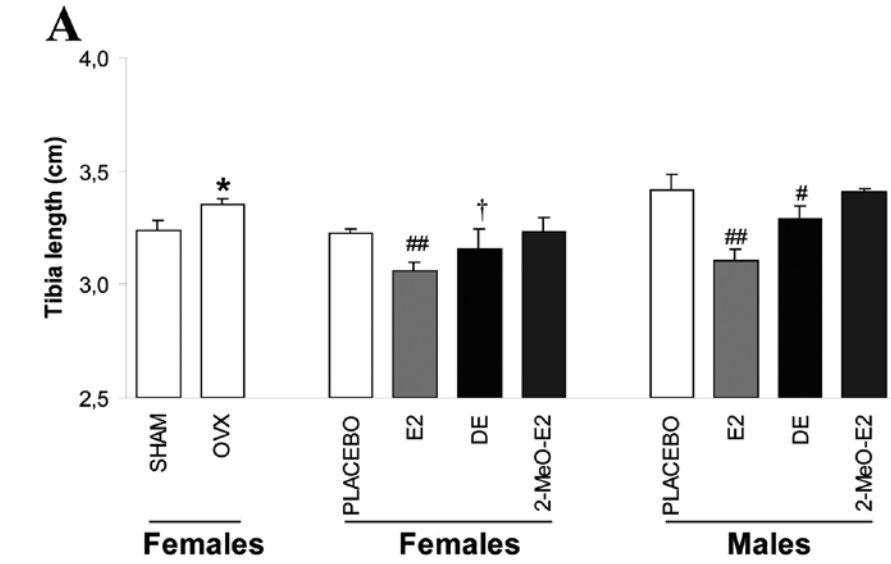


Figure 2 (page 38)

Effects of OVX and estrogen supplementation on tibia length and growth plate width. (A) Tibia length was measured 3 weeks after OVX or E2, DE or 2-MeO-E2 supplementation of 26-day-old female and male rats. (B) Total, proliferating zone and hypertrophic zone widths were determined 3 weeks after OVX or E2, DE or 2-MeO-E2 supplementation of 26-day-old female and male rats. (C) Representative growth plate images of a sham-operated (a) and OVX rat (b) as well as female and male placebo controls (c and e respectively) and E2-supplemented (d and f respectively) rats. The added lines in (a) indicate the borderlines between the growth plate and the epi- and metaphysis and the transition between proliferating and hypertrophic chondrocytes and were used to determine the width of the proliferating and hypertrophic zones. Bars represent 50 μ m. Values are given as means_{SD}. * $P < 0.05$ compared with sham; * $P < 0.05$, ** $P < 0.001$ and † trend towards significance ($P < 0.1$) compared with placebo.

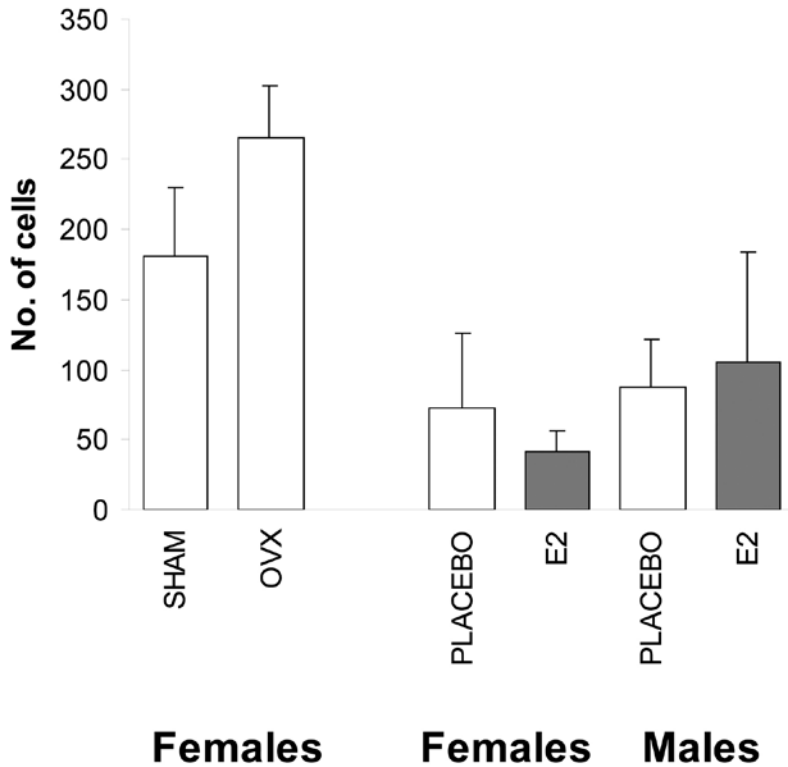


Figure 3

Effects of OVX on PCNA staining in the growth plate. (A) After immunohistochemistry for PCNA, the number of positively stained chondrocytes was determined 3 weeks after OVX of 26-day-old female rats and in E2-supplemented female and male rats by image analysis. Values are given as means_{SD}. * $P < 0.05$ compared with SHAM. (B) Representative growth plate images of a sham-operated (a), OVX rat (b), female placebo (c), female with E2 supplementation (d), male placebo (e) and male with E2 supplementation (f). Note the increased number of immunopositive nuclei in the growth plate of the OVX rat, predominantly in the proliferating zone (b) compared with sham (a). Bars represent 50 μ m.

ER α and β expression in growth plates

Previously, we have demonstrated ER α and β protein expression in the growth plate of the rat (van der Eerden *et al.* 2002). To study whether the expression of the ERs is regulated by OVX or E2, supplementation immunohistochemistry was performed. Positive staining for ER α and β was predominantly detected in late proliferating and early hypertrophic chondrocytes. No differences in staining intensity were seen between the sham (data not shown), placebo (Fig. 4A and D) or OVX rats (Fig. 4B). In contrast, E2 supplementation caused a downregulation of ER α and β staining in growth plates of females and males (Fig. 4C and E respectively). In contrast, E2 supplementation increased ER α and β staining in osteoblastic cells of the primary spongiosum (Fig. 4C and E). Negative controls, including pre-incubation with a corresponding peptide and omission of the first antibody (Fig. 4F), resulted in absence of staining.

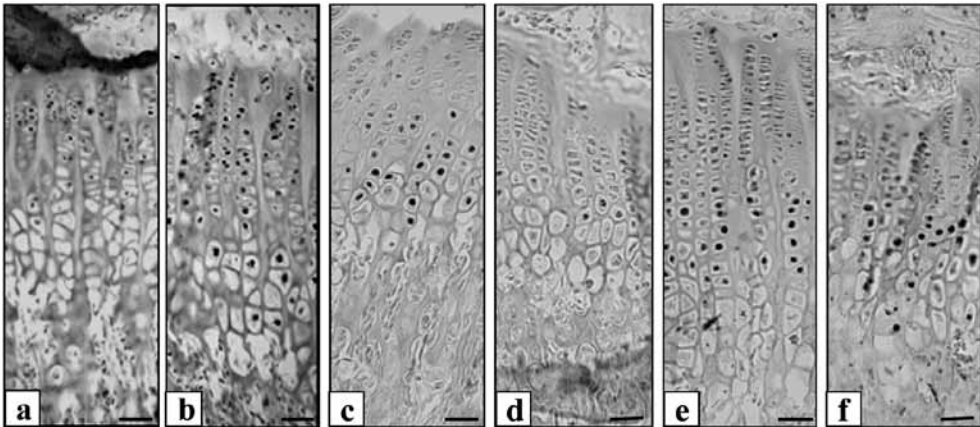


Figure 4

Effects of OVX and E2 supplementation on ER α and β staining in the growth plate. Growth plate sections from the different animal groups were stained for ER α or β . Positive staining was predominantly found in late proliferating (P) and early hypertrophic (H) chondrocytes. No differences in staining intensity were seen between the female placebo (A), OVX (B) or male placebo (D). E2 reduced ER α and β staining in females (C) and males (E) in the growth plate, whereas it increased the expression in osteoblasts of the primary spongiosum (see arrows in C and E). Omission of the first antibody (F) resulted in absence of staining. S, stem cells. Bars represent 50 μ m.

Discussion

We recently found that in female and male rats before sexual maturation (1 and 4 weeks of age), both ER α and ER β were expressed in the tibial growth plate at the mRNA and protein level, implying that this tissue may be responsive to estrogens before sexual maturation (12). To assess this, we either ovariectomized or supplemented female and male rats with E2, DE or 2-MeO-E2 at 26 days of age and analyzed several parameters of longitudinal growth and chondrocyte proliferation 3 weeks later. Rats usually enter sexual maturation around day 30, and maturation takes approximately 4 weeks, implying that rats were still sexually immature at the start of our experiments, while they were halfway to sexual maturation when the experiments were terminated.

OVX of 26-day-old rats caused strong increments in body weight gain, tibia length and growth plate width over a 3-week period compared with sham. The increased growth plate width was explained by a widening of the proliferating zone, which was associated with an increased cell number as well as an increased number of PCNA immunopositive cells. In contrast to OVX, E2 supplementation in female rats of the same age resulted in opposite effects: a dramatically reduced body weight gain, tibial length and growth plate width, the latter being caused by both a reduction in the proliferating zone and hypertrophic zone width. Concomitant with the reduced proliferating zone, E2 tended to decrease the number of PCNA positive chondrocytes as well, although this did not reach significance. In male rats, the parameters of longitudinal growth were similarly decreased compared with females. However, no reduction of PCNA-positive cells was observed.

Turner and co-workers demonstrated increased longitudinal growth rates in ovariectomized 7-week-old sexually maturing rats, whereas subsequent estrogen supplementation reversed this (13). The lowest effective dose of E2 was lower than in our study (1.5 vs 23 $\mu\text{g}/\text{day}$), but these rats were previously ovariectomized (13). Moreover, two reports in which intact 3-month-old female and 2-month-old sexually mature male rats received approximately 200 $\mu\text{g}/\text{day}$ E2, demonstrated a substantial decrease in longitudinal growth (14;15). Our data extend previous data, claiming that as well as in sexually maturing or mature rats, E2 also inhibits longitudinal growth before and at the onset of sexual maturation. OVX of 26-day-old rats results in enhanced parameters of longitudinal growth, despite very low endogenous estrogen levels, suggesting that even in this period, E2 may have an inhibitory effect on growth.

The change in tibial length after OVX or E2 supplementation coincided with changes in growth plate width. Estrogen removal in females caused an increase in proliferating zone width and therefore total growth plate width, whereas estrogen supplementation reduced the width of both the proliferating and hypertrophic zone in both genders. Moreover, the increased width of the proliferating zone after OVX paralleled the increased PCNA staining, whereas E2 supplementation did not significantly alter the number of immunopositive cells in the growth plate. In males, the immunostaining in the hypertrophic zone was quite high, especially in the E2-treated rats, which contributed to an absence of an effect of E2 on PCNA staining compared with placebo. In the E2-supplementation experiment, and to a lesser extent in the OVX experiment, PCNA-positive nuclei were abundantly observed in the pre- and hypertrophic zone. In a study by Aizawa and co-workers, the same phenomenon has been described in rabbit growth plates (26). It appears that subtle changes in the fixation procedure as well as the fact that chondrocytes have a long G1 phase in relation to the S, G2 and M phase contribute to the relatively high number of PCNA-positive hypertrophic chondrocytes (26). In addition, we speculate that E2 may have a sexually dimorphic

effect on the cell cycle G1 phase duration in chondrocytes (27;28). The inhibitory effect of E2 on chondrocyte proliferation is well established. It has been shown that thymidine uptake is reduced following E2 administration in sexually maturing rats and PCNA staining is increased after OVX in sexually immature rabbits (13;16). In the latter study, besides increased PCNA staining, serum IGF-I levels were increased, suggesting that the proliferating effect of OVX was caused in part by serum IGF-I (16). In our study, we did not determine serum levels of IGF-I, since a dramatic decrease of total serum IGF-I did not affect body weight and longitudinal growth in liver-specific IGF-I knockout mice (29). Instead, local effects of IGF-I seemed more important for longitudinal bone growth. Therefore, we quantified the amount of IGF-I mRNA in preparations from tibial growth plates using real-time PCR. We found no difference in relative IGF-I mRNA levels between OVX and sham. This suggests that the effects of E2 status on chondrocyte proliferation cannot be explained by influencing local IGF-I expression. However, we cannot exclude changes in expression levels of other members of the IGF family (IGF-II, IGF-I and II receptors and IGF binding proteins) in the growth plate caused by E2. Removal of E2 has no effect on the width of the hypertrophic zone, whereas E2 administration reduces both proliferating and hypertrophic zone widths. The reduced width of the hypertrophic zone may be a direct effect of E2 itself but it may also be secondary to an effect on chondrocyte proliferation. It was reported that estrogen reduces matrix synthesis, which has been shown to contribute to an age-related decline in longitudinal growth (30). This may be in line with our study, since OVX decreased the cell diameter in the proliferating zone, despite an increase in its width, indicating that matrix synthesis is downregulated when estrogen is deficient. In contrast, it has been shown that E2 stimulates 35S uptake by chondrocytes, implying increased chondrocyte differentiation (31;32). An explanation for a reduced width of the hypertrophic zone could be that estrogen causes the rate of apoptosis or vascular invasion to exceed the rate of cartilage matrix synthesis (21). We recently demonstrated that ER expression levels were relatively unaffected by endogenous estrogen levels (12). In this study, we found that OVX did not affect ER α or ER β expression. However, treatment with a medium dose of E2 caused a reduction in the expression levels of both receptors in male and female rats. From these findings, one may conclude that a substantial rise in endogenous estrogen levels is apparently required to elicit alterations in receptor expression in the rat growth plate. Interestingly, the raised E2 levels increased receptor expression in osteoblasts of the primary spongiosum. This suggests that E2 can either down- or upregulate the expression of its own receptor, depending on the cell type. From our data we cannot exclude effects of E2 on the somatotrophic axis. It has been shown that estrogen augments GH secretion, especially by increasing the secretory pulse mass (4;6). In addition, anti-estrogens lower the basal GH secretion (5). However, direct effects are also likely to occur since the P/H ratio increases strongly following OVX, whereas in dwarf rats (dw/dw), which have reduced GH levels to 5% of normal, the P/H ratio is similar to that in normal rats and this ratio is not affected by subsequent GH treatment (33). These results suggest that E2 inhibits longitudinal bone growth most likely by direct effects on chondrocyte proliferation and differentiation in female and male rats before sexual maturation. Since E2 removal causes such dramatic effects on longitudinal growth, it seems evident that despite its low endogenous levels, E2 may play an important role in controlling longitudinal growth in these animals at this stage.

In analogy with E2 supplementation, we have used the synthetic compound DE, which, based on its lower binding affinity compared with E2, was administered at a

dose 10 times higher than E2 (5 mg/21 days) (18). Despite the fact that supplementation of DE after OVX would result in more pronounced effects, we chose intact rats, since this mimics better the situation when it would be used clinically. DE was recently recognized as an activator of nongenomic estrogen-like signaling (ANGEL) and exhibits anti-apoptotic effects on osteoblasts and osteocytes *in vitro* (19). Moreover, DE increases BMD and bone strength in both estrogen-replete and estrogen-deficient mice (20).

Although to a lesser extent than E2, DE decreased body weight gain in both sexes, tibial length (trend towards significance in females) and growth plate width (not significant in males). In addition, females had a decreased proliferating zone width combined with a reduced P/H ratio. However, despite a 10 times higher dose for DE compared with E2, no effects were found on wet weights of thymus, uterus and testis, whereas E2 severely affected these organs. This suggests that in the classical estrogen target tissues genomic effects are most important, whereas in bone and cartilage genomic and nongenomic pathways mediate the effect of estrogen. These results imply a role for genomic and nongenomic signaling in the regulation of body weight gain, tibia length and growth plate width, although genomic signaling prevails.

In addition to DE, 2-MeO-E2 was administered at a similar dose used for DE, since this naturally occurring metabolite of E2 has a very low binding affinity compared with E2 (25). Our 2-MeO-E2 supplementation experiment was comparable to that by Turner & Evans (21) using intact rats, but there were some differences. The rats in our study were sexually immature at the start of the experiment, whereas the female rats used by Turner & Evans were sexually mature (3 months). Moreover, we used slow-release pellets with a relatively low dose (230 µg/day), establishing relatively constant levels during the experiment, while Turner administered 2-MeO-E2 orally (20 mg/day), not knowing precisely what amount the gastro-intestinal tract absorbs. Furthermore Turner & Evans demonstrated dramatically reduced longitudinal bone growth and growth plate width in the 3-month-old sexually mature intact female rats. Interestingly, no effects were found on radial bone growth and cancellous bone turnover or on uterus wet weight (21). Our results were less pronounced but a significant growth plate width reduction was observed in male rats, which was primarily explained by a reduction of the hypertrophic zone width (trend towards significance). Growth plate width in females did not alter but the proliferating zone width was significantly reduced and, subsequently, the P/H ratio. We found no effects of 2-MeO-E2 on body weight gain, tibial length and wet weights of thymus, uterus/testis or liver. From these results, we may conclude that, although not as pronounced as in an earlier study, effects of 2-MeO-E2 seem to be limited to the regulation of growth plate parameters only, suggesting that it might be used as a SERM in the future.

In conclusion, E2 may exert effects on longitudinal growth before and at the onset of sexual maturation, despite very low serum levels at these stages. There may be a role for nongenomic signaling in body weight gain, tibial length and growth plate width, explaining some of the effects on longitudinal growth, but genomic signaling prevails. DE administration in ovariectomized rats should provide more evidence on the relative contribution of genomic and nongenomic signaling in longitudinal growth.

Acknowledgement and funding

Financial support by Ferring BV, The Netherlands, is gratefully acknowledged.

References

1. **Carani C, Qin K, Simoni M, Faustini-Fustini M, Serpente S, Boyd J, Korach KS, Simpson ER** 1997 Effect of testosterone and estradiol in a man with aromatase deficiency. *N Engl J Med* 337:91-95
2. **Morishima A, Grumbach MM, Simpson ER, Fisher C, Qin K** 1995 Aromatase deficiency in male and female siblings caused by a novel mutation and the physiological role of estrogens. *J Clin Endocrinol Metab* 80:3689-3698
3. **Smith EP, Boyd J, Frank GR, Takahashi H, Cohen RM, Specker B, Williams TC, Lubahn DB, Korach KS** 1994 Estrogen resistance caused by a mutation in the estrogen-receptor gene in a man. *N Engl J Med* 331:1056-1061
4. **Martha PM, Jr., Gorman KM, Blizzard RM, Rogol AD, Veldhuis JD** 1992 Endogenous growth hormone secretion and clearance rates in normal boys, as determined by deconvolution analysis: relationship to age, pubertal status, and body mass. *J Clin Endocrinol Metab* 74:336-344
5. **Metzger DL, Kerrigan JR** 1993 Androgen receptor blockade with flutamide enhances growth hormone secretion in late pubertal males: evidence for independent actions of estrogen and androgen. *J Clin Endocrinol Metab* 76:1147-1152
6. **Veldhuis JD** 1998 Neuroendocrine control of pulsatile growth hormone release in the human: relationship with gender. *Growth Hormone & IGF Research* 8:49-59
7. **Laron Z, Sarel R, Pertzalan A** 1980 Puberty in Laron type dwarfism. *Eur J Pediatr* 134:79-83
8. **Kennedy J, Baris C, Hoyland JA, Selby PL, Freemont AJ, Braidman IP** 1999 Immunofluorescent localization of estrogen receptor-alpha in growth plates of rabbits, but not in rats, at sexual maturity. *Bone* 24:9-16
9. **Kusec V, Viridi AS, Prince R, Triffitt JT** 1998 Localization of estrogen receptor-alpha in human and rabbit skeletal tissues. *J Clin Endocrinol Metab* 83:2421-2428
10. **Nilsson LO, Boman A, Savendahl L, Grigelioniene G, Ohlsson C, Ritzen EM, Wroblewski J** 1999 Demonstration of estrogen receptor-beta immunoreactivity in human growth plate cartilage. *J Clin Endocrinol Metab* 84:370-373
11. **van der Eerden BC, Karperien M, Wit JM** 2001 The estrogen receptor in the growth plate: implications for pubertal growth. *J Pediatr Endocrinol Metab* 14 Suppl 6:1527-1533
12. **van der Eerden BC, Gevers EF, Lowik CW, Karperien M, Wit JM** 2002 Expression of estrogen receptor alpha and beta in the epiphyseal plate of the rat. *Bone* 30:478-485
13. **Turner RT, Evans GL, Wakley GK** 1994 Reduced chondroclast differentiation results in increased cancellous bone volume in estrogen-treated growing rats. *Endocrinology* 134:461-466

14. **Wakley GK, Evans GL, Turner RT** 1997 Short-term effects of high dose estrogen on tibiae of growing male rats. *Calcif Tissue Int* 60:37-42
15. **Tobias JH, Chow J, Colston KW, Chambers TJ** 1991 High concentrations of 17 beta-estradiol stimulate trabecular bone formation in adult female rats. *Endocrinology* 128:408-412
16. **Tajima Y, Yokose S, Kawasaki M, Takuma T** 1998 Ovariectomy causes cell proliferation and matrix synthesis in the growth plate cartilage of the adult rat. *Histochem J* 30:467-472
17. **Cosman F, Lindsay R** 1999 Selective estrogen receptor modulators: clinical spectrum. *Endocr Rev* 20:418-434
18. **VanderKuur JA, Hafner MS, Christman JK, Brooks SC** 1993 Effects of estradiol-17 beta analogues on activation of estrogen response element regulated chloramphenicol acetyltransferase expression. *Biochemistry* 32:7016-7021
19. **Kousteni S, Bellido T, Plotkin LI, O'Brien CA, Bodenner DL, Han L, Han K, DiGregorio GB, Katzenellenbogen JA, Katzenellenbogen BS, Roberson PK, Weinstein RS, Jilka RL, Manolagas SC** 2001 Nongenotropic, sex-nonspecific signaling through the estrogen or androgen receptors: dissociation from transcriptional activity. *Cell* 104:719-730
20. **Manolagas SC, Weinstein RS, Bellido T, Bodenner DL, Jilka RL, Parfitt AM** 1999 Activators of non-genomic estrogen-like signalling (ANGELS): A novel class of small molecules with bone anabolic properties. *Journal of Bone and Mineral Research* 14:S180
21. **Turner RT, Evans GL** 2000 2-Methoxyestradiol inhibits longitudinal bone growth in normal female rats. *Calcif Tissue Int* 66:465-469
22. **Dohler KD, Wuttke W** 1976 Circadian fluctuations of serum hormone levels in prepubertal male and female rats. *Acta Endocrinol (Copenh)* 83:269-279
23. **Saksena SK, Lau IF** 1979 Variations in serum androgens, estrogens, progestins, gonadotropins and prolactin levels in male rats from prepubertal to advanced age. *Exp Aging Res* 5:179-194
24. **van der Eerden BC, Karperien M, Gevers EF, Lowik CW, Wit JM** 2000 Expression of Indian hedgehog, parathyroid hormone-related protein, and their receptors in the postnatal growth plate of the rat: evidence for a locally acting growth restraining feedback loop after birth. *J Bone Miner Res* 15:1045-1055
25. **Merriam GR, MacLusky NJ, Picard MK, Naftolin F** 1980 Comparative properties of the catechol estrogens, I: methylation by catechol-O-methyltransferase and binding to cytosol estrogen receptors. *Steroids* 36:1-11
26. **Aizawa T, Kokubun S, Tanaka Y** 1997 Apoptosis and proliferation of growth plate chondrocytes in rabbits. *J Bone Joint Surg Br* 79:483-486

27. **Leung BS, Potter AH** 1987 Mode of estrogen action on cell proliferation in CAMA-1 cells: II. Sensitivity of G1 phase population. *J Cell Biochem* 34:213-225
28. **Takahashi MM, Noumura T** 1987 Sexually dimorphic and laterally asymmetric development of the embryonic duck syrinx: effect of estrogen on in vitro cell proliferation and chondrogenesis. *Dev Biol* 121:417-422
29. **Yakar S, Liu JL, Stannard B, Butler A, Accili D, Sauer B, LeRoith D** 1999 Normal growth and development in the absence of hepatic insulin-like growth factor I. *Proc Natl Acad Sci U S A* 96:7324-7329
30. **Hunziker EB** 1988 Growth plate structure and function. *Pathol Immunopathol Res* 7:9-13
31. **Blanchard O, Tsagris L, Rappaport R, Duval-Beaupere G, Corvol M** 1991 Age-dependent responsiveness of rabbit and human cartilage cells to sex steroids in vitro. *J Steroid Biochem Mol Biol* 40:711-716
32. **Corvol MT, Carrascosa A, Tsagris L, Blanchard O, Rappaport R** 1987 Evidence for a direct in vitro action of sex steroids on rabbit cartilage cells during skeletal growth: influence of age and sex. *Endocrinology* 120:1422-1429
33. **Gevers EF, Milne J, Robinson IC, Loveridge N** 1996 Single cell enzyme activity and proliferation in the growth plate: effects of growth hormone. *J Bone Miner Res* 11:1103-1111

3

Expression of vascular endothelial growth factor (VEGF) in the growth plate is stimulated by estradiol and increases during pubertal development

Joyce Emons¹, Andrei S. Chagin², Torun Malmlöf², Magnus Lekman², Åsa Tivesten³, Claes Ohlsson³, Jan M. Wit¹, Marcel Karperien^{4,5}, Lars Sävendahl²

J Endocrinol. 2010 Jan 29. PubMed PMID: 20093283

¹Dept of Paediatrics, Leiden University Medical Center, 2300 ZA Leiden, the Netherlands;

²Dept of Women's and Children's Health, Karolinska Institutet, SE-171 76 Stockholm, Sweden;

³Division of Endocrinology, Department of Internal Medicine, Sahlgrenska University Hospital, Gothenburg, Sweden;

⁴Dept of Tissue Regeneration, University of Twente, 7522 NB Enschede, the Netherlands;

⁵Dept of Endocrinology and Metabolism, Leiden University Medical Center, 2300 ZA Leiden, The Netherlands.

Abstract

Longitudinal bone growth is regulated in the growth plate. At the end of puberty, growth velocity diminishes and eventually ceases with fusion of the growth plate through mechanisms not yet completely understood. Vascular Endothelial Growth Factor (VEGF) has an important role in angiogenesis, but also in chondrocyte differentiation, survival and the final stages of endochondral ossification. Estrogen has been shown to up-regulate VEGF expression in the uterus and bone of rats. In this study we investigated the relation between estrogen and VEGF production in growth plate chondrocytes both in vivo and in vitro. The expression of VEGF protein was down-regulated upon ovariectomy and restored upon estradiol supplementation in rat growth plates. In cultured rat chondrocyte cell line RCJ3.1C5.18 estradiol dose-dependently stimulated 121 kDa and 189 kDa isoforms of VEGF but not the 164 kDa isoform. Finally, VEGF expression was observed at both protein and mRNA level in human growth plate specimens. The protein level increased during pubertal development supporting a link between estrogens and local VEGF production in the growth plate. We conclude that estrogens regulate VEGF expression in the epiphyseal growth plate although the precise role of VEGF in estrogen-mediated growth plate fusion remains to be clarified.

Introduction

Longitudinal growth occurs at the epiphyseal plate, a thin layer of cartilage entrapped between epiphyseal and metaphyseal bone, at the distal ends of the long bones (1). In the growth plate, immature cells lie toward the epiphysis, called the resting zone, with flat more mature chondrocytes in the proliferating zone and large chondrocytes in the hypertrophic zone adjacent to this. At the end of puberty longitudinal growth ceases with total replacement of avascular cartilage by highly vascularized bone eventually resulting in epiphyseal fusion. Estrogen is known to be an important hormone in the regulation of growth plate maturation and epiphyseal fusion; it regulates and can accelerate the programmed senescence of the growth plate, leading to proliferative exhaustion of chondrocytes and epiphyseal fusion (2;3). At a low concentration, estrogen is known to increase growth velocity, an effect possibly mediated through the GH-IGF-1 axis, while at a high concentration estrogen inhibits growth and promotes epiphyseal fusion in the long bones (4-6).

A critical step in endochondral ossification is when blood vessels enter from the primary spongiosum and osteoblasts invade from the bone marrow to lay down trabecular bone (7;8). Vascular Endothelial Growth Factor (VEGF) is a potent mediator of angiogenesis but has also been shown to modulate chondrocyte differentiation and survival, osteoblast differentiation and osteoclasts recruitment (9-11). VEGF is expressed by growth plate chondrocytes and osteoblasts in different species including the human (12-15). Human VEGF is present in 6 different proteins, VEGF-A, -B, -C, -D, -E and -F, where VEGF-A has been shown to be expressed in the growth plate and also believed to be most important in the regulation of longitudinal bone growth. VEGFA has six alternatively spliced isoforms: VEGF121, VEGF145, VEGF165, VEGF183, VEGF189, and VEGF206 (16). The receptors involved in VEGF-A signalling are VEGFR-1 (also fms-like tyrosine kinase receptor 1) and VEGFR-2 (also kinase insert domain-containing receptor, KDR) with almost all responses being mediated through the second receptor which has also been detected at the chondro-osseous junction in the mouse growth plate (11;14;17). Inactivating VEGF in mice and monkeys resulted in impaired trabecular bone formation and expansion of the hypertrophic zone indicating inhibition of cartilage resorption (14;18). In addition, Vegfa conditional knockout

mice driven by a col2a1 promotor showed delayed invasion of blood vessels into the primary ossification center and delayed removal of terminal hypertrophic chondrocytes together with massive cell death in chondrocytes throughout the growth plate demonstrating the importance of VEGFA for chondrocyte survival (9). In vitro VEGF expression can be up-regulated by factors known to be important in the regulation of longitudinal bone growth like FGF, TGF-beta and IGF-1 (13). Rat studies showed that in uterus and bone tissue, VEGF expression is upregulated by estrogen (19;20). In humans, bone growth and estrogen levels increase in parallel during earlier phases of puberty while at the end of puberty growth ceases with a total replacement of cartilage by bone resulting in fusion of the growth plate.

We hypothesized that estrogens have the capacity to stimulate local VEGF production in growth plate chondrocytes and that this could be a possible mechanism involved in the process of growth plate maturation and fusion in humans. To address this, we performed in vivo studies in ovariectomized rats supplemented with estradiol and also in vitro studies in cultured rat chondrocytes exposed to estradiol and assessed chondrocyte specific expression of VEGF. In addition, we measured VEGF expression in growth plate specimens obtained from humans in different pubertal stages.

Material and Methods

Animals and study protocol

Female Sprague-Dawley rats were purchased from Scanbur BK AB (Sollentuna, Sweden). The animals were housed in a temperature- and humidity-controlled room with a 6:00 a.m. to 6:00 p.m. light cycle and allowed a soy-free diet containing 0.7% of calcium and 0.5% of phosphorus (R70; Lactamin AB, Kimstad, Sweden) and tap water ad libitum. All procedures were approved by the ethics committee at Göteborg University and conformed to the National Institutes of Health Guide for the Care and Use of Laboratory Animals. The animals were randomly divided into three groups: sham operation + vehicle treatment (sham, n = 12), OVX + vehicle treatment (OVX, n = 10) and OVX + 17 β -estradiol treatment (E2, n = 11). At 12 weeks of age (body weight, 251 \pm 2 g), the rats were either sham-operated or OVX under isoflurane anesthesia (Baxter Medical AB, Kista, Sweden), and small silastic implants were placed subcutaneously in the cervical region. The silastic implants were prepared as previously described, releasing 2.5 μ g/day of E2 (21). Vehicle-treated animals received an empty implant. 17 β -estradiol was obtained from Sigma Chemical. After 6 weeks of treatment, the animals were killed by excision of the heart under isoflurane anesthesia, and the right proximal tibia was fixed in 4% paraformaldehyde, decalcified, and embedded in paraffin. Uterus size, correlating with estrogen levels, was smaller in the ovariectomized rats and slightly larger in the estrogen-supplemented animals compared to sham indicating supra-physiological levels of estrogen in the estrogen treated group. Study details were previously described (22;23).

Patients and tissue preparation

Human proximal and distal femur growth plate tissues were collected from 12 girls at different pubertal stages who were undergoing surgery for different medical indications (Table 1). One fetal sample was collected from a female donor of 23 weeks gestational age. The study protocol was approved by the Local Medical Ethics Committees of the Leiden University Center, Leiden, the Netherlands and the Karolinska University Hospital, Stockholm, Sweden. Informed consent was obtained from all patients and their parents. Epiphyseal samples were either directly frozen in liquid isopentane and stored at -80°C or fixed in 10% formalin, decalcified and embedded in paraffin. All tissue samples were processed in the same way.

Immunohistochemistry

All tissues were cut in 5 μm sections and mounted on histological glass slides (Superfrost plus), dried at 37°C overnight and heated at 60°C for 1 hour before immunohistochemical treatment. Immunohistochemistry was performed as previously described (24) with the modification that antigen retrieval was achieved by incubating with 0.1% trypsin (Invitrogen) for 10 minutes at 37°C. Anti-VEGF antibody was obtained from Santa Cruz Inc. (Santa Cruz Biotechnology, Inc., Santa Cruz, CA, USA) and used in a 1:200 dilution for rat tissues and 1:50 dilution for human tissues. Secondary anti-rabbit biotinylated antibody (Jackson Immunoresearch lab, West Grove, PA, USA) was used in a 1:1000 dilution, followed by incubation with avidin-biotin Vectastain ABC reagent according to manufactures instructions (Vector laboratories, Burlingame, California, USA). Digital images were collected employing a Nikon Eclipse E800 microscope equipped with an Olympus DP70 digital camera.

Image analysis

Images of the central two thirds of the rat growth plates were captured in three visual fields. All pictures were taken in a 200X magnification with a 2040x1536 resolution and further analyzed in Image Pro Plus 5.0® software. Pictures were converted into grey scale-8 mode and inverted in order to obtain correct optical density (OD) values in immuno-positive areas. An automatic bright objects counting was performed to identify the number of immuno-positive objects above the defined thresholds. Threshold level for cell size was defined as objects with an area over 12 μm^2 and 20 μm^2 in the proliferative and hypertrophic zone respectively. The total optical density of the immuno-positive objects was calculated automatically, a function referred as Density sum in the Image Pro Plus software. The analyzed areas were measured in mm^2 and results are expressed as number of positive cells/ mm^2 , protein expression (OD arbitrary unit)/ mm^2 and protein expression (OD arbitrary unit)/per cell. Data are presented as mean +/- SEM.

RNA isolation

Bone was removed from all epiphyseal samples and 40 μm thick sections were cut with a cryostat. Every fifth section was followed by a 5 μm thick section which was studied with Haematoxylin staining to ensure lack of bone contamination. Total RNA isolation was performed with an optimized method for RNA extraction from cartilage as described by Heinrichs et al. (25) except that the protocol was started by homogenizing the sections in 1 ml guanidine thiocyanate solution. RNA samples from bladder and prostate tissue was obtained from Gentaur molecular products (Gentaur molecular products, Brussel, Belgium). RNA extraction was followed by purification with a RNeasy kit according to the manufacturers protocol (Qiagen) and quality and integrity of each sample were checked with the Agilent 2100 Bioanalyzer.

Real-Time RT-PCR (qPCR)

RNA was reverse transcribed into cDNA using a First Strand cDNA Synthesis kit for qPCR (Roche Diagnostics GmbH, Mannheim, Germany) according to the manufacturer's instructions. Expression of VEGFA and VEGFR-2 (KDR) mRNA was quantified by real-time PCR using the Bio-Rad iCycler with SYBR Green. QuantiTect Primer Assays were purchased from Qiagen (Qiagen Benelux B.V., Venlo, the Netherlands) and used according to the manufacturer's protocol. Threshold cycles were estimated and averaged for the triplicates. Relative amounts of mRNA were normalized to β 2-microglobulin expression in the same sample to account for variability in the initial concentration and quality of total RNA and in the efficiency of the reverse transcription reaction.

Western Blotting

Nontransformed clonal rat chondrogenic cells RCJ3.1C5.18 (C5.18 cells) were differentiated for 10 days (26) and subsequently treated 24 hours with a dose-range of 17β -estradiol. Cells were lysated and the protein concentration was measured by the Bradford protein assay (Bio-Rad Laboratories AB, Sundbyberg, Sweden). Proteins were separated on acrylamide gels (Bio-Rad Laboratories) and transferred to PVDF membrane. Three different isoforms of VEGFA were detected employing anti-VEGF rabbit Ab (1:1500; sc-152, Santa Cruz Biotechnology Inc., Santa Cruz, CA). Secondary goat anti-rabbit antibody was peroxidase labelled and used in a 1:10000 dilution (Santa Cruz Biotechnology Inc., Santa Cruz, CA). The resulting bands were confirmed by comparing the size of the protein in the cell extract with known molecular weight markers. The antigen-antibody complexes were then detected by chemiluminescence. After films had been developed, blots were stained with Coomassie Blue to ensure equal loading of total protein. Density measurements were normalized per density of Coomassie blue staining (27). Each experiment was repeated at least three times.

Statistics

The human sections were blinded and a relative staining intensity was scored (score 0 to 3) for the proliferative and hypertrophic zone of each growth plate. Scores were displayed in a scatterplot and a linear regression analyses was performed to calculate significance. The same was done for the qPCR results.

For the rat data, 6 growth plate sections for every animal were analysed by Image analysis protocol described above and means were calculated in terms of VEGF positive cells/ μm^2 and VEGF expression (OD arbitrary unit)/per cell for each animal. Significance was calculated by one way ANOVA followed by Fisher's protected least significance difference test.

Results

VEGF protein expression in the rat growth plate

Sham-operated rats were used as an internal control confirming abundant VEGF expression in the growth plates, both in the proliferative and hypertrophic zone (figure 1A). Pre-incubation of the primary antibody with recombinant VEGF abolished the staining in both proliferative and hypertrophic chondrocytes (figure 1C). Staining was analysed by a computerized method for the proliferative and hypertrophic zone (see Methods section).

To reveal any possible regulation of VEGF expression by estrogens we analyzed the number of VEGF-expressing chondrocytes in rats upon ovariectomy and 17 β -estradiol supplementation. Ovariectomy resulted in a significant decrease in the number of VEGF positive cells in the proliferative zone (1173 \pm 93 vs. 1556 \pm 100 cells/mm² in sham-operated animals; $p < 0.01$), an effect completely restored by 17 β -estradiol replacement (1713 \pm 81 vs. 1173 \pm 93 cells/mm² in vehicle alone; $p < 0.001$; figure 2A). A similar trend was observed in hypertrophic chondrocytes, albeit not statistically significant (figure 2C). The level of VEGF per cell (expressed as OD arbitrary units/cell) did not differ significantly between the groups in the proliferative zone (figure 2B). However, in the hypertrophic zone ovariectomy resulted in a significant decrease in the level of VEGF per cell (35747 \pm 1989 vs. 43240 \pm 1900 in sham-operated animals; $p < 0.01$), an effect which was not restored by estradiol supplementation (36601 \pm 1615 vs. 35747 \pm 1989 in vehicle alone; $p = 0.74$; figure 2D).

VEGFA isoform expression in cultured chondrocytes

In order to distinguish between direct and systemic effects of estrogen on VEGF expression we performed experiments in the rat chondrogenic cell line RCJ3.1C5.18 (C5.18 cells) which can be differentiated into hypertrophic chondrocytes (26). The cells were differentiated for 10 days and then treated with 17 β -estradiol for 24 hours. Estradiol dose-dependently stimulated expression of VEGF-121 and VEGF-189 while VEGF-164 expression was not affected (figure 3). VEGF-189 was suppressed by low estradiol concentrations and increased by high concentrations.

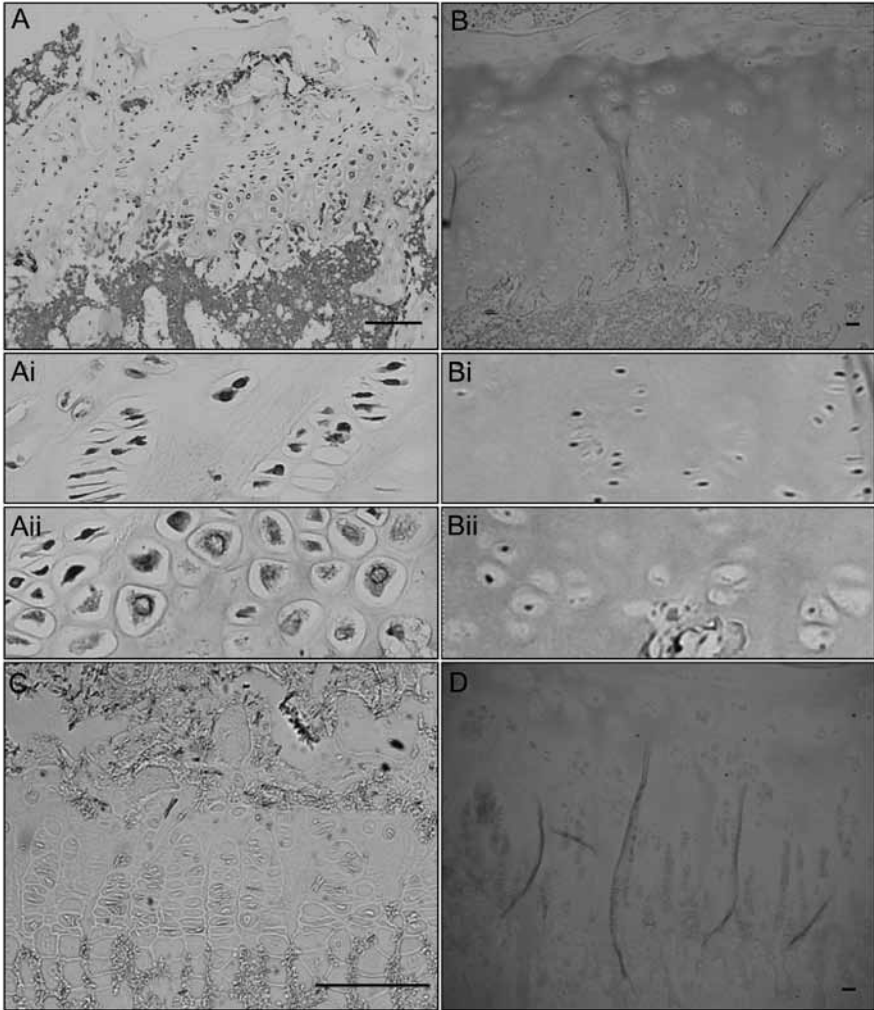


Figure 1. VEGF immunohistochemistry staining.

VEGF protein expression was detected in the rat growth plate (panel A, 100x magnification) and the human pubertal growth plate (panel B, 100x magnification). Panel Ai and Bi show 5x enlargements of the proliferative zone in panel A and B. Panel Aii and Bii show 5x enlargements of the hypertrophic zone in panel A and B. Pre-incubation of the primary antibody with recombinant VEGF abolished the staining in both proliferative and hypertrophic chondrocytes (panel C, 400x). Panel D shows a negative control for the human growth plates. Bars indicate 100 μm .

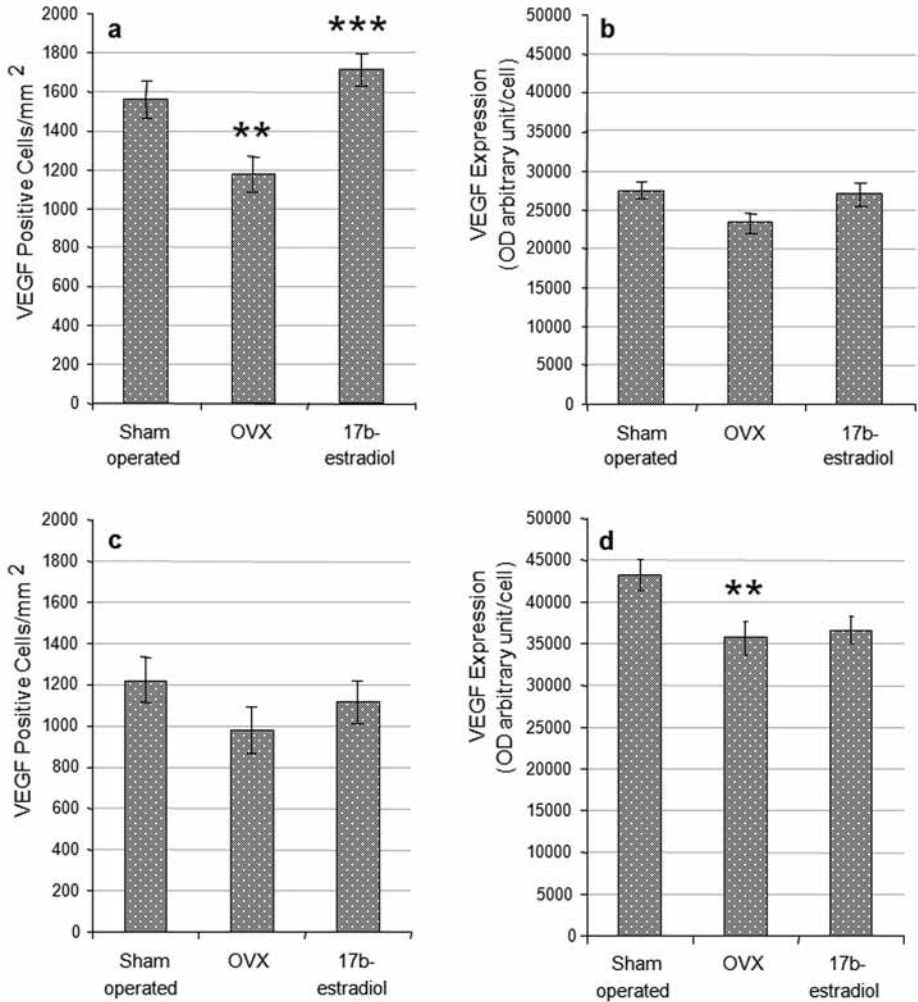
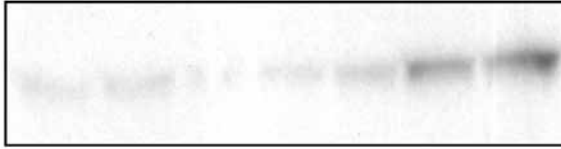


Figure 2. Quantification of VEGF staining in the proliferative and hypertrophic zone.

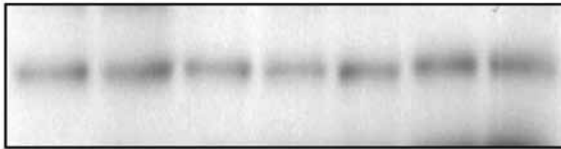
VEGF staining was quantified with a computerized method for the proliferative zone. Panel a. shows a significant decrease in the amount of positive cells/mm² growth plate after ovariectomy which was completely restored by 17 β -estradiol. Staining intensity per cells (OD arbitrary unit/cell), showed no difference between all groups (panel b.). The hypertrophic zone shows the same trend as the proliferative zone, there were however no statistically significant differences (panel c.). Staining intensity per cells (OD arbitrary unit/cell) showed a significant decrease after ovariectomy in the hypertrophic zone, but no restoration with estrogen supplementation (panel d.). Data are presented as mean \pm SEM. * $p < 0.05$, ** $p < 0.01$, *** $p < 0.001$.

a.

VEGF 189



VEGF 164



VEGF 121



Control 1 pM 10 pM 100 pM 1 nM 10 nM 100 nM

b.

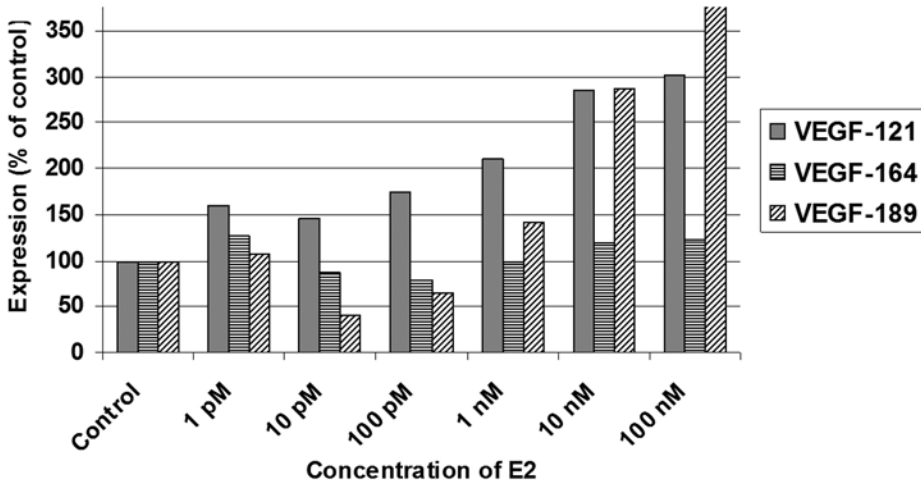


Figure 3. VEGFA isoform Western blot analysis in chondrocyte culture

Panel a illustrates that 17β -estradiol directly stimulated expression of isoforms VEGF 189, VEGF 164, and VEGF 121. The isoforms VEGF-121 and VEGF-189 showed a very strong response, VEGF-164 in contrast just a marginal response. In panel b, the expression levels are calculated as a percentage of the VEGF expression in non-treated control.

VEGF protein and mRNA expressions in human growth plates

Growth plate biopsies were obtained from girls at different stages of pubertal development. To verify how VEGF is distributed in the human pubertal growth plate, we analyzed VEGF expression levels in these rare tissue samples. Out of 13 collected growth plates we analyzed 6 human growth plates for VEGF protein expression and 9 for VEGF mRNA expression (see table 1). In all these human growth plates VEGF protein was detected in both proliferative and hypertrophic zone chondrocytes (figure 1B). When the relative staining intensity was scored (score 0 to 3), a significant increase in VEGF expression with progression of puberty was found in both the proliferative ($p=0.022$) and hypertrophic zone ($p=0.017$) (figure 4 panel a and b). Negative controls showed no staining (data not shown).

Studies of mRNA levels with qPCR confirmed VEGF expression in pubertal as well as fetal human growth plates albeit expression of VEGF mRNA in the prepubertal growth plate was approximately 200 fold lower compared to the expression in prostate and bladder tissue (positive controls). The threshold cycles for VEGF expression were subtracted from the $\beta 2$ -microglobulin threshold cycles in order to calculate the delta Ct (ΔCt). Average values for the different groups were calculated and compared to the prepubertal growth plate. The fetal growth plate showed a 4.2 fold higher expression of VEGF compared to the prepubertal growth plate. The pubertal growth plate samples ($n=6$) showed on average a 1.6-fold higher expression of VEGF mRNA compared to the prepubertal growth plate ($n=2$) but in contrast to VEGF protein expression, we did not find a significant correlation between VEGF mRNA levels assessed by qPCR and the stage of pubertal development ($p=0.183$, $R=0.238$). The VEGF receptor, VEGFR-2, was also expressed at mRNA level in all our growth plate samples analyzed. Similarly to VEGF, the average VEGFR-2 mRNA level was 1.6-fold higher in pubertal girls ($n=6$) compared to prepubertal ($n=2$), but there was no statistically significant correlation with pubertal progression ($p=0.585$, $R=0.045$) likely due to high variation between samples and low number of patients.

Patient	Diagnosis	Bone	age (yr)	Puberty	Experiment
1	leg length difference	distal femur	9	B1-2	IHC
2	hip luxations, femur head resection	proximal femur	12	B2	qPCR, IHC
3	leg length difference	distal femur	12	B2	IHC
4	leg length difference	distal femur	14	B2-3	IHC
5	hip luxations, femur head resection	proximal femur	13	B3	qPCR, IHC
6	cerebral palsy, femur head resection	proximal femur	15	B4	IHC
7	osteosarcoma in tibia	distal femur	8	B1	qPCR
8	Upper limb amputation of the leg	distal femur	9	B1	qPCR
9	tall stature	distal femur	10	B2	qPCR
10	tall stature	distal femur	12	B3	qPCR
11	tall stature	distal femur	15	B4	qPCR
12	hip luxations, femur head resection	proximal femur	14	B4	qPCR
13	fetal, selective abortion	distal femur	23 weeks	Fetal	qPCR

Table 1. Patients information and human tissues

Table showing diagnosis of each patient, location of growth plate, age given in years, Tanner pubertal breast stage (B1-B5) and experiment in which growth plate sample is used (IHC and/or qPCR). IHC indicates immunohistochemistry.

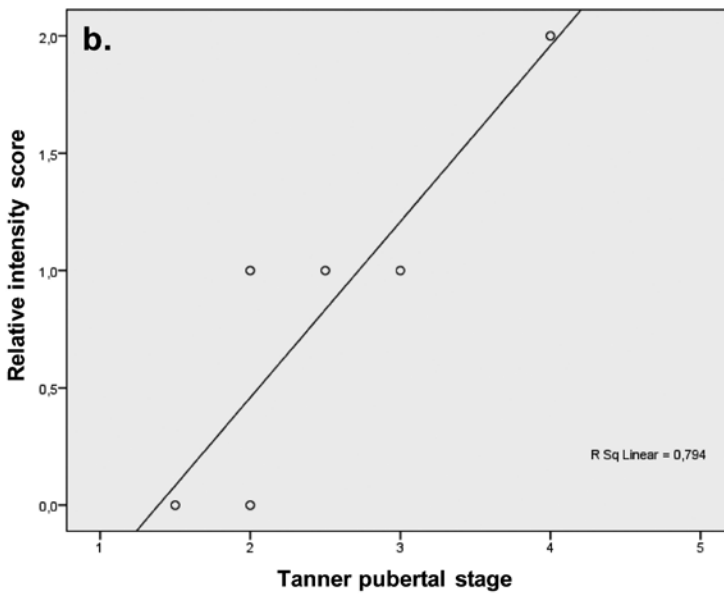
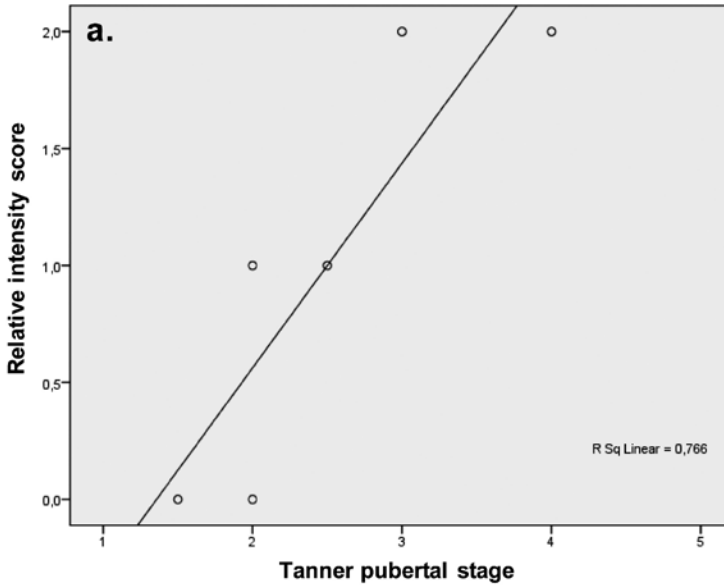


Figure 4. Scatterplot of VEGF expression in the human growth plate

Relative intensity of VEGF protein expression was scored for each growth plate and plotted in relation to the pubertal stage for the proliferative zone (panel a.) and the hypertrophic zone (panel b.). R square values were respectively 0.766 ($p=0.022$) for the proliferative zone and 0.794 ($p=0.017$) for the hypertrophic zone.

Discussion

Our *in vivo* and *in vitro* data demonstrate that estradiol directly stimulates the expression of VEGF in rat growth plate chondrocytes. Furthermore, we confirmed that VEGF is expressed in the human pubertal growth plate and that the VEGF protein level increases with pubertal progression supporting a link between estrogens and local VEGF production in the growth plate.

VEGF was previously detected mostly in hypertrophic chondrocytes of human growth plate samples by immunohistochemistry (15). We observed VEGF expression not only in the hypertrophic zone, but also in the proliferative zone, which is in line with the observations of Horner et al who studied VEGF protein expression in neonatal human growth plate cartilage (Horner 1999 J. Anat). VEGF mRNA was also detected in the proliferative zone of murine growth plate cartilage (Cramer and Pfander 2004). VEGF expression in proliferating chondrocytes and the significant change in expression with alternating estrogen levels were observed in both human and rat growth plates in our study. This slight divergence in results could be due to technical issues attributed to immunohistochemistry such as antigen retrieval or type of antibody.

We confirmed our immunohistochemistry data by Q-PCR analysis. mRNA expression of VEGF and the VEGFR-2 receptor was, to our knowledge for the first time, detected in adolescent and pubertal human growth plates. VEGF mRNA was previously detected in the fetal growth plate by others (Petersen 2002 and Garcia-Ramirez 2000). Expression of VEGFR-2 was earlier detected at the chondro-osseous junction in mice (14), in epiphyseal cartilage of pigs (28), in the avian growth plate (29) and in hypertrophic chondrocytes of the fetal growth plate (30). In contrast to protein levels, mRNA did not reveal a significant increase in VEGF expression with progression of puberty. This discrepancy in results could be due to a difference between mRNA and protein expression, a difference in tissue preparation for RNA extraction when the surrounding bone was removed or alternatively due to a change in morphological organization of the growth plate during progression of puberty (e.g a decreased hypertrophic layer).

This is the first report demonstrating a link between estrogens and VEGF expression in the epiphyseal growth plate. *In vivo* treatment of rats with 17 β -estradiol increased the number of growth plate chondrocytes expressing VEGF. In line with this, in the hypertrophic zone of ovariectomized animals the number of VEGF positive cells/mm² growth plate was decreased. In addition, *in vitro* data in a rat chondrocytic cell line showed a dose-dependent stimulatory effect of estradiol on the expression of VEGF-121 isoform. VEGF-189 was suppressed by low estradiol concentrations and stimulated by higher concentrations. This might counterbalance the slight concomitant increase of VEGF 121 thereby protecting the growth plate when exposed to low concentrations of estradiol. Our growth plate findings are in line with previous reported effects of estrogens on VEGF expression in bone, uterus and breast cancer tissues (20;31;32).

Systemic estrogen levels increase with puberty eventually resulting in epiphyseal fusion by the end of puberty (33), presumably due to acceleration of growth plate senescence through proliferative exhaustion of chondrocytes (3). From our results obtained in the rat we hypothesized that estrogen not only accelerates senescence of the growth plate, but also stimulates chondrocytes to secrete VEGF which might contribute to the process of epiphyseal fusion. VEGF protein was detected in human pubertal growth plates and indeed, the expression level significantly increased during pubertal progression. This observation in humans supports our findings in rats and strengthens our hypothesis that estrogens stimulate VEGF expression in the growth plate.

A 200 fold lower VEGF mRNA level in the growth plate was observed compared to the prostate or bladder tissues. We believe that observed stimulation of VEGF expression by estrogens in avascular growth plate chondrocytes can substantially affect the growth plate. Indeed, VEGF

has an important role in chondrocyte differentiation, chondrocyte survival and endochondral ossification (9-11). Inhibition of VEGF showed in several studies dramatic effects on the growth plate, like expansion of the hypertrophic zone and delayed removal of terminal hypertrophic chondrocytes (9;14). Conversely, one might speculate that an increase in expression leads to a smaller hypertrophic zone, a more rapid removal of terminal hypertrophic chondrocytes and eventually epiphyseal fusion. Reports on an increase in VEGF expression has to our knowledge not been published before.

Estrogen levels were higher in the estrogen-supplemented rats compared to the sham-operated rats. Uterus size, correlating with estrogen levels, was small in ovariectomized rats compared to sham-operated animals and slightly larger in the estrogen-supplemented animals indicating supra-physiological levels of estrogen in the estrogen treated group (22;23). Serum levels of estradiol were not measured in patients from whom growth plate tissue samples were collected. However, serum levels of estradiol are well known to positively correlate with the stage of pubertal development (34).

The collection of human samples is small and consists of a variability of disorders. However, human growth plate samples are extremely difficult to obtain. We believe that even though patients suffered from diverse disorders, the underlying mechanism of epiphyseal maturation and fusion will be the same for all growth plates. Eventually longitudinal growth stops in all patients, with only few exceptions, at the end of puberty. The human data are in line with both in vivo and in vitro rat data thereby strengthening our conclusion that estrogen stimulates VEGF expression in the growth plate. Estrogen levels were not analyzed in these patients and our assumption of different levels of estrogen exposure is based on the fact that tissue samples were obtained from girls in different pubertal stages.

In summary, we demonstrated that VEGF protein expression in the growth plate is elevated by estrogens in vivo in ovariectomized rats and in vitro in a rat chondrocytic cell line. Our findings are supported by human expression studies in girls in different pubertal stages. From this we conclude that estrogens stimulate VEGF expression in the growth plate although the exact role of VEGF in estrogen-mediated growth plate fusion remains to be clarified.

Acknowledgment and funding

The authors thank the orthopaedic surgeons in the Leiden University Medical Center and at the Karolinska University Hospital in Stockholm for providing the growth plate samples.

This study was supported by ZonMw (project # 920-03-358) the Netherlands, the Swedish Research Council (project 2007-54X-15073-04-3); and a visiting scholarship award from the European Society for Paediatric Endocrinology.

References

1. **Kronenberg HM** 2003 Developmental regulation of the growth plate. *Nature* 423:332-336
2. **Chagin AS, Savendahl L** 2007 Estrogens and growth: review. *Pediatr Endocrinol Rev* 4:329-334
3. **Weise M, De Levi S, Barnes KM, Gafni RI, Abad V, Baron J** 2001 Effects of estrogen on growth plate senescence and epiphyseal fusion. *Proc Natl Acad Sci U S A* 98:6871-6876
4. **Klein KO, Martha PM, Jr, Blizzard RM, Herbst T, Rogol AD** 1996 A longitudinal assessment of hormonal and physical alterations during normal puberty in boys. II. Estrogen levels as determined by an ultrasensitive bioassay. *J Clin Endocrinol Metab* 81:3203-3207
5. **Metzger DL, Kerrigan JR** 1994 Estrogen receptor blockade with tamoxifen diminishes growth hormone secretion in boys: evidence for a stimulatory role of endogenous estrogens during male adolescence. *J Clin Endocrinol Metab* 79:513-518
6. **Ross JL, Long LM, Skerda M, Cassorla F, Kurtz D, Loriaux DL, Cutler GB, Jr.** 1986 Effect of low doses of estradiol on 6-month growth rates and predicted height in patients with Turner syndrome. *J Pediatr* 109:950-953
7. **Hunziker EB** 1994 Mechanism of longitudinal bone growth and its regulation by growth plate chondrocytes. *Microsc Res Tech* 28:505-519
8. **Kember NF** 1993 Cell kinetics and the control of bone growth. *Acta Paediatr Suppl* 82 Suppl 391:61-65
9. **Zelzer E, Mamluk R, Ferrara N, Johnson RS, Schipani E, Olsen BR** 2004 VEGFA is necessary for chondrocyte survival during bone development. *Development* 131:2161-2171
10. **Zelzer E, Olsen BR** 2005 Multiple roles of vascular endothelial growth factor (VEGF) in skeletal development, growth, and repair. *Curr Top Dev Biol* 65:169-187
11. **Dai J, Rabie AB** 2007 VEGF: an essential mediator of both angiogenesis and endochondral ossification. *J Dent Res* 86:937-950
12. **Carlevaro MF, Cermelli S, Cancedda R, Descalzi CF** 2000 Vascular endothelial growth factor (VEGF) in cartilage neovascularization and chondrocyte differentiation: auto-paracrine role during endochondral bone formation. *J Cell Sci* 113 (Pt 1):59-69
13. **Garcia-Ramirez M, Toran N, Andaluz P, Carrascosa A, Audi L** 2000 Vascular endothelial growth factor is expressed in human fetal growth cartilage. *J Bone Miner Res* 15:534-540

14. **Gerber HP, Vu TH, Ryan AM, Kowalski J, Werb Z, Ferrara N** 1999 VEGF couples hypertrophic cartilage remodeling, ossification and angiogenesis during endochondral bone formation. *Nat Med* 5:623-628
15. **Haeusler G, Walter I, Helmreich M, Egerbacher M** 2005 Localization of matrix metalloproteinases, (MMPs) their tissue inhibitors, and vascular endothelial growth factor (VEGF) in growth plates of children and adolescents indicates a role for MMPs in human postnatal growth and skeletal maturation. *Calcif Tissue Int* 76:326-335
16. **Robinson CJ, Stringer SE** 2001 The splice variants of vascular endothelial growth factor (VEGF) and their receptors. *J Cell Sci* 114:853-865
17. **Ferrara N, Gerber HP, LeCouter J** 2003 The biology of VEGF and its receptors. *Nat Med* 9:669-676
18. **Ryan AM, Eppler DB, Hagler KE, Bruner RH, Thomford PJ, Hall RL, Shopp GM, O'Neill CA** 1999 Preclinical safety evaluation of rhuMABVEGF, an antiangiogenic humanized monoclonal antibody. *Toxicol Pathol* 27:78-86
19. **Hyder SM, Stancel GM, Chiappetta C, Murthy L, Boettger-Tong HL, Makela S** 1996 Uterine expression of vascular endothelial growth factor is increased by estradiol and tamoxifen. *Cancer Res* 56:3954-3960
20. **Mekraldi S, Lafage-Proust MH, Bloomfield S, Alexandre C, Vico L** 2003 Changes in vasoactive factors associated with altered vessel morphology in the tibial metaphysis during ovariectomy-induced bone loss in rats. *Bone* 32:630-641
21. **Vandenput L, Boonen S, Van HE, Swinnen JV, Bouillon R, Vanderschueren D** 2002 Evidence from the aged orchidectomized male rat model that 17beta-estradiol is a more effective bone-sparing and anabolic agent than 5alpha-dihydrotestosterone. *J Bone Miner Res* 17:2080-2086
22. **Tivesten A, Moverare-Skrtic S, Chagin A, Venken K, Salmon P, Vanderschueren D, Savendahl L, Holmang A, Ohlsson C** 2004 Additive protective effects of estrogen and androgen treatment on trabecular bone in ovariectomized rats. *J Bone Miner Res* 19:1833-1839
23. **Tivesten A, Bollano E, Nystrom HC, Alexanderson C, Bergstrom G, Holmang A** 2006 Cardiac concentric remodelling induced by non-aromatizable (dihydro-)testosterone is antagonized by oestradiol in ovariectomized rats. *J Endocrinol* 189:485-491
24. **Nilsson O, Chrysis D, Pajulo O, Boman A, Holst M, Rubinstein J, Martin RE, Savendahl L** 2003 Localization of estrogen receptors-alpha and -beta and androgen receptor in the human growth plate at different pubertal stages. *J Endocrinol* 177:319-326

25. **Heinrichs C, Yanovski JA, Roth AH, Yu YM, Domene HM, Yano K, Cutler GB, Jr, Baron J** 1994 Dexamethasone increases growth hormone receptor messenger ribonucleic acid levels in liver and growth plate. *Endocrinology* 135:1113-1118
26. **Lunstrum GP, Keene DR, Weksler NB, Cho YJ, Cornwall M, Horton WA** 1999 Chondrocyte differentiation in a rat mesenchymal cell line. *J Histochem Cytochem* 47:1-6
27. **Chrysis D, Zaman F, Chagin AS, Takigawa M, Savendahl L** 2005 Dexamethasone induces apoptosis in proliferative chondrocytes through activation of caspases and suppression of the Akt-phosphatidylinositol 3'-kinase signaling pathway. *Endocrinology* 146:1391-1397
28. **Kim HK, Bian H, ya-Ay J, Garces A, Morgan EF, Gilbert SR** 2009 Hypoxia and HIF-1alpha expression in the epiphyseal cartilage following ischemic injury to the immature femoral head. *Bone*
29. **Rath NC, Huff WE, Huff GR** 2007 Thiram-induced changes in the expression of genes relating to vascularization and tibial dyschondroplasia. *Poult Sci* 86:2390-2395
30. **Petersen W, Tsokos M, Pufe T** 2002 Expression of VEGF121 and VEGF165 in hypertrophic chondrocytes of the human growth plate and epiphyseal cartilage. *J Anat* 201:153-157
31. **Garvin S, Nilsson UW, Huss FR, Kratz G, Dabrosin C** 2006 Estradiol increases VEGF in human breast studied by whole-tissue culture. *Cell Tissue Res* 325:245-251
32. **Kazi AA, Jones JM, Koos RD** 2005 Chromatin immunoprecipitation analysis of gene expression in the rat uterus in vivo: estrogen-induced recruitment of both estrogen receptor alpha and hypoxia-inducible factor 1 to the vascular endothelial growth factor promoter. *Mol Endocrinol* 19:2006-2019
33. **Juul A** 2001 The effects of oestrogens on linear bone growth. *Hum Reprod Update* 7:303-313
34. **Norjavaara E, Ankarberg C, bertsson-Wikland K** 1996 Diurnal rhythm of 17 beta-estradiol secretion throughout pubertal development in healthy girls: evaluation by a sensitive radioimmunoassay. *J Clin Endocrinol Metab* 81:4095-4102

41

The role of p27 kip1 in the regulation of growth plate chondrocyte proliferation in mice

Joyce A.M. Emons^{1,2}, Rose Marino¹, Ola Nilsson¹, Kevin M. Barnes¹, Naomi Even-Zohar¹, Anisia C. Andrade¹, Neal A Chatterjee¹, Jan M. Wit², Marcel Karperien^{2,3}, Jeffrey Baron^{1,4}

Pediatr Res. 2006 Sep;60(3):288-93

¹Developmental Endocrinology Branch, National Institute of Child Health and Human Development, National Institutes of Health, Bethesda, USA

²Department of Pediatrics, Leiden University Medical Center, Leiden, The Netherlands

³Department of Endocrinology and Metabolic Diseases, LUMC, Leiden, The Netherlands

⁴Commissioned Officer in the U.S. Public Health Service

Abstract

p27/Kip1, a cyclin-dependent kinase inhibitor, negatively regulates proliferation of multiple cell types. The goal of this study was to assess the role of p27 in the spatial, temporal and conditional regulation of growth plate chondrocyte proliferation. p27 mRNA expression was detected by real-time RT-PCR in both proliferative/resting and hypertrophic zones of the mouse growth plate at levels approximately 2-fold lower than in the surrounding bone. To determine whether this expression is physiologically important, we studied skeletal growth in 7-wk-old mice lacking a functional p27 gene. In these mice, body length was modestly increased compared to wild-type littermates. In the proximal tibiae, proliferation of growth plate chondrocytes was increased but tibial length was not significantly greater than controls. p27 ablation had no measurable effect on growth plate morphology, including the number of proliferative or hypertrophic chondrocytes, suggesting that p27 is not necessary for the cessation of proliferation and terminal differentiation of chondrocytes as they exit the proliferative zone. Treatment with dexamethasone in vivo inhibited longitudinal bone growth similarly in p27-deficient mice and controls indicating that p27 is not required for the inhibitory effects of glucocorticoid on growth plate function. p27-deficient mice had increased width of the femoral diaphysis, suggesting that p27 acts normally to inhibit periosteal bone growth. In conclusion, our findings suggest that p27 has modest inhibitory effects on growth plate chondrocyte proliferation but is not required for the spatial or temporal regulation of proliferation or the conditional regulation by glucocorticoid.

Introduction

Longitudinal bone growth occurs at the growth plate, a thin layer of cartilage located between the epiphysis and the metaphysis, at the ends of the long bones. Bone elongation occurs by a process called endochondral ossification, in which chondrocytes undergo the sequential steps of proliferation, hypertrophic differentiation, and apoptosis. The chondrocytes and the surrounding cartilage matrix are then replaced by bone tissue.

This process of longitudinal bone growth requires precise regulation of chondrocyte proliferation. First, chondrocyte proliferation is regulated spatially within the growth plate; the proliferation rate varies with distance along the long axis of the bone. In the resting and uppermost proliferative zone, proliferation is slow. Proliferation increases in the mid proliferative zone and then slows again in the lower proliferative zone and finally ceases in the hypertrophic zone (1). Second, chondrocyte proliferation varies temporally; the proliferation rate of chondrocytes declines with increasing age (2-5) causing longitudinal bone growth to slow and eventually stop. Third, chondrocyte proliferation is regulated conditionally, in response to conditions elsewhere in the body (1). Some of the extracellular signaling mechanisms that regulate proliferation are known. For example, spatial regulation involves parathyroid hormone-related protein (PTHrP) and Indian hedgehog (Ihh) and conditional regulation involves circulating IGF-1 and glucocorticoids (6, 7). However, the final portion of the pathway is not understood, that is, how the cell cycle of chondrocytes is modulated temporally, spatially, and conditionally.

One of the suggested mechanisms is through orderly activation and inactivation of cyclin-dependent kinases and cyclin-dependent kinase inhibitors that control the cell cycle. Progression of the cell cycle is promoted by activation of cyclin-dependent kinases. Cyclin-dependent kinase inhibitors play important roles in maintaining growth arrest and cell differentiation by binding

and inactivating these cyclin-dependent kinases. In mammals two known families of cyclin-dependent kinase inhibitors have been identified, INK4 and Cip/Kip. The Cip/Kip family includes p21, p27 and p57, which can act on most cyclin/cyclin-dependent kinase complexes and also on some kinases unrelated to cyclin-dependent kinases, essential for G1 progression and S1 entry (8). Different Cip/Kip inhibitors appear to mediate the growth-inhibiting effects of different stimuli. For example, p21 and p57 expression is increased in cells containing damaged DNA, and p21 expression is also increased in terminally differentiated cells (9). p27 expression, on the other hand, increases in response to extracellular anti-proliferative signals while proliferative signals repress p27 expression (10). Cells grown in the presence of antiproliferative factors, like cAMP or rapamycin, have elevated levels of p27 mRNA (11, 12).

Previous studies suggest that p27 may regulate growth plate chondrocyte proliferation and differentiation (13,14). p27 has been detected immunohistochemically in hypertrophic chondrocytes in fetal and early postnatal mice (15, 16). p27 has also been detected in cultured rat resting zone chondrocytes where its expression is upregulated during thyroid hormone-induced terminal differentiation (13). Targeted disruption of p27 in mice causes multiorgan hyperplasia and increased body weight with all tissues proportionally enlarged and containing more cells (14, 17-19). Kiyokawa et al. (17) reported an increased size and width of tibiae and femora in p27-deficient mice compared to wild-type mice. However, beyond this, little is known about the role of p27 in regulating skeletal growth.

The current study was designed to explore the role of p27 in the spatial, temporal, and conditional regulation of growth plate chondrocyte proliferation. First, we measured p27 expression in the mouse growth plate using real time PCR. Second, we assessed growth plate structure, chondrocyte proliferation, longitudinal bone growth and cortical width in p27-deficient mice. Third, we determined whether p27 mediates the effects of a hormonal modulator of longitudinal bone growth by administering a glucocorticoid to p27-deficient mice.

Materials and Methods

Animals

Heterozygous p27^{+/-} mice from a mixed C57BL/6J and 129 background were provided by Dr. Jack Pledger (H Lee Moffitt Cancer Center, University of South Florida College of Medicine, Tampa, USA). In these mice, originally generated by Matthew Fero and colleagues, the entire coding region for p27 has been replaced by a neomycin resistance cassette (10). The mice were bred in our animal facility to obtain p27^{-/-} and p27^{+/+} mice. Mouse colonies were maintained in a pathogen free environment and fed standard rodent chow (Zeigler Bros, Gardners, PA) with water ad libitum. Animal care was in accordance with the Guide for the Care and Use of Laboratory Animals (National Research council (1996). The protocol was approved by the Animal Care and Use Committee, National Institutes of Child and Human Development, National Institutes of Health.

Mouse genotyping

At three weeks of age, 5 mm of the tail end was excised under local anaesthesia, and genomic DNA was extracted using the DNeasy Tissue Kit (Qiagen, Valencia, CA). Genotypes were analysed by the polymerase chain reaction (PCR). p27 deletions were confirmed by the presence of a 600 bp fragment unique to the mutant genotype amplified with primer p27 KO1 (CCT TCT ATG GCC TTC TTG ACG) and primer P27 KO2 (TGG AAC CCT GTG CCA TCT CTA T) (sequences provided by

Matthew Fero, Fred Hutchinson Cancer Research Center, Seattle, Washington). The PCR reaction mixture (Invitrogen, Carlsbad, CA) contained 5% DMSO. PCR reactions were performed under the following conditions: 94 °C for 3 min, followed by 40 cycles of 94 °C for 1 min, 61 °C for 45 s and 72 °C for 45 s, and ending with primer extension at 72 °C for 5 min. Wild-type alleles were confirmed by the presence of a 190 base-pair fragment amplified with the primers *p27* WT1 (GAT GGA CGC CAG ACA AGC) and *p27* WT2 (CTC CTG CCA TTC GTA TCT GC) (Dr. Jack Pledger, H Lee Moffitt Cancer Center; University of South Florida College of Medicine, Tampa, USA., personal communication). The DNA was amplified with PCR conditions as follows: 94 °C for 3 min, followed by 12 cycles of 94 °C for 20 s, 64 °C for 30 s (subtracting 0.5 °C every cycle) and 72 °C for 35 s, followed by 25 cycles of 94 °C for 20 s, 58 °C for 30 s and 72 °C for 35 s, and ending with 72 °C for 2 min.

Animal procedures and tissue processing

To assess *p27* expression in growth plate, five 5-wk-old wild-type C57BL/6J mice and two 5-wk-old mice homozygous for *p27* deletion were sacrificed by cervical dislocation. Proximal tibial growth plates were rapidly excised, embedded in OCT compound (Electron Microscopy Sciences, Hatfield, PA) and stored at -80 °C for subsequent processing.

To analyze the skeletal phenotype of *p27* deficiency, mice were separated in 4 groups by their genotypes and sex: *p27*^{+/+} female (n = 9), *p27*^{+/+} male (n = 10), *p27*^{-/-} female (n = 9), *p27*^{-/-} male (n = 10). At 7 weeks of age, mice were sacrificed by inhalation of carbon dioxide. 7 weeks was chosen because previous studies (17, 20) demonstrated a significant difference in weight between wild-type and *p27*-deficient mice beginning at this age. Furthermore, at 7 weeks of age mouse growth plates are still active. 200 µl 5-Bromo-2'-deoxy-uridine (BrdU, 10 mg/ml, Sigma-Aldrich, St. Louis, MO) was administered i.p 7 h and 2 h before sacrifice. The animals were weighed, and body length (nose-base of tail and total length including tail) was determined (21). Heart, liver, spleen and kidney were excised and weighed. Tibiae and femora were excised, separated from adjacent muscle, and their lengths were measured using a digital vernier caliper. The left femora were fixed overnight in 10% phosphate buffered formalin and preserved in 70% alcohol for microcomputed tomography. The left tibiae were prepared for histological analysis by fixing overnight in 10% phosphate buffered formalin, decalcifying in 10% EDTA, and embedding in paraffin.

To assess the effect of dexamethasone in the absence of *p27*, 3-wk-old mice were divided into a *p27*^{+/+} (7 males, 10 females) and a *p27*^{-/-} group (6 males, 5 females). The animals were all injected subcutaneously with 20µg dexamethasone once a day, five times a week for four weeks. Body weight and body length was measured weekly. BrdU was administered as before. After sacrifice, tibiae and femora were excised and measured. Measurements were compared to non-treated controls.

Isolation and reverse transcription of RNA

Frozen longitudinal sections (40 µm) of proximal tibial growth plates from 5-week-old mice were mounted on Superfrost Plus slides (Histoserv, Germantown, MD). Slides were thawed 2 min, fixed in 70% ethanol and 95% ethanol, stained in eosin, washed in 100% ethanol and dehydrated in xylene (each step for 60 s, at room temperature). Standard precautions against RNases were employed. Using an inverted microscope and a scalpel, from each section, four different zones were separated: epiphyseal bone, resting plus proliferative zone, hypertrophic zone, and metaphyseal bone. The division between bone tissue and growth plate tissue was readily distinguished visually. To avoid cross-contamination between the resting/proliferative zone and the hypertrophic zone, the boundary segment of cartilage containing the lower proliferative zone and the upper hypertrophic zone was discarded. For each zone, approximately 16 sections from a single animal

were pooled prior to RNA isolation. RNA isolation was performed as previously described except that we scaled down the procedure to use one fifth of each volume and omitted the final precipitation with LiCl (22). RNA concentration was assessed and integrity was confirmed using a Bioanalyzer 2100, RNA Pico Chips, and version A.02.12 of the Bio Sizing software according to manufacturers instructions (Agilent Biotechnologies, Inc., Palo Alto, CA).

Reverse transcription was accomplished by mixing the entire RNA solution generated, 100 ng random hexamers, and 10 μ mol deoxynucleoside triphosphate (dNTP) (Invitrogen). The samples were denatured for 5 min at 65 C then placed on ice. 4 μ l of 5x First strand buffer (Invitrogen), 0.1 M DTT (Invitrogen) and 40 U RNase out (Invitrogen) was added to the mixture followed by 2 min incubation at 42 C. 200 U Superscript III Reverse transcriptase (Invitrogen) was added followed by a 10 min incubation at 25 C and a one hour of incubation at 50 C. Afterwards samples were heated at 70 C for 15 min to inactivate reverse transcriptase.

Real-time RT-PCR

Expression of p27 mRNA was quantified by real-time quantitative PCR using the ABI prism 7300 Sequence Detection System (Applied Biosystems, Foster City, CA) with specific, FAM- labeled probes. The oligonucleotide primers and probes for p27 mRNA and 18S ribosomal RNA were supplied by Applied Biosystems; assays 4319413E and Mm00438168_m1, respectively. PCR reactions were performed with the cDNA solution, TaqMan Universal PCR Master Mix, p27 or 18S primers and probes (Applied Biosystems, Foster City, CA), according to the manufacturer's instructions, using the following thermal cycling conditions: one cycle at 50 °C for 2 min and 95 °C for 10 min, followed by 40 cycles of 15 s at 95 °C and 1 min at 60 °C. Each sample, which represents a single region from a single animal, was assayed in triplicate. The efficiencies of the p27 and 18S PCR reactions were determined using serial dilutions of whole growth plate cDNA.

Quantitative Histology

Longitudinal 5 μ m sections of the proximal tibial growth plate were obtained near the center of the formalin-fixed, decalcified bone, mounted on Superfrost Plus slides (Histoserv, Germantown, MD) and stained with Masson Trichrome. All histological measurements were performed in the central two-third of the growth plate sections. Height was measured at three points parallel to the chondrocyte columns, and results were averaged. The number of proliferative and hypertrophic cells was counted in 15 intact columns per growth plate, and counts were averaged. The terminal hypertrophic chondrocyte was defined as the cell in the last lacuna that was not invaded by metaphyseal blood vessels (5). Height of 10 lacunae per animal were measured and results were averaged. We only measured lacunae with a sharp boundary, which indicates that the lacunar wall is perpendicular to the plane of section and thus the section had been made near the center of the lacuna.

BrdU labeling and detection

In tissues sections from animals injected with BrdU, labeled cells were visualized with a commercial kit (BrdU staining kit, Zymed, San Francisco, CA.), using the kit protocol except that the trypsin was diluted 1:6 with reagent 1B. Labeled and unlabeled cells were counted in 20 chondrocyte columns per animal in the central two-third of the growth plate sections and averaged.

Microcomputed tomography (micro-CT)

Excised and fixed femora from wild type and p27 knock out mice were scanned using a MicroCAT II scanner (Imtek, Inc., Knoxville, TN). Each femur was immobilized on the sample table using plastic foam. The scanning conditions were as follows: resolution 50 μm , voxel size 30 micron, 80 kVp, 500 mA and 720 projections over 360 degrees. After scanning, 3-dimensional images of the whole femora were reconstructed and used to measure total length (most proximal to most distal point), shaft width (measured at mid-shaft), cortex width (measured at mid-shaft at 0, 90, 180 and 270 degrees and averaged), bone volume and bone mineral density.

Statistics

Data were presented as mean \pm SEM.

For the real-time PCR data, triplicate threshold cycle values were averaged and then the relative amounts of p27 mRNA were normalized to an endogenous control, 18S ribosomal RNA, in the same sample to account for variability in the initial concentration and quality of total RNA and in the efficiency of the reverse transcription reaction. This normalization was calculated as described by Pfaffl et al.(23). To analyze differences between tissues, relative expression values were log transformed to achieve a normal distribution, and analyzed by ANOVA followed by Holm-Sidak comparisons between adjacent regions.

Phenotypic comparisons between wild-type and p27-deficient groups were made by two-way ANOVA with sex and genotype as independent variables. One mouse was eliminated from the micro CT-data because of a fractured femur. For the dexamethasone administration experiment, comparisons between wild-type and p27-deficient mice were made using a Generalized Linear Model using 3 independent variables: genotype, sex, and treatment.

Results

Expression of p27 mRNA in the growth plate and surrounding bone

In the wild-type mouse growth plate, p27 mRNA expression was assessed by real-time PCR. p27 mRNA was detected in both resting/proliferative zone and in hypertrophic zone at similar levels. However the concentration of mRNA (normalized to 18S ribosomal RNA concentration in the same sample) in both regions of the growth plate was approximately 2-fold lower than in the surrounding bone (Fig. 1). As a negative control we measured the expression of p27 mRNA in two p27-deficient mice. In both mice the p27 mRNA expression was undetectable in growth plate and surrounding bone tissue. To confirm the accuracy of the dissection, we analyzed mRNA expression for type X collagen and type I collagen. As expected, type X collagen was primarily expressed in the hypertrophic cartilage and type I collagen was primarily expressed in the bone (Fig. 1).

Growth phenotype of p27-deficient mice

Ablation of p27 in mice had a mild positive effect on body size measured at 7 weeks of age (Table 1, ANOVA using sex and genotype as independent variables). p27^{-/-} mice had an increased body weight compared to p27^{+/+} littermates. Weight of the spleen, heart, liver, and kidney were also significant increased in p27^{-/-} mice.

Ablation of p27 increased the body length, suggesting greater longitudinal growth of the vertebrae, but did not significantly affect the length of the tibia or femur. Width of the femur mid-shaft was significantly increased in p27^{-/-} compared to wild-type mice (Table 1). This increase in shaft width did not result in an increase in mid-shaft cortical thickness or in overall femoral bone density, measured by micro CT-scan.

Growth plate morphology and proliferation in p27-deficient mice

p27 deficiency had no discernable effect on tibial growth plate morphology (Fig. 2). Total growth plate width, the number of proliferative and hypertrophic cells per intact column, and the height of the terminal hypertrophic cell did not differ significantly between p27-deficient and wild-type mice (Table 2). However growth plate chondrocyte proliferation, assessed by BrdU-labeling index, was greater in p27-deficient than in wild-type mice (Table 2).

Dexamethasone-induced growth inhibition in p27-deficient mice

Treatment of 3-wk-old mice with dexamethasone for 4 weeks caused a significant decrease in total body weight, tibial length, and femoral length but not in body length when compared to untreated controls (Table 3). This decrease was observed in both wild-type and p27-deficient mice. The magnitude of this growth inhibition did not significantly differ with the genotype ($P = NS$ for body weight, tibial length, and femoral length, and body length). Therefore dexamethasone appeared to have a similar effect on wild-type and p27-deficient mice.

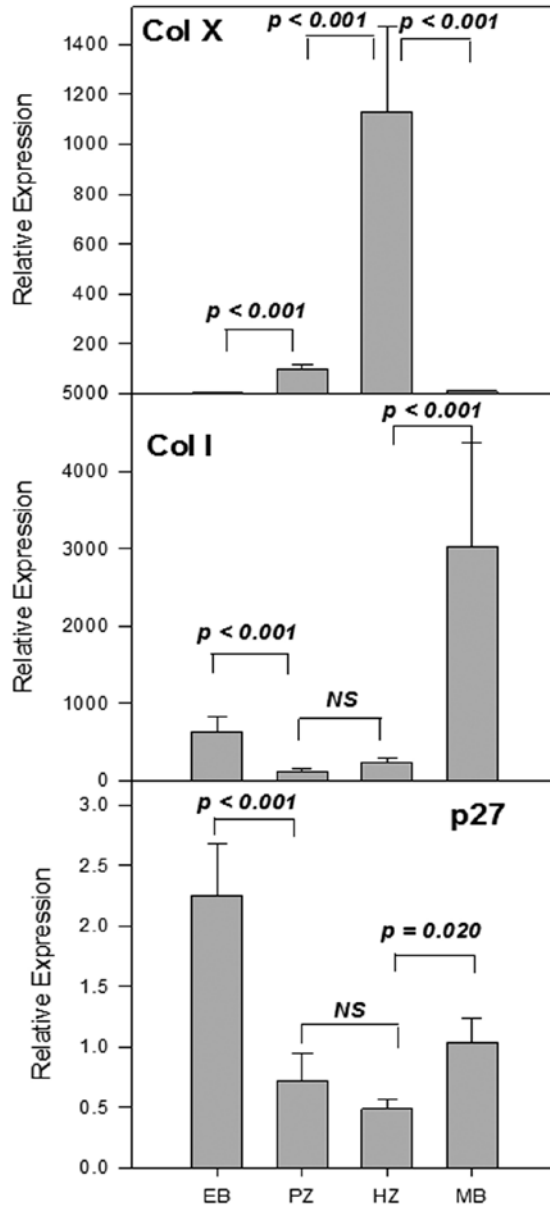


Figure 1

Relative mRNA expression (mean \pm SEM) of type X collagen, type I collagen, and p27 in proximal tibial growth plate and surrounding bone of 5-wk-old mice. Using an inverted microscope and a scalpel, epiphyseal bone, resting plus proliferative zone, hypertrophic zone, and metaphyseal bone samples were isolated from longitudinal sections of proximal tibiae from 5 wild-type mice. For each zone of each animal, approximately 16 sections were pooled prior to RNA isolation and reverse transcription. mRNA expression was measured by real-time PCR using oligonucleotide primers and TaqMan probes. All samples were run in triplicate. The mRNA content of each gene was normalized to 18S ribosomal RNA content in the same sample and, for ease of comparison, multiplied by 10^6 . Statistical significance was assessed by ANOVA, followed by Holm-Sidak. P values shown are not corrected for multiple comparisons.

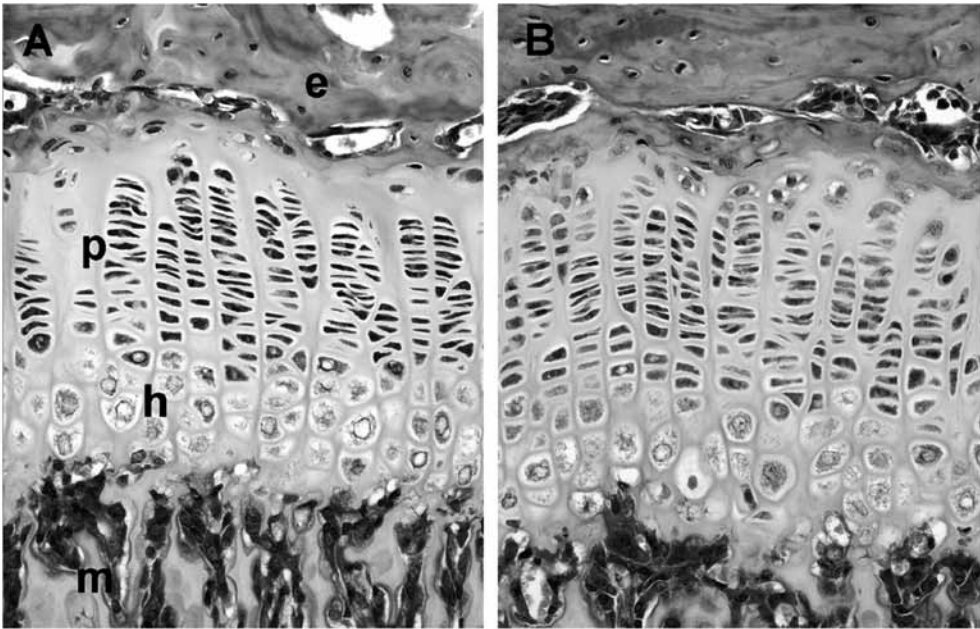


Figure 2

Representative photomicrographs of proximal tibial growth plates of $p27^{+/+}$ (A) and $p27^{-/-}$ (B) mice at 7 weeks of age. Longitudinal 5 μ m sections were obtained near the center of the formalin-fixed, decalcified bone and stained with Masson Trichrome. No differences were observed between the two genotypes. e, epiphyseal bone; p, proliferative zone; h, hypertrophic zone; m, metaphyseal bone.

Table 1. Body and organ size of wild-type and $p27$ -deficient mice .

	Males		Females		Both sexes $p27^{-/-}$ vs $p27^{+/+}$ (ANOVA) P
	$p27^{+/+}$	$p27^{-/-}$	$p27^{+/+}$	$p27^{-/-}$	
	Mean SEM	Mean SEM	Mean SEM	Mean SEM	
weight (g)	22.3± 0.465	26.6± 1.087**	19.4± 0.504	21.8± 0.729*	<0.001
spleen weight (g)	0.063± 0.004	0.102± 0.007**	0.066± 0.006	0.083± 0.007	<0.001
heart weight (g)	0.148± 0.01	0.191± 0.008**	0.133± 0.006	0.141± 0.009	0.005
liver weight (g)	1.3± 0.054	1.90± 0.12**	1.05± 0.049	1.29± 0.066*	<0.001
kidney weight (g)	0.16± 0.007	0.226± 0.018**	0.126± 0.007	0.149± 0.008	<0.001
body length without tail (cm)	9.3± 0.1	9.6± 0.1	9.0± 0.1	9.4± 0.2*	0.003
body length with tail (cm)	16.6± 0.1	17.1± 0.1*	16.1± 0.1	16.3± 0.2	0.025
tibia length (mm)	17.38± 0.19	17.51± 0.1	16.82± 0.21	17.05± 0.11	NS
femur length (mm)	14.49± 0.14	14.42± 0.12	13.85± 0.19	14.07± 0.13	NS
femur shaft width (mm)	1.62± 0.03	1.84± 0.05**	1.63± 0.02	1.79± 0.05**	<0.001
femur cortex width (mm)	0.226± 0.011	0.254± 0.015	0.247± 0.007	0.251± 0.007	NS
bone density/volume	26.26± 1.29	27.44± 1.3	21.21± 1.25	23.96± 1.16	NS

mean ± SEM

*, $p < 0.05$

** , $p < 0.01$

Table 2. Growth plate characteristics of wild-type versus p27-deficient mice.

	Males		Females		Both sexes -/- vs +/+ (ANOVA)
	p27 ^{+/+}	p27 ^{-/-}	p27 ^{+/+}	p27 ^{-/-}	
height growth plate	0.361 ± 0.01	0.371 ± 0.011	0.343 ± 0.007	0.343 ± 0.009	NS
proliferating cells/intact column	11.4 ± 0.5	11.7 ± 0.3	11.0 ± 0.3	11.3 ± 0.3	NS
hypertrophic cells/intact column	3.9 ± 0.2	3.6 ± 0.1	3.9 ± 0.1	3.8 ± 0.1	NS
height terminal hypertrophic cell	0.0222 ± 0.0005	0.0221 ± 0.0006	0.0215 ± 0.0006	0.0217 ± 0.0006	NS
# positive BrdU cells/intact column	2.7 ± 0.1	3.6 ± 0.2**	2.5 ± 0.2	3.1 ± 0.2**	0.001
% positive BrdU cells/intact column	24 ± 1	31 ± 2**	23 ± 2	28 ± 2**	0.002

mean ± SEM

** = p < 0.01

Table 3. Effect of dexamethasone treatment on body and bone growth in wild-type and p27-deficient mice

	p27 ^{-/-}					p27 ^{+/+}				
	Males [†]	% [‡]	Females [†]	% [‡]	P [§]	Males [†]	% [‡]	females [†]	% [‡]	P [§]
weight (g)	-3.7 ± 0.6	-16.6	-2.7 ± 0.7	-13.9	< 0.001	-5.3 ± 1.3	-19.9	-3.5 ± 1.5	-15.6	< 0.001
body length without tail (cm)	-0.08 ± 0.10	-1.1	0.04 ± 0.13	-1.09	NS	-0.28 ± 0.16	-3.1	-0.23 ± 0.21	-2.1	NS
tibia length (mm)	-1.1 ± 0.3	-6.2	-0.8 ± 0.2	-4.5	< 0.001	-1.1 ± 0.2	-6.5	-0.6 ± 0.4	-3.7	< 0.001
femur length (mm)	-0.8 ± 0.2	-5.6	-0.5 ± 0.2	-3.3	< 0.001	-1.1 ± 0.2	-7.5	-0.7 ± 0.2	-4.9	< 0.001

[†] dexamethasone-treated minus untreated controls (mean ± SEM)

[‡] % change = 100* (dexamethasone-treated minus untreated controls)/untreated controls

[§] dexamethasone-treated vs. untreated controls (males and females combined)

Discussion

p27 mRNA was detected in the growth plates of 5-wk-old mice by real-time PCR. The p27 mRNA levels in growth plate were approximately two-fold lower than levels in the surrounding epiphyseal and metaphyseal bone tissue.

The expression of p27 mRNA was not significantly greater in the hypertrophic zone than in the resting/proliferative zone. This finding does not support the hypothesis that upregulation of p27 is involved in terminal differentiation of growth plate chondrocytes (13, 14, 24). Earlier studies using immunohistochemistry reported p27 expression primarily in hypertrophic chondrocytes of fetal mouse long bones. This divergence in results could be due to a difference between mRNA and protein expression, to developmental changes in p27 expression, or to the poor quantitative nature of immunohistochemistry (15, 16). The current study is the first to assess the expression of p27 in the growth plate using a quantitative method and the first to assess expression in the growth plate beyond the neonatal period.

In tissues from p27^{-/-} mice, we did not detect p27 expression, which indicates that our real-time PCR assay was specific for p27 mRNA. The observed p27 expression in the growth plate is unlikely to be due to contamination from the surrounding bone because measurement of type I and type X collagen mRNA levels suggests that the microdissection was quite accurate. The surrounding bone tissue consists of several different cell types, and this study does not determine the level of p27 expression in different bone cells.

To determine whether the p27 expression in the growth plate is physiologically important, we studied skeletal growth in p27-deficient mice. p27-deficient mice had a slightly greater body length than wild-type mice, presumably reflecting greater growth of the vertebrae. In long bones, p27 ablation was associated with a modestly increased rate of chondrocyte proliferation. The tibial and femoral lengths were not significantly different from those of wild-type littermates, suggesting that the increase in growth plate chondrocyte proliferation had begun shortly before 7 weeks of age, the time when the differences in body size are beginning to manifest (17, 20). Alternatively the lack of difference in bone length despite an increase in growth plate chondrocyte proliferation might reflect a decrease in matrix production rate or an increase in apoptosis of non-terminal chondrocytes. Taken together, our findings indicate that p27 has a mild inhibitory effect on the normal proliferation of proliferative zone chondrocytes. Kiyokawa et al also mentioned a positive effect of p27 ablation on bone length in mice although the actual bone length was not presented in that paper (17). The magnitude of the effect on skeletal growth in different studies may depend on genetic background. Previous studies in other backgrounds (coisogenic 129S4 mice) show an approximately 30% greater weight in p27-deficient than wild-type mice (10, 14, 17) whereas we observed only a 19% (male) and 13% (female) difference at 7 weeks of age. Nonetheless, the small magnitude of the effect suggests that p27 is not necessary for the normal growth deceleration that occurs with age. The absence of skeletal growth deceleration would allow continued growth at fetal rates, which would be expected to have yielded a dramatic increase in bone length.

There was no discernable effect of p27 deficiency on growth plate morphology. In particular, the number of proliferative chondrocytes and the number of hypertrophic chondrocytes per column were unaffected. One previous study mentioned that the overall growth plate height was unaffected by p27 ablation but that the proliferative zone of p27^{-/-} mice appeared larger in some sections. However, in that study, no supporting quantitative data were reported (14). The BrdU-labeling index was increased in the proliferative zone of p27^{-/-} compared to p27^{+/+} mice, whereas the number of chondrocytes in the proliferative zone was the same in p27^{-/-} and p27^{+/+} mice. This difference may occur because the number of proliferative chondrocytes depends not only on the

number of cells being generated per column but also on how far down the column the cells undergo terminal differentiation into hypertrophic chondrocytes. Therefore, it is possible to have an effect on proliferation rate and not on number of proliferative chondrocytes. Our findings indicate that p27 is not necessary for the cessation in proliferation and for the terminal differentiation that occurs near the boundary between the proliferative and hypertrophic zones. Thus, p27 is not critical for the spatial regulation of growth plate chondrocyte proliferation.

We next hypothesized that p27 might mediate the growth-suppressing effects of glucocorticoids and thus play an important role in the conditional regulation of growth plate chondrocyte proliferation. The growth-inhibiting effects of glucocorticoids are the result of a decrease in proliferation and possibly an increase in apoptosis (25). The growth-inhibiting effects of glucocorticoids in other cell types may be mediated in part by p27 (26). Thus, p27-deficient murine embryonic fibroblasts are partially resistant to the growth-inhibitory effects of glucocorticoids (27). However in our experiment, dexamethasone administration slowed longitudinal bone growth in p27-deficient mice and wild-type mice to a similar extent. Thus, p27 does not appear to be necessary for the decreased proliferation of growth plate chondrocytes induced by excess glucocorticoid in mice.

p27 affected not only the process of longitudinal bone growth but also radial growth of the diaphyseal cortex. p27^{-/-} mice showed a greater diaphyseal width of the femur. This finding is consistent with a previous report (14). In contrast to the overall shaft width, we found that the cortical thickness (from endosteal to periosteal surface) was not increased. Similarly, overall femoral bone density, which is highly dependent on cortical thickness, was not affected by p27 ablation. Taken together these data suggest that periosteal bone growth is increased in the absence of p27, but that endosteal resorption may also be increased, thus negating any effect on cortical thickness. The increase in diaphyseal width might be caused by increased mechanical load due to increased body weight or to a direct effect of p27 on periosteal growth.

We choose to study the role of p27 in the regulation of longitudinal growth because of the suggestion from previous studies (13:14) that it may regulate growth plate chondrocyte proliferation and differentiation. Other cell cycle regulators may also be important in the regulation of longitudinal growth. For example, mice lacking p57 have altered cell proliferation and differentiation, leading to endochondral bone ossification defects with incomplete differentiation of hypertrophic chondrocytes (28). Also p21^{CIP1/WAF1} might play a role in skeletal growth since it is shown to be expressed in both the proliferative and hypertrophic zones in the growth plate of mice, rats and pigs (29, 30).

In conclusion, our findings suggest that p27 is expressed in the growth plate. p27 ablation modestly increases growth plate chondrocyte proliferation, the process of longitudinal bone growth, and periosteal bone growth. However, p27 does not appear to be required for the inhibition of chondrocyte proliferation that occurs during hypertrophic differentiation, with increasing age, or in response to glucocorticoid excess. Thus, our findings suggest that p27 negatively modulates growth plate chondrocyte proliferation, but it is not required for spatial, temporal, or conditional regulation of chondrocyte proliferation in the growth plate.

Funding

This study is supported by the Intramural Research Program of the National Institute of Child Health and Human Development, NIH and the Ter Meulen Foundation, The Netherlands. There is

no conflict of interest.

References

1. **Kember NF, Walker KV.** Control of bone growth in rats. *Nature* 1971; 229:428-9.
2. **Aizawa T, Kokubun S, Tanaka Y.** Apoptosis and proliferation of growth plate chondrocytes in rabbits. *J Bone Joint Surg Br* 1997; 79:483-6.
3. **Farquharson C, Loveridge N.** Cell proliferation within the growth plate of long bones assessed by bromodeoxyuridine uptake and its relationship to glucose 6-phosphate dehydrogenase activity. *Bone Miner* 1990; 10:121-30.
4. **Hunziker EB, Schenk RK.** Physiological mechanisms adopted by chondrocytes in regulating longitudinal bone growth in rats. *J Physiol* 1989; 414:55-71.
5. **Weise M, De Levi S, Barnes KM, Gafni RI, Abad V, Baron J.** Effects of estrogen on growth plate senescence and epiphyseal fusion. *Proc Natl Acad Sci U S A* 2001; 98:6871-6.
6. **van der Eerden BC, Karperien M, Gevers EF, Lowik CW, Wit JM.** Expression of Indian hedgehog, parathyroid hormone-related protein, and their receptors in the postnatal growth plate of the rat: evidence for a locally acting growth restraining feedback loop after birth. *J Bone Miner Res* 2000; 15:1045-55.
7. **van der Eerden BC, Karperien M, Wit JM.** Systemic and local regulation of the growth plate. *Endocr Rev* 2003; 24:782-801.
8. **Johnson DG, Walker CL.** Cyclins and cell cycle checkpoints. *Annu Rev Pharmacol Toxicol* 1999; 39:295-312.
9. **Gartel AL, Serfas MS, Tyner AL.** p21--negative regulator of the cell cycle. *Proc Soc Exp Biol Med* 1996; 213:138-49.
10. **Fero ML, Rivkin M, Tasch M, Porter P, Carow CE, Firpo E et al.** A syndrome of multiorgan hyperplasia with features of gigantism, tumorigenesis, and female sterility in p27(Kip1)-deficient mice. *Cell* 1996; 85:733-44.
11. **Kato JY, Matsuoka M, Polyak K, Massague J, Sherr CJ.** Cyclic AMP-induced G1 phase arrest mediated by an inhibitor (p27Kip1) of cyclin-dependent kinase 4 activation. *Cell* 1994; 79:487-96.
12. **Nourse J, Firpo E, Flanagan WM, Coats S, Polyak K, Lee MH et al.** Interleukin-2-mediated elimination of the p27Kip1 cyclin-dependent kinase inhibitor prevented by rapamycin. *Nature* 1994; 372:570-3.
13. **Ballock RT, Zhou X, Mink LM, Chen DH, Mita BC, Stewart MC.** Expression of cyclin-dependent kinase inhibitors in epiphyseal chondrocytes induced to terminally differentiate with thyroid hormone. *Endocrinology* 2000; 141:4552-7.

14. **Drissi H, Hushka D, Aslam F, Nguyen Q, Buffone E, Koff A et al.** The cell cycle regulator p27kip1 contributes to growth and differentiation of osteoblasts. *Cancer Res* 1999; 59:3705-11.
15. **Horner A, Shum L, Ayres JA, Nonaka K, Nuckolls GH.** Fibroblast growth factor signaling regulates Dach1 expression during skeletal development. *Dev Dyn* 2002; 225:35-45.
16. **Sunters A, McCluskey J, Grigoriadis AE.** Control of cell cycle gene expression in bone development and during c-Fos-induced osteosarcoma formation. *Dev Genet* 1998; 22:386-97.
17. **Kiyokawa H, Kineman RD, Manova-Todorova KO, Soares VC, Hoffman ES, Ono M et al.** Enhanced growth of mice lacking the cyclin-dependent kinase inhibitor function of p27(Kip1). *Cell* 1996; 85:721-32.
18. **Nagahama H, Hatakeyama S, Nakayama K, Nagata M, Tomita K, Nakayama K.** Spatial and temporal expression patterns of the cyclin-dependent kinase (CDK) inhibitors p27Kip1 and p57Kip2 during mouse development. *Anat Embryol (Berl)* 2001; 203:77-87.
19. **Teixeira LT, Kiyokawa H, Peng XD, Christov KT, Frohman LA, Kineman RD.** p27Kip1-deficient mice exhibit accelerated growth hormone-releasing hormone (GHRH)-induced somatotrope proliferation and adenoma formation. *Oncogene* 2000; 19:1875-84.
20. **Lin J, Della-Fera MA, Li C, Page K, Choi YH, Hartzell DL et al.** P27 knockout mice: reduced myostatin in muscle and altered adipogenesis. *Biochem Biophys Res Commun* 2003; 300:938-42.
21. **Hughes PC, Tanner JM.** A longitudinal study of the growth of the black-hooded rat: methods of measurement and rates of growth for skull, limbs, pelvis, nose-rump and tail lengths. *J Anat* 1970; 106:349-70.
22. **Heinrichs C, Yanovski JA, Roth AH, Yu YM, Domene HM, Yano K et al.** Dexamethasone increases growth hormone receptor messenger ribonucleic acid levels in liver and growth plate. *Endocrinology* 1994; 135:1113-8.
23. **Pfaffl MW.** A new mathematical model for relative quantification in real-time RT-PCR. *Nucleic Acids Res* 2001; 29:e45.
24. **Beier F, Taylor AC, LuValle P.** The Raf-1/MEK/ERK pathway regulates the expression of the p21(Cip1/Waf1) gene in chondrocytes. *J Biol Chem* 1999; 274:30273-9.
25. **Smink JJ, Gresnigt MG, Hamers N, Koedam JA, Berger R, Buul-Offers SC.** Short-term glucocorticoid treatment of prepubertal mice decreases growth and IGF-I expression in the growth plate. *J Endocrinol* 2003; 177:381-8.
26. **Rogatsky I, Hittelman AB, Pearce D, Garabedian MJ.** Distinct glucocorticoid receptor transcriptional regulatory surfaces mediate the cytotoxic and cytostatic effects of glucocorticoids. *Mol Cell Biol* 1999; 19:5036-49.

27. **Wang Z, Garabedian MJ.** Modulation of glucocorticoid receptor transcriptional activation, phosphorylation, and growth inhibition by p27Kip1. *J Biol Chem* 2003; 278:50897-901.
28. **Zhang P, Liegeois NJ, Wong C, Finegold M, Hou H, Thompson JC et al.** Altered cell differentiation and proliferation in mice lacking p57KIP2 indicates a role in Beckwith-Wiedemann syndrome. *Nature* 1997; 387:151-8.
29. **Stewart MC, Farnum CE, MacLeod JN.** Expression of p21CIP1/WAF1 in chondrocytes. *Calcif Tissue Int* 1997; 61:199-204.
30. **Zenmyo M, Komiya S, Hamada T, Hiraoka K, Suzuki R, Inoue A.** p21 and parathyroid hormone-related peptide in the growth plate. *Calcif Tissue Int* 2000; 67:378-81.

5

Catch-up growth: testing the hypothesis of delayed growth plate senescence in humans

Joyce A.M. Emons^{1,3}, Bart Boersma², Jeffrey Baron^{3,4}, Jan Maarten Wit¹

J of Pediatrics 2005. 147(6):843-6

¹ Department of Pediatrics, Leiden University Medical Center, Leiden, The Netherlands

² Department of Pediatrics, Medical Center Alkmaar, Alkmaar, The Netherlands

³ Developmental Endocrinology Branch, National Institute of Child Health and Human Development, National Institutes of Health, Bethesda, MD, 20982

⁴ Commissioned Officer in the U.S. Public Health Service

After a period of growth inhibition, the linear growth rate usually exceeds the normal range. This phenomenon, known as catch-up growth, was first described more than 40 years ago by Prader et al (1). It has been observed in humans and other mammals, after a wide variety of growth-inhibiting conditions, including malnutrition, Cushing syndrome, hypothyroidism, growth hormone deficiency, and many other systemic diseases (2).

Tanner proposed the hypothesis that catch-up growth is regulated by a central nervous system mechanism that compares the individual's actual body size to an age-appropriate set point and then adjusts the growth rate accordingly (3). However, this hypothesis is not supported by observations that transient growth inhibition within a single growth plate is followed by local catch-up growth in rabbits (4). This local catch-up growth suggests a mechanism intrinsic to the growth plate. Evidence from animal studies suggests that catch-up growth is due, in large part, to a delay in growth plate senescence. Growth plate senescence refers to the normal, programmed changes that occur in the growth plate over time. With increasing age, there is a decrease in the linear growth rate, the chondrocyte proliferation rate, the height of the growth plate, and the number of cells in each growth plate zone (5).

Animal studies suggest that growth plate senescence is not a function of time per se, but of cell proliferation (6). In particular, growth plate chondrocytes may have a finite proliferative capacity that is gradually exhausted, causing growth to slow and eventually to stop (6;7). Conditions that suppress growth plate chondrocyte proliferation conserve the proliferative capacity of the chondrocytes, thus slowing senescence. Consequently, after transient growth inhibition, growth plates retain a greater proliferative capacity, are less senescent, and, hence, show a greater growth rate than expected for age, resulting in catch-up growth.

However, the relationship between catch-up growth and delayed growth plate senescence has only been studied in rabbits (6) and rats (8). Thus it is not known whether catch-up growth is caused by delayed growth plate senescence in humans. Testing this hypothesis in humans is more difficult because most of the known hallmarks of growth plate senescence require microscopic examination of the growth plate. In children, we are restricted to indirect measures of growth plate senescence, including bone age and linear growth rate. Bone age assesses the degree to which the embryonic cartilaginous skeleton has been transformed into the adult bony skeleton. Bone age has been used as a surrogate marker for growth plate senescence (9) on the basis of 2 lines of evidence. First, the determination of bone age is based partly on the thickness of the radiolucent bands between the epiphyses and metaphyses, and thus bone age depends in part on growth plate height, a structural marker of senescence (7). Second, bone age is inversely associated with the remaining linear growth potential. This association is the basis for most height prediction methods (10). Thus bone age is associated with a functional marker of senescence, the decline in growth potential of the growth plates.

If catch-up growth in humans is indeed due to delayed growth plate senescence, and if bone age is a marker for growth plate senescence, then catch-up growth should be associated with delayed bone age. Abundant clinical data support this association. A delayed bone age is observed in essentially all conditions that impair growth, including nutritional, endocrine, rheumatologic, gastrointestinal, heart, lung, and kidney disease (11). Thus multiple conditions, which span the breadth of pediatric medicine, are all associated with growth inhibition, bone age delay, and, if the condition resolves, catch-up growth. This broad association supports the hypothesis that catch-up growth in humans is due, at least in part, to delayed growth plate senescence.

Linear growth rate can also be used as a marker for growth plate senescence. With age, the linear growth rate declines dramatically. The human fetus grows at a rate of over 100 cm/y. By birth, the linear growth rate has decreased to 50 cm/y, and in later childhood to 5 cm/y. In humans, this

decline is briefly interrupted by the pubertal growth spurt, after which the growth rate declines to zero. Animal studies suggest that this decline in growth rate is due to a mechanism intrinsic to the growth plate (4).

We propose that the linear growth rate in prepubertal children can be used to test the hypothesis that catch-up growth in children is due to delayed growth plate senescence. If catch-up growth is due solely to a delay in growth plate senescence, then the linear growth rate of a child experiencing catch-up growth should be equal to the growth rate of a normal younger child. Thus the growth curve during catch-up growth should represent a simple time shift of the normal growth curve of a younger child (Figure 1, A). A steeper curve would suggest that other (or additional) mechanisms besides delayed senescence are responsible for the catch-up growth.

As a first test of this approach, we examined catch-up growth in children with celiac disease placed on a gluten free diet. We reanalyzed data from an earlier study (12) using a new mathematical approach designed to test our hypothesis. A total of 28 prepubertal children, consisting of 9 boys (chronological age [CA] 3.9 ± 3.0 years, bone age [BA] 3.6 ± 2.5 years, height standard deviation score SDS for CA 21.3 ± 1.1 , BMI SDS 20.1 ± 1.0 , mean \pm SD) and 19 girls (CA 3.9 ± 3.4 yr, BA 3.2 ± 2.7 yr, height SDS for CA 21.4 ± 1.0 , BMI SDS 20.7 ± 1.1), from the Netherlands with celiac disease were included in this study. The following inclusion criteria were used: (1) symptoms and small intestinal biopsy typical for celiac disease, (2) no signs of puberty, and (3) no other known diagnoses or treated diseases. Height was measured 0.5, 1, 2, 3, 6, 12, 18, 24, 30, 36, and 50 months after introduction of a gluten-free diet with standard equipment. The study was approved by the hospital ethical committees, and informed consent was obtained from parents and/or patients.

The height at initiation of treatment was used to determine the baseline height age, defined as the age at which the median height for normal children was equal to the child's baseline height. For each child we then calculated the baseline growth delay, defined as the chronological age at initiation of treatment minus the height age at initiation of treatment. The growth delay for each child was calculated only once, using the data from the baseline visit. For each subsequent data point, we calculated the adjusted age, defined as the chronological age at that visit minus the baseline growth delay. Use of the adjusted age rather than the chronological age allowed us to assess whether growth was normal for a younger child, that is, whether the child's growth curve represented a simple time shift of the normal growth curve. We therefore calculated the child's height SDS for adjusted age. A similar analysis was done using initial bone age instead of height age. Our hypothesis predicts that the height SDS for adjusted age would remain close to 0 SDS over time (Figure 1, B, dashed curve). An increasing SDS for adjusted age (Figure 1, B, solid curve) would indicate that the growth rate was increased even for adjusted age, which would not be consistent with the delayed senescence hypothesis.

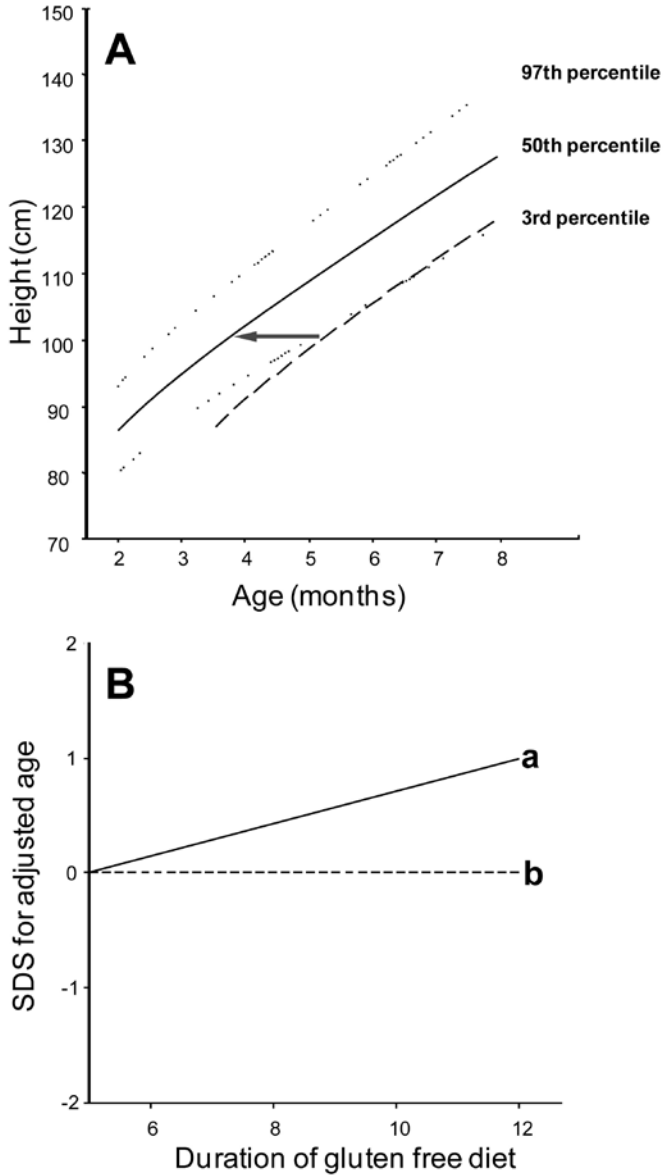


Figure 1

Theoretical catch-up growth curves predicted by the delayed senescence hypothesis. A, The delayed senescence hypothesis predicts that the height curve during catch-up growth (dashed line) should represent simple time-shift of normal (50 percentile, solid line) height curve. B, Therefore the delayed senescence hypothesis also predicts that, during catch-up growth, height should remain normal for a younger child (based on initial height age). Consequently, the height SDS for adjusted age should remain close to 0 (curve b). If the height SDS for adjusted age increases over time, this would indicate that the child's growth rate is rapid even for a younger child (curve a). Curve a would be inconsistent with the delayed senescence hypothesis.

The height SDS for chronological age (Figure 2, A) at onset of gluten-free diet was 21.5, and in the following 36 months this value increased to 20.6 SDS,¹² indicating that the linear growth rate was greater than normal for CA. Thus these children experienced catch-up growth.

However, height SDS for adjusted age on the basis of initial height age remained very close to 0 SDS (Figure 2, B), and height SDS for adjusted age on the basis of initial bone age did the same (Figure 2, C), although with a wider 95% confidence interval (SEM 0.23-0.34) compared with the analysis with height age (SEM 0.02-0.19). Both analyses indicate that the growth rate was normal for a younger child based on initial height age and bone age. Specifically, at baseline, the height age was 0.7 ± 0.8 years less than the CA, and the BA was 0.7 ± 1.0 year (mean \pm SD) less than the CA. Subsequently, the children grew at a rate that was normal for a child 0.7 years younger than chronological age. The larger SEM values for the analysis with BA probably reflect the subjective nature and lower precision of BA measurement compared with height measurement. Because linear growth and bone maturation reflect longitudinal bone growth at the growth plate, the data imply that growth plate function was appropriate for a younger child.

These findings are therefore consistent with the hypothesis that catch-up growth is due to delayed senescence of the growth plate. Indeed, if the height SDS for adjusted age had increased or decreased over time, it would have implied that mechanisms other than growth plate senescence were involved. Although the actual data match the predictions of the delayed senescence hypothesis well, they do not provide a definitive proof of the hypothesis; it is possible that the catch-up growth is due to a completely different mechanism that happens to produce a growth curve that is a time-shift of the normal curve. For example, the neuroendocrine hypothesis, that catch-up growth is regulated by a central nervous system mechanism, does not predict any specific growth pattern, and therefore the current findings neither support nor refute that hypothesis. It is also possible that a gluten-free diet does not fully reverse the growth inhibition, or compliance with a gluten-free diet was not fully accomplished, and thus the observed catch-up growth curve was artifactually dampened.

Indeed, anecdotal observations of individual children have shown catch-up growth curves that appear too steep to be consistent with a delayed senescence mechanism alone (3;13). These observations suggest that an additional mechanism may contribute to human catch-up growth in some conditions, although it is possible that these individual cases might instead reflect individual confounding factors, for example, a pubertal growth spurt superimposed on catch-up growth.

We conclude that the pattern of catch-up growth during recovery from celiac disease is consistent with the hypothesis of delayed growth plate senescence. Analogous studies could be performed in children experiencing catch-up growth after other conditions. The delayed senescence hypothesis predicts that the time course of catch-up growth will vary dramatically with the age of the subjects studied. In infancy, the normal grow rate declines rapidly. Thus delayed growth plate senescence should produce a markedly increased growth rate in infants, and catch-up growth should occur over a brief time course. Conversely, in older children, the hypothesis predicts that catch-up growth should occur gradually, over years. Perhaps in the future, the resolution of noninvasive imaging methods will improve to the point where the histologic markers of growth plate senescence can be assessed in humans. Until then, we may have to extrapolate from animal studies, relying on bone age and linear growth rate to provide indirect tests of the delayed senescence hypothesis in children.

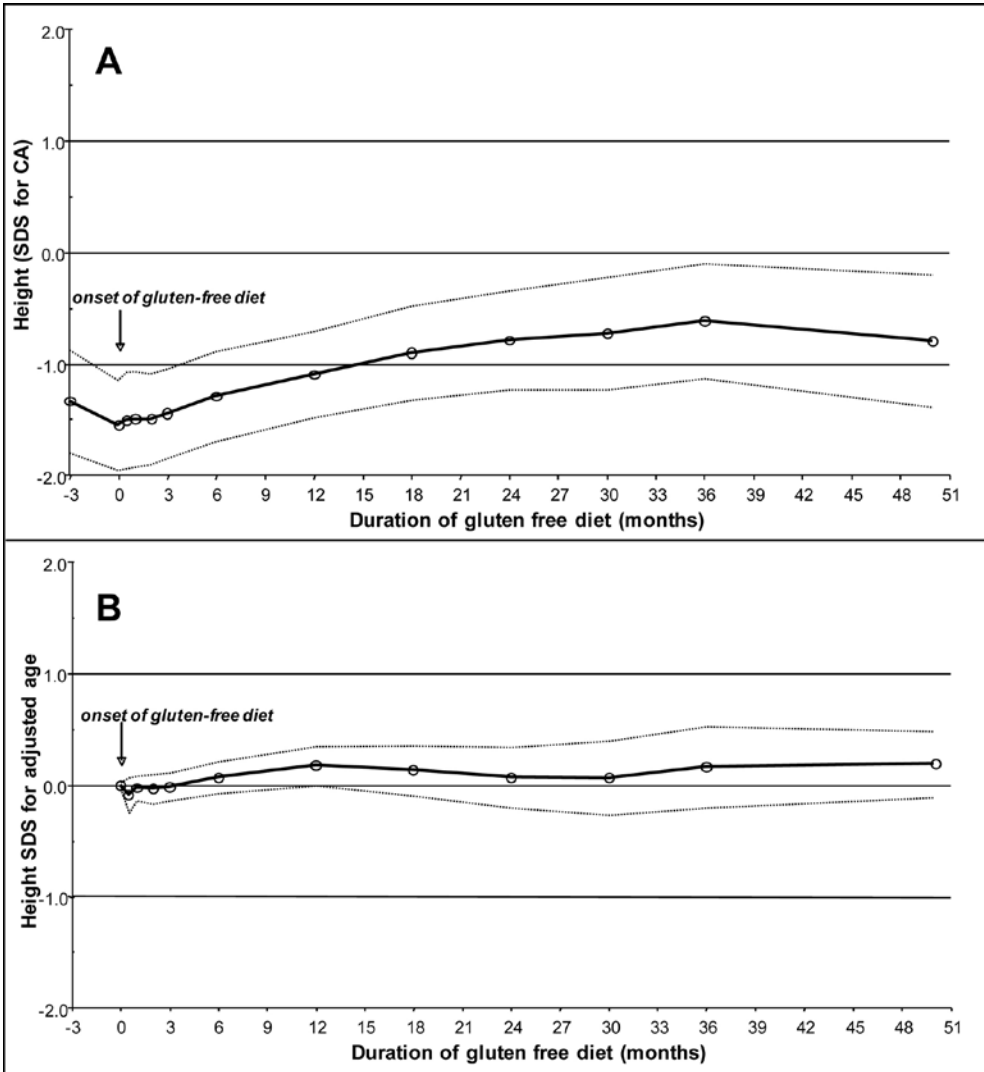


Figure 2

Height SDS for chronological age (A) and for adjusted age (B and C) after institution of a gluten-free diet for celiac disease. A, Before initiation of the gluten-free diet, the average height SDS for chronological age (CA) was negative, indicating short stature. On the gluten-free diet, the height SDS increased, indicating catch-up growth. B, Age was adjusted for height age (HA) at diagnosis. C, Age was adjusted for bone age (BA) at diagnosis. The upper and lower curves in each panel represent 95% confidence interval of the mean. In both B and C the height SDS for adjusted age remained close to 0, indicating that growth was normal for a younger child.

References

1. **Prader A, Tanner JM, von Harnack G** 1963 Catch-up growth following illness or starvation. An example of developmental canalization in man. *J Pediatr* 62:646-659
2. **Boersma B, Wit JM** 1997 Catch-up growth. *Endocr Rev* 18:646-661
3. **Tanner JM** 1963 REGULATION OF GROWTH IN SIZE IN MAMMALS. *Nature* 199:845-850
4. **Baron J, Klein KO, Colli MJ, Yanovski JA, Novosad JA, Bacher JD, Cutler GB, Jr.** 1994 Catch-up growth after glucocorticoid excess: a mechanism intrinsic to the growth plate. *Endocrinology* 135:1367-1371
5. **Nilsson O, Baron J** 2005 Impact of growth plate senescence on catch-up growth and epiphyseal fusion. *Pediatr Nephrol* 20:319-322
6. **Gafni RI, Weise M, Robrecht DT, Meyers JL, Barnes KM, De Levi S, Baron J** 2001 Catch-up growth is associated with delayed senescence of the growth plate in rabbits. *Pediatr Res* 50:618-623
7. **Weise M, De Levi S, Barnes KM, Gafni RI, Abad V, Baron J** 2001 Effects of estrogen on growth plate senescence and epiphyseal fusion. *Proc Natl Acad Sci U S A* 98:6871-6876
8. **Marino R, Hegde A, Barnes KM, Schrier L, Emons JA, Nilsson O, Baron J** 2008 Catch-up growth after hypothyroidism is caused by delayed growth plate senescence. *Endocrinology* 149:1820-1828
9. **Weise M, Flor A, Barnes KM, Cutler GB, Jr., Baron J** 2004 Determinants of growth during gonadotropin-releasing hormone analog therapy for precocious puberty. *J Clin Endocrinol Metab* 89:103-107
10. **Preece MA** 1988 Prediction of adult height: methods and problems. *Acta Paediatr Scand Suppl* 347:4-11
11. **De Luca F, Baron J** 1999 Skeletal maturation. *Endocrinologist* 9:286-293
12. **Boersma B, Houwen RH, Blum WF, van Doorn J, Wit JM** 2002 Catch-up growth and endocrine changes in childhood celiac disease. *Endocrine changes during catch-up growth. Horm Res* 58 Suppl 1:57-65
13. **Boersma B, Otten BJ, Stoeltinga GB, Wit JM** 1996 Catch-up growth after prolonged hypothyroidism. *Eur J Pediatr* 155:362-367

6

Genome wide screening in human growth plates at early and progressed stage puberty of a single patient suggests a role of Elk1, Stat5b and RunX2 in growth plate maturation.

Joyce Emons¹, Bas E. Dutilh², Eva Decker³, Heide Pirzer³, Carsten Sticht⁴, Norbert Gretz⁴, Gudrun Rappold³, Jan Maarten Wit¹, Marcel Karperien^{5,6}.

¹Dept of Paediatrics, Leiden University Medical Center, Leiden, the Netherlands;

² Centre for Molecular and Biomolecular Informatics, Radboud University Nijmegen Medical Center, Nijmegen, the Netherlands;

³Department of Human Molecular Genetics, University of Heidelberg, Heidelberg, Germany;

⁴Medical Research Center, Medical Faculty Mannheim, Mannheim, Germany;

⁵Dept of Tissue Regeneration, University of Twente, 7522 NB Enschede, the Netherlands;

⁶Dept of Endocrinology and Metabolism, Leiden University Medical Center, 2300 ZA Leiden, The Netherlands.

Abstract

In late puberty, estrogen is responsible for the deceleration of growth by stimulating growth plate maturation. The mechanism of action is largely unknown. We obtained pubertal growth plate specimens of the same girl at Tanner stage B2 and B3, which allowed us to address this issue in more detail. Histological analysis showed that progression of puberty coincided with characteristic morphological changes associated with growth plate maturation, such as decreases in total growth plate height ($p=0.002$), height of the individual zones ($p<0.001$) and an increase in intercolumnar space ($p<0.001$). Microarray analysis identified 394 genes (72% upregulated, 28% downregulated) changing with progression of puberty. Overall changes in gene expression were small (average 1.38-fold upregulated and 1.36-fold downregulated genes). The 394 genes mapped to 13 significantly changing pathways ($p<0.05$) in majority belonging to extracellular matrix, cell cycle and cell death, all related to growth plate maturation. We next scanned the upstream promoter regions of the 394 genes for the presence of evolutionarily conserved binding sites for transcription factors implemented in growth plate maturation such as Estrogen Receptor, Androgen Receptor, Elk1, Stat5b, CREBP and Runx2. High quality motif sites for Runx2 (87 genes), Elk1 (43 genes) and Stat5b (31 genes), but not estrogen receptor, were evolutionarily conserved, indicating their functional relevance across primates.

In conclusion, our data suggest a role for Runx2, Elk1 and Stat5b in growth plate maturation and provides suggestive evidence that the effect of estrogen on growth plate maturation is not mediated by activating genomic estrogen signalling in growth plate chondrocytes.

Introduction

Longitudinal growth occurs at the epiphyseal growth plate, a thin layer of cartilage entrapped between epiphyseal and metaphyseal bone at the distal ends of the long bones. In the normal growth plate, immature cells are located towards the epiphysis, called the resting zone, with mature chondrocytes in the proliferating zone, which hypertrophy in the hypertrophic zone adjacent to this (1). At the beginning of puberty longitudinal growth rate first increases, but with progression of puberty, growth rate is decelerating due to growth plate maturation, and at the end of puberty the growth plate eventually disappears due to epiphyseal fusion. The molecular mechanisms underlying these distinct phases of growth plate activity during puberty are largely unknown but a role for estrogen has been suggested (2;3).

Endocrinological observations suggest that at the beginning of puberty relatively low levels of estrogen initiate the growth spurt. With progression of puberty, estrogen levels further increase which drives growth plate maturation and finally growth plate fusion. The most compelling evidence for a role of estrogen is provided by clinical observations in a patient with an inactivating mutation in the estrogen receptor alpha and in patients with a mutation in the aromatase gene resulting in lack of estrogen. These patients did not experience a growth spurt, and lack growth plate maturation and fusion (4;5). Furthermore, from clinical observations it is known that high levels of estrogen inhibit longitudinal bone growth (6).

The mechanism by which estrogens exert these effects on growth plate activity is not fully understood. It has been postulated that estrogen accelerates the senescent decline of the growth plate (7). Senescence is a term for the structural and functional changes over time in the growth plate, such as a gradual decline in the overall growth plate height, proliferative zone height, hypertrophic zone height, size of hypertrophic chondrocytes, proliferation rate and column

density (7). It is believed that the growth plate fuses when senescence reaches a critical point in the growth plate. Recent evidence indicates that senescence might occur because stem-like cells in the resting zone have a finite proliferative capacity, which is exhausted gradually. This process is accelerated by estrogen (8;9).

Estrogen induces cell responses by activating the so-called genomic signaling pathway involving the nuclear estrogen receptor alpha (ERa) and beta (ERb) or of a non-genomic signaling pathway involving membrane bound receptors like GPR30 resulting in activation of adenylyl cyclase and MAPKs (10-13). ERa, ERb and GPR30 are all expressed in human growth plate chondrocytes (14;15). Their expression is not limited to the stem-like cells of the resting zone, which are the main target cells of estrogen action based on the senescence hypothesis, but is more broadly distributed in the growth plate. It is still largely unknown whether the pubertal phenomena in relation to growth rate are caused by direct effects of estrogen on chondrocytes or by indirect effects via, for example, activation of the Growth Hormone/IGF-I axis.

During puberty both sex steroids, growth hormone (GH) and IGF-1 levels increase (16). It is well known that GH and IGF-1 can increase growth velocity as well as accelerate bone maturation measured by a decrease in growth plate height in children (17;18). Also receptors for GH and IGF-1 are present on human chondrocytes (19), indicating that both hormones can have direct effects on the growth plate. Stimulation of the GH-receptor activates an intracellular signal transduction cascade eventually converging to the transcription factor Stat5b (20). Likewise, IGF-1 signalling results in the activation of signalling routes involving for example the transcription factor Elk1 (21). The exact contributions of these hormones in growth plate maturation and epiphyseal fusion still need to be clarified.

Alternatively, estrogen may regulate, either directly or indirectly, the expression of paracrine regulators of growth plate activity such as Parathyroid hormone-related peptide (PTHrP) and Indian hedgehog (Ihh). These secreted growth factors coordinate endochondral ossification by regulating chondrocyte proliferation and differentiation as well as osteoblast differentiation (22;23). PTHrP signals, amongst others, via activation of the cyclic AMP response element binding protein (24). Both factors have been identified in the postnatal growth plate and have been postulated to play a role in growth plate fusion (25).

In the growth plate, the transcription factor Runx2 plays an important role in the regulation of chondrocyte hypertrophy and the associated changes in the extracellular matrix (26). The expression and activation of this transcription factor is in part regulated by PTHrP and Ihh (27). Studies on the regulation of growth plate activity during puberty are hampered by the lack of easy accessible and representative animal models. For example, rodents do not fuse their growth plates at the end of sexual maturation and discrepancies exist between human and mouse models with respect of the role of ERa in growth plate regulation (28-30). In addition, human growth plate specimens are very difficult to obtain.

We were fortunate to obtain growth plate samples of a single patient at two different stages of puberty. The growth plate tissues are genetically identical and from the same anatomical location. In this study we have performed a morphological analysis of these growth plate specimens complemented with a detailed microarray and bioinformatic analysis and identified 394 differentially expressed genes which were representative for processes that occur during growth plate maturation. We subsequently searched the promoter regions of these genes for evidence of involvement of hormones and paracrine factors in their expression regulation during growth plate maturation. Assuming that the regulation of processes such as growth plate maturation is conserved across primates, we identified functional transcription factor binding sites as those motif sites with a better evolutionary conservation than sites occurring by chance, related to

phylogenetic footprinting (31). More specifically, we searched the promoter regions of genes that were differentially expressed in the two growth plate specimens for evidence of direct effects of estrogen, androgen, GH, IGF-I, PTHrP and Runx2 on their expression.

Material and Methods

The study was approved by the local medical ethical committee and informed consent was obtained. Two epiphyseal growth plate samples, from the left and right proximal femur were obtained from the same girl with a 1 year interval. In this period the girl progressed from early (Tanner B2) to a progressed stage of puberty (Tanner B3). The patient suffered from cerebral palsy and underwent resection of her femur head twice because of painful luxations. She did not use any long-term medication. Both epiphyseal samples were longitudinally cut with a bone saw and pieces were covered by Tissue-Tek (Sakura Finetek Europe B.V., Zoeterwoude, the Netherlands), directly frozen in liquid isopentane and stored at -80°C or fixed in 10% formalin, decalcified with EDTA and embedded in paraffin.

Histological analysis

Paraffin embedded samples were cut into longitudinal 5 mm thick sections using a Reichert Jung 2055 microtome (Leica, Rijswijk, The Netherlands). The sections were mounted on glass slides and stained with Haematoxylin. Total height was measured at three points parallel to the chondrocyte columns, height of each zone was measured at 10 different places for each zone and results were averaged. The space between columns in the proliferative and hypertrophic zone was measured at 20 different places.

RNA isolation

Bone was removed from both epiphyseal growth plate samples and 40 μm thick sections were cut with a cryostat. Every fifth section was followed by a 5 μm thick section which was studied with Hematoxylin staining to ensure lack of bone contamination. Total RNA isolation was performed with an optimized method for RNA extraction from cartilage as described by Heinrichs et al. (32) except that the protocol was started by homogenizing the sections in 1 ml guanidine thiocyanate solution. RNA extraction was followed by purification with a RNeasy kit according to the manufacturers protocol (Qiagen) and quality and integrity of each sample were checked with the Agilent 2100 Bioanalyzer.

Microarray

RNA was tested by capillary electrophoresis on an Agilent 2100 bioanalyzer (Agilent) and high quality was confirmed. 100 ng of total RNA was then amplified and labeled using the GeneChip Two-Cycle cDNA Synthesis Kit (Affymetrix) and the MEGAscript T7 Kit (Ambion). The labeled cRNA was further used for the hybridization to Affymetrix Human Genome U133 PLUS 2.0 Array Genechips and hybridized according to Affymetrix manufacturer's protocol. RNA was extracted from two different sections of each growth plate. A Custom CDF Version 11 with Entrez based gene definitions was used to annotate the arrays (33). The Raw fluorescence intensity values were normalized applying quantile normalization using a commercial software package SAS JMP7 Genomics, version 3.1, from SAS (SAS Institute, Cary, NC, USA). Gene annotation was obtained through the Affymetrix NetAffx website (<http://www.affymetrix.com/analysis/index.affx>). The quality control, normalisation and statistical modelling were performed by array group correlation,

mixed model normalisation and mixed model analysis respectively. For the presence/absence analysis for a single-array, GeneChip® Operating Software version 1.4 (GCOS) from Affymetrix was used. Analysis of differential gene expression was based on loglinear mixed model of perfect matches (34). A false discovery rate of $\alpha=0.05$ with FDR-correction for multiple testing was used to make a selection of most differentially expressed genes. These affected genes were further investigated to identify pathways that are likely to be affected by differential expression. Pathways were generated either from the KEGG database (Kyoto Encyclopedia of Genes and Genomes, <http://www.genome.ad.jp/kegg/pathway.html>) or from manual annotation. The selection of affected genes were also analysed with a genome wide analysis of gene sets defined by the Gene Ontology (GO) Consortium and classified as GO-terms (35). In this analysis, an enrichment of affected genes within a GO-term suggests that this GO-term is affected by maturation of the growth plates. Analyses were done with the Gene Ontology Tree Machine program (<http://bioinfo.vanderbilt.edu/gotm>). The raw and normalized data are deposited in the Gene Expression Omnibus database (<http://www.ncbi.nlm.nih.gov/geo/>; accession No. GSE-18338).

Reverse transcription- Polymerase Chain Reaction (RT-PCR)

RNA was reverse transcribed into cDNA using First Strand cDNA Synthesis kit for qPCR (Roche Diagnostics GmbH, Mannheim, Germany) according to the manufacturer's instructions. Expression of collagen 3A1 (COL3A), CDKN1B (p27Kip1), dolichyl-phosphate mannosyltransferase polypeptide 1 (DPM1), Thrombospondin 4 (THBS4), and ribosomal protein L15 (RPL15) mRNA was quantified by real-time PCR using the Bio-Rad iCycler with SYBR Green. QuantiTect Primer Assays for each of these genes were purchased from Qiagen (Qiagen Benelux B.V., Venlo, the Netherlands) and used according to the manufacturer's protocol. Threshold cycles were estimated and averaged for the triplicates. Relative amounts of mRNA were normalized to β_2 -microglobulin expression in the same sample to account for variability in the initial concentration, quality of total RNA and in the efficiency of the reverse transcription reaction. Delta Ct was calculated by extracting the threshold cycle for β_2 -microglobulin from the threshold cycle for the gene of interest followed by calculation of the change in delta Ct with progression of puberty.

Transcription factor binding sites

Upstream regions of 5000nt were downloaded from the 394 genes that changed with progression of puberty. The promoter regions were scanned for six transcription factor binding motifs selected from Jaspar 3.0 (36) and Transfac 7.0 (<http://www.gene-regulation.com>). The motifs were (see supplemental table 1): estrogen receptor (Jaspar MA0112), androgen receptor (Jaspar MA0007), Elk-1 (Transfac M00025), CREB (Jaspar MA0018), Runx2 (Jaspar MA0002) and STAT5B (Transfac M00459). A selection was made of the fraction of the highest scoring positions as potential regulatory sites. Two types of randomization controls were included. Firstly, we scanned the 5,000nt upstream regions of 100 sets of 394 randomly chosen genes for the six motifs mentioned above (random genes). Secondly, we scanned the 5,000nt upstream regions of the 394 differentially expressed genes for 100 versions of the six motifs with randomized columns (random motifs). Because we expected that meaningful binding sites may be distinguished from spurious high scoring hits by their evolutionary conservation, we assessed the conservation of each of the binding sites across nine primate genomes. For this purpose the phastCons (37) primates conservation track was downloaded from the UCSC Genome Browser download page (38) and the average conservation score for all positions aligned with the motif were calculated.

Results

Quantitative Histology

Histology of the samples showed a clear decrease in overall height of the growth plate at the more progressed stage of puberty (figure 1). This was confirmed by quantitative measurements showing a significant decrease in the average height of the growth plate, and a significant decrease in the height of the resting, proliferative and hypertrophic zone at Tanner stage 3. The mean space between columns was increased in the more matured growth plate. These data are summarized in table 1.

Gene expression microarray analysis

RNA of both growth plate samples was amplified, labelled and subjected to Affymetrix microarray analysis (HG-U133 Plus 2) in duplicate. The technical and biological reproducibility was good, with correlations above 0.97. The raw and normalized data are deposited in the Gene Expression Omnibus database (<http://www.ncbi.nlm.nih.gov/geo/>; accession no. GSE-XXXX). Presence and Absence analysis for each probe set was employed by using the GeneChip® Operating Software version 1.4 (GCOS) from Affymetrix. On average 5043 genes were present; with progression of puberty the number of genes present in the growth plate increased slightly (5069 vs 5016) (table 2). The microarray data was validated by quantitative PCR for 5 randomly chosen genes. Similar trends in gene expression (up- or downregulation) were found in qPCR and microarray analysis for all genes (Figure 2). THSB4 showed a more pronounced increase in expression in the microarray results compared to the qPCR results.

Analysis with a loglinear mixed model of perfect matches and a false discovery rate of $\alpha=0.05$ and a Bonferroni-correction for multiple testing revealed 460 affymetrix probe IDs changing in expression, of which 330 were upregulated and 130 were downregulated. Using BioMart 0.7 (39) these probes were mapped to 394 genes changing with maturation of the growth plate (see table 2 supplemental data). The overall changes in gene expression were small; on average 1.38-fold increase for upregulated and 1.36-fold decrease for down regulated genes. Cytokine-like 1 was the most upregulated gene showing a 6.48 fold increase in expression and the most affected downregulated gene, pannexin 3, showed a 2.02 fold decrease in expression level.

The 394 differentially expressed genes were further investigated with Fisher's exact tests using SAS and the KEGG database. 111 of the 394 genes could be mapped to 13 enriched pathways ($p<0.05$) (Table 3). Several of the differentially expressed genes were present in more than one of the above pathways. These pathways were mostly related to the extracellular matrix, cell communication and metabolism. We studied these genes independently for their up or down regulation (see table 3 supplemental data). Most genes, 89 out of 111, were upregulated in the growth plate with progression of puberty. In addition, differentially expressed genes were further investigated with the Gene Ontology Tree Machine. This revealed 49 different Gene Ontology terms (GO terms) relatively enriched ($p<0.01$). Enriched GO terms were related to the extracellular matrix, cell cycle, cell growth and ligase activity (see figure 1 supplemental data).

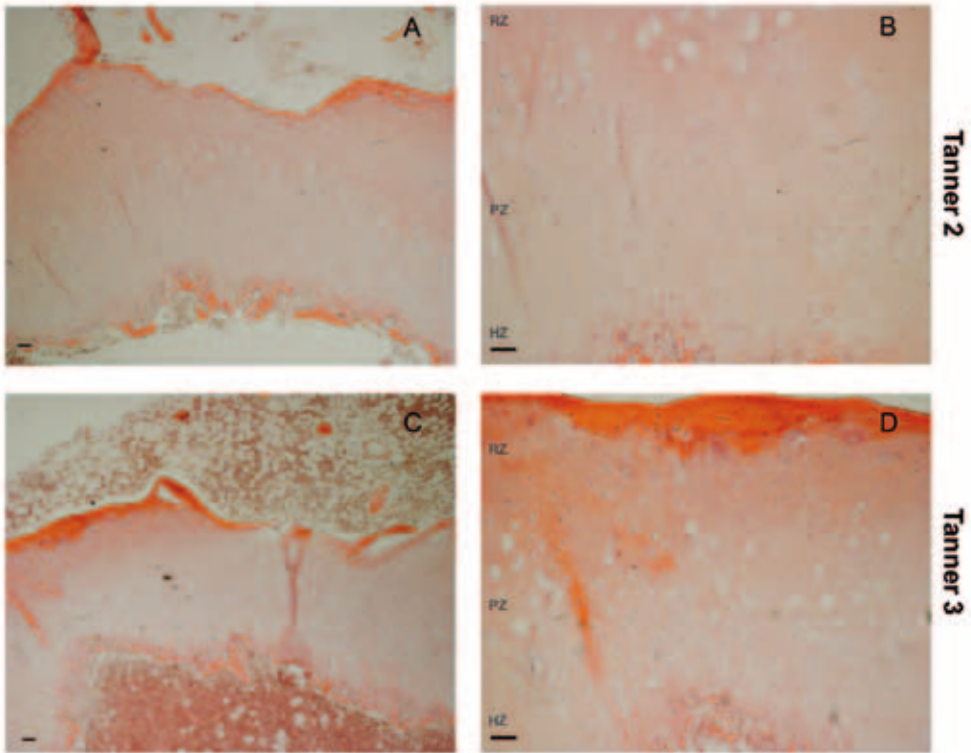


Figure 1: Histology of growth plate Tanner 2 and Tanner 3.

Panel A and B; pictures of growth plate of patient in Tanner stage 2 in respectively 40x and 100x magnification. Panel C and D; pictures of growth plate of patient in Tanner stage 3 in respectively 40x and 100x magnification. The more mature growth plate (Tanner stage 3) shows a decrease in total growth plate height, a decrease in height of each separate zone and an increase in the mean space between columns. RZ means resting zone, PZ means proliferative zone and HZ means hypertrophic zone. Bars indicate 200µm.

Table 1: Quantitative Histology growth plate Tanner stage 2 and 3.

	Tanner stage 2	Tanner stage 3	P-value
Total height (mm)	0.16 ± 0.01	0.097 ± 0.012	0.002
Height resting zone (mm)	0.073 ± 0.003	0.037 ± 0.009	<0.001
Height proliferative zone (mm)	0.047 ± 0.003	0.033 mm ± 0.004	<0.001
Height hypertrophic zone (mm)	0.024 ± 0.003	0.016 ± 0.003	<0.001
Intercolumn space (mm)	4.87*10 ⁻⁴ ± 0.34*10 ⁻⁴	7.52*10 ⁻⁴ ± 0.45*10 ⁻⁴	<0.001

Table showing measurements of total height, height of each individual zone and intercolumn space of the growth plate in Tanner stage 2 and the more progressed growth plate in Tanner stage 3.

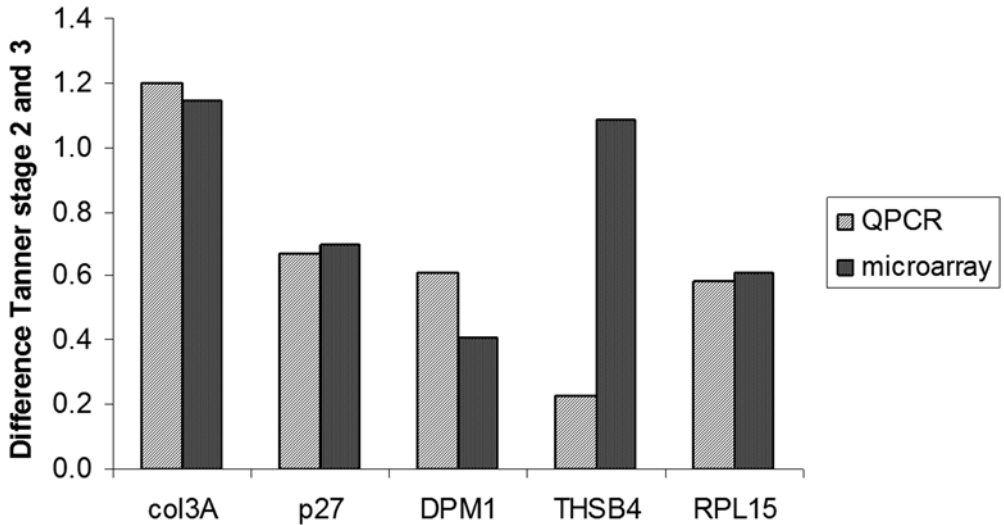


Figure 2: RT-PCR validation of microarray data.

Correlation between RT-PCR and microarray results for (A) collagen 3A1 (COL3A), (B) Thrombospondin 4 (THBS4), (C) CDKN1B (p27Kip1), (D) ribosomal protein L15 (RPL15), (E) dolichyl-phosphate mannosyltransferase polypeptide 1 (DPM1). Results are expressed as changes with progression of puberty (value Tanner B3- Tanner B4) for both the RT-PCR ($\Delta Ct = Ct_{\text{gene of interest}} - Ct_{\beta 2\text{-microglobulin}}$) and microarray results (least square means). Similar trends in gene expression (up- or downregulation) were found in qPCR and microarray analysis for all genes, however THSB4 showed a more pronounced increase in expression in the microarray results compared to the qPCR results.

Table 2: Number of expressed and non-expressed genes.

	Absent	Present	Unknown
Growth plate Tanner 2	10255	5016	5555
Growth plate Tanner 3	10118	5069	5639

Table showing the number of genes absent or present in each of the growth plate. In the column defined as unknown is the number of genes not consistent in the present/absent analysis.

Table 3: Pathways significantly changing with progression of puberty.

	pathway	genes found	total genes pathway	%	p.
1	Proteasome	9	23	39	***
2	Cholera_infection	10	30	33	***
3	Oxidative_phosphorylation	20	89	22	***
4	N_Glycan_biosynthesis	9	27	33	**
5	ATP_synthesis	9	28	32	**
6	Adherens_junction	14	60	23	**
7	Aminosugars_metabolism	6	17	35	**
8	Regulation_of_autophagy	6	17	35	**
9	Ribosome	9	35	26	**
10	ECM_receptor_interaction	14	67	21	**
11	Cell_cycle	15	84	18	*
12	Cell_Communication	13	74	18	*
13	Ubiquitin_mediated_proteolysis	7	32	22	*

*= $p < 0.05$, **= $p < 0.01$, ***= $p < 0.001$

Table showing the 13 significant pathways associated with pubertal maturation of the growth plate.

Table 4: Top 0.001% genes with a transcription factor binding site for 6 motifs; Estrogen receptor, Elk-1, STAT5B, RunX2, Androgen receptor and CREB.

Motif	no. genes	% of 394 genes	p-value	average conservation score	% genes up	% genes down
Estrogen receptor	49	13	0,25	0,19	73	27
Elk-1	43	9	<0,01	0,33	70	30
STAT5B	31	8	0,04	0,25	81	19
RunX2	87	22	<0,01	0,23	76	24
Androgen receptor	46	12	0,07	0,22	80	20
CREB	44	11	0,16	0,20	75	25

Number and percentage of genes plus the average conservation score containing an transcription factor binding site for each of the 6 motifs. Results are presented for the top 0.0001% of sites and 0.001% of sites. For each motif is the percentage given of genes going up and down in expression.

Transcription factor binding sites

We next scanned the promoter regions of the 394 differentially expressed genes for the presence of conserved transcription factor binding sites. We limited our search to transcription factor binding sites which are activated by hormones and paracrine factors that have previously been implicated in growth plate maturation: Estrogen response elements (EREs) and androgen response elements (ARE) for activity of sex-steroids, Stat5b for GH (20), Elk-1 for IGF-I (21), Cyclic AMP response element (CREB) for PTHrP (24) and Runx2 for growth plate hypertrophy (40). We limited our analysis to the top 0.001% of the highest scoring motifs and determined the evolutionary conservation score of these sites. We found 215 genes with one or more transcription factor binding motif using the cut off of 0.001% of the top scoring motifs. The motifs and genes are listed in table 4 of the supplemental data. As a control, a similar analysis was performed using 100 sets of 394 randomly chosen genes. In addition, the promoter regions of the 394 genes were screened with randomized motifs for each transcription factor binding site and their evolutionary conservation score was also determined. These randomizations were used to calculate the statistical confidence score (p-value). The data are summarized in table 4.

We found 87 genes with a transcription factor binding site for RUNX2, 76% of genes going up and 24% going down in expression. The average evolutionary conservation score of the motif was significantly higher ($p < 0.01$) compared to the findings in randomly chosen genes. Likewise, evolutionary conservation of the ELK-1 (49 genes) and STAT5B (31 genes) binding sites in the panel of 394 genes associated with growth plate maturation was significantly higher than random. We subsequently repeated the statistical analysis of the conservation score by including the top 0.01, top 0.1, top 1 and top 10% of the highest scoring sites in the analysis. By including up to 10% of the highest scoring sites of ELK-1 and STAT5B, the evolutionary conservation score was still significantly higher than for the controls. Significance for RUNX2 was lost by increasing the number of motif sites from the top 0.001 to the top 0.01 % (data not shown).

In marked contrast, the average evolutionary conservation scores of EREs (49 genes), AREs (46 genes) and CREB (44 genes) in the set of 394 genes were not significantly higher than in the randomly chosen controls.

In summary, the highest scoring motif sites for RUNX2, Elk-1 and STAT5B were also the most conserved across primates, suggesting that the presence of these motifs may play a functional role in the regulation of expression of the genes related to growth plate maturation. Conversely, high scoring ER, AR and CREBP motif sites were not better conserved than those in random gene sets, suggesting that their presence is coincidental.

Discussion

In the present study we compared gene expression levels in two epiphyseal growth plate samples obtained from one girl at early and mid puberty (Tanner stage 2 and 3) with a 1 year interval. Maturation of the epiphyseal growth plate in mid puberty is associated with a multitude of changes in morphology and expression levels of genes associated with the extracellular matrix, cell death, cell communication and metabolism. In the panel of 394 genes changing with growth plate maturation we found evidence, based on the evolutionary conservation of the highest scoring transcription factor binding sites, for regulation of expression by the transcription factors RUNX2, ELK-1 and STAT5B.

Histological experiments and measurements showed a clear decrease in total growth plate height with maturation. This is in line with the observations in rabbits, where growth plate height gradually declines with age and even more rapidly under the influence of estrogen (7). In humans it is known and widely used for assessing skeletal maturation that radiographically the epiphyseal width varies in different stages and declines in its progress toward maturity. In the more mature growth plate, columns were more widely spaced with more intervening extracellular matrix. These changes are described as senescence of the growth plate and confirm earlier results in rabbits and rats (7;41). Histological observations and measurements were in line with the microarray results, showing significant changes in the extracellular matrix compartment with maturation of the growth plate. The ECM receptor interaction pathway changed significantly with 14 out of 67 genes affected in this pathway. Associated with the extracellular matrix are the aminosugars metabolism pathway and the N-Glycan biosynthesis pathway, both changing significantly with maturation. The ECM is composed of a variety of macromolecules like proteoglycans and polysaccharides (glycosaminoglycans) that are secreted locally and assembled into an organized network (42;43). Most genes in these three pathways are upregulated with maturation suggesting an increase in pathway activity and extracellular matrix production. In addition to the pathway and morphology data, the GO term analyses also showed many enriched GO categories that are involved and associated to the extracellular matrix, which strengthens our findings. Blanchard et al demonstrated previously that estrogens and testosterone stimulate proteoglycan synthesis *in vitro* in male and female human epiphyseal chondrocytes, consistent with our results (44). Besides extracellular matrix pathways, also cell death pathways were enriched in the differentially expressed gene sets, e.g. proapoptotic and anti-apoptotic genes, but also genes involved in the regulation of autophagy. Apoptosis and autophagy are closely related and there is an overlap in signaling proteins (45;46). Previously, we found no signs of classical apoptosis in the human growth plate with pubertal maturation and epiphyseal fusion (47). The results of this study are in line with this and suggestive for a non-classical and perhaps intermediate mechanism of different types of cell death.

The overall change in gene expression levels in growth plate chondrocytes with progression of puberty was unexpectedly small, particularly since puberty is associated with dramatic changes in growth velocity and hormone levels like sex steroids, Growth Hormone and IGF-I (48-50). Our microarray data is in line with the histological changes observed with growth plate maturation providing support that the differentially expressed gene set is representative for the changes that occur during growth plate maturation. We hypothesized that analysis of the promoter regions of these genes may provide clues for transcription factors and signaling pathways that are involved in growth plate maturation. More specifically the promoter regions were analyzed for the presence

of evolutionarily conserved binding sites for Estrogen and Androgen Receptors, ELK-1 for IGF-I, STAT5b for GH, CREB for PTHrP and RUNX2 for growth plate hypertrophy.

Despite strong clinical and experimental evidence for the role of sex steroids and in particular estrogen in growth plate maturation, the potential EREs and also AREs in the promoter regions of the 394 genes were not conserved in other primate species. Although these motif sites may still be functional in human, the fact that they are uniquely human makes this less likely since sequences conserved along species are more likely to have functional roles (37). Thus, estrogen may not have a direct genomic effect in pubertal growth plate maturation. This contrasts with findings of Windahl et al., who previously detected an ERE-mediated response in the hypertrophic zone of mice (51). This discrepancy might be explained by a species difference, as illustrated before by the divergent phenotypes of the ER α knockout mice and man with respect to growth plate regulation. Our data does not exclude a role for non-genomic estrogen signalling in growth plate maturation nor for an indirect effect of estrogen. Likewise, no enrichment was found for CREB binding sites which are activated by intracellular cAMP levels via for example PTHrP.

Interestingly, the high scoring ELK-1, STAT5b and RUNX2 motif sites were conserved across primates. ELK-1 and STAT5b are activated by, amongst others, IGF-I and GH for which receptors are present in growth plate chondrocytes. In animal models local effects of GH and IGF-1 on growth plate chondrocytes have been established (52;53). Besides the increase in levels of estrogen, also the levels of GH and IGF-I increase significantly with the progression of puberty. In addition, it is well known that GH-treatment accelerates growth as well as growth plate maturation, either directly or indirectly via IGF-I. Our conservation analysis of the transcription factor binding motifs in the promoters of differentially expressed genes supports a direct role for GH and IGF-I in growth plate maturation, resulting in activation of STAT5b and ELK-1 mediated gene transcription, respectively. The effect of estrogen on the activity of the GH/IGF-I axis is well appreciated, demonstrated by increasing GH levels in patients with oral estrogen treatment (54;55). This may suggest that effects of estrogen on growth plate maturation might be mediated, at least in part, by GH and/or IGF-I.

Runx2 plays an important role in chondrocyte maturation and is involved in the production of bone matrix proteins (56). Our results are in line with this hypothesis, since we found many genes changing with maturation of the growth plate in puberty that contained evolutionarily conserved transcription factor binding site for Runx2. Previous studies have shown that Runx2 can mediate actions of estrogen in an osteoblastic cell line and that selective estrogen receptor modulators like tamoxifene and raloxifene can increase Runx2 promoter activity in an osteosarcoma cell line (57;58). This provides an additional mechanism by which estrogen can indirectly influence growth plate maturation.

While the changes in growth plate morphology are in line with the senescence hypothesis, our data do not allow testing the proposed effect of estrogen on the depletion of stem-like cells in the growth plate with progression of puberty.

The major limitation of our study is the small sample number. However these growth plate samples are unique and enable a longitudinal analysis within one patient, therefore excluding genetic confounders. Adult height is determined for 80-90% by genetic factors (58;59). Including additional patients would therefore result in increasing variability, which would complicate all subsequent analysis. To the best of our knowledge, no other microarray studies have been performed on human growth plate tissues. The observed changes in gene expression and subsequent pathway analysis were fully in line with morphological changes that were characteristic for growth plate maturation in animal studies. In addition, microarray data were confirmed by qPCR. This strengthens our

confidence that the set of 394 genes is representative for changes in growth plate maturation and that our findings are biologically relevant. However, additional studies have to be done in a larger number of samples and with more pubertal stages to confirm our findings.

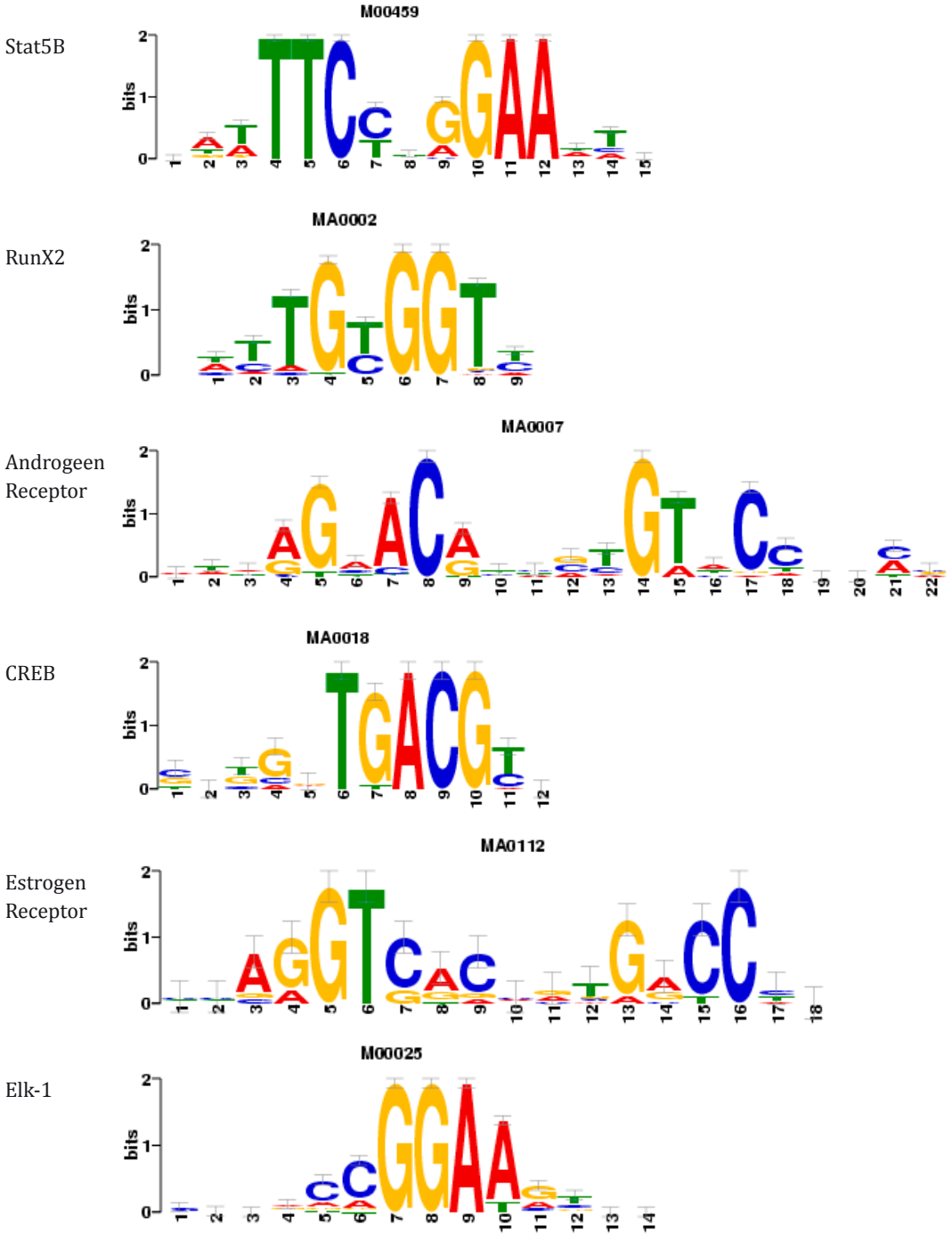
In conclusion, maturation of the epiphyseal growth plate in mid-puberty is associated with morphological changes in line with the senescence theory. This was corroborated by a multitude of changes in gene expression. Thirteen pathways were affected with maturation, several related to the extracellular matrix, the cell cycle, and programmed cell death. Evolutionary conservation of binding sites provides evidence for a direct role for GH, IGF-I and RUNX2 in growth plate maturation. We did not find support for direct genomic effects of estrogen, suggesting that the well appreciated role of estrogen in growth plate maturation might perhaps be indirect by modulating GH, IGF-I and RUNX2 activity.

Acknowledgement and funding

The authors thank the orthopaedic surgeons in the Leiden University Medical Center for providing the growth plate samples.

This study was supported by a Research Unit grant of the European Society for Paediatric Endocrinology. J. Emons was supported by a grant from ZonMW, the Netherlands Organisation of Health and Research and Development (grant number 920-03-358). E. Decker and H. Pirzer were supported by a grant from the Deutsche Forschungsgemeinschaft.

Supplemental table 1



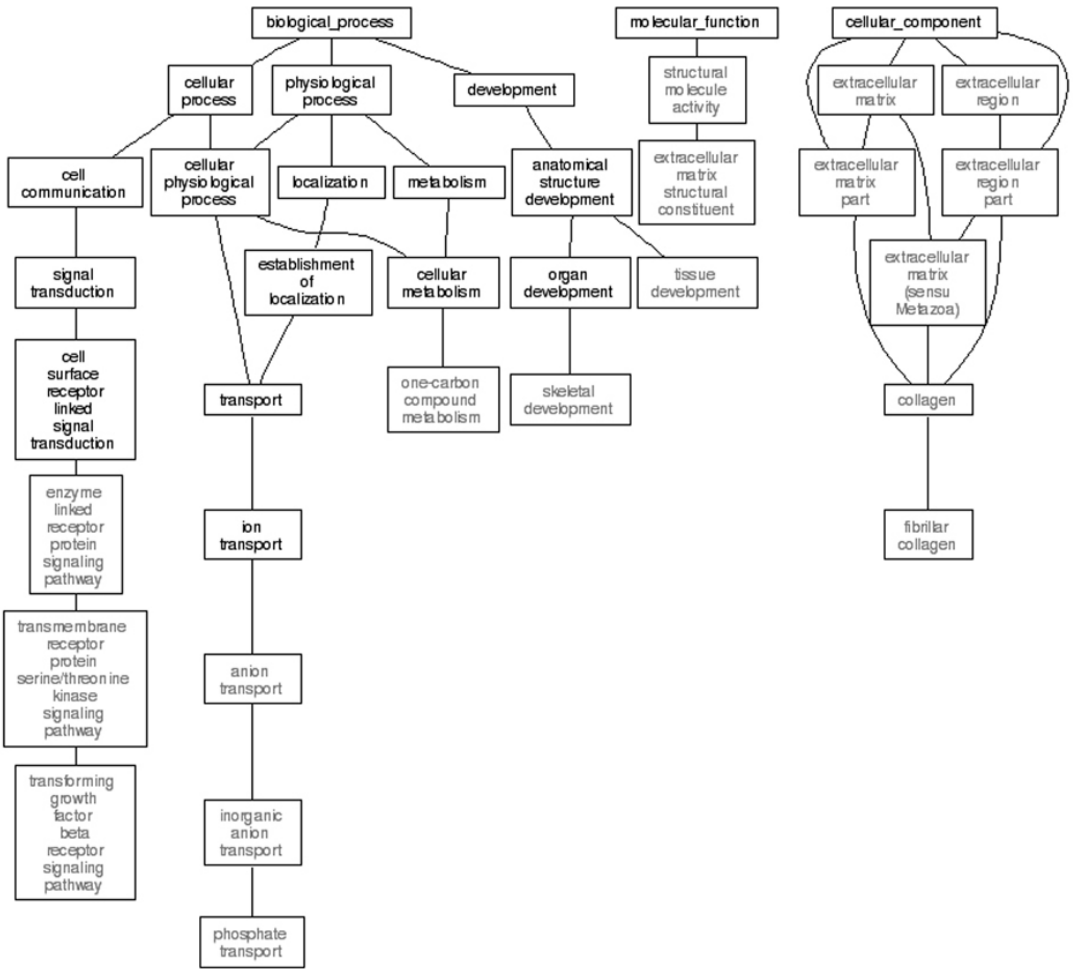
Supplemental table 2

Gene symbol	Ensemble ID	Gene symbol	Ensemble ID	Gene symbol	Ensemble ID
ABLIM1	ENSG00000099204	CD59	ENSG00000085063	FAM134B	ENSG00000154153
AC005921.3-1	ENSG00000108848	CDKN1B	ENSG00000111276	FAM162A	ENSG00000114023
AC010642.5-1	ENSG00000166718	CFH	ENSG00000000971	FAM70A	ENSG00000125355
AC015922.3	ENSG00000220036	CFL2	ENSG00000165410	FAM96A	ENSG00000166797
AC022868.10-1	ENSG00000215034	CHCHD4	ENSG00000163528	FAU	ENSG00000149806
AC091047.10-3	ENSG00000218599	CHMP2B	ENSG00000083937	FBLN7	ENSG00000144152
ACADM	ENSG00000117054	CHMP4A	ENSG00000100931	FBXO28	ENSG00000143756
ACBD3	ENSG00000182827	CILP	ENSG00000138615	FCGBP	ENSG00000090920
ACPL2	ENSG00000155893	CIRBP	ENSG00000099622	FECH	ENSG00000066926
ACTL6A	ENSG00000136518	CLC	ENSG00000105205	FGD2	ENSG00000146192
ADAMTS9	ENSG00000163638	CLDND1	ENSG00000080822	FKBP5	ENSG00000096060
ADD3	ENSG00000148700	CLEC11A	ENSG00000105472	FKBP7	ENSG00000079150
AGPAT5	ENSG00000155189	CLTA	ENSG00000122705	FLRT3	ENSG00000125848
AGPS	ENSG00000018510	CLU	ENSG00000120885	FMOD	ENSG00000122176
AL121893.21-2	ENSG00000214612	CNN3	ENSG00000117519	FNDC1	ENSG00000164694
AL157394.15	ENSG00000180139	CNOT8	ENSG00000155508	FOSB	ENSG00000125740
AL662789.11	ENSG00000198599	COL10A1	ENSG00000123500	FOS	ENSG00000170345
ALS2CR4	ENSG00000155755	COL3A1	ENSG00000168542	FST	ENSG00000134363
ANAPC5	ENSG00000089053	COL6A3	ENSG00000163359	FUBP1	ENSG00000162613
ANKRD13C	ENSG00000118454	COL9A1	ENSG00000112280	FUT11	ENSG00000196968
ANXA1	ENSG00000135046	CoTC_ribozyme	ENSG00000221031	FXYD6	ENSG00000137726
ANXA7	ENSG00000138279	COX4NB	ENSG00000131148	FZD6	ENSG00000164930
ARF4	ENSG00000168374	COX7A2	ENSG00000112695	GABARAPL2	ENSG00000034713
ARL6IP1	ENSG00000170540	COX7A2L	ENSG00000115944	GABRG1	ENSG00000163285
ARMC1	ENSG00000104442	CPEB4	ENSG00000113742	GAK	ENSG00000178950
ARNT	ENSG00000143437	CPNE3	ENSG00000085719	GAP43	ENSG00000172020
ASPA	ENSG00000108381	CPSF6	ENSG00000111605	GCA	ENSG00000115271
ASPN	ENSG00000106819	CREG1	ENSG00000143162	GHITM	ENSG00000165678
ATP5C1	ENSG00000165629	CRIPAK	ENSG00000179979	GLT8D2	ENSG00000120820
ATP5E	ENSG00000124172	CRIPT	ENSG00000119878	GMDS	ENSG00000112699
ATP5EP2	ENSG00000180389	CRISP3	ENSG00000096006	GMFB	ENSG00000197045
ATP5I	ENSG00000169020	CRNKL1	ENSG00000101343	GNA13	ENSG00000120063
ATP6V0D2	ENSG00000147614	CTGF	ENSG00000118523	GOLGA5	ENSG00000066455
ATP6V0E	ENSG00000113732	CTHRC1	ENSG00000164932	GOLGA7	ENSG00000147533
ATPIF1	ENSG00000130770	CTNND1	ENSG00000198561	GPR160	ENSG00000173890
AZIN1	ENSG00000155096	CTR9	ENSG00000198730	GREM1	ENSG00000166923
B4GALT4	ENSG00000121578	CTSK	ENSG00000143387	GSTA4	ENSG00000170899
BBS4	ENSG00000140463	CYP39A1	ENSG00000146233	HBA1	ENSG00000206172
BCAT1	ENSG00000060982	CYTL1	ENSG00000170891	HBA2	ENSG00000188536
BEX5	ENSG00000184515	CYR1	ENSG00000166265	HDAC1	ENSG00000116478
BIN1	ENSG00000136711	DCLRE1C	ENSG00000152457	HDAC4	ENSG00000068024
BTAF1	ENSG00000095564	DCTN4	ENSG00000132912	HEMGN	ENSG00000136929
BUB3	ENSG00000154473	DCUN1D5	ENSG00000137692	HIST1H4C	ENSG00000197061
BXDC5	ENSG00000117133	DDX17	ENSG00000100201	HLA-DQB1	ENSG00000179344
C10orf104	ENSG00000166295	DDX18	ENSG00000088205	HLF	ENSG00000108924
C11orf10	ENSG00000134825	DENND5A	ENSG00000184014	HNRNPUL2	ENSG00000214753
C11orf57	ENSG00000150776	DHRS8	ENSG00000198189	HTRA1	ENSG00000166033
C12orf57	ENSG00000111678	DNAJA1	ENSG00000080661	IFRD1	ENSG00000006652
C13orf18	ENSG00000102445	DNAJC10	ENSG00000077232	IGF1R	ENSG00000140443
C15orf15	ENSG00000137876	DNAJC1	ENSG00000136770	IGFBP7	ENSG00000163453
C15orf24	ENSG00000134153	DPM1	ENSG00000000419	IL1B	ENSG00000125538
C16orf80	ENSG00000070761	DSTN	ENSG00000125868	IL6ST	ENSG00000134352
C1S	ENSG00000182326	EEF2	ENSG00000167658	IRF2BP2	ENSG00000168264
C20orf108	ENSG00000124098	EFHA1	ENSG00000165487	ITGA6	ENSG00000091409
C20orf199	ENSG00000177410	EGR3	ENSG00000179388	ITM2A	ENSG00000078596
C2orf28	ENSG00000138085	EIF1	ENSG00000173812	IVNS1ABP	ENSG00000116679
C2orf40	ENSG00000119147	EIF2A	ENSG00000144895	JMJD1B	ENSG00000120733
C4orf32	ENSG00000174749	EIF3H	ENSG00000147677	JTB	ENSG00000143543
C5orf43	ENSG00000188725	EIF5	ENSG00000100664	KCTD13	ENSG00000174943
C6orf49	ENSG00000124593	ELK3	ENSG00000111145	KDELRL2	ENSG00000136240
C7orf60	ENSG00000164603	EPAS1	ENSG00000116016	KIAA1370	ENSG00000047346
C8orf40	ENSG00000176209	EPYC	ENSG00000083782	KIAA1377	ENSG00000110318
CALD1	ENSG00000122786	ETS1	ENSG00000134954	KIAA1432	ENSG00000107036
CAPS2	ENSG00000180881	ETV5	ENSG00000171656	KIAA1524	ENSG00000163507
CCL18	ENSG00000006074	EVI2A	ENSG00000126860	KLHDC2	ENSG00000165516
CCPG1	ENSG00000214882	F13A1	ENSG00000124491	KRT10	ENSG00000186395
CD164	ENSG00000135535	FAM126B	ENSG00000155744	LAMP1	ENSG00000185896

Gene symbol	Ensemble ID	Gene symbol	Ensemble ID	Gene symbol	Ensemble ID
LAPTM4B	ENSG00000104341	PLBD1	ENSG00000121316	SNX16	ENSG00000104497
LDB2	ENSG00000169744	PLOD2	ENSG00000152952	SNX3	ENSG00000112335
LEPREL1	ENSG00000090530	PLS1	ENSG00000120756	SOCS4	ENSG00000180008
LIX1	ENSG00000145721	PLSCR1	ENSG00000188313	SORL1	ENSG00000137642
LIX1L	ENSG00000152022	PLSCR4	ENSG00000114698	SPATA6	ENSG00000132122
LPAR1	ENSG00000198121	PM20D2	ENSG00000146281	SPRED1	ENSG00000166068
LPL	ENSG00000175445	PMEPA1	ENSG00000124225	SPRY2	ENSG00000136158
LRP4	ENSG00000134569	POMP	ENSG00000132963	SSFA2	ENSG00000138434
LRRFIP2	ENSG00000093167	PPAP2A	ENSG00000067113	STARD13	ENSG00000133121
LRRTM4	ENSG00000176204	PPIC	ENSG00000168938	STK38L	ENSG00000211455
LT44H	ENSG00000111144	PPP1R14C	ENSG00000198729	STT3B	ENSG00000163527
LYPLA1	ENSG00000120992	PPP1R2P4	ENSG00000215471	SUB1	ENSG00000113387
LYRM5	ENSG00000205707	PPP6C	ENSG00000119414	SULF1	ENSG00000137573
LYSMD3	ENSG00000176018	PPT1	ENSG00000131238	SYNP1	ENSG00000198765
MAP4K3	ENSG00000011566	PRDX4	ENSG00000123131	SYNCR	ENSG00000182253
MARK3	ENSG00000075413	PSMB4	ENSG00000159377	TAC1	ENSG00000006128
MBNL1	ENSG00000152601	PSMD12	ENSG00000197170	TAX1BP1	ENSG00000106052
MCCC1	ENSG00000078070	PSMD14	ENSG00000115233	TBC1D12	ENSG00000108239
MCC	ENSG00000171444	PTPLAD1	ENSG00000074696	TCEAL7	ENSG00000182916
MED28	ENSG00000118579	PTPN4	ENSG00000088179	TCF4	ENSG00000196628
MED30	ENSG00000164758	PXDN	ENSG00000130508	TGFB1	ENSG00000120708
MED4	ENSG00000136146	RAB11A	ENSG00000103769	TGFB3R3	ENSG00000069702
METTL3	ENSG00000165819	RAB11FIP2	ENSG00000107560	THBS2	ENSG00000186340
MGAT2	ENSG00000168282	RAB18	ENSG00000099246	THBS4	ENSG00000113296
MNDA	ENSG00000163563	RAB2	ENSG00000104388	TIMM17A	ENSG00000134375
MOXD1	ENSG00000079931	RAP2A	ENSG00000125249	TIMP3	ENSG00000100234
MPO	ENSG00000005381	RCN2	ENSG00000117906	TIPARP	ENSG00000163659
MRPL47	ENSG00000136522	RGS18	ENSG00000150681	TMCO3	ENSG00000150403
MRPS22	ENSG00000175110	RHOB	ENSG00000143878	TMED2	ENSG00000086598
MRPS35	ENSG00000061794	RHOBTB1	ENSG00000072422	TMEM100	ENSG00000166292
MTMR6	ENSG00000139505	RNF7	ENSG00000114125	TMEM161B	ENSG00000164180
MYCBP2	ENSG00000005810	RPL15	ENSG00000174748	TMEM38B	ENSG00000095209
NCOA4	ENSG00000138293	RPN1	ENSG00000163902	TMEM39A	ENSG00000176142
NCUBE1	ENSG00000198833	RPN2	ENSG00000118705	TMEM45A	ENSG00000181458
NDFIP2	ENSG00000102471	RPS19P3	ENSG00000105372	TMEM46	ENSG00000180730
NDP	ENSG00000124479	RPS21	ENSG00000171858	TNFAP6	ENSG00000123610
NET1	ENSG00000173848	RBN1	ENSG00000008109	TNFRSF11B	ENSG00000164761
NFAT5	ENSG00000102908	RSPO3	ENSG00000146374	TNFSF11	ENSG00000120659
NFIB	ENSG00000147862	RYK	ENSG00000163785	TOMM6	ENSG00000214736
NFIX	ENSG00000008441	S100A12	ENSG00000163221	TOX	ENSG00000198846
NFKBIA	ENSG00000100906	S100A8	ENSG00000143546	TRAM1	ENSG00000067167
NMI	ENSG00000123609	SDC1	ENSG00000115884	TRAM2	ENSG00000065308
NNMT	ENSG00000166741	SDC2	ENSG00000169439	TRAPP4	ENSG00000196655
NPC2	ENSG00000119655	SDCBP	ENSG00000137575	TSN	ENSG00000211460
NPEPPS	ENSG00000141279	SEC22C	ENSG00000093183	TXNIP	ENSG00000117289
NRK	ENSG00000123572	SEC23A	ENSG00000100934	UBE2B	ENSG00000119048
NUP107	ENSG00000111581	SEC23B	ENSG00000101310	UGP2	ENSG00000169764
OAT	ENSG00000065154	SEC61G	ENSG00000132432	VAMP7	ENSG00000124333
OMD	ENSG00000127083	SEMA3C	ENSG00000075223	VCAM1	ENSG00000162692
PAN3	ENSG00000152520	SEMA6D	ENSG00000137872	VCIPI1	ENSG00000175073
PANX3	ENSG00000154143	SERP1	ENSG00000120742	VEZF1	ENSG00000136451
PCDH8	ENSG00000136099	SERPINH1	ENSG00000149257	VTA1	ENSG00000009844
PCDHGA11	ENSG00000214567	SERTAD4	ENSG00000082497	WAPAL	ENSG00000062650
PCDHGA12	ENSG000000081853	SF3B1	ENSG00000115524	YES1	ENSG00000176105
PCDHGA2	ENSG00000204955	SFRP1	ENSG00000104332	YIPF5	ENSG00000145817
PCDHGA3	ENSG00000214594	SFRS5	ENSG00000100650	ZBTB10	ENSG00000205189
PCDHGA6	ENSG00000214580	SH3BGR1	ENSG00000131171	ZDHHC6	ENSG00000023041
PCDHGA8	ENSG00000214574	SHMT2	ENSG00000182199	ZNF281	ENSG00000162702
PCDHGB7	ENSG00000214570	SLC15A4	ENSG00000139370	ZNF652	ENSG00000198740
PCM1	ENSG00000078674	SLC2A13	ENSG00000151229		
PDCD10	ENSG00000114209	SLC39A11	ENSG00000133195		
PENK	ENSG00000181195	SLC41A3	ENSG00000114544		
PFDN2	ENSG00000143256	SLITRK6	ENSG00000184564		
PFDN5	ENSG00000123349	SMG7	ENSG00000116698		
PIGK	ENSG00000142892	SMOC1	ENSG00000198732		
PITPNB	ENSG00000180957	SMOC2	ENSG00000112562		
PLAG1	ENSG00000181690	SNAI2	ENSG0000019549		



Supplemental figure 1



References

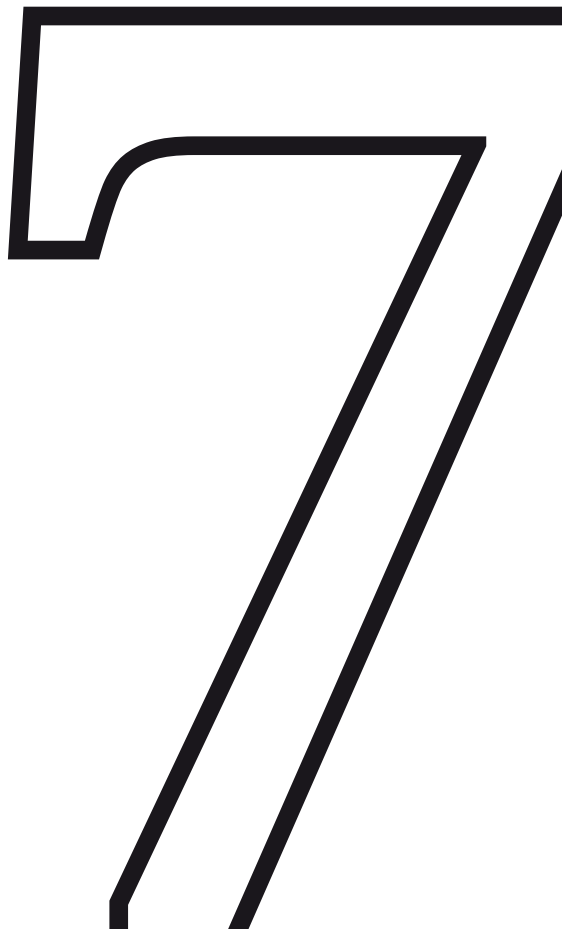
1. **Kronenberg HM** 2003 Developmental regulation of the growth plate. *Nature* 423:332-336
2. **Chagin AS, Savendahl L** 2007 Estrogens and growth: review. *Pediatr Endocrinol Rev* 4:329-334
3. **MacGillivray MH, Morishima A, Conte F, Grumbach M, Smith EP** 1998 Pediatric endocrinology update: an overview. The essential roles of estrogens in pubertal growth, epiphyseal fusion and bone turnover: lessons from mutations in the genes for aromatase and the estrogen receptor. *Horm Res* 49 Suppl 1:2-8
4. **Smith EP, Boyd J, Frank GR, Takahashi H, Cohen RM, Specker B, Williams TC, Lubahn DB, Korach KS** 1994 Estrogen resistance caused by a mutation in the estrogen-receptor gene in a man. *N Engl J Med* 331:1056-1061
5. **Morishima A, Grumbach MM, Simpson ER, Fisher C, Qin K** 1995 Aromatase deficiency in male and female siblings caused by a novel mutation and the physiological role of estrogens. *J Clin Endocrinol Metab* 80:3689-3698
6. **Turner RT, Riggs BL, Spelsberg TC** 1994 Skeletal effects of estrogen. *Endocr Rev* 15:275-300
7. **Weise M, De Levi S, Barnes KM, Gafni RI, Abad V, Baron J** 2001 Effects of estrogen on growth plate senescence and epiphyseal fusion. *Proc Natl Acad Sci U S A* 98:6871-6876
8. **Gafni RI, Weise M, Robrecht DT, Meyers JL, Barnes KM, De Levi S, Baron J** 2001 Catch-up growth is associated with delayed senescence of the growth plate in rabbits. *Pediatr Res* 50:618-623
9. **Schrier L, Ferns SP, Barnes KM, Emons JA, Newman EI, Nilsson O, Baron J** 2006 Depletion of resting zone chondrocytes during growth plate senescence. *J Endocrinol* 189:27-36
10. **Greene GL, Gilna P, Waterfield M, Baker A, Hort Y, Shine J** 1986 Sequence and expression of human estrogen receptor complementary DNA. *Science* 231:1150-1154
11. **Kuiper GG, Enmark E, Peltö-Huikko M, Nilsson S, Gustafsson JA** 1996 Cloning of a novel receptor expressed in rat prostate and ovary. *Proc Natl Acad Sci U S A* 93:5925-5930
12. **Revankar CM, Cimino DF, Sklar LA, Arterburn JB, Prossnitz ER** 2005 A transmembrane intracellular estrogen receptor mediates rapid cell signaling. *Science* 307:1625-1630
13. **Filardo EJ, Quinn JA, Frackelton AR, Jr., Bland KI** 2002 Estrogen action via the G protein-coupled receptor, GPR30: stimulation of adenylyl cyclase and cAMP-mediated attenuation of the epidermal growth factor receptor-to-MAPK signaling axis. *Mol Endocrinol* 16:70-84
14. **Chagin AS, Savendahl L** 2007 GPR30 estrogen receptor expression in the growth plate declines as puberty progresses. *J Clin Endocrinol Metab* 92:4873-4877

15. **Nilsson O, Chrysis D, Pajulo O, Boman A, Holst M, Rubinstein J, Martin RE, Savendahl L** 2003 Localization of estrogen receptors-alpha and -beta and androgen receptor in the human growth plate at different pubertal stages. *J Endocrinol* 177:319-326
16. **Perry RJ, Farquharson C, Ahmed SF** 2008 The role of sex steroids in controlling pubertal growth. *Clin Endocrinol (Oxf)* 68:4-15
17. **de ZF, Butenandt O, Chatelain P, bertsson-Wikland K, Jonsson B, Lofstrom A, Chaussain JL** 1997 Growth hormone treatment of short children born small for gestational age: reappraisal of the rate of bone maturation over 2 years and metanalysis of height gain over 4 years. *Acta Paediatr Suppl* 423:207-212
18. **Kamp GA, Waelkens JJ, de Muinck Keizer-Schrama SM, Delemarre-van de Waal HA, Verhoeven-Wind L, Zwinderman AH, Wit JM** 2002 High dose growth hormone treatment induces acceleration of skeletal maturation and an earlier onset of puberty in children with idiopathic short stature. *Arch Dis Child* 87:215-220
19. **Werther GA, Haynes K, Edmonson S, Oakes S, Buchanan CJ, Herington AC, Waters MJ** 1993 Identification of growth hormone receptors on human growth plate chondrocytes. *Acta Paediatr Suppl* 82 Suppl 391:50-53
20. **Rosenfeld RG, Hwa V** 2009 The growth hormone cascade and its role in mammalian growth. *Horm Res* 71 Suppl 2:36-40
21. **Bruning JC, Gillette JA, Zhao Y, Bjorbaeck C, Kotzka J, Knebel B, Avci H, Hanstein B, Lingohr P, Moller DE, Krone W, Kahn CR, Muller-Wieland D** 2000 Ribosomal subunit kinase-2 is required for growth factor-stimulated transcription of the c-Fos gene. *Proc Natl Acad Sci U S A* 97:2462-2467
22. **Karp SJ, Schipani E, St-Jacques B, Hunzelman J, Kronenberg H, McMahon AP** 2000 Indian hedgehog coordinates endochondral bone growth and morphogenesis via parathyroid hormone related-protein-dependent and -independent pathways. *Development* 127:543-548
23. **van der Eerden BC, Karperien M, Gevers EF, Lowik CW, Wit JM** 2000 Expression of Indian hedgehog, parathyroid hormone-related protein, and their receptors in the postnatal growth plate of the rat: evidence for a locally acting growth restraining feedback loop after birth. *J Bone Miner Res* 15:1045-1055
24. **Mak KK, Bi Y, Wan C, Chuang PT, Clemens T, Young M, Yang Y** 2008 Hedgehog signaling in mature osteoblasts regulates bone formation and resorption by controlling PTHrP and RANKL expression. *Dev Cell* 14:674-688
25. **Kindblom JM, Nilsson O, Hurme T, Ohlsson C, Savendahl L** 2002 Expression and localization of Indian hedgehog (Ihh) and parathyroid hormone related protein (PTHrP) in the human growth plate during pubertal development. *J Endocrinol* 174:R1-R6

26. **Yoshida CA, Komori T** 2005 Role of Runx proteins in chondrogenesis. *Crit Rev Eukaryot Gene Expr* 15:243-254
27. **Yoshida CA, Yamamoto H, Fujita T, Furuichi T, Ito K, Inoue K, Yamana K, Zanma A, Takada K, Ito Y, Komori T** 2004 Runx2 and Runx3 are essential for chondrocyte maturation, and Runx2 regulates limb growth through induction of Indian hedgehog. *Genes Dev* 18:952-963
28. **Nilsson O, Chrysis D, Pajulo O, Boman A, Holst M, Rubinstein J, Martin RE, Savendahl L** 2003 Localization of estrogen receptors-alpha and -beta and androgen receptor in the human growth plate at different pubertal stages. *J Endocrinol* 177:319-326
29. **Vidal O, Lindberg M, Savendahl L, Lubahn DB, Ritzen EM, Gustafsson JA, Ohlsson C** 1999 Disproportional body growth in female estrogen receptor-alpha-inactivated mice. *Biochem Biophys Res Commun* 265:569-571
30. **Smith EP, Boyd J, Frank GR, Takahashi H, Cohen RM, Specker B, Williams TC, Lubahn DB, Korach KS** 1994 Estrogen resistance caused by a mutation in the estrogen-receptor gene in a man. *N Engl J Med* 331:1056-1061
31. **Tagle DA, Koop BF, Goodman M, Slightom JL, Hess DL, Jones RT** 1988 Embryonic epsilon and gamma globin genes of a prosimian primate (*Galago crassicaudatus*). Nucleotide and amino acid sequences, developmental regulation and phylogenetic footprints. *J Mol Biol* 203:439-455
32. **Heinrichs C, Yanovski JA, Roth AH, Yu YM, Domene HM, Yano K, Cutler GB, Jr, Baron J** 1994 Dexamethasone increases growth hormone receptor messenger ribonucleic acid levels in liver and growth plate. *Endocrinology* 135:1113-1118
33. **Sandberg R, Larsson O** 2007 Improved precision and accuracy for microarrays using updated probe set definitions. *BMC Bioinformatics* 8:48
34. **Chu TM, Weir B, Wolfinger R** 2002 A systematic statistical linear modeling approach to oligonucleotide array experiments. *Math Biosci* 176:35-51
35. **Beissbarth T** 2006 Interpreting experimental results using gene ontologies. *Methods Enzymol* 411:340-352
36. **Sandelin A, Wasserman WW, Lenhard B** 2004 ConSite: web-based prediction of regulatory elements using cross-species comparison. *Nucleic Acids Res* 32:W249-W252
37. **Siepel A, Bejerano G, Pedersen JS, Hinrichs AS, Hou M, Rosenbloom K, Clawson H, Spieth J, Hillier LW, Richards S, Weinstock GM, Wilson RK, Gibbs RA, Kent WJ, Miller W, Haussler D** 2005 Evolutionarily conserved elements in vertebrate, insect, worm, and yeast genomes. *Genome Res* 15:1034-1050

38. **Kuhn RM, Karolchik D, Zweig AS, Wang T, Smith KE, Rosenbloom KR, Rhead B, Raney BJ, Pohl A, Pheasant M, Meyer L, Hsu F, Hinrichs AS, Harte RA, Giardine B, Fujita P, Diekhans M, Dreszer T, Clawson H, Barber GP, Haussler D, Kent WJ** 2009 The UCSC Genome Browser Database: update 2009. *Nucleic Acids Res* 37:D755-D761
39. **Haider S, Ballester B, Smedley D, Zhang J, Rice P, Kasprzyk A** 2009 BioMart Central Portal-unified access to biological data. *Nucleic Acids Res* 37:W23-W27
40. **Solomon LA, Berube NG, Beier F** 2008 Transcriptional regulators of chondrocyte hypertrophy. *Birth Defects Res C Embryo Today* 84:123-130
41. **Kember NF** 1973 Aspects of the maturation process in growth cartilage in the rat tibia. *Clin Orthop Relat Res* 288-294
42. **Toole BP, Linsenmayer TF** 1977 Newer knowledge of skeletogenesis: macromolecular transitions in the extracellular matrix. *Clin Orthop Relat Res* 258-278
43. **Toole BP, Okayama M, Orkin RW, Yoshimura M, Muto M, Kaji A** 1977 Developmental roles of hyaluronate and chondroitin sulfate proteoglycans. *Soc Gen Physiol Ser* 32:139-154
44. **Blanchard O, Tsagris L, Rappaport R, Duval-Beaupere G, Corvol M** 1991 Age-dependent responsiveness of rabbit and human cartilage cells to sex steroids in vitro. *J Steroid Biochem Mol Biol* 40:711-716
45. **Codogno P, Meijer AJ** 2006 Atg5: more than an autophagy factor. *Nat Cell Biol* 8:1045-1047
46. **Heath-Engel HM, Chang NC, Shore GC** 2008 The endoplasmic reticulum in apoptosis and autophagy: role of the BCL-2 protein family. *Oncogene* 27:6419-6433
47. **Emons J, Chagin AS, Hultenby K, Zhivotovsky B, Wit JM, Karperien M, Savendahl L** 2009 Epiphyseal Fusion in the Human Growth Plate does not involve Classical Apoptosis. *Pediatr Res*
48. **Casazza K, Goran MI, Gower BA** 2008 Associations among insulin, estrogen, and fat mass gain over the pubertal transition in African-American and European-American girls. *J Clin Endocrinol Metab* 93:2610-2615
49. **Juul A, Bang P, Hertel NT, Main K, Dalgaard P, Jorgensen K, Muller J, Hall K, Skakkebaek NE** 1994 Serum insulin-like growth factor-I in 1030 healthy children, adolescents, and adults: relation to age, sex, stage of puberty, testicular size, and body mass index. *J Clin Endocrinol Metab* 78:744-752
50. **Abbassi V** 1998 Growth and normal puberty. *Pediatrics* 102:507-511
51. **Windahl SH, Lagerquist MK, Andersson N, Jochems C, Kallkopf A, Hakansson C, Inzunza J, Gustafsson JA, van der Saag PT, Carlsten H, Pettersson K, Ohlsson C** 2007 Identification of target cells for the genomic effects of estrogens in bone. *Endocrinology* 148:5688-5695

52. **Isgaard J, Nilsson A, Lindahl A, Jansson JO, Isaksson OGP** 1986 Effects of Local-Administration of Gh and Igf-1 on Longitudinal Bone-Growth in Rats. *American Journal of Physiology* 250:E367-E372
53. **Ohlsson C, Nilsson A, Isaksson O, Lindahl A** 1992 Growth hormone induces multiplication of the slowly cycling germinal cells of the rat tibial growth plate. *Proc Natl Acad Sci U S A* 89:9826-9830
54. **Coutant R, de Casson FB, Rouleau S, Douay O, Mathieu E, Gatelais F, Bouhours-Nouet N, Voinot C, Audran M, Limal JM** 2004 Divergent effect of endogenous and exogenous sex steroids on the insulin-like growth factor I response to growth hormone in short normal adolescents. *J Clin Endocrinol Metab* 89:6185-6192
55. **Veldhuis JD, Keenan DM, Bailey JN, Adeniji A, Miles JM, Paulo R, Cosma M, Soares-Welch C** 2008 Estradiol supplementation in postmenopausal women attenuates suppression of pulsatile growth hormone secretion by recombinant human insulin-like growth factor type I. *J Clin Endocrinol Metab* 93:4471-4478
56. **Komori T** 2003 Requisite roles of Runx2 and Cbfb in skeletal development. *J Bone Miner Metab* 21:193-197
57. **Sasaki-Iwaoka H, Maruyama K, Endoh H, Komori T, Kato S, Kawashima H** 1999 A trans-acting enhancer modulates estrogen-mediated transcription of reporter genes in osteoblasts. *J Bone Miner Res* 14:248-255
58. **Tou L, Quibria N, Alexander JM** 2001 Regulation of human cbfa1 gene transcription in osteoblasts by selective estrogen receptor modulators (SERMs). *Mol Cell Endocrinol* 183:71-79
59. **Perola M, Sammalisto S, Hiekkalinna T, Martin NG, Visscher PM, Montgomery GW, Benjamin B, Harris JR, Boomsma D, Willemsen G, Hottenga JJ, Christensen K, Kyvik KO, Sorensen TI, Pedersen NL, Magnusson PK, Spector TD, Widen E, Silventoinen K, Kaprio J, Palotie A, Peltonen L** 2007 Combined genome scans for body stature in 6,602 European twins: evidence for common Caucasian loci. *PLoS Genet* 3:e97



A cross-sectional microarray study of human epiphyseal growth plates during pubertal maturation.

Joyce A.M. Emons¹, Andrei Chagin², Jeroen Leijten³, Eva Decker⁴, Sandy van Gool¹, Erik van Zwet⁵, Jelle Goeman⁵, Carsten Sticht⁶, Xiaolei Yu⁶, Heide Pirzer⁴, Gudrun A. Rappold⁴, Norbert Gretz⁶, Jan Maarten Wit¹, Lars Savendahl² and Marcel Karperien³.

¹Department of Pediatrics, Leiden University Medical Center, Leiden, the Netherlands;

²Department of Pediatric Endocrinology, Karolinska Institutet, Stockholm, Sweden;

³Department of Tissue Regeneration, Twente University, Enschede, the Netherlands;

⁴Department of Human Molecular Genetics, University of Heidelberg, Heidelberg, Germany;

⁵Department of Medical Statistics and Bioinformatics, Leiden University Medical Center, Leiden, the Netherlands;

⁶Medical Research Center, Medical Faculty Mannheim, Mannheim, Germany.

Abstract

In puberty growth velocity first accelerates, followed by a phase of deceleration and eventually cessation of growth with fusion of the epiphyses. Little is known about the exact mechanisms underlying the pubertal growth spurt, growth plate maturation and epiphyseal fusion. In this study, human growth plate specimens were collected during distinct phases of puberty. High quality RNA was isolated, amplified, labelled and subjected to Affymetrix microarray analysis (HG-U133 Plus 2). We compared growth plate tissue from the distal femur and proximal tibia and found no great difference between expression patterns of these two growth plates from different anatomical locations. Secondly, we performed a cross-sectional microarray study with female tibial growth plate specimens obtained at different stages of pubertal development (prepuberty, early puberty and more progressed puberty). Progression of puberty is associated with many, however mostly small, changes in gene expression that occurred most frequently late in puberty. Pathway analysis revealed 11 pathways, associated with the extracellular matrix homeostasis, hormonal pathways and programmed cell death, changing with maturation of the growth plate. Significance in this comparison was lost when the results were corrected for multiple testing, probably due to the small sample size. Power calculations revealed that at least 5 growth plates are needed in each group to detect a 1.5 fold difference. For the first time we show a developmental regulation of the gene expression pattern in the human epiphyseal growth plate with most alterations occurring during late puberty. However more future studies are needed to validate our findings.

Introduction

Longitudinal growth occurs at the epiphyseal growth plate, a thin layer of cartilage entrapped between epiphyseal and metaphyseal bone, at the distal ends of the long bones (1). Epiphyseal chondrocytes are under tight control of a variety of hormones and growth factors acting directly or indirectly on the growth plate (2). At onset of puberty, the levels of various hormones, including sex steroids, increase in circulation. Sex steroids induce the external signs of puberty (secondary sex characteristics) and the accompanying rise in growth velocity, called the pubertal growth spurt. Typically, pubertal growth consists of a phase of acceleration, followed by a phase of deceleration, and the eventual cessation of growth with the fusion of the epiphyses. One of the important hormones regulating pubertal bone growth in both males and females is estrogen. Estrogen levels increase about 10-fold along with a 1.5 to 3-fold increase in GH and IGF-1 secretion in puberty (3;4).

In puberty, humans gain on average 27.5-31 centimeters in height, accounting for approximately 17% of adult height (5). The dramatic effects on growth velocity during distinct phases of puberty are a reflection of the activity of the growth plate which consequently undergoes substantial changes over time. Little is known about the exact mechanisms underlying the pubertal growth spurt, growth plate maturation and epiphyseal fusion. Most previous studies studying growth plate regulation have used animal models, which poorly represent characteristic growth patterns of human during puberty.

In chapter 6 we investigated gene expression levels during pubertal growth plate maturation within one patient. This revealed a multitude of changes in gene expression. In addition, 13 pathways changed with maturation. Several of these pathways were related to the extracellular matrix. An increase in matrix / cell ratio is a typical characteristic of a maturing growth plate. These analyses were, however, based on one single patient. In order to validate these findings in

a larger population we have started collecting human growth plate specimens. Human growth plate specimens become occasionally available during surgical procedures for diverse medical indications. These medical indications are founded in various diseases, some related to growth others. These specimens were processed for histology and for RNA extraction. In this study, we report preliminary results of the microarray analysis of human growth plate specimens collected during distinct phases of puberty.

Material and Methods

Patients and tissue preparation

Human proximal tibia growth plate tissues were collected from patients at different pubertal stages, undergoing surgery for different medical indications (Table 1). The study protocol was approved by the Local Medical Ethics Committees of The Leiden University Center, Leiden, the Netherlands and The Karolinska University Hospital, Stockholm, Sweden. Informed consent was obtained from all patients and their parents. Epiphyseal samples were embedded in Tissue-Tek (Sakura Finetek Europe B.V., Zoeterwoude, the Netherlands) and frozen in liquid isopentane or immediately fixed in 10% formaldehyde for 24hrs, decalcified in 10% EDTA and embedded in paraffin. RNA was extracted and checked for quality and integrity as previously described in chapter 6.

Table 1

sample	diagnosis	sex	location in fumer	age (yr:m)	Tanner	paraffin/RNA	origin	code
1	elective abortion	f	tibia	fetal		RNA	Leiden	fetal
2	constitutional tall stature	f	distal	11:06	B1	paraffin	Stockholm	pt2
3	leg length difference	f	distal	9:06	B1	paraffin	Stockholm	pt22
4	Osteosarcoma	f	distal	8	B1	RNA	Leiden	GP1234
5	Upper limb amputation of the leg, tibia	f	proximal	9	B1	RNA	Leiden	GP t 8
6	Upper limb amputation of the leg, femur	f	distal	9	B1	RNA	Leiden	GP f 6
7	Chondroid osteosarcoma, Rothmund Thompson S	f	distal	12	B1	RNA	Leiden	GP1142
8	leg length difference	f	distal	9:06	B1-2	paraffin	Stockholm	pt23
9	hip luxations, femur head resection	f	proximal	12:05	B2	paraffin/RNA	Leiden	GS 3
10	leg length difference	f	distal	12:08	B2	paraffin	Stockholm	pt19
11	constitutional tall stature	f	distal	13:07	B2	paraffin	Stockholm	pt25
12	constitutional tall stature	f	distal	12:01	B2	paraffin	Stockholm	pt30
13	Tall stature	f	distal	10:06	B2	RNA	Stockholm	GP 12h
14	leg length difference	f	distal	14:02	B2-3	paraffin	Stockholm	pt17
15	Tall stature	f	distal	11:05	B2-3	RNA	Stockholm	GP 10h
16	hip luxations, femur head resection	f	proximal	13:05	B3	paraffin/RNA	Leiden	GS 7
17	leg length difference	f	distal	13:08	B3	paraffin	Stockholm	pt15
18	Tall stature	f	distal	12	B3	RNA	Stockholm	GP 22h
19	cerebral palsy, femur head resection	f	proximal	15:01	B4	paraffin	Leiden	GS 8
20	leg length difference	f	distal	13:03	B4	paraffin	Stockholm	pt8
21	femur head resection	f	proximal	14:00	B4	RNA	Leiden	5233
22	Tall stature	f	distal	15:07	B4	RNA	Stockholm	GP 21h
23	cerebral palsy, femur head resection	f	proximal	17:00	B5	paraffin	Leiden	GS 9
24	leg length difference	f	distal	1:00	B5	paraffin	Stockholm	pt31
25	CHD, femur head resection	m	proximal	13:01	G1	RNA	Leiden	GS 13
26	Marfan	m	distal	12:03	G1	paraffin	Stockholm	pt 5
27	cerebral palsy, AIS, femur head resection	m	proximal	10	G1/B1	RNA	Leiden	GP6
28	cerebral palsy, femur head resection	m	proximal	16:10	G2	RNA	Leiden	GP25
29	leg length difference	m	distal	12:06	G3	paraffin	Stockholm	pt 24
30	leg length difference	m	distal	15:04	G3-4	paraffin	Stockholm	pt 26
31	leg length difference	m	distal	14:08	G4	paraffin	Stockholm	pt 18
32	47XYY	m	distal	14	G4-5	paraffin	Stockholm	pt 27

Patients information. Samples #4 and 5 are derived from the same patient. Samples #8 and 15 are derived from the same patient

Microarray analyses

100 ng of total RNA was amplified and labeled using the GeneChip Two-Cycle cDNA Synthesis Kit (Affymetrix, Santa Clara, CA) and the MEGAscript T7 Kit (Ambion, Austin, TX). The labeled cRNA was further used for the hybridization to Affymetrix Human Genome U133 PLUS 2.0 Array Genechips and hybridized according to Affymetrix manufacturers protocol. In a first approach we compared growth plate tissue from the distal femur and proximal tibia to investigate the influence of location on gene expression profiles. In this analysis samples #4 and #5 were used.

In a second approach we performed a cross-sectional microarray study with growth plate specimens obtained at different stages of pubertal development. To minimize the variability we only included growth plate specimens from the female sex derived from the proximal tibia. The samples were divided in 3 different groups: 1. prepubertal (pt #3 and #4); 2. early puberty (defined as Tanner stage B2 and B2-3, pt #12 and #14); 3. more progressed stage puberty (defined as Tanner stage B3 and B4 pt #17 and #20). A genewise linear model was fitted to the six arrays using the R package Limma to test differences between the three stages of puberty. Because of the limited power due to the small sample size, no adjustment was made for multiple testing, but attention was focused on the patterns in the uncorrected P values. Differentially expressed genes were further investigated as previously described with a global test in order to identify pathways that are likely to be affected by growth plate maturation (6).

Thirdly, a power calculation was performed to see how many growth plate specimens are needed to ensure that with 80% probability a 1.5 fold change can be detected at 5% level of significance after correction for multiple testing.

Besides the growth plate samples used in the experiments described in the above table 1 also contains additional growth plate samples not just yet, but available for future experiments.

Results

Proximal vs distal femoral growth plate expression

The expression profiles of distal and proximal femoral growth plate were largely overlapping. Most genes showed a small non-significant change (<1.4 fold). Only eight genes were showing a more than 2-fold difference. Figure 1 shows a volcano plot of all genes. From this we conclude that growth plates from different anatomical locations are similar in gene expression pattern. Subsequently, they can be used together in one comparison studying other parameters like pubertal maturation.

Pubertal maturation

Because of the small sample size (n=2 in each group) attention was focused on the patterns in the uncorrected P values. This revealed 605 genes changing from prepuberty to early puberty, while 1275 genes changed from early to late puberty and as many as 2362 genes changed from prepuberty to late puberty. Many genes were changing in more than one comparison (Figure 2). Significance was lost when results were corrected for multiple testing. The changes in expression level were mostly in a small range. The most affected upregulated gene (matrilin-1) showed a 32 fold change in expression from prepuberty to late puberty. The most affected downregulated gene showed a 11 fold change in expression level from prepuberty to late puberty (TCDD-inducible poly(ADP-ribose) polymera). The percentage of probes, out of the genes changing with maturation, with ≥ 2 fold change are shown in table 2. Results indicate that most alterations occurred during late puberty with 48.6% of genes increasing in expression level and 51.4% of genes decreasing in expression level.

Power calculation

Although the expression of many genes tended to change with progression of puberty, in this limited analysis none of these changes reached significance after correction for multiple testing. This was due to the small sample size, the biological variability between the specimens and the unexpectedly low levels of fold change. Based on this first analysis, we performed a power calculation to determine the number of growth plate specimens needed to ensure that with 80% probability a 1.5 fold change at 5% level of significance after correction for multiple testing can be detected.

In this analysis the total number of genes has to be considered, given that including many genes which are not involved in the regulation of growth during puberty makes it more difficult to flag the genes that do play a role. The variance of the expression levels between the samples also has to be considered. If a given gene naturally varies very much between individuals, it will consequently be hard to detect a signal. To get an idea of the amount of variability we might expect, we computed the variance for each gene in our data. We found that the mean variance was around 0.2, but variances above 0.8 did also occur.

In Figure 3 we plotted the required sample size (in each group) as a function of the variance. The red line is based on testing 200 genes, the black line on testing 1000 genes. From this can be concluded that about 5 growth plates in each group are needed to detect a fold change of 1.5 when the variance is 0.2.

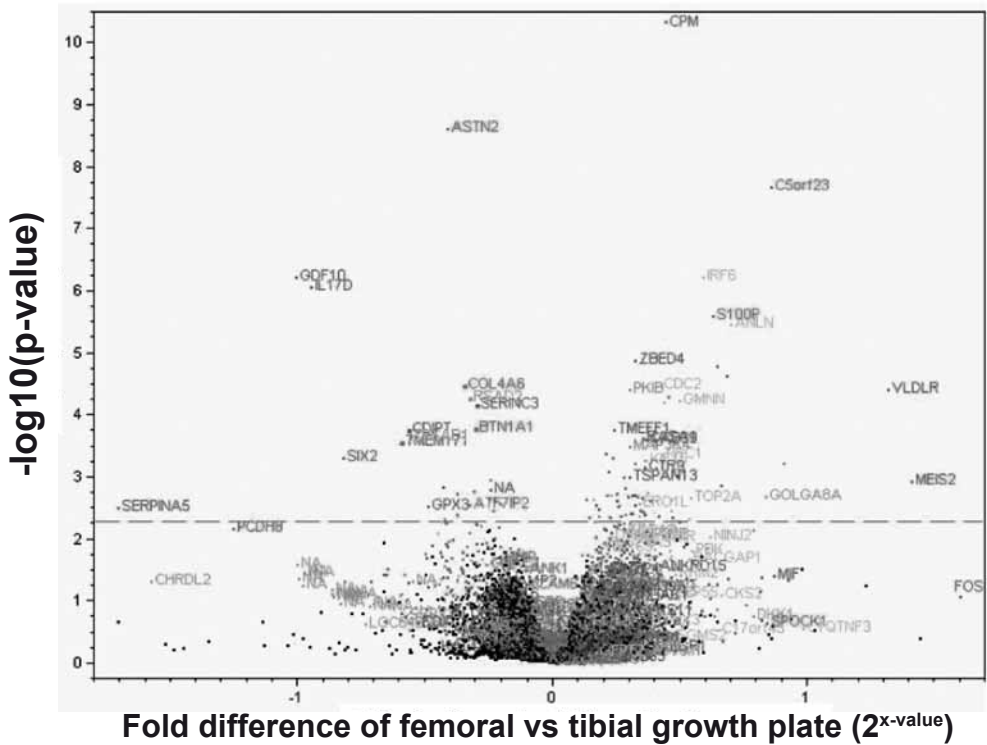


Figure 1. Proximal vs distal femoral growth plate expression.

In this figure the gene expression levels of the tibial growth plate versus the femoral growth plate is plotted. On the x-axis is written the fold-difference which can be calculated by 2^x -value. On the y-axis the $-\log_{10}(\text{p-value})$ which indicates the level of significance. The higher these value the more significant and values above the dashed line are significant without correction for multiple testing. Expression profiles were largely overlapping. Most genes showed a small non-significant change ($x < 0.5 = \text{fold change} < 1.4 \text{ fold}$). Only eight genes were showing a more than 2-fold difference.

prepubertal vs early puberty

prepubertal vs late puberty

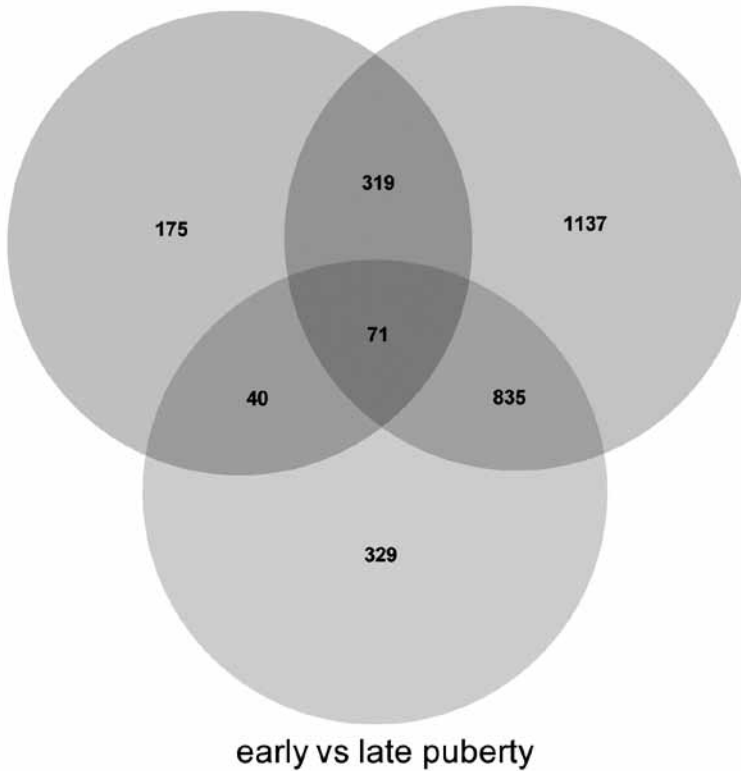


Figure 2: Venn diagram of significantly different genes in each group.

This figure shows the number of genes significantly different in each of the 3 comparisons between the different groups. It also shows the number of genes significant in more than one comparison.

Table 2

	Percentage of probes ≥ 2 fold change
prepuberty to early puberty	0.4%
early puberty to late puberty	2.0%
prepuberty to late puberty	3.1%

Percentage of probes with a ≥ 2 fold change between the different groups of pubertal maturation.

A pathway-based analysis with a global test for all genes revealed 11 pathways changing significantly from early to late puberty (table 3). Affected pathways associated with the extracellular matrix homeostasis, hormonal pathways and programmed cell death. Significance was lost when the results were corrected for multiple testing.

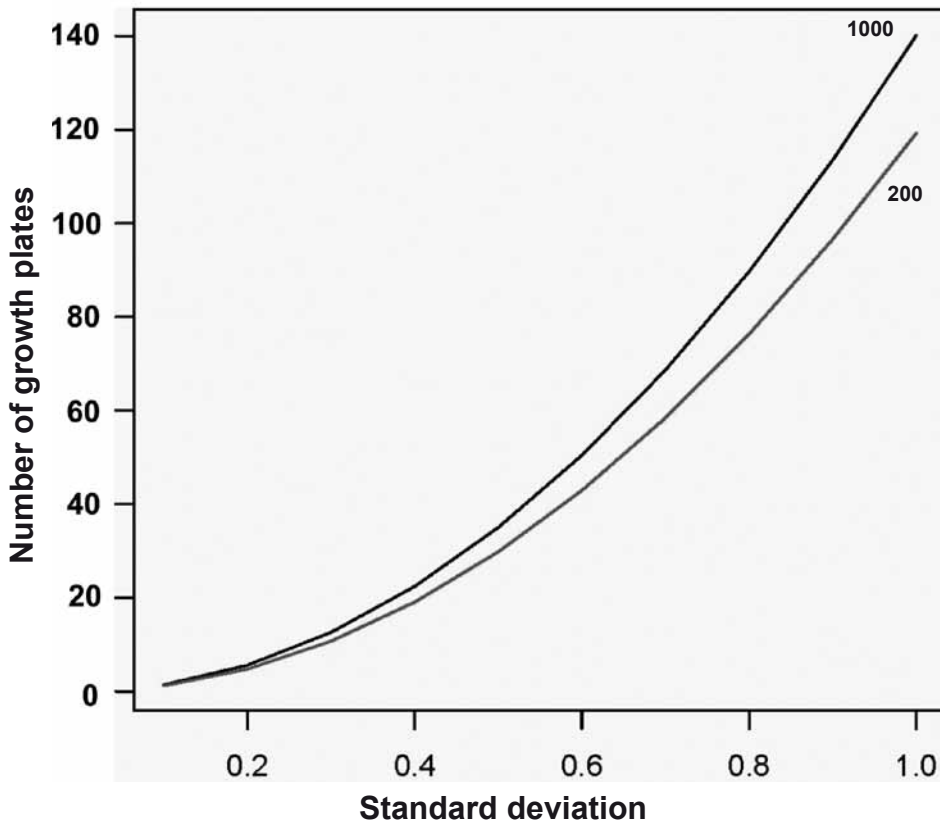


Figure 3: Required number of growth plates for different standard deviation scores.

One line is based on a selection of 200 genes and the other one for a selection of 1000 genes.

Tabel 3

	prepubertal. vs.early puberty	prepubertal.vs.late puberty	early.vs.late puberty
Regulation of autophagy	0.518	0.046	0.005
N-Glycan biosynthesis	0.879	0.403	0.006
RNA polymerase	0.767	0.195	0.016
Peptidoglycan biosynthesis	0.266	0.053	0.020
Lysine degradation	0.631	0.151	0.026
Biosynthesis of steroids	0.802	0.262	0.026
Terpenoid biosynthesis	0.749	0.358	0.028
Apoptosis	0.658	0.106	0.034
Complement + coagulation cascades	0.677	0.199	0.042
Fc epsilon RI signaling pathway	0.749	0.314	0.047
GnRH signaling pathway	0.715	0.168	0.049

Affected pathways and p-values for each comparison.

Discussion

A limited microarray analyses of 6 human growth plate samples at prepuberty, early puberty and advanced puberty revealed a large number of changes in gene expression with progression of puberty. Changes in expression levels were on average small and most alterations occurred during late stage of puberty. Furthermore, the variations in gene expression in between growth plate samples isolated from different patients at an identical stage of pubertal development were relatively large. Given the high impact of genetic composition on growth and final height this is not surprising.

A number of pathways changed with progression of puberty. Affected pathways were associated with extracellular matrix homeostasis, hormonal pathways and programmed cell death which have all been implicated in growth plate maturation. None of the identified changes reached significance when the statistical analyses were corrected for multiple testing. This was due to small sample size, large variation between specimens at the same developmental stage and overall small changes in gene expression levels.

The overall small change in gene expression levels in growth plate chondrocytes with progression of puberty was unexpected, since puberty is associated with dramatic changes in growth velocity which is mediated by the activity of growth plate chondrocytes. This is exemplified by the pubertal growth spurt, which accounts for approximately 17% of final height (3-5). In addition, puberty is related to a large increase in expression of hormones like sex steroids, Growth Hormone and IGF-I. These hormones have been postulated to regulate the changes in growth plate activity in part by exerting direct effects on growth plate chondrocytes. Of these hormones, estrogen demonstrates the most dramatic changes particularly in girls who were subject of the present study and is postulated to be the driving factor of the growth spurt, growth plate maturation and fusion. This might indicate that gene expression in the human growth plate is not as sensitive to circulating estrogen levels as was expected.

Estrogen accelerates the senescent decline (7). Senescence is a term for the structural and functional changes over time in the growth plate. Stem-like cells in the resting zone have a finite proliferative capacity, which is gradually exhausted resulting eventually in epiphyseal fusion (8;9). Based on this hypothesis, cells that are most sensitive to estrogen are growth plate stem cells. These cells are located in the resting zone of the growth plate adjacent to the epiphyseal bone and form a minority in the growth plate. By removing the bone from the cartilage by micro dissection, it is likely that many of the growth plate stem cells are removed as well. Likewise, to prevent contamination of the RNA preparations with cells of the metaphyseal bone, large parts of the terminal hypertrophic cell layer will be sacrificed as well. Our growth plate RNA samples are therefore enriched in proliferating and early hypertrophic cells. If stem cells are indeed most responsive to estrogen by changes in gene expression it is likely that such an effect will be missed in our experiment. Micro dissection with a laser for example, which allows a more precise selection of cell types for RNA isolation than manual micro dissection, might be considered as an alternative approach. Our findings do not support nor contradict the senescence hypothesis. A suggested biological marker for growth plate senescence is loss of DNA methylation and this cannot be detected by gene expression microarray analysis (10).

Although the analysis of the microarray data did not reveal findings that could withstand correction for multiple testing, it was remarkable that genes changing over time could be mapped to pathways like 'regulation of autophagy' and 'apoptosis'. Chondrocyte death is presumed to be a characteristic of growth plate maturation and fusion. In a previous study we studied apoptosis in a collection of growth plate tissues together with a unique growth plate specimen in the process

of epiphyseal fusion (11). In this study we were not able to detect any signs of autophagy and/or classical apoptosis with pubertal maturation morphologically nor at the protein level. We did observe early signs of necrosis and signs of hypoxia. The results from this microarray study are indicative for more cell death markers in late stages of puberty. Results do not identify the exact mechanism since both pathways contain many genes, and also overlapping genes, suggestive for some sort of programmed cell death which might be a combination of autophagy, apoptosis and perhaps a third kind of cell death like necrosis.

The exact mechanism through which chondrocytes disappear during epiphyseal fusion in humans still needs to be clarified. By increasing the power of the analysis by including new growth plate specimens, microarray analysis may shed more light on the process of chondrocyte death during the advanced stages of puberty. Alterations in genes associated with hormonal pathways are in line with a rat study, reporting an increase in sex steroid synthesis in sexually maturing rats (12). A number of growth plates in our collection were derived from pathological conditions. We believe that it is a safe assumption that the underlying mechanism of epiphyseal maturation and fusion is the same for all growth plates regardless of the underlying disease of each patient since eventually longitudinal growth stops in all patients by the end of puberty and all patients undergo growth plate maturation as a function of puberty.

Power calculations showed that 5 growth plates in each group are needed to detect a fold change of 1.5 with an overall variance of 0.2. Unfortunately, we did not have that many growth plates derived from female tibias. Differences in genetic background were omitted in the longitudinal analysis of the 2 growth plate samples from one patient as described in chapter 6. Comparing data from this longitudinal analysis with the present cross-sectional study did not show a perfect match in respect to individual genes. However, results of pathway analysis are more in agreement with the longitudinal study. Both analyses showed changes in pathways associated with the extracellular matrix and programmed cell death. In addition, the longitudinal study confirmed extracellular matrix changes on protein level.

Our microarray results are promising and contain a great amount of data; however more samples are needed to validate our findings. With a larger collection, results could serve as a database and clarify multiple research questions involving the growth plate. In addition, we now have a large collection of paraffin embedded tissues on which studies can be performed on protein expression. In conclusion, for the first time we show a developmental regulation of the gene expression pattern in the human epiphyseal growth plate. Most alterations occurred during late puberty suggesting that the affected pathways may be involved in the regulation of human epiphyseal growth plate maturation and fusion. However, more future studies are needed to validate our findings.

References

1. **Kronenberg HM** 2003 Developmental regulation of the growth plate. *Nature* 423:332-336
2. **van der Eerden BC, Karperien M, Wit JM** 2003 Systemic and local regulation of the growth plate. *Endocr Rev* 24:782-801
3. **Casazza K, Goran MI, Gower BA** 2008 Associations among insulin, estrogen, and fat mass gain over the pubertal transition in African-American and European-American girls. *J Clin Endocrinol Metab* 93:2610-2615
4. **Juul A, Bang P, Hertel NT, Main K, Dalgaard P, Jorgensen K, Muller J, Hall K, Skakkebaek NE** 1994 Serum insulin-like growth factor-I in 1030 healthy children, adolescents, and adults: relation to age, sex, stage of puberty, testicular size, and body mass index. *J Clin Endocrinol Metab* 78:744-752
5. **Abbassi V** 1998 Growth and normal puberty. *Pediatrics* 102:507-511
6. **Goeman JJ, van de Geer SA, de Kort F, van Houwelingen HC** 2004 A global test for groups of genes: testing association with a clinical outcome. *Bioinformatics* 20:93-99
7. **Weise M, De Levi S, Barnes KM, Gafni RI, Abad V, Baron J** 2001 Effects of estrogen on growth plate senescence and epiphyseal fusion. *Proc Natl Acad Sci U S A* 98:6871-6876
8. **Gafni RI, Weise M, Robrecht DT, Meyers JL, Barnes KM, De Levi S, Baron J** 2001 Catch-up growth is associated with delayed senescence of the growth plate in rabbits. *Pediatr Res* 50:618-623
9. **Schrier L, Ferns SP, Barnes KM, Emons JA, Newman EI, Nilsson O, Baron J** 2006 Depletion of resting zone chondrocytes during growth plate senescence. *J Endocrinol* 189:27-36
10. **Nilsson O, Mitchum RD, Jr, Schrier L, Ferns SP, Barnes KM, Troendle JF, Baron J** 2005 Growth plate senescence is associated with loss of DNA methylation. *J Endocrinol* 186:241-249
11. **Emons J, Chagin AS, Hultenby K, Zhivotovsky B, Wit JM, Karperien M, Savendahl L** 2009 Epiphyseal Fusion in the Human Growth Plate does not involve Classical Apoptosis. *Pediatr Res*
12. **van der Eerden BC, Van D, V, Lowik CW, Wit JM, Karperien M** 2002 Sex steroid metabolism in the tibial growth plate of the rat. *Endocrinology* 143:4048-4055

8

Epiphyseal Fusion in the Human Growth Plate does not involve Classical Apoptosis

Joyce Emons¹, Andrei S. Chagin², Kjell Hultenby³, Boris Zhivotovsky⁴, Jan M. Wit¹, Marcel Karperien^{5,6}, Lars Sävendahl²

Pediatr Res. 2009 Dec;66(6):654-9

¹Dept of Paediatrics, Leiden University Medical Center, 2300 ZA Leiden, the Netherlands;

²Dept of Pediatric Endocrinology, Karolinska Institutet, SE-171 76 Stockholm, Sweden;

³ Dept of Laboratory Medicine, Karolinska Institutet, 14186 Stockholm, Sweden;

⁴Division of Toxicology, Institute of Environmental Medicine, Karolinska Institutet, S-171-77 Stockholm, Sweden;

⁵Dept of Tissue Regeneration, University of Twente, 7522 NB Enschede, the Netherlands;

⁶Dept of Endocrinology and Metabolism, Leiden University Medical Center, 2300 ZA Leiden, The Netherlands.

Abstract

By the end of puberty, growth ceases and epiphyseal fusion occurs through mechanisms not yet completely understood. Human growth plate tissues were collected in various pubertal stages including a unique late pubertal growth plate, which was about to fuse. Apoptosis was studied by TUNEL (terminal deoxynucleotidyl transferase (TdT)-mediated deoxy-UTP nick end labeling) staining, immunolocalization of pro- and anti-apoptotic proteins and electron microscopy. Morphological analyses of the fusing growth plate revealed disorganized, large chondrocytes surrounded by a border of dense, cortical-like bone. In the unfused growth plates, few chondrocytes were TUNEL-positive. In contrast, the fusing growth plate contained no single TUNEL-positive cell. Anti-apoptotic (Bcl-2 and Bcl-X_L) and pro-apoptotic (Bax, Bad and cleaved caspase-3) proteins were detected in all growth plate zones without change in intensity during pubertal progression. Expression of anti-apoptotic proteins was found in the fusing growth plate but of the pro-apoptotic proteins only Bad was detected. Electron microscopy revealed no typical signs of apoptosis or autophagy in any of the growth plates. In contrast, morphological signs of hypoxia as well as necrosis were observed. We conclude that classical apoptosis is not likely to be involved in the process of human growth plate fusion.

Introduction

Longitudinal growth occurs at the epiphyseal plate, a thin layer of cartilage entrapped between epiphyseal and metaphyseal bone, located at the distal ends of the long bones. The epiphyseal plate consists of three principal layers with immature cells lying toward the epiphysis, called the resting zone, more mature flat chondrocytes in the proliferating zone and the hypertrophic zone adjacent to this. Stem-like cells in the resting zone have a finite proliferative capacity that is gradually exhausted which consequently results in fusion of the growth plate at the end of puberty (1). At the chondro-osseous junction site of the growth plate, a nowadays generally accepted hypothesis is that terminally hypertrophic chondrocytes die by undergoing apoptosis leaving behind a scaffold of cartilage matrix for osteoblasts that invade and lay down bone resulting in growth plate fusion (1, 2). Apoptotic cells in general show typical morphological changes like cell shrinkage, intact organelles and integrity of membranes, pyknotic nuclei by aggregation of chromatin, fragmented DNA, partitioning of the cytoplasm and nucleus into membrane bound-vesicles (apoptotic bodies) and absence of an inflammatory response (3, 4). The Nomenclature Committee on Cell Death suggested to describe apoptosis at a biochemical level as a caspase-dependent process (5). Apoptosis in growth plate chondrocytes has been reported in many *in vivo* and *in vitro* studies performed in different species applying mostly the TUNEL (Terminal deoxynucleotidyl transferase (TdT)-mediated deoxy-UTP nick end labeling) technique to label fragmented DNA (6-8). Additional studies in animals show that apoptosis-regulating proteins are predominantly expressed in the proliferative and hypertrophic zones with an increase of pro-apoptotic factors by age (7, 9). Others have questioned apoptosis as the final mechanism through which chondrocytes die in the terminal hypertrophic zone. Ahmed et al. hypothesized non-apoptotic mechanisms to be involved and described morphological changes distinct from classical apoptosis (10). In addition, Roach et al. re-examined microscopic pictures of hypertrophic chondrocytes of *in vitro* cultured chick growth plates and hypothesized that terminal hypertrophic chondrocytes not only die through apoptosis but some also go through transdifferentiation to endochondral osteoblasts (11). In later studies Roach et al studied rabbit growth plates and described chondrocytes with condensed chromatin,

suggestive of apoptosis, but the "morphology of the cytosol" was unlike that of necrotic, apoptotic, or normal cells (12, 13). In 2004, they came up with the name chondroptosis instead of apoptosis to describe the appearance of these cells (14). This study also reported autophagic vacuoles in the chondroptotic cells, suggesting a role for autophagy in the process of cell death of the terminal hypertrophic cell. Autophagy and autophagosomes were also observed in avian hypertrophic chondrocytes and in chondrocytes of newborn mice (15, 16).

Previous studies focusing on the fate of growth plate chondrocytes have been performed mostly in different animal models. It is uncertain whether the chick growth plate is comparable to the human, and studies in rodents are limited by the fact that growth plate fusion does not occur during sexual maturation in rats and mice. The only studies done in human tissues are not very extensive involving TUNEL analyses performed in spinal growth plates and slipped capital femoral epiphysis growth plates (6, 17, 18). To resolve this issue, we decided to jointly collect human growth plate tissue samples obtained during epiphyseal surgery performed in children at different stages of development. When analyzing all these samples of human growth plate tissues, we were lucky to discover that in one of the patients, a 17-year-old late pubertal female, the growth plate was captured just when it was in the process of undergoing epiphyseal fusion. This growth plate tissue can be considered as unique since epiphyseal fusion is a rapid process which is extremely difficult to capture. This specific human tissue specimen is therefore like a snapshot of epiphyseal fusion and could help us to better understand how growth plate fusion occurs and the underlying mechanisms involved. Using these tissues, we here aimed to describe the morphological characteristics of a fusing human growth plate and possible mechanisms involved in the process of human epiphyseal fusion and discuss these in relation to previous published data obtained in different animal models.



Figure 1: X-ray of patient #13. Complete luxation of the right hip.

Methods

Patients and tissue preparation

Human proximal and distal femur growth plate tissues were collected from 14 girls and 5 boys at different pubertal stages who were undergoing surgery for different medical indications (Table 1). The study protocol was approved by the Local Medical Ethics Committees of The Leiden University Center, Leiden, the Netherlands and The Karolinska University Hospital, Stockholm, Sweden. Informed consent was obtained from all patients and their parents. No patient used any continuous medication. Patient #13, the patient with a growth plate in the process of epiphyseal fusion, was mostly wheelchair bound and mentally retarded. Because of frequent painful hip luxations hip replacement surgery was performed. Figure 1 shows an X-ray of her right hip where a complete luxation can be observed. All tissue samples were processed in the same way. Specimens were immediately fixed in 10% formaldehyde overnight, decalcified in 10% EDTA for 5 days and then embedded in paraffin.

Table 1: IHC Total growth plate staining

Pt #	diagnosis	sex	(distal/prox femur)	age (yr:m)	Tanner	TUNEL	Bcl-2	Bcl-X _L	Bax	Bad	Casp3
1	constitutional tall stature	f	distal	11:6	B1	0	x	x	x	x	x
2	leg length difference	f	distal	9:6	B1	0	x	x	x	x	x
3	leg length difference	f	distal	9:6	B1-2	0	x	x	x	x	2
4	hip luxations, femur head resection	f	proximal	12:5	B2	0	1	2	1	1	2
5	leg length difference	f	distal	12:8	B2	1	x	3	x	2	2
6	constitutional tall stature	f	distal	13:7	B2	0	x	x	x	x	x
7	constitutional tall stature	f	distal	12:1	B2	0	2	x	x	x	x
8	leg length difference	f	distal	14:2	B2-3	0	x	2	1	2	2
9	hip luxations, femur head resection	f	proximal	13:5	B3	0	2	2	2	2	1
10	leg length difference	f	distal	13:8	B3	0	x	1	1	x	0
11	cerebral palsy, femur head resection	f	proximal	15:1	B4	0	2	2	1	2	1
12	leg length difference	f	distal	13:3	B4	0	x	x	x	x	x
13	cerebral palsy, femur head resection	f	proximal	17:0	B5	0	2	2	0	2	0
14	leg length difference	f	distal	12:1	B5	0	x	x	x	x	x
15	Marfan	m	distal	12:3	G1	0	x	x	x	x	1
16	leg length difference	m	distal	12:6	G3	0	x	x	x	x	x
17	leg length difference	m	distal	15:4	G3-4	0	x	x	x	x	x
18	leg length difference	m	distal	14:8	G4	0	x	x	x	x	x
19	47XYY	m	distal	14:0	G4-5	0	x	x	x	x	x

TUNEL and histology staining for Bcl-2, Bcl-X_L, Bax, Bad and caspase-3 were scored from 0 to 3 for each patient (Pt). 0 indicating no staining in the growth plate and 3 indicating many positive chondrocytes throughout the growth plate. x indicates that no staining was performed. Age is given in years and months (yr:m)

Immunohistochemistry

Immunohistochemistry was performed as previously described (19) with the following modifications. After antigen retrieval by incubating with trypsin (Invitrogen) for 10 minutes at 37°C, the sections were additionally treated with 5 mg/ml hyaluronidase (Sigma-Aldrich, Inc, Steinheim, Germany) for 30 min at 37°C. Anti-Collagen-X antibody was from Quartett (Berlin, Germany) and used in a 1:100 dilution. Anti-Bcl-2 antibody was from Upstate (#06-474 Upstate Biotechnology, Lake Placid, NY, USA) and used in a 1:300 dilution. Anti-Bax antibody (P19) and anti-Bad antibody (C-20) were purchased from Santa Cruz Inc., (Santa Cruz Biotechnology, Inc., Santa Cruz, CA, USA) and respectively used in a 1:300 and 1:200 dilution. Anti-Bcl-X_L antibody was purchased from Transduction Laboratories (Becton Dickinson AB, Stockholm, Sweden) and used in a 1:100 dilution. Anti-cleaved-caspase 3 primary antibody was purchased from Cell Signaling Technology (In Vitro Sweden AB, Stockholm, Sweden) and used in a 1:50 dilution. Secondary anti-rabbit biotinylated antibody (Jackson Immunoresearch lab, West Grove, PA, USA) or anti-mouse biotinylated antibody (DAKO, Glostrup, Denmark) were respectively used in a 1:1000 and 1:300 dilution, followed by incubation with avidin-biotin Vectastain ABC reagent according to manufactures instructions (Vector laboratories, Burlingame, California, USA). Digital images were collected employing a Nikon Eclipse E800 microscope equipped with an Olympus DP70 digital camera.

Apoptosis assay (TUNEL)

Apoptotic cells were identified by terminal deoxynucleotidyl transferase (TdT)-mediated deoxy-UTP nick end labeling (TUNEL) immunohistochemistry according to instructions for the TdT-FragEL™ DNA fragmentation kit (Oncogene Research, Boston, MA) with the following modifications. The sections were treated with 5 µg/ml proteinase K for 15 min (20-22). Control experiments showed that when pre-treating sections with distilled water instead of TdT, all cells were negative, whereas pretreatment with DNase enabled labeling of all cells.

Tartrate-resistant acid phosphatase (TRACP) staining

TRACP staining was performed using a combination of solutions that include naphthol-AS BI phosphate, dimethylformamide, tartaric acid, acetate buffer, vermoal buffer, sodium nitrite, and pararosaniline pH 5.2. Tissue sections were deparaffinized, rehydrated, and incubated with the reactive solution for 30 min as described in detail previously (23). After washing with distilled water, the tissue sections were counterstained with Mayer's hematoxylin.

Transmission electron microscopy (TEM)

Small tissue pieces were cut out from blocks of paraffin embedded bone/cartilage tissue and the paraffin was dissolved in Xylene at 60°C. The tissue was re-hydrated in alcohol into distilled water and fixed in 2% glutaraldehyde + 0.5% paraformaldehyde in 0.1M sodiumcacodylate buffer containing 0.1M sucrose and 3mM CaCl₂, pH 7.4, 24 hours at 4°C. Specimens were rinsed in 0.15 M sodiumcacodylate buffer containing 3mM CaCl₂, pH 7.4 postfixed in 2% osmium tetroxide in 0.07 M sodiumcacodylate buffer containing 1.5 mM CaCl₂, pH 7.4 at 4°C for 2 hour, dehydrated in ethanol followed by acetone and embedded in LX-112 (Ladd, Burlington, Vermont, USA). Semithin sections were cut and stained with toluidine blue and used for light microscopic analysis. Ultrathin section were cut and contrasted with uranyl acetate followed by lead citrate and examined in a Tecnai 10 transmission electron microscope at 80 kV. Digital images were captured by a MegaView III digital camera (Soft Imaging System, GmbH, Münster, Germany).

Results

Light microscopy

Figure 2a and c show representative pictures of an early pubertal female growth plate (patient #4) at 40x (a) and 100x (c) magnification. Figure 2b and d show pictures of the late pubertal patient (patient #13) with ongoing fusion of her growth plate stained with H&E at respectively 40x and 100x magnification. As expected, early pubertal growth plate chondrocytes were found to be organized in parallel columns maturing from resting to proliferative and then to large hypertrophic cells. In the late pubertal patient, growth plate remnants were found at the site where in less mature bones the epiphyseal plate is located. These remnants were small and surrounded by dense cortical-like bone. Chondrocytes within these growth plate remnants were disorganized and no columns could be found. In addition, the cells were very large with big lacunae and some of them were fused together. In order to study in more detail the interface of the fusing growth plate, immunohistochemistry for collagen type X and TRACP staining were performed. The unfused growth plates showed expectedly positive staining for collagen type X in the hypertrophic zone (Figure 2e). However, the growth plate remnant with large hypertrophic-like cells did surprisingly not show any positive staining (Figure 2f). TRACP staining, a marker for osteoclasts, was seen at the chondro-osseous junction of prepubertal growth plates (Figure 2g), as well as in early pubertal growth plates (data not shown). However, at the interface of the growth plate remnant no TRACP staining could be detected (Figure 2h).

Transmission electron microscopy

To allow comparative electron microscopic studies of cell death characteristics, small pieces were cut out from paraffin blocks containing growth plate tissues from the patient with ongoing epiphyseal fusion. For comparative analysis, three younger pubertal female growth plates (patients #4, 9 and 11) were processed in a similar way.

The fusing growth plate was found to be entirely surrounded by a border of very dense, cortical-like bone clearly isolating the growth plate from any vessels or osteoclasts (figure 3f). In contrast, in nonfusing growth plates, there was a small distinct border between loosely packed collagen type II in the cartilage matrix and collagen type I in the bone matrix (figure 3e). Collagen type I contains thick fibers compared to the very thin collagen type II fibers and therefore these two types of collagen could easily be distinguished. There were no signs of classical apoptosis in the fusing growth plate; e.g. no apoptotic bodies or patched chromatin and proteins could be found (figure 3b, d). In addition, no typical signs of inflammation were found although we did observe some signs of early necrosis like empty vacuoles (see arrows figure 3b). Additionally we observed signs of hypoxia, e.g. patchy distributed chromatin and defect plasma cell membranes. No double-membrane autophagosomes, like typically seen in cells undergoing autophagy, were found in the fusing growth plate.

In early-pubertal and mid-pubertal growth plates (figure 3a, c), we observed normal chondrocytes with non-pyknotic nuclei containing homogenous dense chromatin without signs of DNA fragmentation. We specifically focused on the terminal hypertrophic chondrocytes that were about to be incorporated into the newly formed bone. In these cells some chromatin condensation was seen, but this was clearly different from what normally is seen in cells undergoing classical apoptosis. Cell membranes were intact and the cytoplasm mostly empty. No autophagosomes could be found and no sign of necrosis was present.

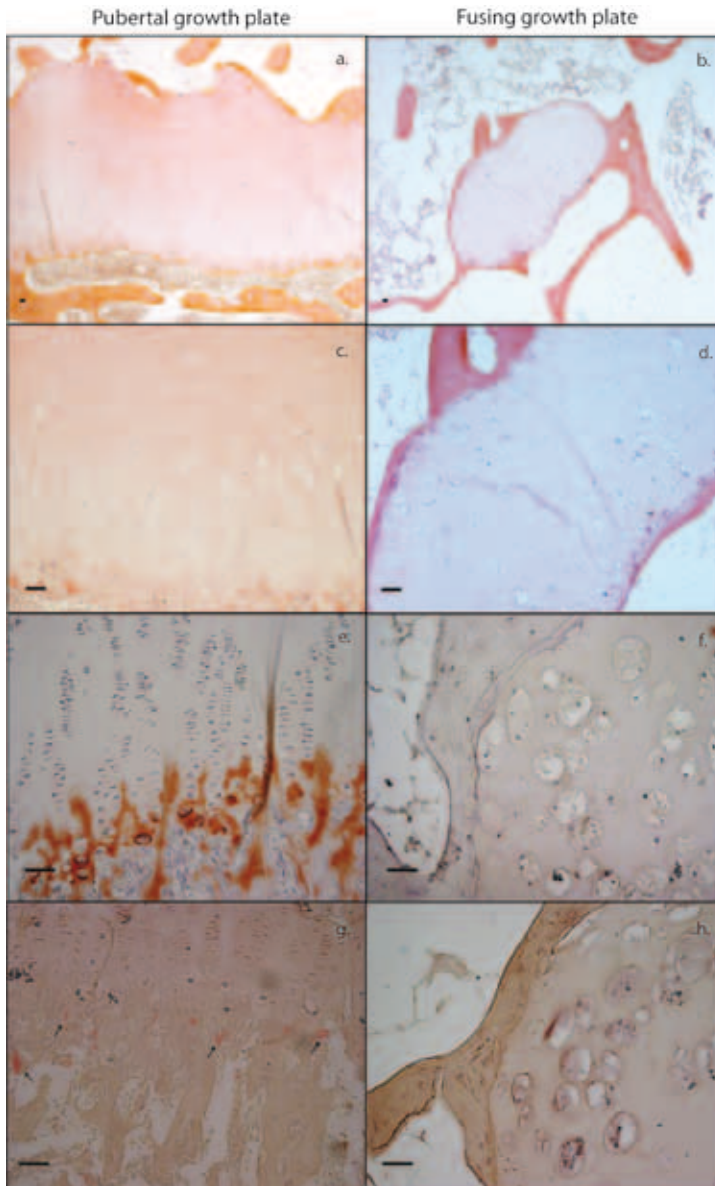


Figure 2. H&E staining of sectioned human growth plates.

In early pubertal patients, growth plate chondrocytes were organized in parallel columns; (patient#4; panel a. 40x and panel c. 100x magnification). In a late pubertal patient, the growth plate was diminished to a small remnant surrounded by dense cortical-like bone (patient #13; panel b. 40x and panel d. 100x magnification). All unfused growth plates stained positive for collagen type X in the hypertrophic zone (patient #2; panel e. 100x magnification) while the fusing growth plate did not show any staining (patient #13; panel f. 100x magnification). Panel g. shows positive TRACP staining in an early pubertal growth plate, indicated by arrows (patient #2, 100x magnification) while the fusing growth plate stained negative (patient #13; panel h. 100x magnification). Bars in all figures indicate 200µm.

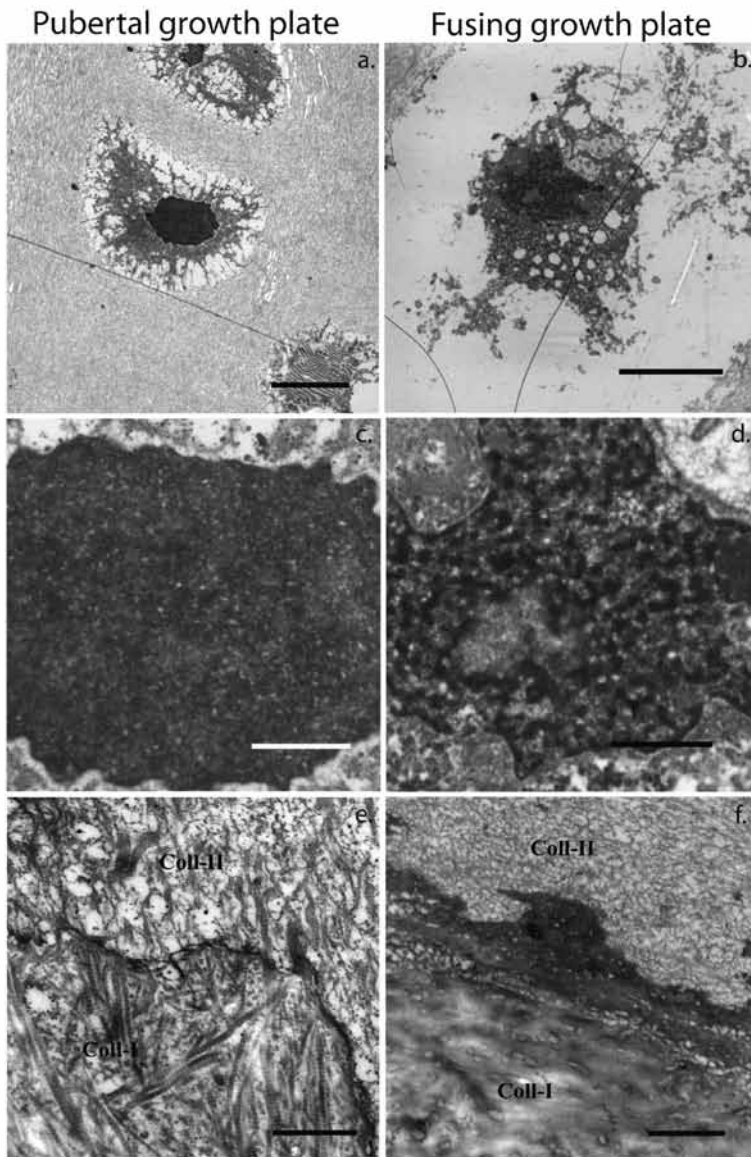


Figure 3

TEM images from the proximal femur epiphyseal growth plate in a mid-pubertal patient (patient #9; left panels, **a**, **c**, and **e**) and the late pubertal patient with a fusing growth plate (patient #13; right panels **b**, **d**, and **f**). In the mid-pubertal patient, hypertrophic zone chondrocytes displayed a normal morphology (**a**) and at a higher magnification dense chromatin was found in the cell nucleus (**c**). In contrast, the fusing growth plate displayed a patchy chromatin pattern (**b** and **d**). At high power magnifications of the interphase between cartilage and bone matrix, a distinct border between loosely packed cartilage matrix collagen type II (Coll-II) and bone matrix collagen type I (Coll-I) was found in the mid-pubertal patient (**e**) while in the fusing growth plate, the border was thicker and the bone matrix collagen type I more dense (**f**). Bars: **a**, **b** = 5 μ m; **c**, **d** = 2 μ m; **e**, **f** = 1 μ m.

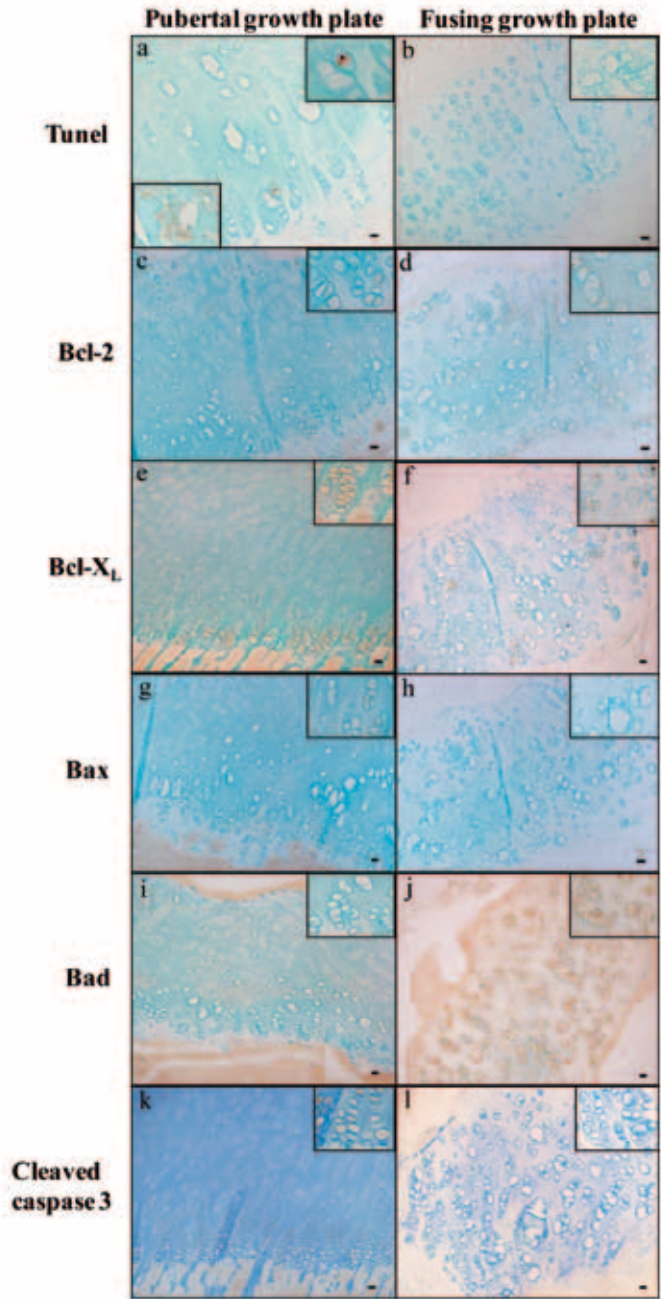


Figure 4

TUNEL and immunohistochemistry staining of prepubertal, pubertal and fusing growth plates (100x and inserts 200x magnification). Panel **a**: TUNEL analysis patient #4, left insert showing positive cells in surrounding bone marrow. Panel **b**: TUNEL analysis fusing growth plate (patient #13). Panel **c+d**: Bcl-2 staining patient #4 and fusing growth plate. Panel **e+f**: Bcl-X_L staining patient #10 and fusing growth plate. Panel **g+h**: Bax staining patient #4 and fusing growth plate. Panel **i+j**: Bad staining patient #3 and fusing growth plate. Panel **k+l**: cleaved caspase-3 patient #3 and fusing growth plate. Bars indicate 100 μm.

TUNEL analysis

In all female (2 prepubertal and 12 pubertal) and male (5 pubertal) subjects, very few growth plate chondrocytes stained positive or showed an apoptotic-like morphology when applying the TUNEL method (figure 4a). The staining intensity was scored (0 to 3 points; 0 indicating no staining and 3 indicating many positive cells throughout the growth plate) and the results are shown in table 1, ranked according to pubertal stages. It is important to point out that when evaluated by experienced scientists in the field, most TUNEL-positive cells indeed were considered to have a viable appearance, as indicated by a complete absence of apoptosis-related morphological changes, and should therefore be considered as non-specifically stained. In the fusing growth plate, no single TUNEL-positive cell was detected (figure 4b). In contrast, the surrounding bone marrow was abundantly stained with the TUNEL technique and could therefore serve as an internal positive control as previously described (21, 24). Negative controls showed no staining.

Anti-apoptotic proteins

Bcl-2 staining was detected in cells throughout the whole growth plate in patients with non-fused growth plates (n=4, table 1) (figure 4c). When the relative staining intensity was scored (score 0 to 3), a possible tendency towards increased expression was found during maturation (table 1). The fusing growth plate did show some staining for Bcl-2 (score 2; figure 4d).

Bcl-X_L, another anti-apoptotic factor, was also localized in cells throughout the whole growth plate (n=6, table 1, figure 4e). No change in percentage positive cells or staining intensity was seen during maturation. Also in the fusing growth plate some cells stained positive for Bcl-X_L (score 2; fig 4f).

Pro-apoptotic proteins and caspase 3

Staining for Bax, a proapoptotic factor, was seen in chondrocytes throughout the whole growth plate (n=5, table 1, figure 4g). No change in staining intensity or percentage Bax positive cells was seen during pubertal development. Interestingly, in the fusing growth plate no staining for Bax could be detected (figure 4h).

Staining for Bad, another proapoptotic factor, was found throughout the whole growth plate (n=5, table 1, figure 4i). No change in staining intensity or percentage of positive cells was seen during development. Some staining for Bad proteins was observed in the fusing growth plate (score 2; fig 4j), unfortunately with abundant background staining.

Cleaved caspase 3, an effector caspase in the apoptotic cascade, was seen throughout the whole growth plate in all pubertal stages (n= 8, table 1) with no change during maturation (figure 4k). In the fusing growth plate, no staining for cleaved caspase 3 was detected (figure 4l).

Negative controls showed no staining for all analyzed pro- and anti-apoptotic proteins.

Discussion

Based on well established morphological and histological criteria of apoptosis, we could not detect any signs of classical apoptosis in human terminal hypertrophic growth plate chondrocytes. These findings were also confirmed by electron microscopy. In a unique tissue specimen of a late pubertal fusing human growth plate, we found clear evidence that chondrocyte apoptosis is not likely to be involved in the end phase of growth plate fusion in humans. In contrast, signs of hypoxia and early necrosis were present in the fusing growth plate.

This is the first detailed study of apoptosis in the human pubertal growth plate which includes expression levels of pro- and anti-apoptotic proteins together with morphological analysis based on light and electron microscopy. Our study includes the characterization of a unique tissue sample from a growth plate in the process of undergoing fusion where we made the novel observation that the chondrocytes were markedly enlarged, disorganized, and surrounded by a border of dense, cortical-like bone. No morphological signs of classical apoptosis were found in this fusing growth plate. Our findings are in agreement with earlier studies describing terminal hypertrophic zone chondrocytes at the chondro-osseous junction to have a morphology which is not typically seen in cells undergoing classical apoptosis (11, 14, 25, 26). However, it is important to point out that all these previous studies were performed in animal growth plates; avians or rodents that do not fuse their growth plates by the end of sexual maturati.

The mechanism by which terminal hypertrophic chondrocytes disappear during endochondral ossification is believed to be related to the underlying cause of eventual growth plate fusion. However, these two events involving the epiphyseal growth plate might as well be two different and independent processes. In this paper we compared both. Interestingly, we found some signs of early apoptosis and also some signs of necrosis such as empty vacuoles in the fusing growth plate, suggesting that fusing growth plate chondrocytes appear in a sort of intermittent stage between apoptosis and necrosis. Importantly, no signs of inflammation were observed around the fusing growth plate. Erenpreisa and Roach also reported signs of necrosis in dark chondrocytes of the embryonic chick growth plate (26), however such dark chondrocytes were not found in our human growth plate tissue samples. To our knowledge, no other signs of necrosis have previously been reported in the growth plate. Interestingly, Shapiro et al. has reported that the morphology of terminal hypertrophic chondrocytes suggest autophagy, a type II programmed cell death, to occur in the growth plate (16). However, we did not see any double membrane structures like autophagosomes suggestive for autophagy, but only vesicles with a single membrane that we interpreted as vacuoles.

Apoptosis is the most widely accepted and described mode of cell death through which terminal hypertrophic chondrocytes disappear and are replaced by bone (27). Most studies rely on TUNEL technique only, which often overestimates the number of apoptotic nuclei, as it labels not only fragmented DNA but also DNA in the process replication and repair. In many studies TUNEL positive chondrocytes were observed not only in the hypertrophic layer where cells are assumed to die prior to being incorporated into the newly formed bone, but in all zones of the growth plate (6, 17, 18). When re-evaluating pictures of growth plate chondrocytes positive for TUNEL staining, a high diversity of results could be found. Cell morphology is not always complementing TUNEL positivity and when data are presented, cells often do not look like cells in the process of undergoing apoptosis, but as healthy viable cells without showing signs of cell shrinkage and pyknotic nuclei (6, 17, 18). Thus, the TUNEL method is very sensitive and it requires precise temporal control of each step (28) and must be verified by other techniques like EM or molecular markers of apoptosis.

Molecular markers of apoptosis include cleavage of caspases and often regulation of pro- and anti-apoptotic proteins of the Bcl-2 family (29). In the current study we are the first to investigate these proteins in the human postnatal growth plate and we found that they are indeed expressed throughout the whole growth plate. We did not observe any caspase-3 cleavage, the effector caspase of apoptosis in the fusing growth plate. Moreover, in the fusing growth plate we observed clear expression of the anti-apoptotic proteins Bcl-2 and Bcl-X_L and a possible down-regulation of the pro-apoptotic protein Bax. Thus, all three approaches including TUNEL technique, analysis of cell morphology by electron microscopy and molecular markers by immunohistochemistry altogether suggest that there is no classical apoptosis occurring in the fusing human growth plate. A novel and clear observation was that the fusing human growth plate is surrounded by a border of very dense thick bone, shelling the growth plate remnant. There are no vessels seen in or surrounding the fusing growth plate. Moreover, there were some signs of hypoxia in the fusing growth plate like patchy distributed chromatin. From these findings one can hypothesize that this border of dense bone is functioning as a physical barrier for oxygen and nutrients to reach the fusing growth plate resulting in hypoxia and eventually cell death in a non-classical apoptotic way through necrosis or a mixture of apoptosis and necrosis. White et al. recently demonstrated by light microscopy bridging bone in the center of a distal human tibial growth plate obtained from a 12 years and 11 months old girl, which might be an early sign of this shelling process (30). A limitation of this study is the relatively small number of growth plates that were analysed and the fact that some were derived from pathological conditions. To some extent, this is compensated by the fact that we were fortunate to obtain a tissue sample from a human growth plate just in the rapid process of undergoing epiphyseal fusion, which allowed us to investigate possible underlying mechanisms. In addition, the underlying mechanism of epiphyseal maturation and fusion will be the same for all growth plates regardless of the underlying disease of each patient since eventually longitudinal growth stopped in all patients by the end of puberty. When performing electron microscopy, the gold standard in cell death research, we found no clear signs of classical apoptosis in any of the human growth plates studied including the fusing one. It should be mentioned that fixation was not performed in the optimal way for electron microscopy. However membranes were not disrupted in the way one would expect if tissue damage had occurred secondary to fixation problems. Furthermore, all tissues were processed in the same way and there were clear differences in chromatin pattern and collagen fibres which were nicely preserved. In summary, a unique piece of fusing human growth plate tissue clearly demonstrate that classical apoptosis is not likely to be involved in the process of human growth plate fusion. We found signs suggestive for hypoxia and necrosis, but the exact mechanism through which chondrocytes disappear during epiphyseal fusion in humans still needs to be defined.

Acknowledgment and funding

The authors thank the orthopaedic surgeons in the Leiden University Medical Center and at the Karolinska University Hospital in Stockholm for providing the growth plate samples.

This study is supported by ZonMw (project # 920-03-358) the Netherlands, the Swedish Research Council; and a visiting scholarship award from the European Society for Paediatric Endocrinology. No author has a conflict of interest to report.

References

1. **Hunziker EB** 1994 Mechanism of longitudinal bone growth and its regulation by growth plate chondrocytes. *Microsc Res Tech* 28:505-519
2. **Kronenberg HM** 2003 Developmental regulation of the growth plate. *Nature* 423:332-336
3. **Cohen JJ** 1993 Apoptosis. *Immunol Today* 14:126-130
4. **Zimmermann KC, Green DR** 2001 How cells die: apoptosis pathways. *J Allergy Clin Immunol* 108:S99-103
5. **Kroemer G, Martin SJ** 2005 Caspase-independent cell death. *Nat Med* 11:725-730
6. **Adamczyk MJ, Weiner DS, Nugent A, McBurney D, Horton WE, Jr.** 2005 Increased chondrocyte apoptosis in growth plates from children with slipped capital femoral epiphysis. *J Pediatr Orthop* 25:440-444
7. **Chrysis D, Nilsson O, Ritzen EM, Savendahl L** 2002 Apoptosis is developmentally regulated in rat growth plate. *Endocrine* 18:271-278
8. **Smink JJ, Gresnigt MG, Hamers N, Koedam JA, Berger R, Buul-Offers SC** 2003 Short-term glucocorticoid treatment of prepubertal mice decreases growth and IGF-I expression in the growth plate. *J Endocrinol* 177:381-388
9. **Wang Y, Toury R, Hauchecorne M, Balmain N** 1997 Expression of Bcl-2 protein in the epiphyseal plate cartilage and trabecular bone of growing rats. *Histochem Cell Biol* 108:45-55
10. **Ahmed YA, Tatarczuch L, Pagel CN, Davies HM, Mirams M, Mackie EJ** 2007 Physiological death of hypertrophic chondrocytes. *Osteoarthritis Cartilage* 15:575-586
11. **Roach HI, Erenpreisa J** 1996 The phenotypic switch from chondrocytes to bone-forming cells involves asymmetric cell division and apoptosis. *Connect Tissue Res* 35:85-91
12. **Roach HI, Clarke NM** 1999 "Cell paralysis" as an intermediate stage in the programmed cell death of epiphyseal chondrocytes during development. *J Bone Miner Res* 14:1367-1378
13. **Roach HI, Clarke NM** 2000 Physiological cell death of chondrocytes in vivo is not confined to apoptosis. New observations on the mammalian growth plate. *J Bone Joint Surg Br* 82:601-613
14. **Roach HI, Aigner T, Kouri JB** 2004 Chondroptosis: a variant of apoptotic cell death in chondrocytes? *Apoptosis* 9:265-277
15. **Settembre C, rtega-Solis E, McKee MD, de PR, Al AQ, Ballabio A, Karsenty G** 2008 Proteoglycan desulfation determines the efficiency of chondrocyte autophagy and the extent of FGF signaling during endochondral ossification. *Genes Dev* 22:2645-2650
16. **Shapiro IM, Adams CS, Freeman T, Srinivas V** 2005 Fate of the hypertrophic chondrocyte: microenvironmental perspectives on apoptosis and survival in the epiphyseal growth plate. *Birth Defects Res C Embryo Today* 75:330-339

17. **Wang S, Qiu Y, Zhu Z, Ma Z, Xia C, Zhu F** 2007 Histomorphological study of the spinal growth plates from the convex side and the concave side in adolescent idiopathic scoliosis. *J Orthop Surg* 2:19
18. **Zhu F, Qiu Y, Yeung HY, Lee KM, Cheng JC** 2006 Histomorphometric study of the spinal growth plates in idiopathic scoliosis and congenital scoliosis. *Pediatr Int* 48:591-598
19. **Nilsson O, Chrysis D, Pajulo O, Boman A, Holst M, Rubinstein J, Martin RE, Savendahl L** 2003 Localization of estrogen receptors-alpha and -beta and androgen receptor in the human growth plate at different pubertal stages. *J Endocrinol* 177:319-326
20. **Chagin AS, Chrysis D, Takigawa M, Ritzen EM, Savendahl L** 2006 Locally produced estrogen promotes fetal rat metatarsal bone growth; an effect mediated through increased chondrocyte proliferation and decreased apoptosis. *J Endocrinol* 188:193-203
21. **Chagin AS, Karimian E, Zaman F, Takigawa M, Chrysis D, Savendahl L** 2007 Tamoxifen induces permanent growth arrest through selective induction of apoptosis in growth plate chondrocytes in cultured rat metatarsal bones. *Bone* 40:1415-1424
22. **Martensson K, Chrysis D, Savendahl L** 2004 Interleukin-1beta and TNF-alpha act in synergy to inhibit longitudinal growth in fetal rat metatarsal bones. *J Bone Miner Res* 19:1805-1812
23. **van der Pluijm G, Most W, Van DW-P, de GH, Papapoulos S, Lowik C** 1991 Two distinct effects of recombinant human tumor necrosis factor-alpha on osteoclast development and subsequent resorption of mineralized matrix. *Endocrinology* 129:1596-1604
24. **Ramos F, Fuertes-Nunez M, Suarez-Vilela D, Fernandez-Lopez A** 2002 What does apoptosis have to do with clinical features in myelodysplastic syndrome? *Haematologica* 87:381-391
25. **Adams CS, Shapiro IM** 2002 The fate of the terminally differentiated chondrocyte: evidence for microenvironmental regulation of chondrocyte apoptosis. *Crit Rev Oral Biol Med* 13:465-473
26. **Erenpreisa J, Roach HI** 1998 Aberrant death in dark chondrocytes of the avian growth plate. *Cell Death Differ* 5:60-66
27. **Cetin E, Girsch W, Brand G, Thurnher D, Cetin EM, Trieb K** 2004 Distinct expression of APO-1/Fas and caspase-8 in the human growth plate. *Calcif Tissue Int* 74:181-186
28. **Rohwer F, Azam F** 2000 Detection of DNA damage in prokaryotes by terminal deoxyribonucleotide transferase-mediated dUTP nick end labeling. *Appl Environ Microbiol* 66:1001-1006
29. **Robertson JD, Orrenius S, Zhivotovsky B** 2000 Review: nuclear events in apoptosis. *J Struct Biol* 129:346-358
30. **White JR, Wilsman NJ, Leiferman EM, Noonan KJ** 2008 Histomorphometric analysis of an adolescent distal tibial physis prior to growth plate closure. *J Child Orthop* 2:315-319

9

Preferential chondrogenic differentiation potential of human bone marrow-derived mesenchymal stem cells

M.E. Bernardo M.D.¹, J.A.M. Emons M.D.², A.J. Nauta Ph.D.³, H. Roelofs Ph.D.⁴, S. Romeo M.D.⁵, A. Marchini⁶, G.A. Rappold⁶, S. Vucikevic⁷, M. Karperien Ph.D.², F. Locatelli M.D.¹, R. Willemze Ph.D., M.D.³, W.E. Fibbe Ph.D., M.D.^{3,4}

Connect Tissue Res. 2007;48(3):132-40

¹Pediatric Hematology/Oncology, IRCCS Policlinico San Matteo, Pavia, Italy.

²Department of Endocrinology, ³Department of Experimental Hematology,

⁴Department of Immunohematology and Blood Transfusion,

⁵Department of Pathology, Leiden University Medical Center, Leiden, The Netherlands,

⁶Institute of Human Genetics, University of Heidelberg, Heidelberg, Germany, and

⁷Laboratory for Mineralized Tissues, University of Zagreb, Zagreb, Croatia

Abstract

Objective: Mesenchymal stem cells are multipotent cells capable of differentiation into several mesenchymal lineages. These cells have been isolated from various tissues such as adult bone marrow, placenta and fetal tissues. Since a specific phenotypical marker for MSCs is lacking, MSCs are currently characterized on the basis of phenotype and capacity to differentiate into multiple mesenchymal lineages. However, how the potential of these cells to differentiate into the chondrogenic lineage is influenced by the tissue of origin has not been examined. The aim of this study was to investigate whether MSCs isolated from different sources exhibit differential multilineage differentiation potential.

Design: MSCs from fetal and adult tissues were phenotypically characterized and examined for their differentiation capacity, based on morphological criteria and expression of extracellular matrix components.

Results: Our results show that both fetal and adult MSCs undergo chondrogenesis under appropriate conditions. Nevertheless, MSCs of bone marrow origin, either fetal or adult, exhibit a higher chondrogenic potential than fetal lung and placenta derived MSCs, as demonstrated by the appearance of typical morphological features of cartilage, the intensity of Toluidine Blue staining and the expression of collagen type II, IX and X after culture under chondrogenic conditions. In addition, the capacity of MSCs to differentiate into chondrocytes was reduced upon passaging of cells.

Conclusions: MSCs are an attractive source for cartilage tissue engineering strategies. Hence, exploring the chondrogenic potential of different sources is of great interest for such a purpose. Our study indicates that bone marrow is to be considered as the preferred MSC source for cartilage engineering.

Introduction

Articular cartilage has a limited capacity of healing after injury. Traumatic damage and degenerative diseases of the cartilage such as osteoarthritis or rheumatoid arthritis are common health problems worldwide. Therefore a lot of interest has recently emerged in techniques for cartilage tissue engineering. The current strategies of cartilage repair, based on the use of autologous chondrocytes, have some limitations including the small number of cells available with restricted proliferative capacity and the further damage at donor site of harvest. For these reasons, new techniques are now focusing on the use of mesenchymal progenitor cells to be delivered within an appropriate carrier system to repair and regenerate pathologically altered cartilage^{1,2}. In fact, mesenchymal stem cells (MSCs) play a role in bone and cartilage homeostasis and it has been shown that the chondrogenic activity of these cells is reduced in patients with advanced osteoarthritis (OA)³. One of the mechanisms involved in the repair of damaged articular cartilage may be the *de novo* chondrogenesis from MSCs^{4,5}. Therefore, based on the *in vitro* observation of the differentiation into chondrocytes, on their expandability and availability, MSCs can be considered as an attractive candidate for purposes of cartilage engineering^{6,7}.

MSCs are multipotent cells with the ability to differentiate into several mesenchymal lineages, including osteoblasts, adipocytes and chondrocytes⁸⁻¹⁰. Although MSCs were originally isolated from bone marrow¹¹, they have also been isolated from other tissue sources. MSCs have been identified in fetal tissues such as lung, bone marrow, liver and spleen in first- and second-trimester^{12,13}. Placenta has been shown to be another rich source of MSCs of both fetal and maternal origin¹⁴;

and MSCs have been also isolated from umbilical cord blood, although in low frequency, and adipose tissue. At present no unique phenotype has been identified for MSCs; therefore the isolation and characterization of MSCs relies on the expression of a number of characteristic markers on culture expanded cells and on their ability to differentiate into the various mesenchymal differentiation lineages.

In the present study, we investigate the multilineage differentiation potential of MSCs derived from 4 different sources and whether this capacity is influenced by the tissue of origin.

Materials and methods

Isolation and culture of human MSCs

Fetal tissues

Fetal lung (fL) and fetal bone marrow (fBM) were obtained from the same fetus from women undergoing elective termination of pregnancy between 15 and 22 weeks of gestation. The study was approved by the hospital ethical committees and informed consent was obtained. Single cell suspensions of fetal lung were made by mincing and flushing the organ through a 100 mm nylon filter with IMDM medium (Cambrex, Verviers, Belgium) containing 1% penicillin/streptomycin (P/S; Cambrex, Verviers, Belgium) and 2% heat-inactivated fetal calf serum (FCS; Cambrex, Verviers, Belgium), i.e. washing medium. Single cell suspensions of fetal bone marrow were obtained by penetrating the long bones with a needle (23 gauge) and flushing the bones with washing medium. After washing, the cell suspension was depleted of red cells by incubation for 10 minutes in NH₄Cl (8,4 g/L)/KHCO₃ (1/g) buffer at 4 °C. The cells were subsequently plated at 160.000/cm² in culture medium consisting of M199 (Gibco, Paisley, Scotland) supplemented with 10% FCS, P/S, Endothelial Cell Growth Factor (ECGF) 20 mg/ml (Roche Diagnostics GmbH, Mannheim, Germany) and heparin 8 U/ml in tissue culture flasks (Greiner Bio-One GmbH, Mannheim, Germany) previously coated with 1% gelatin for 30 minutes at room temperature.

Placenta

Placentas (PL) were derived from second- and third-trimester pregnancies after informed consent and approval by the hospital ethical committees. Tissue specimens of placenta (maternal origin) were first washed with PBS; single cell suspensions were made by mincing and flushing the tissue through a 100 mm nylon filter with washing medium. The cells were subsequently cultured as described above. To confirm the maternal origin of these cells, molecular HLA-typing was performed on the PL-MSCs cultures.

Adult bone marrow

Adult bone marrow (aBM) samples were obtained from healthy donors for allogeneic stem cell transplantation under a protocol approved by the Ethical Review Board. Mononuclear cells were isolated by density gradient (Ficoll, 1.077 g/ml) and plated at 160.000/cm² in culture medium consisting of DMEM-Low Glucose (Gibco, Paisley, Scotland) supplemented with 10% FCS and P/S.

All cells were kept in a humidified atmosphere at 37 °C with 5% CO₂. Three to five days after plating, non-adherent cells were removed and the medium was refreshed. When grown to confluency, adherent cells were detached with trypsin/EDTA (Cambrex, Verviers, Belgium) for 5 minutes at 37 °C and reseeded for expansion or differentiation.

Flow cytometric analysis

Culture expanded fL-, fBM-, aBM- and PL-MSCs were phenotypically characterized by flow cytometry (FACSScan, Becton Dickinson). Fluorescein isothiocyanate (FITC) or phycoerythrin (PE) conjugated antibodies against CD166 (CLB, Amsterdam The Netherlands), CD105 (Ancell Corporation, Bayport, MN, USA), CD90 (Pharmlingen, San Diego, CA), CD34, CD45 and CD80 (Beckton Dickinson, San Jose, CA), CD31 (DAKO, Glostrup, Denmark), HLA-ABC (Instruchemie, Hilversum, The Netherlands), HLA-DR (Beckton Dickinson, San Jose, CA) were used, as well as isotype controls.

Osteogenic and adipogenic differentiation

The adipogenic and osteogenic differentiation capacity of MSCs from the 4 different sources was determined as previously described¹³. In short, to induce osteogenic differentiation, cells were cultured in a-MEM supplemented with 10% FCS, P/S, dexametasone (10^{-7} M) and ascorbic acid (50 mg/ml). b-glycerophosphate (5 mM) was added from day 7 onwards. For adipogenesis, insulin (10 mg/ml), indomethacin (0,25 M) and 1-methyl-3-isobutylxantine (IBMX, 50 mM) were added to this medium. Cells were incubated in differentiation medium for 3 weeks, with medium replacement twice a week, at 37°C with 5% CO₂. To detect the osteogenic differentiation cells were stained for alkaline phosphatase (AP) activity using Fast Blue and for calcium depositions with Alzarin Red. The adipogenic differentiation was evaluated through the morphological appearance of fat droplets.

Chondrogenic differentiation

For chondrocyte differentiation, 200,000 MSCs were placed per well in 96-well suspension culture plates, U-shape, (Greiner Bio-One GmbH, Mannheim, Germany) and centrifuged at 1200 rpm for 4 minutes to a pellet. Pellets were cultured at 37 °C with 5% CO₂ in 200 ml of serum-free chondrogenic medium consisting of DMEM-High Glucose (Gibco, Paisley, Scotland), 40 mg/ml proline (Sigma, USA), 100 mg/ml sodium pyruvate (Sigma, USA), 50 mg/ml ITS+Premix (BD Biosciences, Bedford, MA), 1% Glutamax (Gibco, Paisley, Scotland), P/S, 50 mg/ml ascorbate-2-phosphate (Sigma, USA), 10^{-7} dexametasone (Sigma, USA), 10 ng/ml Transforming growth Factor-b3 (TGF-b3, R&D Systems, Minneapolis) and 500 ng/ml Bone Morphogenetic Protein-6 (BMP-6, kindly provided by dr. S. Vucikevic) The medium was refreshed every 3 days for 21 days. We investigated at least three samples per source and 3 different passages per sample.

Reverse Transcription-Polymerase Chain Reaction (RT-PCR)

Total RNA was extracted from 1 million undifferentiated MSCs and from pellets at day 21 of the differentiation period, from each source, using RNAeasy kit (Quiagen GmbH, Hilden). RNA was reverse transcribed into cDNA using First Strand cDNA Synthesis kit for RT-PCR (Roche Diagnostics GmbH, Mannheim, Germany) according to the manufacturer's instructions. cDNA was amplified using a GeneAmp PCR System 2400 (Applied Biosystems, Foster City, CA). Expression of collagen type II, IX and X mRNA was quantified by real-time quantitative PCR using the Bio-Rad iCycler with SYBR Green. Data were corrected for β_2 -microglobulin expression. The following oligonucleotide primers were used: collagen type II: forward 5'-CCCTCTCCACACCTTCCTC-3' and reverse 5'-GGGTGAGGGATTCCAGGAAAA-3'; collagen type

IX: forward 5'-AGGACACAAGGGTGAAGAAGGT-3' and reverse 5'-TTTTCCCTTTGTCCCCAACTATG-3'; collagen type X: forward 5'-TTTTGCTGCTAGTATCCTTGAACCTT-3' and reverse 5'-AGGAGTACCTTGCTCTCCTCTTACT-3'; β_2 -microglobulin: forward 5'-TGCTGTCTCCATGTTTGATGTAT CT-3' and reverse 5'-TCTCTGCTCCCCACCTCTAAGT-3'. All PCR reactions were performed with 5 ng cDNA and according to the manufacturer's protocol of the qPCR Core Kit (Eurogentec, Southampton, UK) in a final volume of 25 μ l.

The cDNA was amplified using the following thermal cycling conditions: one cycle at 50 °C for 2 min and 95 °C for 10 min, followed by 40 cycles of 15 s at 95 °C and 1 min at 60 °C. Each sample was assayed in triplicate and water was used as a negative control. Fluorescence spectra were recorded and the threshold cycle number (Ct) was read. For each source mean Ct was calculated and from this value the fold difference from expression in the human growth plate according to the equation $2^{-\Delta\Delta Ct}$. For visualization, this value was log-transformed and expressed in figure 2C.

Histological analysis

After 21 days of culture in chondrogenic medium, pellets were fixed in 10% formalin, dehydrated by treatment with graded ethanols and incubated in butanol overnight. Thereafter pellets were embedded in paraffin and cut into 5 mm sections using a Reichert Jung 2055 microtome (Leica, Rijswijk, The Netherlands). The sections were then mounted on glass slides and stained with Toluidine Blue.

The immunohistochemical staining for collagen type X was performed on deparaffinized sections. To block non-specific activity, sections were pretreated with hydrogen peroxidase. Sections were stained with mouse monoclonal antibody against collagen type X (Quartett, Berlin, Germany). The binding of mouse IgG was detected by biotinylated rabbit-anti-mouse IgG (DAKO, Glostrup, Denmark), followed by incubation with horseradish-peroxidase-conjugated-streptavidine (Amersham Biosciences, UK). The peroxidase activity was revealed using 3-amino-9-ethylcarbazole (AEC) substrate. After sections were washed, they were counterstained with hematoxylin.

Results

Morphology and immunophenotypic characterization of MSCs

MSCs isolated from all four different sources displayed the characteristic MSC-like spindle-shape, however subtle differences in morphology were present (Figure 1A). fL- and PL-MSCs showed a more elongated and thin shape compared to the rounder and thicker shape of BM-MSCs.

MSCs from all samples were immunophenotypically analyzed at passage 2 or 3. The phenotypes of fL-, fBM-, aBM- and PL-MSCs were similar and in agreement with previous publication^{9,13,14}, i.e. CD90, CD105, CD166, HLA-ABC positive and CD34, CD45, CD31, CD80, HLA-DR negative (Figure 1B).

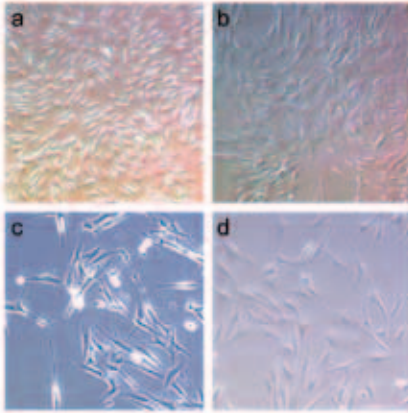
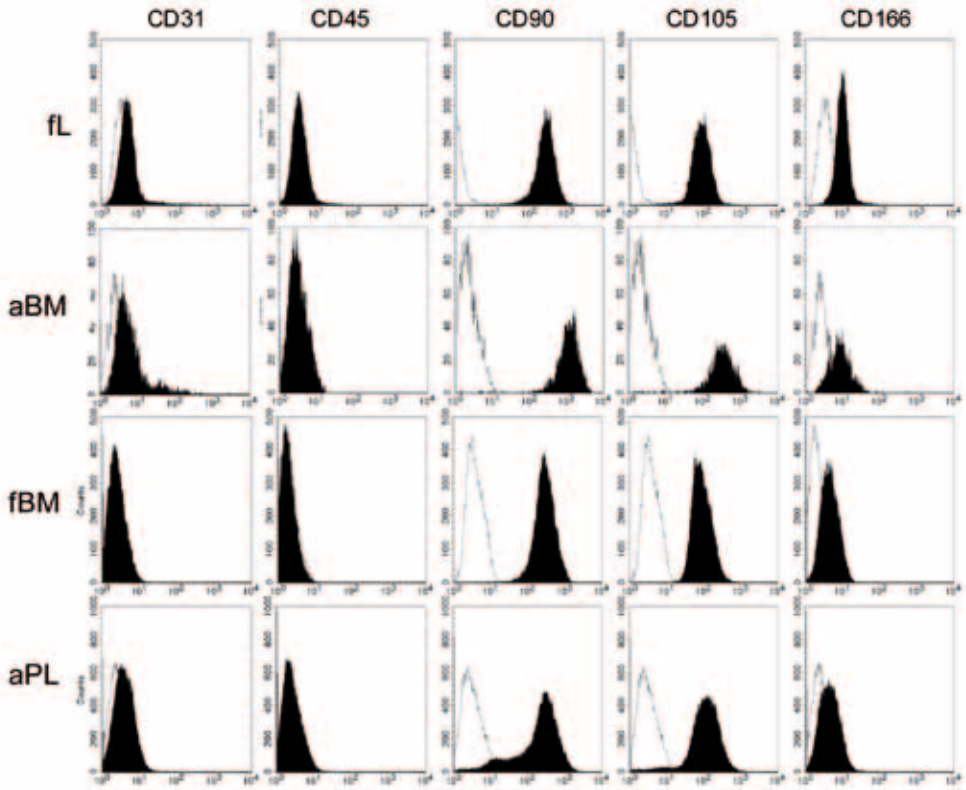
A**B**

Figure 1. Morphology and immunophenotype of culture-expanded MSCs.

(A) MSCs from the four different sources display the characteristic spindle-shaped morphology, however subtle differences are present. **a, b:** Morphology of fBM- and aBM-MSCs respectively, showing a spindle-round shape. Magnification x5. **c, d:** Morphology of fL- and PL-MSCs respectively, displaying a spindle-thin shape. Magnification x10. **(B)** Immunophenotypic characterization of MSCs from a representative sample.

Osteogenic and adipogenic differentiation

To examine the differentiation capacity of MSCs from the different sources, cells were induced into osteoblasts and adipocytes and examined by histological stainings. fL-, fBM-, aBM-MSCs and PL-MSCs were all able to differentiate into osteoblasts as demonstrated by the histologic detection of alkaline phosphatase activity and calcium depositions, and into adipocytes as revealed by the formation of lipid droplets (data not shown). However, PL-MSCs showed a lower ability to form both osteoblasts and adipocytes, while fL-MSCs were less capable to differentiate into the adipogenic lineage, as compared to bone marrow sources (Table 1).

The differentiation capacity into osteoblasts and adipocytes was maintained, unmodified, until passage 7 (P7).

Table 1. Differentiation potential of MSCs derived from different tissue sources

	Adipocyte-like morphology	Alzarin Red staining Intensity	Toluidine Blue Intensity	Chondrocyte-like morphology	N. of positive pellets/total N. of pellets evaluated
fL-MSC	+	++	+/-	+/-	0/4
fBM-MSC	++	++	++	++	3/3
aBM-MSC	++	++	+	++	4/4
PL-MSC	+/-	+/-	-	-	0/4

The presence of adipocyte-like morphology, the intensity of Alzarin Red and Toluidine Blue staining and the chondrocyte-like morphology are scored as: -, +/-, +, ++. The adipocyte-like morphology is defined by the appearance of fat droplets. The chondrocyte-like morphology is defined by the following features: decrease in cell density with distance between cells, rounded morphology of cells and nuclei, deposition of extracellular matrix, presence of chondrocytic lacunae. Only pellets that are scored + or ++ for both the Toluidine Blue staining and the chondrocyte-like morphology are considered positive for cartilage formation (last column on the right).

The chondrogenic differentiation capacity of MSCs is influenced by the tissue of origin

Next, the chondrogenic differentiation capacity of MSCs of different origin was examined and compared. fL- (n= 4 samples), fBM- (n= 3 samples, derived from the same fetus), aBM- (n= 4 samples) and PL-MSCs (n= 4 samples, maternal origin) were centrifuged into micromasses, cultured as pellets and differentiated in serum-free medium containing ascorbate-2-phosphate, dexamethasone, TGF- β 3 and BMP-6.

MSCs from all sources formed a pellet after centrifugation, although pellets consisting of fL- and PL-MSCs were frequently less stable and showed a more irregular shape compared to the pellets from fBM- and aBM-MSCs that were firm and spherical. Pellets derived from fBM- and aBM-MSCs were larger in size after 21 days of culture compared to those derived from fL- and PL-MSCs. In particular, fBM- and aBM-MSCs showed an increase in both the diameter and the area of the pellets after 3 weeks of culture in chondrogenic medium (data not shown). Furthermore, a 4.2- and a 2.9-fold increase in weight was observed in pellets formed by fBM and aBM-MSCs respectively at day 21 of culture, whereas fL- and PL-MSCs exhibited a decrease in weight of pellets over the culture period (Figure 2A). These observations suggest that cartilage extracellular matrix has been synthesized and deposited in pellets from bone marrow cells, leading to the increase in size and weight.

To more specifically analyze the process of chondrogenesis, the expression of collagen type II, IX and X was measured by Q-PCR on undifferentiated cells and on pellets 3 weeks after induction (Figure 2B). Pellets formed by fBM- and aBM-MSCs showed a marked increase in the expression of collagen type II, IX and X after the induction period, compared to fL- and PL-MSCs pellets. These data were confirmed by the histological analysis: fBM- and aBM-MSCs produced more proteoglycans, hence more extracellular matrix, and expressed more chondrocyte-like *lacunae*, as indicated by the intensity of the Toluidine Blue staining (Figure 2C). Moreover, the immunohistochemical staining for collagen type X was positive only in sections derived from fBM and aBM samples, suggesting that only these cells started to terminally differentiate into hypertrophic chondrocytes (Figure 2D). A scoring system was used to compare the different degrees of chondrogenic differentiation between the 4 sources; evaluating the intensity of the Toluidine Blue staining and the appearance of the typical chondrocyte-like morphology, both scored from - to ++. The stained sections from both fBM- and aBM-MSCs obtained the highest score with 100% of the samples evaluated demonstrating differentiation into chondrocytes; in fact, fBM- and aBM- cells showed the most intense Toluidine Blue staining and the typical morphological features of differentiated cartilage such as the decrease in cell density with distance between cells, the rounded morphology of cells, the deposition of extracellular matrix stained in purple and the presence of chondrocytic lacunae, whereas samples from fL- and PL-MSCs didn't (Table 1).

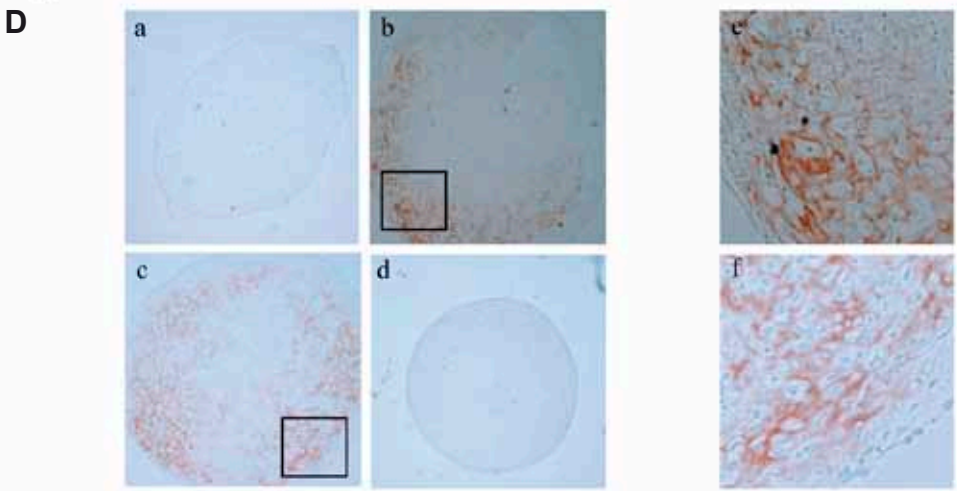
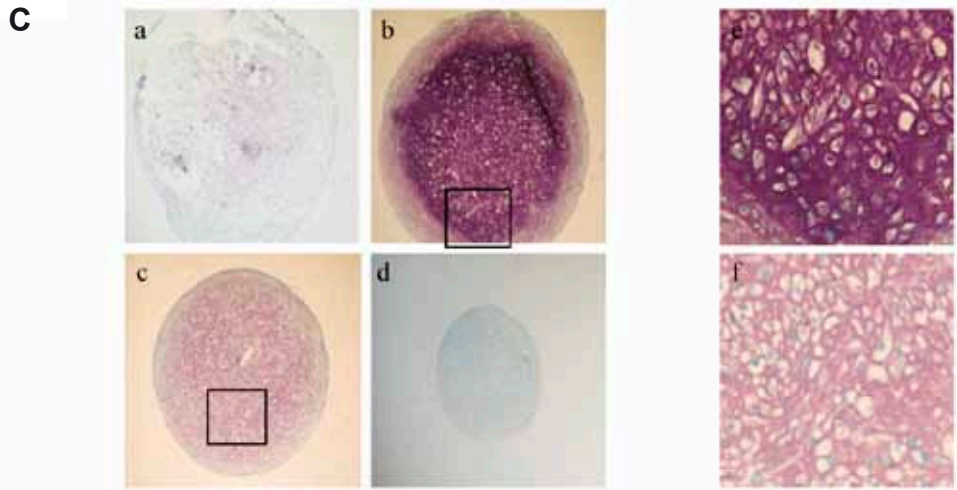
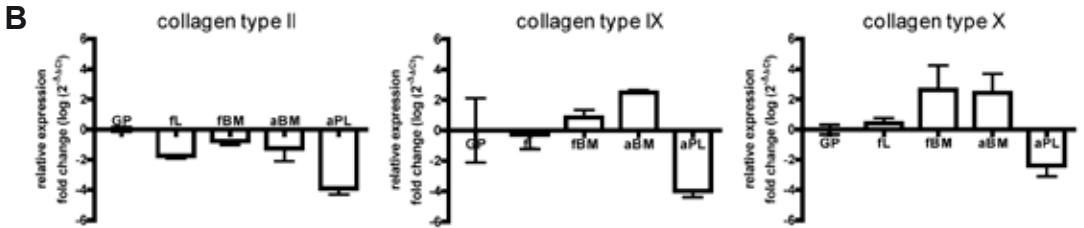
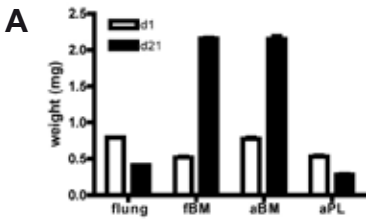


Figure 2. Chondrogenic differentiation of MSCs from different sources. (page 156)

(A) Wet weights of the pellets from the four different sources at day 1 and 21 of the induction period ($n = 3$). **(B)** Real-time RT-PCR analysis of collagen type II, IX and X during chondrogenic differentiation corrected for the housekeeping gene b2 microglobulin. Values are fold difference compared to expression in human growth plate (GP) and expressed as $\log(2^{-\Delta\Delta Ct})$. **(C)** Toluidine Blue staining on paraffin embedded sections after 3 weeks of differentiation. Representative pictures from each source at passage 3 are shown: a) fL-MSCs; b) fBM-MSCs; c) aBM-MSCs; d) PL-MSCs; e) and f) are enlargements of figure 2C b) and c) respectively, for detailed morphology. **(D)** Immunohistochemical staining for collagen type X on deparaffinized sections after the induction period. Representative pictures at passage 3 are depicted: a) fL-MSCs; b) fBM-MSCs; c) aBM-MSCs; d) PL-MSCs; e) and f) are enlargements of figure 2D b) and c) respectively, for detailed morphology.

The chondrogenic differentiation capacity of MSCs decreases with passage number

In order to examine whether the number of cell passages has an influence on the chondrogenic differentiation capacity of MSCs, different passages of fL-, fBM-, aBM- and PL-MSCs were evaluated. When considering fBM- and aBM-MSCs, a passage-dependent decrease in cartilage formation was observed (Table 2). In particular, the early passages (P2-3) displayed the most intense Toluidine Blue staining and all the typical features of differentiated cartilage, whereas the later passages (P4-5 and P6-7) showed only a moderate or mild staining with less evidence of cartilage differentiation (data not shown). Moreover, the capacity of BM-MSCs to differentiate into chondrocytes declined between passage 6 and 8. For fL- and PL-MSCs, the influence of cell passage was not evident since little or no differentiation towards the chondrogenic lineage was observed overall.

Table 2. Influence of cell passage on the chondrogenic capacity of MSCs from different tissue sources.

	P2-3	P4-5	P6-7
fL-MSC	0/4	0/4	0/4
fBM-MSC	3/3	3/3	1/3
aBM-MSC	4/4	4/4	2/4
PL-MSC	0/3	0/3	0/4

The differentiation capacity is expressed as number of positive samples on the total number of samples evaluated per passage-group. A sample is scored positive when satisfying the criteria described in Table 1.

Discussion

Skeletal defects resulting from disease, malformation or injury are an interesting area of application for stem cell therapy. The therapeutic effect of the transplantation of MSCs in children with *Osteogenesis Imperfecta*, a genetic disorder resulting in the abnormal production of collagen type I¹⁵⁻¹⁷, suggests the potential of MSCs to ameliorate bone disorders. MSCs are an ideal candidate for strategies of tissue engineering since they are easily isolated and can be rapidly expanded to numbers that are required for clinical application^{10,18,19}.

In this study we compared the chondrogenic differentiation potential of culture expanded MSCs derived from fetal BM and lung, placenta and adult BM. In comparison with fetal lung and placenta, fetal BM derived MSCs exhibited a significant enhanced capacity to differentiate into chondrocytes, as evidenced by the increase in weight, diameter and area of pellets formed by bone marrow cells over the differentiation period, the increased levels in the expression of mRNA of extracellular matrix components, such as collagen type II, IX and X, the positivity of the immunohistochemical staining for collagen type X and the marked intensity of the Toluidine Blue staining. A similar preferred chondrogenic potential was observed for adult BM-derived MSCs, showing that BM as a source of MSCs was responsible for this differentiation potential, rather than the fetal developmental stage of the tissue. The chondrogenic differentiation was reduced and ultimately lost, after prolonged passages of the cultures. Although *in vivo* experiments are required to further substantiate the biological significance of these findings, our results suggest BM as the preferred source for cartilage tissue engineering.

MSCs have been shown to require specific culture conditions to induce differentiation towards the chondrogenic lineage. These requirements include a high cell density facilitating cell-cell contact and the use of serum-free medium with the addition of bioactive factors²⁰. In particular BMP-6, a member of the TGF- β superfamily of growth factors, has been demonstrated to enhance the chondrogenic differentiation of human MSCs in a pellet culture system^{21,22}. Our results confirm these findings and add that not only aBM-MSCs but also MSCs isolated from fetal tissues, namely lung and bone marrow, can undergo chondrogenesis under the same conditions.

In a study from *in't Anker* and colleagues¹³ it was shown that MSCs isolated from second-trimester fetal bone marrow, lung, liver and spleen exhibit a different potential to differentiate into osteoblast and adipocytes, despite a similar immunophenotype. Moreover, a recent study from *Im et al*²³ demonstrated that adipose tissue-derived MSCs possess a lower osteogenic and chondrogenic potential than BM-derived MSCs. Also in our experiments, despite MSCs derived from the four different sources showed a comparable phenotypic characterization and morphology, the capacity to form cartilage was more expressed in fBM- and aBM-MSCs. Moreover, we found that PL-MSCs were less capable to form both osteoblasts and adipocytes, while fL-MSCs showed to have a lower ability to differentiate into the adipogenic lineage compared to bone marrow sources. These differences in the differentiation potential might reflect some intrinsic diversities of MSCs residing in the various tissues, suggesting that the relation between immunophenotype and function of MSCs needs to be further investigated. Alternatively, the frequency of cells with lineage-specific differentiation capacity may differ between tissue sources. Indeed, the identification of specific markers enabling to distinguish between different populations of MSCs would be an important tool in the understanding and employment of these cells in the clinical setting.

We found that the chondrogenic potential of MSCs decreases with the increase of the cell passage, as shown by the inferior growth in size and the mild intensity of the Toluidine Blue staining in pellets from the later passages (P6-7). These findings are in agreement with the study from *Sekiya*

*et al*²² in which a decrease in the chondrogenic potential of adult bone marrow-derived MSCs was seen after each consecutive passage under very similar culture conditions. In *Sekiya* experience, only a selected population of MSCs, the so called small and rapidly self-renewing cells (RS cells), retained the ability to form cartilage at P5. This loss of chondrogenic potential may be due to the graduate elimination of MSCs with chondrogenic potential and overgrowth by MSCs that lack differentiation potential, or may be due to functional alterations in chondrogenic MSCs.

In conclusion, our results show that: I) MSCs of both fetal and adult origin undergo chondrogenesis under appropriate culture conditions; II) fBM- and aBM-MSCs express a higher chondrogenic ability than fL- and PL-MSCs, based on morphological, molecular, histochemical and immunohistochemical criteria; III) an inverse correlation between passage number and chondrogenic differentiation capacity of MSCs is present. Based on these observations and considering the attractive role that MSCs could play in strategies of cartilage tissue engineering, our data suggest that bone marrow cells are to be considered as the preferred MSC source to be employed for cartilage repair.

Acknowledgement and funding

The authors would like to thank Carin Kleijburg for providing PL-MSC samples and Fawzia Sheikariem for technical assistance.

Supported by grants from the European Community (FP6 Program, Allostem) and CNR (Consiglio Nazionale delle Ricerche) to F.L., research grant 03-3014 from the Dutch Cancer Society, the Netherlands, EuroCord Nederland Foundation and the Netherlands Organization for Scientific Research (920-03-358).

References

1. **Heng BC, Cao T, Lee EH.** Directing stem cell differentiation into the chondrogenic lineage in vitro. *Stem Cells* 2004;22:1152-1167.
2. **Jorgensen C, Gordeladze J, Noel D.** Tissue engineering through autologous mesenchymal stem cells. *Curr Opin Biotechnol* 2004;15:406-410.
3. **Murphy JM, Dixon K, Beck S, Fabian D, Feldman A, Barry F.** Reduced chondrogenic and adipogenic activity of mesenchymal stem cells from patients with advanced osteoarthritis. *Arthritis Rheum* 2002;46:704-713.
4. **Alsalameh S, Amin R, Gemba T, Lotz M.** Identification of mesenchymal progenitor cells in normal and osteoarthritic human articular cartilage. *Arthritis Rheum* 2004;50:1522-1532.
5. **Tallheden T, Dennis JE, Lennon DP, Sjogren-Jansson E, Caplan AI, Lindahl A.** Phenotypic plasticity of human articular chondrocytes. *J Bone Joint Surg Am* 2003;85-A Suppl 2:93-100.
6. **van der Kraan PM, Buma P, van Kuppevelt T, van den Berg WB.** Interaction of chondrocytes, extracellular matrix and growth factors: relevance for articular cartilage tissue engineering. *Osteoarthritis Cartilage* 2002;10:631-637.
7. **Risbud MV, Sittinger M.** Tissue engineering: advances in in vitro cartilage generation. *Trends Biotechnol* 2002;20:351-356.
8. **Caplan AI.** The mesengenic process. *Clin Plast Surg* 1994;21:429-435.
9. **Pittenger MF, Mackay AM, Beck SC, Jaiswal RK, Douglas R, Mosca JD.** Multilineage potential of adult human mesenchymal stem cells. *Science* 1999;284:143-147.
10. **Deans RJ, Moseley AB.** Mesenchymal stem cells: biology and potential clinical uses. *Exp Hematol* 2000;28:875-884.
11. **Friedenstein A.** Stromal mechanisms of bone marrow: cloning in vitro and retransplantation in vivo. In: Thienfelder S, Rodt H, Kolb HJ, eds. *Immunology of Bone Marrow Transplantation*. Berlin: Springer-Verlag; 1980:19-20.
12. **Campagnoli C, Roberts IA, Kumar S, Bennet PR, Bellantuono I, Fisk NM.** Identification of mesenchymal stem/progenitor cells in human first-trimester fetal blood, liver, and bone marrow. *Blood* 2001;98:2396-2402.
13. **in 't Anker PS, Noort WA, Scherjon SA, Kleijburg-van der Keur C, Kruisselbrink AB, van Bezooijen RL.** Mesenchymal stem cells in human second-trimester bone marrow, liver, lung, and spleen exhibit a similar immunophenotype but a heterogeneous multilineage differentiation potential. *Haematologica* 2003;88:845-852.

14. **in 't Anker PS, Scherjon SA, Kleijburg-van der Keur C, de Groot-Swings GM, Claas FH, Fibbe WE.** Isolation of mesenchymal stem cells of fetal or maternal origin from human placenta. *Stem Cells* 2004;22:1338-1345.
15. **Horwitz EM, Prockop DJ, Fitzpatrick LA, Koo WW, Gordon PL, Neel M.** Transplantability and therapeutic effects of bone marrow-derived mesenchymal cells in children with osteogenesis imperfecta. *Nat Med* 1999;5:309-313.
16. **Horwitz EM, Gordon PL, Koo WK, Marx JC, Neel MD, McNall RY.** Isolated allogeneic bone marrow derived mesenchymal stem cells engraft and stimulate growth in children with osteogenesis imperfecta: implications for cell therapy of bone. *PNAS* 2002; 99: 8932-8937.
17. **Le Blanc K, Gotherstrom C, Ringden O, Hassan M, McMahon R, Horwitz E.** Fetal mesenchymal stem-cell engraftment in bone after in utero transplantation in a patient with severe osteogenesis imperfecta. *Transplantation* 2005; 79:1607-1614.
18. **Fibbe WE, Noort WA.** Mesenchymal stem cells and hematopoietic stem cell transplantation. *Ann N Y Acad Sci* 2003;996:235-244.
19. **Barry FP, Murphy JM.** Mesenchymal stem cells: clinical applications and biological characterization. *Int J Bioch & Cell Biol* 2004; 36: 568-584.
20. **Yoo JU, Barthel TS, Nishimura K, Solchaga L, Caplan AI, Goldberg VM.** The chondrogenic potential of human bone-marrow-derived mesenchymal progenitor cells. *J Bone Joint Surg Am* 1998; 80: 1745-1757.
21. **Indrawattana N, Chen G, Tadokoro M, Shann LH, Ohgushi H, Tateishi T.** Growth factor combination for chondrogenic induction from human mesenchymal stem cell. *Biochem Biophys Res Commun* 2004;320:914-919.
22. **Sekiya I, Colter DC, Prockop DJ.** BMP-6 enhances chondrogenesis in a subpopulation of human marrow stromal cells. *Biochem Biophys Res Commun* 2001;284:411-418.
23. **Im G-I, Shin Y-W, Lee K-B.** Do adipose tissue-derived mesenchymal stem cells have the same osteogenic and chondrogenic potential as bone marrow-derived cells? *Osteoarthritis Cartilage* 2005; 13(10): 845-853.

10

Fetal mesenchymal stem cells differentiating towards chondrocytes display a similar gene expression profile as growth plate cartilage.

J.A.M. Emons^{1*}, S.A. van Gool^{1*}, J.C.H. Leijten², E. Decker³, X. Yu⁴, C. Sticht⁴, J.C. van Houwelingen⁵, J.J. Goeman⁵, C. Kleijburg⁶, S. Scherjon⁶, N. Gretz⁴, J.M. Wit¹, G. Rappold³, M. Karperien^{1,2}.

¹Department of Pediatrics, Leiden University Medical Center, Leiden, the Netherlands;

²Department of Tissue Regeneration, Twente University, Enschede, the Netherlands;

³Department of Human Molecular Genetics, and

⁴Medical Research Center, Medical Faculty Mannheim, University of Heidelberg, Heidelberg, Germany;

⁵Department of Medical Statistics and Bioinformatics, and

⁶Department of Obstetrics, Leiden University Medical Center, Leiden, the Netherlands.

**These authors contributed equally to this work*

Abstract

Most studies on growth plate (GP) maturation and fusion have been carried out in animal models not fully representing the human epiphyseal GP. We used human fetal bone marrow-derived mesenchymal stem cells (hfMSCs) differentiating towards chondrocytes as an alternative model for the GP. Our aims were to assess whether chondrocytes derived from hfMSCs are a valid model for the GP and to study gene expression patterns associated with chondrogenic differentiation.

Microarray and principal component analysis were applied to study gene expression profiles during chondrogenic differentiation. A set of 315 genes was found to correlate with *in vitro* cartilage formation. Several identified genes are known to be involved in cartilage formation and validate the robustness of the differentiating hfMSC model. Other genes like Bradykinin and IFN- γ signaling, CCL20, and KIT were not described in association with chondrogenesis before. KEGG pathway analysis using the 315 genes revealed 9 significant signaling pathways correlated with cartilage formation.

To determine which type of hyaline cartilage is formed, we compared the gene expression profile of differentiating hfMSCs with previously established expression profiles of human articular (AC) and epiphyseal GP cartilage. As differentiation towards chondrocytes proceeds, hfMSCs gradually obtain a gene expression profile similar to epiphyseal GP cartilage, but less resembling the fingerprint of AC. This study validates differentiating bone marrow-derived hfMSCs as an excellent model for the epiphyseal GP. The hfMSC model offers the opportunity to unravel molecular mechanisms underlying growth regulation as they occur in the human growth plate.

Introduction

Growth of the long bones of the human skeleton occurs as the result of a tightly orchestrated proliferation and differentiation program called endochondral ossification. In the epiphyseal growth plate of long bones, chondrocytes originating from mesenchymal stem cells subsequently undergo proliferation, hypertrophic differentiation, and programmed cell death before being replaced by bone. At the time of sexual maturation, growth first increases but at the end of puberty epiphyseal fusion and termination of growth occur. Our knowledge on the molecular mechanisms underlying growth regulation is limited, although estrogen has been identified as a key regulator of growth plate maturation and fusion (1). Gaining a detailed understanding of growth regulatory processes is essential to facilitate the development of novel strategies for the treatment of various growth disorders.

Commonly used animal models for studying growth plate regulation do not fully represent the human epiphyseal plate. For example, rodent growth plates do not fuse at the end of sexual maturation (2), and therefore do not display an important hallmark of human growth plate development. The shortcoming of the mouse model is clearly demonstrated by the contrast between the marginally affected growth phenotype of the estrogen receptor alpha (ER α) knock out mouse (α ERKO) (3) and the prominent growth phenotype of a male patient lacking functional ER α (4), characterized by the absence of epiphyseal fusion and continuation of growth into adulthood. The lack of representative animal models has led to the realization that alternative human models are essential to elucidate the mechanisms involved in growth plate regulation and fusion. However, human growth plate specimens are difficult to obtain, whereas *in vitro* models such as chondrosarcoma cell lines or articular cartilage-derived chondrocyte cultures have limited differentiation capacity, are often difficult to maintain under laboratory conditions or

tend to dedifferentiate. Furthermore, articular cartilage and growth plate cartilage have distinct functions and it is therefore questionable whether articular cartilage-derived chondrocytes are representative for epiphyseal growth plate chondrocytes.

Multipotent human mesenchymal stem cells (hMSCs) are a promising *in vitro* model to study chondrogenesis. They have been postulated as an alternative cell source for articular cartilage reconstruction and for studying endochondral ossification as it occurs in the epiphyseal growth plate (5). In this study, we explored the cartilage forming capacity of human fetal (hf)MSCs to create an *in vitro* model for the human growth plate. We have chosen human fetal bone marrow-derived MSC for their superior differentiation characteristics compared to adult bone marrow-derived MSCs (6). Efficient cartilage formation was demonstrated by immunohistochemical analysis and gene expression profiling was applied to identify genetic pathways involved in the differentiation process. In addition, the gene expression profiles of the differentiating hfMSCs were compared with global gene expression patterns of human articular and growth plate cartilage to assess whether differentiating hfMSCs represent either articular or growth plate chondrocytes.

Materials and methods

Cell culture

The use of human fetal material was approved by the medical ethical committee of the Leiden University Medical Center and an informed consent was obtained from the women undergoing elective abortion. Cell suspensions of fetal bone marrow were obtained by flushing the long bones of fetuses with M199 washing medium. For the chondrogenic differentiation and microarray analysis, cells derived from a single 22 weeks old fetus were used. MSCs derived from other fetuses were also stimulated to undergo chondrogenic differentiation. Red cells were depleted by incubation for 10 minutes in NH_4Cl (8.4 g/L)/ KHCO_3 (1g /L) buffer at 4°C. Mononuclear cells were plated at a density of 16×10^4 cells/cm² in M199 culture medium (Gibco) supplemented with 10% fetal bovine serum (FBS), 1% penicillin/streptavidin (P/S), fungizone, endothelial cell growth factor (ECGF) 20 µg/ml (Roche Diagnostics) and heparin 8 U/ml in culture flasks (Greiner) coated with 1% gelatin. Cultures were kept in a humidified atmosphere at 37°C with 5% CO₂. The culture medium was changed twice per week. After reaching near-confluence at passage 4 to 5, hfMSCs were harvested by treatment with 0.5 % trypsin and 0.5% ethylene diamine tetra acetic acid (EDTA; Gibco) for 5 minutes at 37°C and replated for chondrogenic differentiation.

In vitro chondrogenic differentiation

hfMSCs (2×10^5 cells/well) were positioned into pellets by centrifugation at 1200 rpm for 4 minutes in U-shaped 96-well suspension culture plates (Greiner) and cultured at 37°C with 5% CO₂ in 200 µl of serum-free chondrogenic medium consisting of high-glucose (25 mM) Dulbecco's modified Eagle's medium (DMEM; Gibco) supplemented with 40 µg/ml proline (Sigma), 100 µg/ml sodium pyruvate (Sigma, USA), 50 mg/ml ITS (insulin-transferrin-selenic acid) with Premix (BD Biosciences), 1% Glutamax (Gibco), 1% penicillin/streptavidin, 50 g/ml ascorbate-2-phosphate (Sigma), 10^{-7} M dexamethasone (Sigma), 10 ng/ml transforming growth factor-β3 (TGF-β3; R&D Systems), 500 ng/ml bone morphogenetic protein 6 (BMP6) and antibiotic and antimycotic mix (0.06% polymixin, 0.2% kanamycin, 0.2% penicillin, 0.2% streptavidin, 0.02% nystatin and 0.5% amphotericin. The medium was changed twice per week for 5 weeks.

Histological analysis

Two pellets per time point (after 1, 2, 3, 4, or 5 weeks of chondrogenesis) were used for histological evaluation. Pellets were fixed in 10% formalin, dehydrated by treatment with graded ethanols and processed for paraffin embedding. 5 μ m sections were cut using a Reichert Jung 2055 microtome (Leica). For each pellet, only the sections from exactly the center of the pellets were mounted on glass slides. Before histological (toluidine blue) or immunohistochemical staining, sections were deparaffinized in xylene and graded ethanols followed by three washing steps phosphate buffered saline (PBS).

For immunohistochemistry, sections were preincubated with blocking buffer (1% H₂O₂ in 40% methanol, 60% tris buffered saline) twice for 15 minutes at room temperature, followed by overnight incubation at 4°C with mouse monoclonal antibody against collagen type II or type X in a 1:100 dilution (Quartett). Next, sections were incubated with the secondary antibody biotinylated rabbit-anti-mouse IgG (DAKO) in a 1:300 dilution, followed by incubation with horseradish-peroxidase-conjugated-streptavidine (Amersham Biosciences). Staining was visualized with 3-amino-9-ethylcarbazole substrate in 0.2 mg/ml acetate buffer (pH 5.2) with 0.04% H₂O₂. After counterstaining with hematoxylin, the sections were mounted in Histomount (National Diagnostics). Pictures of the stained pellets were taken with a Nikon DXM 1200 digital camera using standardized settings.

RNA isolation

Total RNA from 2·10⁶ undifferentiated hMSCs derived from the 22-weeks old fetus was extracted with Trizol (Invitrogen). After 1, 2, 3, 4, or 5 weeks of chondrogenesis, 60 pellets (per time point) were pooled and homogenized in 1ml 4M guanidine isothiocyanate solution (Sigma) and RNA was extracted according to the optimized method for RNA extraction from cartilage as described by Heinrichs et al. (43). The extracted total RNA was purified using the RNeasy kit according to recommendations of the manufacturer (Qiagen).

Gene expression profiling

High RNA quality was confirmed by capillary electrophoresis on an Agilent 2100 bioanalyzer (Agilent). Total RNA (100 ng) was amplified and labeled using the GeneChip Two-Cycle cDNA Synthesis Kit (Affymetrix) and the MEGAscript T7 Kit (Ambion). For gene expression profiling, labeled cRNA was hybridized in duplicate to Affymetrix Human Genome U133 PLUS 2.0 Array Genechips. All procedures were carried out according to the manufacturer's recommendations.

Raw data from Affymetrix CEL files were analyzed using SAS software package Microarray Solution version 1.3 (SAS Institute). Custom CDF version 10 with Entrez based gene definitions (44) was applied to map the probes to genes. Gene annotation was obtained using the Affymetrix NetAffx website (<http://www.affymetrix.com/analysis/index.affx>). Quality control, normalization and statistical modeling were performed by array group correlation, mixed model normalization and mixed model analysis respectively. The normalized expression values for each gene were standardized by linearly scaling the values across all samples of the time course to a mean of 0 with an SD of 1. Analysis of differential gene expression was based on loglinear mixed model of perfect matches (45). A false discovery rate of $\alpha=0.05$ with Bonferroni-correction for multiple testing was used to set the level of significance. The raw and normalized data are deposited in the Gene Expression Omnibus database (<http://www.ncbi.nlm.nih.gov/geo/>; accession no. GSE-XXXX).

Microarray data analysis

The statistical analysis of the microarray data was based on the normalized mean expression values per probe at 6 time points with 2 replications at each time point (12 observations per probe).

In order to identify subgroups of probes with similar expression profiles over time, a principal component analysis (PCA) of the covariance matrix was carried out on the mean expression value for each probe at each time point. For each probe, factor scores for principal components 1, 2 and 3 were obtained by regression analysis of the 12 array results (6 time points in duplicate) for that specific probe to those components. The first principal component corresponded with the general expression level during the whole experiment, whereas the second and third component corresponded with changes over time. Since our interest was to identify genes associated with the changes that occur during differentiation from stem cells towards chondrocytes, we focused our analysis on the second and third component. By construction, these factor scores had a mean of 0 with an SD of 1. Generally, the distribution over the factor scores showed a normal distribution with outliers. We used a cut-off of ± 3.29 to select outlying probes. This cut-off would select 0.1% of the probes, if the factors scores would follow a pure normal distribution that could be expected if the data were pure noise. The presence of replications allowed us to assess the statistical significance of the factor scores and to remove probes that were not significant at the $\alpha=5\%$ level. In a separate study we compared the gene expression profiles of human articular cartilage (AC) and epiphyseal growth plate (GP) cartilage. A set of 1818 significant differentially expressed genes was identified, that can be used to discriminate between the two hyaline cartilage subtypes (Leijten et al., manuscript in preparation). All AC (n=5) and GP (n=5) samples were derived from 9 to 17 year old female donors with no history of growth disorders. The gene expression profiles of the stem cells differentiating towards chondrocytes were compared with this list. Principal component analysis (PCA) with Pearson product-moment correlation was performed to compute correlations between the expression profiles.

Pathway analysis

Using sets of probes emerging from PCA, a search for relevant KEGG pathways was performed using the DAVID® Knowledgebase, a publicly available bioinformatics tool for functional annotation (<http://david.abcc.ncifcrf.gov>).

Quantitative real-time polymerase chain reaction (qPCR)

RNA was transcribed into cDNA using the First Strand cDNA Synthesis kit for qPCR (Roche Diagnostics) according to the manufacturer's protocol. Specific primer sets (available on request) were designed to amplify aggrecan (ACAN), pannexin 3 (PANX3), epiphygan (EPYC), collagen type II (COL2), and type X (COL10), SRY-box 9 (SOX9), WNT11, lymphoid enhancer-binding factor 1 (LEF1), Gremlin 1 (GREM1), and the housekeeping genes β_2 -microglobulin, and glyceraldehyde 3-phosphate dehydrogenase (GAPDH). In order to test donor inter-variation, differentiated MSCs isolated from other fetal donors were used for qPCR analysis as well.

All PCR reactions were performed in triplicate with 5 ng cDNA and according to the manufacturer's protocol of the iQ™ SYBR® Green Kit (Biorad) in a final volume of 25 μ l. The cDNA was amplified using the following thermal cycling conditions: one cycle at 50°C for 2 min and 95°C for 10 min, followed by 40 cycles of 15 s at 95°C and 1 min at 56°C. Fluorescence spectra were recorded and the threshold cycle number (Ct) was read. For each time point mean Ct was calculated and from this value the fold difference in expression between undifferentiated hfMSCs and differentiating cells according to the equation $2^{-\Delta\Delta Ct}$ (normalized fold expression). For visualization, this value was log-transformed.

Results

Chondrogenic differentiation by hfMSCs

Evaluation of protein and mRNA expression

Immunohistological evaluation showed an increasing expression of cartilage markers with time and a gradual morphological change from stem cells to mature and hypertrophic chondrocytes (figure 1). The mean diameter of the pellets increased with time, as well as the amount of glycosaminoglycans, a major constituent of the cartilaginous extracellular matrix. Immunohistochemical staining for collagen type II demonstrated the presence of chondrocytes after 1 week of pellet culture. Hypertrophic chondrocytes were first detected after 3 weeks, as detected by immunohistochemical staining for collagen type X. At the last stage of differentiation, the pellets display a two-layered structure with a core that consists of chondrocytes and that is surrounded by a thin outer layer of undifferentiated thin spindle-shaped cells.

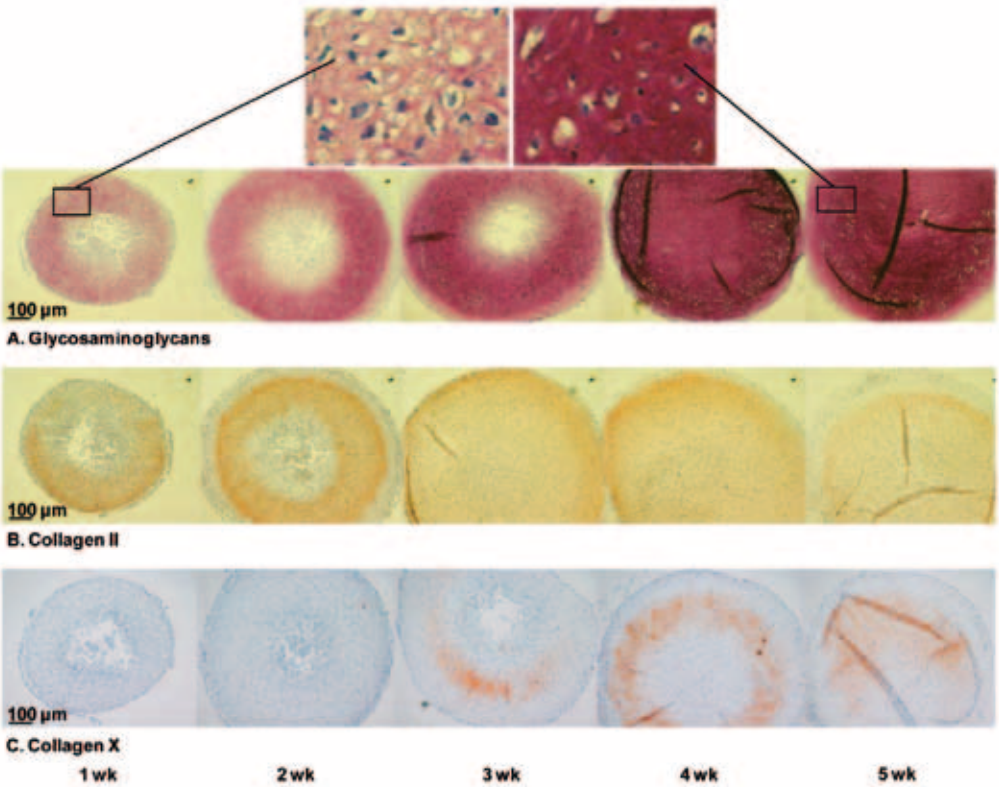


Figure 1

Expression of (A) glycosaminoglycans visualized by toluidine blue staining, (B) collagen type II immunohistochemistry (brown), and (C) collagen type X immunohistochemistry (brown) during 5 weeks of chondrogenic differentiation of hfMSCs to chondrocytes.

From each time point RNA was isolated and subjected to microarray analysis. Changes in gene expression of a subset of genes consisting of both established marker genes for chondrogenesis and differentially expressed genes identified by microarray analysis were validated using qPCR (figure 2). In concordance with the observations of immunohistological markers of chondrogenesis, microarray data and qPCR showed time-dependent increases in the expression of the cartilage markers collagen type II, and type X, SOX9, and aggrecan mRNA. To further extend this analysis, we randomly selected 7 genes (pannexin 3, epiphycan, WNT11, LEF1, gremlin 1, Dickkopf 1, matrilin) that showed marked regulation over time based on microarray analysis. Again, qPCR demonstrated a strong correlation between the expression patterns revealed by both techniques (results for 5 of these genes are shown in figure 2E-I), providing further support for the robustness of our dataset. Repeating the qPCR analysis using RNA isolated from other fetal donors of MSCs that were stimulated to undergo chondrogenic differentiation rendered similar gene expression patterns as observed for the single 22-weeks old donor derived cells (data not shown).

Principal component analysis and KEGG pathway analysis

The sequential changes that occur during chondrogenic differentiation in the hfMSC model were studied with bioinformatics analysis of the microarray data. Using principal component analysis, three components were found to explain 99.6% of the variance within our dataset (figure 3.A). The factor loadings in figure 3.B show that component 1 describes a general level of gene expression, as expected. Component 2 shows to what extent gene expression changed with time during chondrogenic differentiation and component 3 signifies whether there was an additional, short term elevation or dip in expression around 2 to 3 weeks of differentiation. Since components 2 and 3 were most likely to contain genes associated with the loss of stem cell characteristics or the gain of a chondrocyte phenotype, we focused on those components.

Using the ± 3.29 cut-off in combination with a 5% significance test, we distinguished four subgroups of probes. The precise definitions and the resulting numbers of these subgroups are given in figure 3.C. The scatter plot in figure 3.D illustrates that the numbers of probes in subgroups 1 and 2 are much larger than the 9 probes (0.05%) that would have been expected under purely random selection. Moreover, in these two subgroups nearly all probes in the first selection are significant at the 5% level, suggesting that the number of false discoveries in these two groups is quite small. More noise is presumably present in the smaller subgroups 3 and 4 based on factor 3 scores.

The profiles of the selected probes demonstrate that subgroup 1 containing the largest number of probes ($n=146$) describes a peak of expression on t_0 followed by a decrease in expression thereafter. In contrast, the second largest subgroup of probes ($n=105$) in profile 2 demonstrates increasing expression levels from t_0 onward. The smaller subgroups 3 and 4 demonstrate lower levels of expression with profile 3 ($n=49$) showing a short-term increase in expression at t_1 followed by decreases thereafter and profile 4 ($n= 15$) displaying a short-term expression dip between t_1 - t_2 .

A total of 83 out of 315 probes could not be annotated and was discarded from further analysis. The remaining 232 probes that could be matched to genes (supplementary table 1) were used to identify 9 KEGG pathways that were significantly associated with chondrogenic differentiation and contained 39 genes. (figure 4). Some genes were present solely in one pathway ($n= 23$), but others were found in 2 ($n= 6$) or 3 ($n= 10$) pathways (table 1). Three functional groups of genes were recognized: 1) growth factor (GF) and GF-related genes; 2) genes associated with the extracellular matrix; and 3) genes associated with signal transduction, cell cycle, and cell survival.

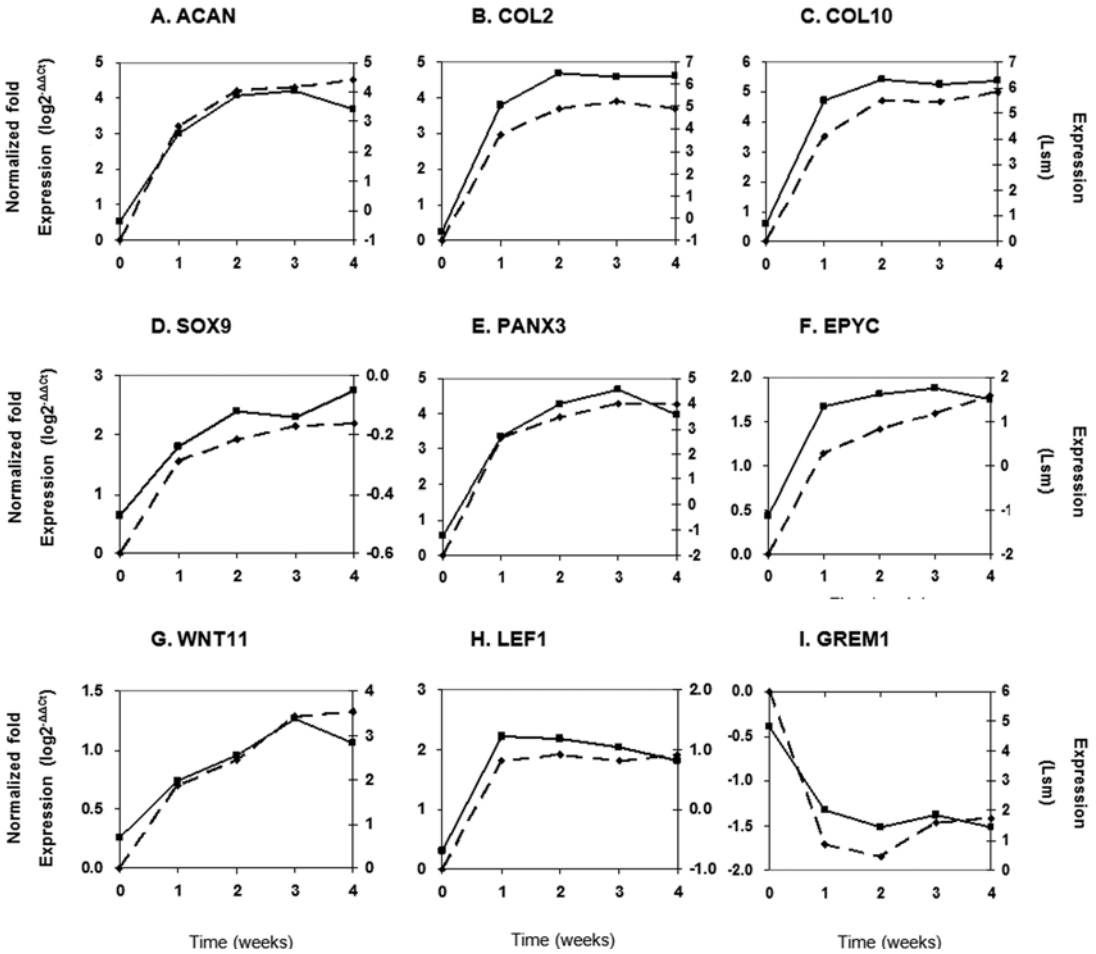


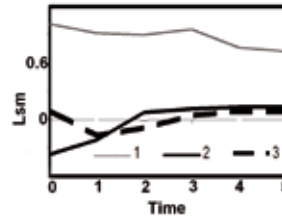
Figure 2

Correlation between qPCR and microarray expression data for (A) aggrecan, (B) collagen II, (C) collagen X, (D) SOX9, (E) pannexin 3, (F) epiphykan, (G) WNT11, (H) LEF1, and (I) gremlin 1 during 5 weeks of chondrogenic differentiation of hMSCs. qPCR data are expressed as delta delta CT values corrected for the housekeeping gene $\beta 2$ -microglobulin. The primary y-axis (left) indicates the qPCR results as normalized fold expression on a log-scale. The secondary y-axis (right) indicates the microarray analysis results as least square means (Lsm).

A. Variance explained by PCA

Component	Variance (%)	Cumulative variance (%)
1	95.16	95.16
2	3.24	98.40
3	1.15	99.55
4+5+6	0.45	100

B. Principal components



C. Subgroup definitions

Subgroup	Factor 2 score	Factor 3 score	Nº. of probes	Sign. probes
1	≤ -3.29		149	146
2	≥ 3.29		118	105
3	< -3.29	≤ -3.29	135	49
4	> 3.29	≥ -3.29	64	15

D. Expression profiles

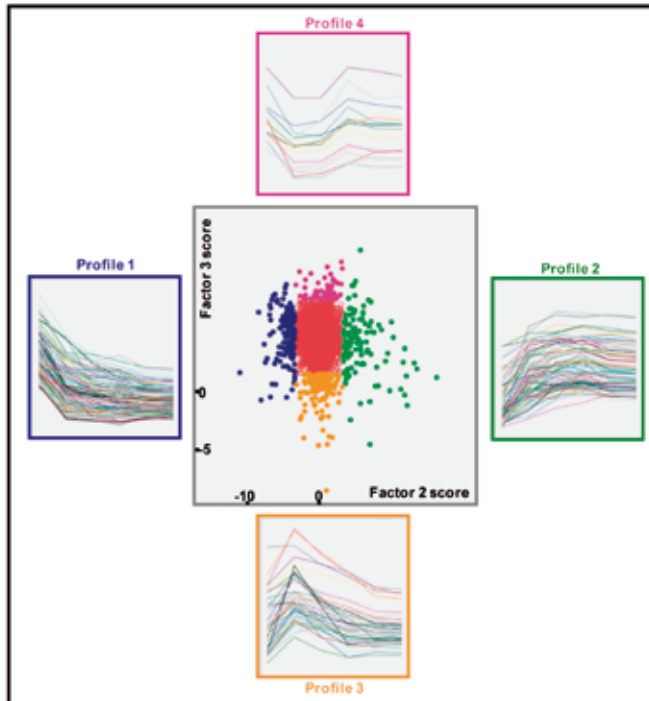


Figure 3

Gene selection based on principal component analysis. A) variance explained by components 1-6 from principal component analysis. B) principal components 1, 2, and 3 as expression profiles. C) selection of probes based on their factor 2 and 3 scores. D) scatterplot view of gene data in respect to their correlation (factor score) to principal components 2 and 3. Subgroups 1, 2, 3, and 4 are represented by blue, green, yellow, and pink dots, respectively. Side-placed graphs depict the gene expression profiles for genes found in the four subgroups.

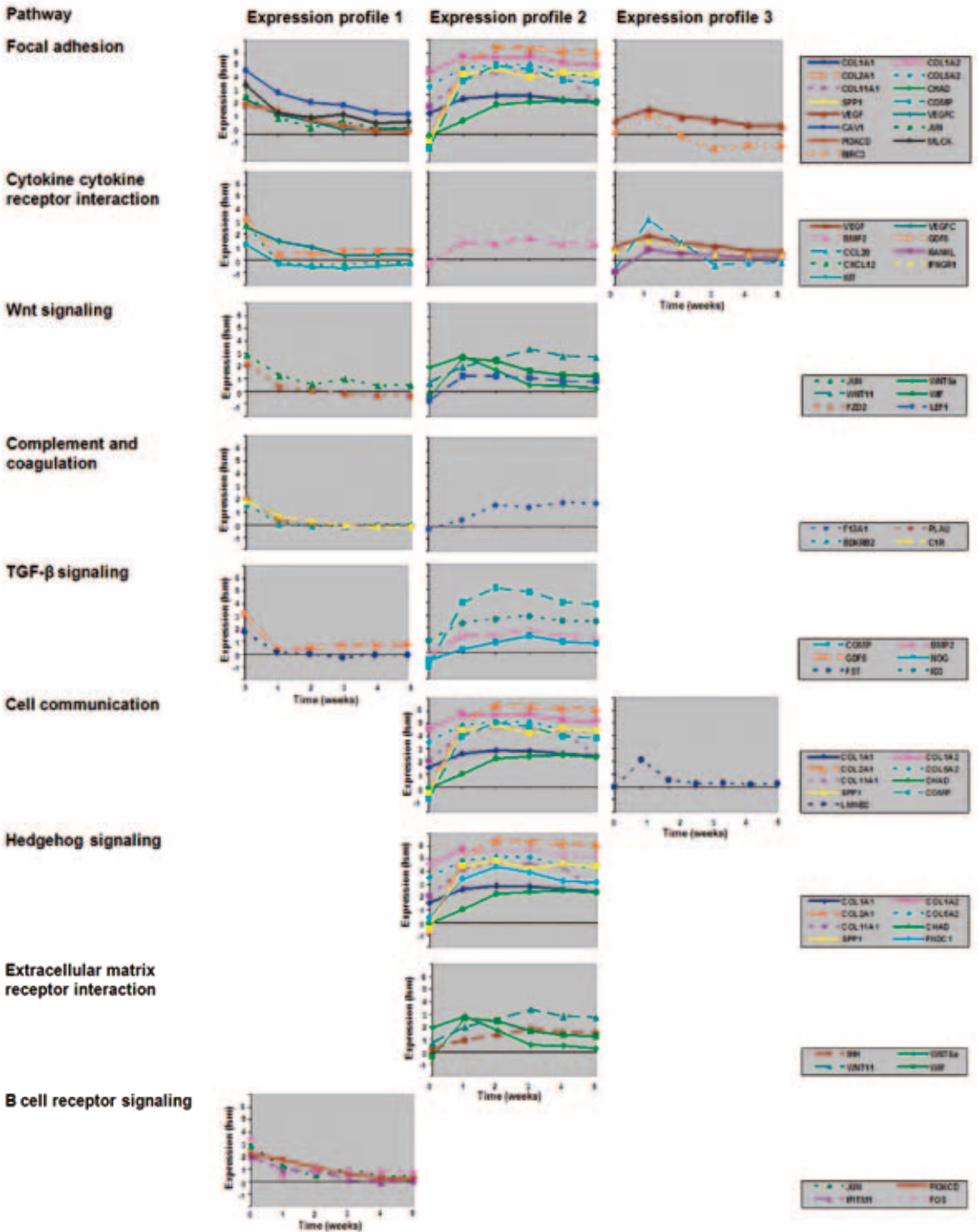


Figure 4

KEGG signaling pathways significantly associated with chondrogenic differentiation of hMSCs. For each pathway, genes showing the same distinct expression profile during 5 weeks of chondrogenic differentiation are depicted as groups.

Gene expression fingerprinting for cartilage subtype

Histological and gene expression analyses showed that the differentiating hfMSCs acquire a hyaline cartilage phenotype. Two major types of hyaline cartilage can be distinguished, namely articular and epiphyseal cartilage. In order to serve as a model for the epiphyseal growth plate, differentiating hfMSCs should obtain a growth plate signature. To test this, we compared the expression profiles of the differentiating hfMSCs with previously established profiles of human articular and growth plate cartilage (AC and GP, respectively, Leijten et al., in preparation). In a three-dimensional schematic representation, samples of AC and GP plot in two different groups (figure 5). As expected, AC, GP, and undifferentiated hfMSCs (hMSC_t0) plotted as distinct entities in a three-dimensional space. As differentiation progressed, the expression profile of the hfMSCs changed, and the differentiating chondrocytes gradually acquired a fingerprint resembling GP, but not AC. This analysis demonstrated that the hfMSCs differentiating towards chondrocytes acquired a GP cartilage phenotype.

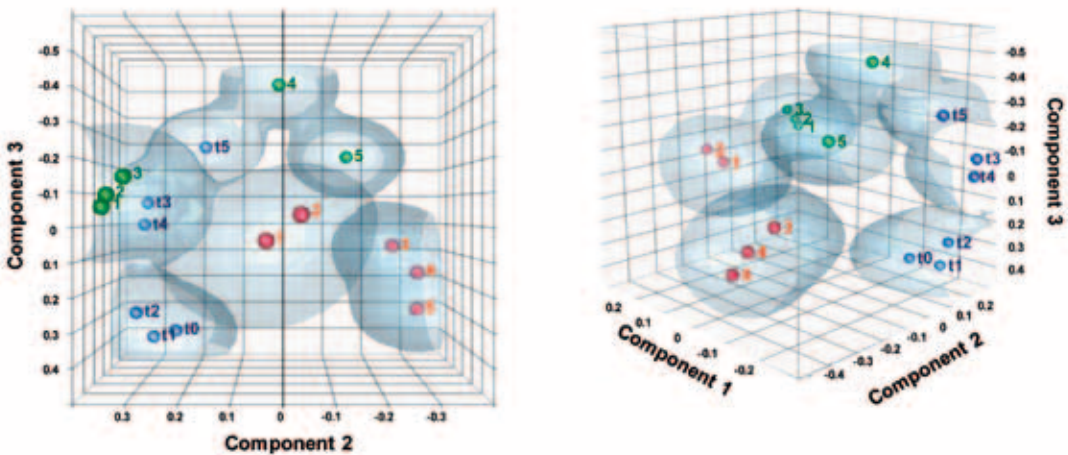


Figure 5

Three-dimensional overviews of gene expression data in respect to their correlation (factor score) to principal components 1, 2, and 3. Red dots, samples of articular cartilage; Green dots, samples of growth plates; Blue dots, differentiation time-range of hfMSCs (t0, undifferentiated hfMSCs; t5, mature chondrocytes). Dots indicate the mean factor score for all genes on the Affymetrix chip on the three principal components for one cartilage sample. Clouds represent the spread around the mean factor score in three dimensions.

Discussion

The present study was conducted in order to determine whether fetal bone marrow-derived MSCs are a representative human model for studying processes taking place in the epiphyseal growth plate and to identify associated signaling pathways. It has been reported that human bone marrow-derived MSCs display a better chondrogenic differentiation capacity than those derived from other sources, with fetal being superior over adult MSCs (6). Consequently, it seems appropriate to use fetal bone marrow-derived MSCs as a model for chondrogenesis. However, fetal MSCs are not easily obtained, due to ethical and legal considerations, and as a consequence, adult bone marrow-derived MSCs have been used in many previous studies (7-14).

Chondrogenic differentiation occurred in our *in vitro* model, as illustrated by the progressive expression of the chondrocyte markers collagen type II and X and the cartilaginous matrix constituent glycosaminoglycan. The two-layered structure that developed in the pellet during chondrogenic differentiation indicates that the differentiation was more successful in the core of the pellet.

Further confirmation of chondrogenesis was obtained by analysis of mRNA expression of cartilage markers, which, in addition, also validated our microarray results. The observation of similar gene expression patterns for all analyzed markers during chondrogenic development of MSCs derived from other fetal donors indicates that the selected 22-weeks old fetal MSC-donor was representative for fetal bone marrow in general.

Matrix mineralization was not observed after 5 weeks of differentiation, suggesting that the matrix was not ready for mineralization or that environmental stimuli necessary to induce this process were absent.

Microarray analysis generated a multidimensional dataset of differentially expressed genes for each time point. Several methods for analyzing such complex data have been reported, many based on presence/absence analysis, which starts with the list of differentially expressed genes and applies a strict but arbitrary cut-off for differential expression of individual genes (9;14). Misinterpretation of the data can easily occur, since genes are assumed to be independent, whereas it is more likely that sets of correlated genes play a role in complex biological processes (15). Genes that are not considered differentially expressed, but that do play a role in important signaling pathways, may be wrongfully eliminated. Another analysis strategy applied by many groups is to report on *a priori* selected pathway(s) of interest, thereby disregarding the relative importance of this pathway in view of other potentially co-regulated or interacting pathways. Alternatively, we have applied PCA with restrictive criteria as a statistical selection method for identification of gene expression profiles associated with the acquisition of chondrocyte characteristics or the loss of a stem cell phenotype. Since biological replicates were not included in this study, such a stringent approach was necessary in order to minimize potentially false-positive results.

The gene expression data generated with this analytic approach are consistent with previous reports on *in vitro* cartilage formation by adult mesenchymal stem cells. We therefore conclude that PCA is a suitable and unbiased analysis tool for data reduction in multidimensional and complex microarray experiments. Using this method, 232 genes were identified to be significantly associated with chondrogenic differentiation, 39 of which were present in 9 significantly enriched KEGG pathways. These 39 genes could be classified in three major functional groups that are discussed in the following sections.

Growth factor (GF) and GF-related genes

Growth factors from the transforming growth factor β (TGF- β), Wnt, Hedgehog and VEGF families have been recognized as major regulators of endochondral bone formation in embryonic and postnatal cartilage development (16;17). Some family members were also identified to be involved in chondrocyte differentiation in our *in vitro* model.

BMP2 and its downstream effector ID3 are upregulated early in differentiation consistent with previous reports on the importance of BMP signaling in chondrogenesis (18;19). Growth and differentiation factor 5 (GDF5), previously reported as stimulator of chondrocyte proliferation (20), was highly expressed at the earliest time point observed and downregulated thereafter. A similar expression profile was found for the BMP inhibitor follistatin (FST) that was previously shown to be expressed by proliferative, but not by hypertrophic chondrocytes (21).

Previous *in vitro* studies have demonstrated that BMP2 interacts with Wnt and hedgehog family members and their downstream effectors, indicating that functional crosstalk between regulatory pathways occurs during chondrogenesis (19;22). Such interactions may have taken place in our *in vitro* model as well since several genes out of the Wnt and Hedgehog family were affected during differentiation, e.g. WNT5a, WNT11, FZD2, WIF1 and IHH. IHH expression reached a maximum after 3 weeks of differentiation, which is in agreement with a stimulatory, PTHrP-independent effect of IHH on terminal chondrocyte differentiation in the postnatal growth plate.

Another major group of regulatory factors found to be involved in chondrogenesis was the superfamily of cytokines. Several genes in this group were changing significantly over time, e.g. CXCL12, CCL20, interferon- γ (IFN- γ), IFN- γ receptor IFNGR1, interferon-induced transmembrane protein 1 (IFITM1) and the cytokine RANKL (receptor activator for nuclear factor κ B ligand). To our knowledge a role for CCL20, IFITM1, IFN- γ and its receptor IFNGR1 has not been described before in chondrogenesis.

Vascular endothelial growth factors (VEGF and VEGFC), originally described to promote epiphyseal vascularization prior to endochondral ossification, also regulate *in vitro* chondrogenesis (23-25). Both VEGF and VEGFC were significantly changing in expression level early in our model.

Genes associated with the extracellular matrix

Progression of chondrogenic differentiation depends on the coordinated expression of ECM components and on cell-matrix interactions (16). Several genes involved in focal adhesion, cell-matrix communication, ECM receptor interaction and matrix remodeling were found to play a role in our *in vitro* model of chondrogenesis.

The expression of cartilaginous ECM proteins, such as collagens (COL1A1, COL1A2, COL2A1, COL5A2, COL11A1), chondroadherin (CHAD), cartilage oligomeric matrix protein (COMP), secreted phosphoprotein 1 (osteopontin, SPP1), and fibronectin type III (FNDC1), was upregulated. Apart from a structural role in the extracellular matrix, FNDC1, SPP1 and CHAD also function as integrin ligands and regulate cell-matrix signaling by binding to the cell surface plasma membrane protein integrinT. Aggregation of integrins in focal adhesions is induced by activity of myosin light chain kinase (MLCK) (26). Upon ligand-integrin binding, signaling complexes are activated that mediate downstream effectors of integrin signaling such as phosphoinositide-3-kinase (PI3K) (27), thereby stimulating cell proliferation (28). We observed early downregulation of integrin signaling-related proteins such as PI3K and MLCK.

Members of the complement and coagulation family of proteins were expressed during *in vitro* chondrogenic differentiation. Coagulation factor XIII (F13A1) expression was upregulated, other genes like complement component I (C1R), urokinase-type plasminogen activator (PLAU) and bradykinin receptor B2 (BDKRB2) were downregulated during differentiation in our model. These

proteins are associated with matrix mineralization (29-31) or matrix degradation in the growth plate (32-34).

Genes associated with signal transduction, cell cycle, and cell survival

Several genes involved in the regulation of cell survival and proliferation and signal transduction were found to be important in our *in vitro* model of chondrogenesis. Caveolin 1 (CAV1), a multifunctional scaffolding protein located at cell surface caveolae, regulates TGF, Wnt, cytokine and VEGF signaling by modulating their downstream signaling cascades such as JAK/STAT, β -catenin/LEF1, MAPK/ERK and PI3K/AKT (35-38). The anti-apoptotic baculoviral IAP repeat containing 3 (BIRC3) has been shown to increase the survival of cultured human chondrocytes (39). Phosphoinositide-3-kinase (PI3K), proto-oncogene KIT, transcription factor JUN and FOS are all associated to the regulation of cell proliferation (40; 41). Expression of the nuclear envelope protein lamin B2 (LMNB2) was first upregulated and later in differentiation downregulated in our model. Constantinescu et al suggested a role for LMNB2 in suppressing differentiation of undifferentiated embryonic stem cells (42).

Conclusion

Many genes identified in this study were previously reported in association with chondrogenesis, validating the robustness of differentiating hfMSC as a model for cartilage formation. The implication of bradykinin and IFN- γ signaling, CCL20, and KIT are novel findings. Discrepancies between our results and reports by others may rely on differences between the source, and chondrogenic capacity of MSCs used, the experimental conditions for inducing chondrogenesis, and the gene expression analysis methods (9;10;13). Developmental genes essential for chondrogenic differentiation (e.g. SOX genes, IGF-I) were not identified, in line with other reports (11). Marginal changes in the expression of these genes may be sufficient for inducing major effects, but too subtle to be detected by most gene expression analysis methods, including PCA. Alternatively, changes occurring within the first days of differentiation may have been unnoticed due to the chosen time interval of analysis.

This study has demonstrated for the first time that bone marrow-derived hfMSCs acquire a GP-, but less an AC-like signature during differentiation towards chondrocytes. These findings validate differentiating hfMSCs as an excellent model for the epiphyseal growth plate. The application of this model in future studies creates the opportunity to unravel molecular mechanisms underlying growth regulation in the human epiphyseal plate and allows the analysis of even the earliest stages of chondrogenic differentiation. The effects of specific signaling pathways and growth-associated hormones (e.g. estrogen), can be studied and (genetically) manipulated in this model, which may give an impulse to the development of novel treatment strategies in various growth disorders.

Acknowledgement and funding

This work was supported by a grant from the European Society for Paediatric Endocrinology Research Unit and by grants from ZonMW, the Netherlands Organisation for Health Research and Development, to S.A. van Gool (grant number 920-03-392) and J.A.M. Emons (grant number 920-03-358) and a grant from the Deutsche Forschungsgemeinschaft to G.Rappold (Ra380/12-1). The authors gratefully acknowledge the TeRM Smart Mix Program of the Netherlands Ministry of Economic Affairs and the Netherlands Ministry of Education, Culture and Science.

Supplemental table 1

Affymetrix ID	Gene code	Gene title
205856_at	SLC14A1	solute carrier family 14 (urea transporter), member 1 (Kidd blood group)
205911_at	PTHFR1	parathyroid hormone receptor 1
219148_at	PBK	PDZ binding kinase
213182_x_at	CDKN1C	cyclin-dependent kinase inhibitor 1C (p57, Kip2)
206737_at	WNT11	wingless-type MMTV integration site family, member 11
203868_s_at	VCAM1	vascular cell adhesion molecule 1
218730_s_at	OGN	osteolectin (osteoinductive factor, mimecan)
200665_s_at	SPARC	secreted protein, acidic, cysteine-rich (osteonectin)
223484_at	C15orf48	chromosome 15 open reading frame 48
206315_at	CRLF1	cytokine receptor-like factor 1
205497_at	ZNF175	zinc finger protein 175
204724_s_at	COL9A3	collagen, type IX, alpha 3
219410_at	TMEM45A	transmembrane protein 45A
218391_at	SNF8	SNF8, ESCRT-II complex subunit, homolog (S. cerevisiae)
210538_s_at	BIRC3	baculoviral IAP repeat-containing 3
201487_at	CTSC	cathepsin C
219134_at	ELTD1	EGF, latrophilin and seven transmembrane domain containing 1
212551_at	CAP2	CAP, adenylate cyclase-associated protein, 2 (yeast)
206421_s_at	SERPINB7	serpin peptidase inhibitor, clade B (ovalbumin), member 7
219837_s_at	CYTL1	cytokine-like 1
210220_at	FZD2	frizzled homolog 2 (Drosophila)
207064_s_at	AOC2	amine oxidase, copper containing 2 (retina-specific)
218542_at	CEP55	centrosomal protein 55kDa
206423_at	ANGPTL7	angiopoietin-like 7
231227_at	---	Transcribed locus, strongly similar to WNT-5A protein precursor
229494_s_at	CD63	CD63 molecule
223734_at	OSAP	ovary-specific acidic protein
206614_at	GDF5	growth differentiation factor 5 (cartilage-derived morphogenetic protein-1)
205713_s_at	COMP	cartilage oligomeric matrix protein
230372_at	---	Transcribed locus, PREDICTED: similar to hyaluronan synthase 2 [Pan troglodytes]
1563724_at	SACS	Spastic ataxia of Charlevoix-Saguenay (sacsin)
203499_at	EPHA2	EPH receptor A2
1556499_s_at	COL1A1	collagen, type I, alpha 1
219230_at	TMEM100	transmembrane protein 100
206790_s_at	NDUFB1	NADH dehydrogenase (ubiquinone) 1 beta subcomplex, 1, 7kDa
204825_at	MELK	maternal embryonic leucine zipper kinase
212565_at	STK38L	serine/threonine kinase 38 like
1554997_a_at	PTGS2	prostaglandin-endoperoxide synthase 2 (prostaglandin G/H synthase & cyclooxygenase)
204894_s_at	AOC3	amine oxidase, copper containing 3 (vascular adhesion protein 1)
203886_s_at	FBLN2	fibulin 2
203153_at	IFIT1	interferon-induced protein with tetratricopeptide repeats 1
242517_at	KISS1R	KISS1 receptor
1552340_at	SP7	Sp7 transcription factor
203963_at	CA12	carbonic anhydrase XII
1554950_at	AGC1	aggrecan 1 (chondroitin sulfate proteoglycan 1, large aggregating proteoglycan)
232451_at	---	MRNA; cDNA DKFZp564I0816 (from clone DKFZp564I0816)
227705_at	TCEAL7	transcription elongation factor A (SII)-like 7
1570574_at	GPR177	G protein-coupled receptor 177
218273_s_at	PPM2C	protein phosphatase 2C, magnesium-dependent, catalytic subunit
224735_at	CYBASC3	cytochrome b, ascorbate dependent 3
239787_at	KCTD4	potassium channel tetramerisation domain containing 4
226281_at	DNER	delta-notch-like EGF repeat-containing transmembrane
218839_at	HEY1	hair/enhancer-of-split related with YRPW motif 1
214710_s_at	CCNB1	cyclin B1
231798_at	NOG	Noggin
204595_s_at	STC1	stanniocalcin 1
209189_at	FOS	v-fos FBJ murine osteosarcoma viral oncogene homolog
203297_s_at	JARID2	Jumonji, AT rich interactive domain 2
230137_at	TMEM155	transmembrane protein 155

208078_s_at	SNF1LK	SNF1-like kinase // SNF1-like kinase
217989_at	DHR58	dehydrogenase/reductase (SDR family) member 8
229125_at	ANKRD38	ankyrin repeat domain 38
205141_at	ANG /// RNASE4	angiogenin, ribonuclease, RNase A family, 5 /// ribonuclease, RNase A family, 4
204712_at	WIF1	WNT inhibitory factor 1
1552960_at	LRRC15	leucine rich repeat containing 15
225155_at	SNHG5	small nucleolar RNA host gene (non-protein coding) 5
204351_at	S100P	S100 calcium binding protein P
1569372_at	TUBB2B	Tubulin, beta 2B
205097_at	SLC26A2	solute carrier family 26 (sulfate transporter), member 2
204881_s_at	UGCG	UDP-glucose ceramide glucosyltransferase
203434_s_at	MME	membrane metallo-endopeptidase (neutral endopeptidase, enkephalinase)
1568574_x_at	SPP1	Secreted phosphoprotein 1 (osteopontin, bone sialoprotein I)
206908_s_at	CLDN11	claudin 11 (oligodendrocyte transmembrane protein)
1556153_s_at	NFKBIZ	Nuclear factor of kappa light polypeptide gene enhancer in B-cells inhibitor, zeta
210643_at	TNFSF11	tumor necrosis factor (ligand) superfamily, member 11, RANKL
203305_at	F13A1	coagulation factor XIII, A1 polypeptide
213791_at	PENK	proenkephalin
242324_x_at	CCBE1	collagen and calcium binding EGF domains 1
213338_at	TMEM158	transmembrane protein 158
213139_at	SNAI2	snail homolog 2 (Drosophila)
217979_at	TSPAN13	Tetraspanin 13
215420_at	IHH	Indian hedgehog homolog (Drosophila)
229645_at	C18orf51	chromosome 18 open reading frame 51
218717_s_at	LEPREL1	leprecan-like 1
238332_at	ANKRD29	ankyrin repeat domain 29
205828_at	MMP3	matrix metalloproteinase 3 (stromelysin 1, progelatinase)
209395_at	CHI3L1	chitinase 3-like 1 (cartilage glycoprotein-39)
204337_at	RGS4	regulator of G-protein signalling 4
201939_at	PLK2	polo-like kinase 2 (Drosophila)
228844_at	SLC13A5	solute carrier family 13 (sodium-dependent citrate transporter), member 5
218468_s_at	GREM1	gremlin 1, cysteine knot superfamily, homolog (Xenopus laevis)
201467_s_at	NQO1	NAD(P)H dehydrogenase, quinone 1
224482_s_at	RAB11FIP4	RAB11 family interacting protein 4 (class II)
206239_s_at	SPINK1	serine peptidase inhibitor, Kazal type 1
213492_at	COL2A1	collagen, type II, alpha 1
1552737_s_at	WWP2	WW domain containing E3 ubiquitin protein ligase 2
204162_at	KNTC2	kinetochore associated 2
213622_at	COL9A2	collagen, type IX, alpha 2
202497_x_at	SLC2A3	solute carrier family 2 (facilitated glucose transporter), member 3
206309_at	LECT1	leukocyte cell derived chemotaxin 1
1556427_s_at	LOC221091	similar to hypothetical protein
201762_s_at	PSME2	proteasome (prosome, macropain) activator subunit 2 (PA28 beta)
201795_at	LBR	lamin B receptor
209946_at	VEGFC	vascular endothelial growth factor C
210432_s_at	SCN3A	sodium channel, voltage-gated, type III, alpha
206439_at	DSPG3	dermatan sulfate proteoglycan 3
203498_at	DSCR1L1	Down syndrome critical region gene 1-like 1
202912_at	ADM	adrenomedullin
221729_at	COL5A2	collagen, type V, alpha 2
1555345_at	SLC38A4	solute carrier family 38, member 4
210095_s_at	IGFBP3	insulin-like growth factor binding protein 3
201601_x_at	IFITM1	interferon induced transmembrane protein 1 (9-27)
205483_s_at	ISG15	ISG15 ubiquitin-like modifier
1554685_a_at	KIAA1199	KIAA1199
221019_s_at	COLEC12	collectin sub-family member 12 /// collectin sub-family member 12
240448_at	KIAA0802	KIAA0802
200790_at	ODC1	ornithine decarboxylase 1
206932_at	CH25H	cholesterol 25-hydroxylase
205352_at	SERPINI1	serpin peptidase inhibitor, clade I (neuroserpin), member 1
228640_at	---	CDNA clone IMAGE:4800096
205051_s_at	KIT	v-kit Hardy-Zuckerman 4 feline sarcoma viral oncogene homolog
204731_at	TGFBR3	transforming growth factor, beta receptor III (betaglycan, 300kDa)

221823_at	C5orf30	chromosome 5 open reading frame 30
1554736_at	ARHGAP29	Rho GTPase activating protein 29
217997_at	PHLDA1	pleckstrin homology-like domain, family A, member 1
226907_at	PPP1R14C	protein phosphatase 1, regulatory (inhibitor) subunit 14C
223235_s_at	SMOC2	SPARC related modular calcium binding 2
202403_s_at	COL1A2	collagen, type I, alpha 2
204469_at	PTPRZ1	protein tyrosine phosphatase, receptor-type, Z polypeptide 1
223614_at	C8orf57	chromosome 8 open reading frame 57
212850_s_at	LRP4	low density lipoprotein receptor-related protein 4
202965_s_at	CAPN6	calpain 6
223316_at	CCDC3	coiled-coil domain containing 3
200974_at	ACTA2	actin, alpha 2, smooth muscle, aorta
213293_s_at	TRIM22	tripartite motif-containing 22
222020_s_at	HNT	neurotrimin
210609_s_at	TP53I3	tumor protein p53 inducible protein 3
201739_at	SGK	serum/glucocorticoid regulated kinase
217995_at	SQRDL	sulfide quinone reductase-like (yeast)
204682_at	LTBP2	latent transforming growth factor beta binding protein 2
201195_s_at	SLC7A5	solute carrier family 7 (cationic amino acid transporter, y+ system), member 5
206764_x_at	MPPE1	metallophosphoesterase 1
213060_s_at	CHI3L2	chitinase 3-like 2 /// chitinase 3-like 2
205334_at	S100A1	S100 calcium binding protein A1
209955_s_at	FAP	fibroblast activation protein, alpha
204035_at	SCG2	secretogranin II (chromogranin C)
217875_s_at	TMEPAI	transmembrane, prostate androgen induced RNA
203879_at	PIK3CD	phosphoinositide-3-kinase, catalytic, delta polypeptide
202709_at	FMOD	fibromodulin
1554737_at	FBN2	fibrillin 2 (congenital contractural arachnodactyly)
205941_s_at	COL10A1	collagen, type X, alpha 1 (Schmid metaphyseal chondrodysplasia)
202727_s_at	IFNGR1	interferon gamma receptor 1
226930_at	FNDC1	fibronectin type III domain containing 1
207001_x_at	TSC22D3	TSC22 domain family, member 3
206960_at	GPR23	G protein-coupled receptor 23
203666_at	CXCL12	chemokine (C-X-C motif) ligand 12 (stromal cell-derived factor 1)
204320_at	COL11A1	collagen, type XI, alpha 1
203058_s_at	PAPSS2	3'-phosphoadenosine 5'-phosphosulfate synthase 2
205870_at	BDKRB2	bradykinin receptor B2
201464_x_at	JUN	v-jun sarcoma virus 17 oncogene homolog (avian)
226989_at	RGMB	RGM domain family, member B
229740_at	LOC643008	PP12104
203304_at	BAMBI	BMP and activin membrane-bound inhibitor homolog (<i>Xenopus laevis</i>)
218899_s_at	BALC	brain and acute leukemia, cytoplasmic
224348_s_at	H19	H19, imprinted maternally expressed untranslated mRNA
209560_s_at	DLK1	delta-like 1 homolog (<i>Drosophila</i>)
222162_s_at	ADAMTS1	ADAM metalloproteinase with thrombospondin type 1 motif, 1
206115_at	EGR3	early growth response 3
1562094_at	MGC26963	Hypothetical protein MGC26963
216952_s_at	LMNB2	lamin B2
210948_s_at	LEF1	lymphoid enhancer-binding factor 1
1563466_at	MYLK	Myosin, light polypeptide kinase
212689_s_at	JMJD1A	jumonji domain containing 1A
205347_s_at	TMSL8	thymosin-like 8
204967_at	SHROOM2	shroom family member 2
218009_s_at	PRC1	protein regulator of cytokinesis 1
212067_s_at	C1R /// LOC643676	complement component 1, r subcomponent
1560259_at	RORA	RAR-related orphan receptor A
206432_at	HAS2	hyaluronan synthase 2
1561065_at	ANKRD6	Ankyrin repeat domain 6
1555800_at	ZNF533	zinc finger protein 533
219747_at	C4orf31	chromosome 4 open reading frame 31
1558636_s_at	ADAMTS5	ADAM metalloproteinase with thrombospondin type 1 motif, 5 (aggrecanase-2)
227497_at	---	CDNA FLJ11723 fis, clone HEMBA1005314
1555527_at	COL9A1	collagen, type IX, alpha 1

202768_at	FOSB	FBJ murine osteosarcoma viral oncogene homolog B
204221_x_at	GLIPR1	GLI pathogenesis-related 1 (glioma)
204774_at	EVI2A	ecotropic viral integration site 2A
206157_at	PTX3	pentraxin-related gene, rapidly induced by IL-1 beta
202643_s_at	TNFAIP3	tumor necrosis factor, alpha-induced protein 3
234994_at	KIAA1913	KIAA1913
227475_at	FOXQ1	forkhead box Q1
219334_s_at	OBFC2A	oligonucleotide/oligosaccharide-binding fold containing 2A
218986_s_at	FLJ20035	hypothetical protein FLJ20035
228382_at	FAM105B	family with sequence similarity 105, member B
205523_at	HAPLN1	hyaluronan and proteoglycan link protein 1
224967_at	UGCG	UDP-glucose ceramide glucosyltransferase
213817_at	---	CDNA FLJ13601 fis, clone PLACE1010069
212900_at	SEC24A	SEC24 related gene family, member A (S. cerevisiae)
1552619_a_at	ANLN	anillin, actin binding protein
224609_at	SLC44A2	solute carrier family 44, member 2
203755_at	BUB1B	BUB1 budding uninhibited by benzimidazoles 1 homolog beta (yeast)
1555724_s_at	TAGLN	transgelin
202450_s_at	CTSK	cathepsin K (pyncnodysostosis)
213861_s_at	FAM119B	family with sequence similarity 119, member B
213248_at	LOC221362	hypothetical protein LOC221362
203570_at	LOXL1	lysyl oxidase-like 1
230407_at	---	Transcribed locus, strongly similar to strawberry notch homolog 1; MOP-3
209567_at	RRS1	RRS1 ribosome biogenesis regulator homolog (S. cerevisiae)
210512_s_at	VEGF	vascular endothelial growth factor
205289_at	BMP2	bone morphogenetic protein 2
203065_s_at	CAV1	caveolin 1, caveolae protein, 22kDa
203758_at	CTSO	cathepsin O
205476_at	CCL20	chemokine (C-C motif) ligand 20
207826_s_at	ID3	inhibitor of DNA binding 3, dominant negative helix-loop-helix protein
205479_s_at	PLAU	plasminogen activator, urokinase
201136_at	PLP2	proteolipid protein 2 (colonic epithelium-enriched)
203764_at	DLG7	discs, large homolog 7 (Drosophila)
209160_at	AKR1C3	aldo-keto reductase family 1, member C3 (3-alpha hydroxysteroid dehydrogenase, type II)
207977_s_at	DPT	dermatopontin
205125_at	PLCD1	phospholipase C, delta 1
207980_s_at	CITED2	Cbp/p300-interacting transactivator, with Glu/Asp-rich carboxy-terminal domain, 2
204475_at	MMP1	matrix metalloproteinase 1 (interstitial collagenase)
1556209_at	CLEC2B	C-type lectin domain family 2, member B
205830_at	CLGN	calmegin
219295_s_at	PCOLCE2	procollagen C-endopeptidase enhancer 2
205907_s_at	OMD	osteomodulin
206869_at	CHAD	chondroadherin
223836_at	KSP37	Ksp37 protein
204948_s_at	FST	folliostatin
240955_at	PANX3	pannexin 3

References

1. **Chagin AS, Savendahl L** 2007 Estrogens and growth: review. *Pediatr Endocrinol Rev* 4: 329-334
2. **Nilsson O, Chrysis D, Pajulo O, Boman A, Holst M, Rubinstein J, Martin RE, Savendahl L** 2003 Localization of estrogen receptors-alpha and -beta and androgen receptor in the human growth plate at different pubertal stages. *J Endocrinol* 177:319-326
3. **Vidal O, Lindberg MK, Hollberg K, Baylink DJ, Andersson G, Lubahn DB, Mohan S, Gustafsson JA, Ohlsson C** 2000 Estrogen receptor specificity in the regulation of skeletal growth and maturation in male mice. *Proc Natl Acad Sci U S A* 97:5474-5479
4. **Smith EP, Boyd J, Frank GR, Takahashi H, Cohen RM, Specker B, Williams TC, Lubahn DB, Korach KS** 1994 Estrogen resistance caused by a mutation in the estrogen-receptor gene in a man. *N Engl J Med* 331:1056-1061
5. **Pelttari K, Steck E, Richter W** 2008 The use of mesenchymal stem cells for chondrogenesis. *Injury* 39 Suppl 1:S58-S65
6. **Bernardo ME, Emons JA, Karperien M, Nauta AJ, Willemze R, Roelofs H, Romeo S, Marchini A, Rappold GA, Vukicevic S, Locatelli F, Fibbe WE** 2007 Human mesenchymal stem cells derived from bone marrow display a better chondrogenic differentiation compared with other sources. *Connect Tissue Res* 48:132-140
7. **Djouad F, Delorme B, Maurice M, Bony C, Apparailly F, Louis-Pence P, Canovas F, Charbord P, Noel D, Jorgensen C** 2007 Microenvironmental changes during differentiation of mesenchymal stem cells towards chondrocytes. *Arthritis Res Ther* 9:R33
8. **Larson BL, Ylostalo J, Prockop DJ** 2008 Human multipotent stromal cells undergo sharp transition from division to development in culture. *Stem Cells* 26:193-201
9. **Mrugala D, Dossat N, Ringe J, Delorme B, Coffy A, Bony C, Charbord P, Haupl T, Daures JP, Noel D, Jorgensen C** 2009 Gene Expression Profile of Multipotent Mesenchymal Stromal Cells: Identification of Pathways Common to TGFbeta3/BMP2-Induced Chondrogenesis. *Cloning Stem Cells*
10. **Phinney DG, Prockop DJ** 2007 Concise review: mesenchymal stem/multipotent stromal cells: the state of transdifferentiation and modes of tissue repair--current views. *Stem Cells* 25:2896-2902
11. **Sekiya I, Vuoristo JT, Larson BL, Prockop DJ** 2002 In vitro cartilage formation by human adult stem cells from bone marrow stroma defines the sequence of cellular and molecular events during chondrogenesis. *Proc Natl Acad Sci U S A* 99:4397-4402

12. **Sekiya I, Larson BL, Smith JR, Pochampally R, Cui JG, Prockop DJ** 2002 Expansion of human adult stem cells from bone marrow stroma: conditions that maximize the yields of early progenitors and evaluate their quality. *Stem Cells* 20:530-541
13. **Shahdadfar A, Fronsdal K, Haug T, Reinholt FP, Brinchmann JE** 2005 In vitro expansion of human mesenchymal stem cells: choice of serum is a determinant of cell proliferation, differentiation, gene expression, and transcriptome stability. *Stem Cells* 23:1357-1366
14. **Ylostalo J, Smith JR, Pochampally RR, Matz R, Sekiya I, Larson BL, Vuoristo JT, Prockop DJ** 2006 Use of differentiating adult stem cells (marrow stromal cells) to identify new downstream target genes for transcription factors. *Stem Cells* 24:642-652
15. **Goeman JJ, Buhlmann P** 2007 Analyzing gene expression data in terms of gene sets: methodological issues. *Bioinformatics* 23:980-987
16. **DeLise AM, Fischer L, Tuan RS** 2000 Cellular interactions and signaling in cartilage development. *Osteoarthritis Cartilage* 8:309-334
17. **Zelzer E, Olsen BR** 2005 Multiple roles of vascular endothelial growth factor (VEGF) in skeletal development, growth, and repair. *Curr Top Dev Biol* 65:169-187
18. **De LF, Barnes KM, Uyeda JA, De-Levi S, Abad V, Palese T, Mericq V, Baron J** 2001 Regulation of growth plate chondrogenesis by bone morphogenetic protein-2. *Endocrinology* 142:430-436
19. **Minina E, Wenzel HM, Kreschel C, Karp S, Gaffield W, McMahon AP, Vortkamp A** 2001 BMP and Ihh/PTHrP signaling interact to coordinate chondrocyte proliferation and differentiation. *Development* 128:4523-4534
20. **Buxton P, Edwards C, Archer CW, Francis-West P** 2001 Growth/differentiation factor-5 (GDF-5) and skeletal development. *J Bone Joint Surg Am* 83-A Suppl 1:S23-S30
21. **Funaba M, Ogawa K, Murata T, Fujimura H, Murata E, Abe M, Takahashi M, Torii K** 1996 Follistatin and activin in bone: expression and localization during endochondral bone development. *Endocrinology* 137:4250-4259
22. **Tuan RS** 2003 Cellular signaling in developmental chondrogenesis: N-cadherin, Wnts, and BMP-2. *J Bone Joint Surg Am* 85-A Suppl 2:137-141
23. **Bluteau G, Julien M, Magne D, Mallein-Gerin F, Weiss P, Daculsi G, Guicheux J** 2007 VEGF and VEGF receptors are differentially expressed in chondrocytes. *Bone* 40:568-576
24. **Maes C, Stockmans I, Moermans K, Van LR, Smets N, Carmeliet P, Bouillon R, Carmeliet G** 2004 Soluble VEGF isoforms are essential for establishing epiphyseal vascularization and regulating chondrocyte development and survival. *J Clin Invest* 113:188-199

25. **Mayer H, Bertram H, Lindenmaier W, Korff T, Weber H, Weich H** 2005 Vascular endothelial growth factor (VEGF-A) expression in human mesenchymal stem cells: autocrine and paracrine role on osteoblastic and endothelial differentiation. *J Cell Biochem* 95:827-839
26. **Clark K, Langeslag M, Figdor CG, van Leeuwen FN** 2007 Myosin II and mechanotransduction: a balancing act. *Trends Cell Biol* 17:178-186
27. **Howe A, Aplin AE, Alahari SK, Juliano RL** 1998 Integrin signaling and cell growth control. *Curr Opin Cell Biol* 10:220-231
28. **Ulici V, Hoenselaar KD, Gillespie JR, Beier F** 2008 The PI3K pathway regulates endochondral bone growth through control of hypertrophic chondrocyte differentiation. *BMC Dev Biol* 8:40
29. **Johnson K, Hashimoto S, Lotz M, Pritzker K, Terkeltaub R** 2001 Interleukin-1 induces pro-mineralizing activity of cartilage tissue transglutaminase and factor XIIIa. *Am J Pathol* 159:149-163
30. **Nurminskaya MV, Linsenmayer TF** 2002 Immunohistological analysis of transglutaminase factor XIIIa expression in mouse embryonic growth plate. *J Orthop Res* 20:575-578
31. **Aeschlimann D, Mosher D, Paulsson M** 1996 Tissue transglutaminase and factor XIII in cartilage and bone remodeling. *Semin Thromb Hemost* 22:437-443
32. **Madsen CD, Sidenius N** 2008 The interaction between urokinase receptor and vitronectin in cell adhesion and signalling. *Eur J Cell Biol* 87:617-629
33. **Sakiyama H, Nakagawa K, Kuriwa K, Imai K, Okada Y, Tsuchida T, Moriya H, Imajoh-Ohmi S** 1997 Complement C1s, a classical enzyme with novel functions at the endochondral ossification center: immunohistochemical staining of activated C1s with a neoantigen-specific antibody. *Cell Tissue Res* 288:557-565
34. **Weber KT, Sun Y, Tyagi SC, Cleutjens JP** 1994 Collagen network of the myocardium: function, structural remodeling and regulatory mechanisms. *J Mol Cell Cardiol* 26:279-292
35. **Bauer PM, Yu J, Chen Y, Hickey R, Bernatchez PN, Looft-Wilson R, Huang Y, Giordano F, Stan RV, Sessa WC** 2005 Endothelial-specific expression of caveolin-1 impairs microvascular permeability and angiogenesis. *Proc Natl Acad Sci U S A* 102:204-209
36. **Galbiati F, Volonte D, Brown AM, Weinstein DE, Ben-Ze'ev A, Pestell RG, Lisanti MP** 2000 Caveolin-1 expression inhibits Wnt/beta-catenin/Lef-1 signaling by recruiting beta-catenin to caveolae membrane domains. *J Biol Chem* 275:23368-23377
37. **Grande-Garcia A, del Pozo MA** 2008 Caveolin-1 in cell polarization and directional migration. *Eur J Cell Biol* 87:641-647
38. **Jasmin JF, Mercier I, Sotgia F, Lisanti MP** 2006 SOCS proteins and caveolin-1 as negative regulators of endocrine signaling. *Trends Endocrinol Metab* 17:150-158

39. **Gagarina V, Carlberg AL, Pereira-Mouries L, Hall DJ** 2008 Cartilage oligomeric matrix protein protects cells against death by elevating members of the IAP family of survival proteins. *J Biol Chem* 283:648-659
40. **Hirsch E, Costa C, Ciruolo E** 2007 Phosphoinositide 3-kinases as a common platform for multi-hormone signaling. *J Endocrinol* 194:243-256
41. **Miettinen M, Lasota J** 2005 KIT (CD117): a review on expression in normal and neoplastic tissues, and mutations and their clinicopathologic correlation. *Appl Immunohistochem Mol Morphol* 13:205-220
42. **Constantinescu D, Gray HL, Sammak PJ, Schatten GP, Csoka AB** 2006 Lamin A/C expression is a marker of mouse and human embryonic stem cell differentiation. *Stem Cells* 24:177-185
43. **Heinrichs C, Yanovski JA, Roth AH, Yu YM, Domene HM, Yano K, Cutler GB, Jr, Baron J** 1994 Dexamethasone increases growth hormone receptor messenger ribonucleic acid levels in liver and growth plate. *Endocrinology* 135:1113-1118
44. **Dai M, Wang P, Boyd AD, Kostov G, Athey B, Jones EG, Bunney WE, Myers RM, Speed TP, Akil H, Watson SJ, Meng F** 2005 Evolving gene/transcript definitions significantly alter the interpretation of GeneChip data. *Nucleic Acids Res* 33:e175
45. **Chu TM, Weir B, Wolfinger R** 2002 A systematic statistical linear modeling approach to oligonucleotide array experiments. *Math Biosci* 176:35-51

11

General discussion

General Discussion

Longitudinal bone growth occurs throughout childhood and is the key characteristic that distinguishes children from adults. During puberty longitudinal growth rate first increases, but finally as the growth plate further matures growth decreases and eventually ceases with epiphyseal fusion at the end of puberty. Mechanisms underlying growth plate maturation and epiphyseal fusion with termination of longitudinal growth are still largely unknown. With puberty estrogen levels increase and this is supposed to play an important role in growth plate maturation and epiphyseal fusion. In this thesis we investigated:

1. The route and effects of estrogens (17 β -estradiol or/and SERMs) on growth plate structure and VEGF expression.
2. Maturation of the growth plate: regarding proliferation and the cell cycle, the delayed growth plate senescence theory, pubertal changes and epiphyseal fusion.
3. A relatively new human growth plate model using mesenchymal stem cells.

Actions of estrogens and selective estrogen receptor modulators

Estrogens play a key role in longitudinal bone growth through growth plate maturation, epiphyseal fusion and augmentation of accrual of bone. In the human lack of estrogen action leads to continuation of growth and subsequently tall stature by absence of growth plate fusion (1;2). Conversely high levels of estrogen inhibit longitudinal bone growth and can clinically be used to prevent tall stature, but treatment is associated with side-effects (3). Therefore it is important to investigate the actions of estrogens in more detail.

In the sexually immature rat we observed an increase in body weight gain, tibia length and width of the growth plate with an increased proliferating zone after removal of estrogens by ovariectomy. Suppletion of estrogen showed the reverse effects in line with the clinical observations in humans. The effects of estrogen have been suggested to be mediated mainly through the nuclear receptors ER α and ER β , which are both expressed in growth plate chondrocytes of several species, including the human (4-7). We detected these estrogen receptors in the rat predominantly in late proliferating and early hypertrophic chondrocytes and observed a decrease in ER α and ER β staining with estrogen suppletion in chapter 2.

Estrogen can exert its effects through a genomic or non-genomic pathway, however the contribution of these routes to longitudinal growth has not been clarified up to now. Desoxyestrone administration, a synthetic compound that exclusively acts through the non-genomic pathway, resulted in a decrease in longitudinal growth although to a smaller extent than 17 β -estradiol. This indicates that estrogenic effects on longitudinal growth are regulated both through genomic and nongenomic pathways with genomic signalling prevailing.

Estrogen acts on a number of diverse tissues resulting in potential side-effects of estrogen treatment (3). Selective estrogen receptor modulators (SERMs) were developed to circumvent these side effects (8). 2-methoxyestradiol was suggested to be tissue-selective in the growth plate of female rats (9). We administered 2-methoxyestradiol to sexually immature rats and indeed found a decreased thickness of the proliferative zone in female rats and a decrease in the thickness of the total growth plate and of the hypertrophic zone in the male rat, but no general

effect on longitudinal growth was observed. Sibonga et al did find an effect on longitudinal bone growth when 2-methoxyestradiol was administered orally to older (10 weeks) and more mature rats (10). Therefore we conclude that 2-methoxyestradiol indeed has a growth plate selective estrogenic effect. However, more studies in animal and human models are needed to optimize the effects on longitudinal bone growth and to assess potential side-effects before clinical use can be considered. Recent studies have assigned 2-methoxyestradiol as a promising anticancer agent in the treatment of cancer, since it induces apoptosis in cancer cells (11;12). Nowadays more extensively investigated SERMs in relation to skeletal growth are raloxifene and tamoxifen. Both compounds act as estrogen agonists and impair longitudinal bone growth (13-15).

Estrogens can have a direct effect, but also an indirect effect on growth by stimulating the GH-IGF-I axis resulting in an increase of IGF-I levels (16;17). In our estrogen treated rats we were unable to measure circulating IGF-1 levels, but we did investigate local IGF-1 expression. We did not observe an effect on IGF-1 expression in the growth plate.

VEGF expression in the growth plate

Estrogen and its receptors interact with various growth factors in order to control longitudinal growth (16-19). One of these growth factors is Vascular Endothelial Growth Factor (VEGF). It was previously shown that estrogen up-regulated VEGF expression in uterus and bone tissue (20;21). In chapter 3 we demonstrate that VEGF expression in chondrocytes was elevated by estrogen treatment *in vivo* and *in vitro*. Removal of estrogens by ovariectomy resulted in a decrease in VEGF expression. Moreover, pubertal human growth plate maturation resulted in an increase in VEGF expression. From these observations we concluded that estrogens regulate VEGF expression in the growth plate.

Vascular Endothelial Growth Factor (VEGF) is important in the final event of endochondral ossification, as it has a function in chondrocyte differentiation and chondrocyte survival (22-24). Inhibition of VEGF resulted in dramatic effects on longitudinal growth and the growth plate in previous studies (22;25). At the end of puberty longitudinal growth ceases with total replacement of avascular cartilage by highly vascularized bone eventually resulting in epiphyseal fusion. VEGF could play an important role in this process. Our results are in line with this hypothesis, since estrogen and pubertal maturation both upregulated VEGF expression in growth plate chondrocytes suggesting a potential role for VEGF in estrogen-induced growth plate fusion. However, this suggested role needs to be confirmed in future experiments.

Growth plate senescence, proliferation and p27

One of the postulated hypotheses for epiphyseal fusion is that estrogen accelerates the senescent decline and that the growth plate fuses when senescence reaches a critical point (26). Senescence is a term for structural changes like a decrease in height of different zones in the growth plate, but also for the decline in chondrocyte proliferation (26;27). Senescence might influence proliferation and the cell cycle of chondrocytes by orderly inactivation and activation of cyclin-dependent kinases and kinase inhibitors like p27Kip1 (p27). p27-deficient mice have an increased size of long bones and weight compared to wild-type mice, suggestive for a functional role for p27 in the regulation of longitudinal growth (28-30). In chapter 4 we detected p27 mRNA in the growth plates of 5-wk-old mice by real-time PCR. The p27 mRNA levels in growth plate tissues were

approximately 2-fold lower than levels in the surrounding bone tissue. No significant difference was detected in p27 expression in the separate zones. Previous studies suggested a role for p27 in the differentiation of terminal growth plate chondrocytes. However, our results are in contrast with this since no elevated expression was seen in the hypertrophic zone (28;31;32). p27 ablation modestly increased chondrocyte proliferation in the growth plate and body length of 7 weeks old mice, however tibia length was not significantly greater than in controls. Presumably the increase in total length was a result of greater growth in the vertebrae and the increase in proliferation may have started shortly before sacrifice. The latter is supported by observations made by others who reported an increase in body size later in life, therefore most likely the increase in proliferation was too short to result in an increase in length of long bones (29;33). Another explanation for the modest effect of p27 in our study might be a difference in genetic background. Previous studies used a different background and have reported a more prominent growth phenotype (coisogenic 129S4 mice).

Treatment with glucocorticoids inhibited longitudinal growth in p27-deficient mice and controls to the same extent, indicating that p27 is not required for the negative effects of dexamethasone on longitudinal growth. Our findings in chapter 4 suggest that p27 negatively modulates growth plate chondrocyte proliferation, but it is not required for the conditional regulation of chondrocyte proliferation as induced by dexamethasone in the growth plate of rats.

In chapter 7 we used microarray techniques on human growth plate tissues and detected a significant change in the cell cycle pathway with progression of puberty. 15 out of 84 genes in this pathway were affected and among these was p27. p27 showed an up-regulation in expression with pubertal maturation of the growth plate. This indicates that the cell cycle activity and thereby proliferation decreased in line with the senescence hypothesis in the human pubertal growth plate and the reduced chondrocyte proliferation during growth plate maturation.

The delayed growth plate senescence hypothesis and catch-up growth

After a period of growth inhibition, the linear growth rate usually exceeds the normal range. This phenomenon is known as catch-up growth (34). Evidence from animal studies suggests that catch-up growth is due, at least in large part, to a delay in growth plate senescence. However, the relationship between catch-up growth and delayed growth plate senescence has only been studied in rabbits and rats (27;35). In chapter 5 we re-evaluated height and bone age measurements in patients with celiac disease before and on gluten-free diet. On gluten-free diet these patients experienced catch-up growth. We concluded that the pattern of catch-up growth in patients with celiac disease is consistent with the hypothesis of delayed growth plate senescence. We are the first showing human data in line with this hypothesis, however we cannot exclude that additional mechanisms like for example microRNAs and changes in gene expression may have contributed to the increase in height velocity as well.

Pubertal growth plate maturation

We had the unique opportunity to obtain two epiphyseal samples of one patient in different stages of puberty. Microarray analyses of these two samples were used to receive a first insight in the molecular processes and interactions occurring during human growth plate maturation in chapter 6. Histological experiments and measurements showed a clear decrease in width of the total

growth plate, more widely spaced columns with less cells and consequently more extracellular matrix in the more mature growth plate. This confirmed earlier observations in rabbits and rats (36;37). Our microarray results were in line with our morphological data obtained with histology, showing many genes and pathways related to the extracellular matrix significantly affected with maturation. Progression of puberty did affect many genes in the cell cycle pathway.

In addition, we have performed a detailed bioinformatic analysis on these two growth plate specimens. More specifically, we searched the promoter regions of genes that are differentially expressed in the two growth plate specimens with pubertal maturation for evidence of direct effects of estrogen, androgen, GH, IGF-I and PTHrP on their expression and analyzed these genes for their evolutionary conservation across 9 primates. Sequences evolutionary conserved along species are likely to have critical functional roles (38). This data provides for the first time evidence that Estrogen receptor, androgen receptor, STAT5B, ELK-1 and RUNX2 were found to have transcription factor binding motifs in genes involved in growth plate maturation, suggestive for a role of these transcription factors in pubertal maturation of the human growth plate.

In order to extend our microarray analyses in relation to pubertal growth plate maturation we collected additional human growth plate tissues. Growth plate tissues were obtained from patients who were undergoing surgery for a variety of disorders. Even though patients suffered from diverse disorders, we assume that the underlying mechanism of epiphyseal maturation and fusion is the same for all growth plates. Eventually longitudinal growth stops in all patients at the end of puberty. In chapter 7 a cross-sectional microarray analysis was performed on 6 female tibial growth plates of various pubertal stages. Results suggested many genes changing from prepuberty to early puberty, however most alterations occurred during late puberty. Overall changes in gene expression were very small and only few genes changed more than 2 fold with progression of puberty. This shows that there is no large change in expression patterns with progression of puberty and that there rather might be an effect of multiple small factors. The fact that we did not observe large changes is also in line with the senescence theory. This theory suggests that stem-like cells in the resting zone have a finite proliferative capacity, which is gradually exhausted resulting eventually in epiphyseal fusion (27;39). Loss of DNA methylation is suggested to be a biological marker for growth plate senescence and this can not be detected by microarray analysis (40).

Affected pathways were associated with extracellular matrix homeostasis, hormonal pathways and programmed cell death. These findings in affected pathways are in agreement with the observed results in the longitudinal study in chapter 6, however gene profiles were not fully overlapping and sets of other genes were at times in contrast as well.

Epiphyseal fusion

The exact mechanism by which epiphyseal fusion occurs is not yet completely understood. In chapter 8 we investigated apoptosis as the final mechanism by which chondrocytes eventually die and are replaced by bone. At the chondro-osseous junction site of the growth plate, apoptosis is nowadays generally accepted as the mechanism by which terminally hypertrophic chondrocytes die (41;42). It is generally assumed that the same mechanism eventually also results in epiphyseal fusion. We performed a detailed study on apoptosis in terminal hypertrophic chondrocytes in the pubertal female growth plate and found no signs of classical apoptosis. In addition, we studied a unique tissue specimen of a late pubertal human growth plate in the process of epiphyseal fusion and found clear evidence that apoptosis is not likely to be involved in the end phase of growth plate fusion. We did observe a dense border of thick bone surrounding the growth plate remnant, signs

of hypoxia and early necrosis in this fusing growth plate. We hypothesize that the border of dense bone is functioning as a physical barrier for oxygen and nutrients to reach the fusing growth plate resulting in hypoxia and eventually cell death in a non-classical apoptotic way through necrosis or a mixture of apoptosis and necrosis. In line with this new hypothesis White et al. recently demonstrated bridging bone in the center of a distal human tibial growth plate obtained from a 12.9 years old girl which might be an early sign of this shelling process (43).

Interestingly, in chapters 6 and 7 we found a significant increase in expression of the hypoxia-inducible factor 2 alpha gene from prepuberty to early and late stage puberty. The HIF-1alpha gene was also found to be expressed, but no change was seen with maturation. These findings are in line with Stewart et al, who reported an up-regulated expression of HIF-2alpha mRNA during chondrocytes differentiation in vitro, but no change in HIF-1alpha mRNA expression (44). Hif-2alpha knockout mice are small, what might indicate that this gene has an important role in the growth plate and subsequently in the regulation of longitudinal growth (45).

Therefore we believe it could be a hypoxia related process leading eventually to cell death of growth plate chondrocytes. Indeed with our microarray experiments in chapters 6 and 7 we did find many affected genes changing with pubertal maturation that are involved in programmed cell death, e.g. proapoptotic and anti-apoptotic genes, but also genes involved in the regulation of autophagy. However, histological and electron microscopy analyses thus far showed no signs of classical apoptosis and no autophagosomes in the fusing growth plate in chapter 8. Apoptosis and autophagy are closely related and there is an overlap in signaling proteins (46;47). The results of our studies are in line with this and suggestive for a non-classical and perhaps intermediate mechanism of different types of cell death.

Growth plate models

Most of our knowledge regarding the regulation of the growth plate is based on animal studies. However most animal models only partially correspond to the human situation and many species differences are present. In mouse and rat for example, in contrast to humans, growth plates do not fuse under the influence of estrogen at the end of puberty (48;49). This indicates that rodents are not perfectly representative for studies on growth plate fusion, excluding the use of transgenic approaches.

In chapter 9 we investigated a promising relatively new human model for the growth plate, human mesenchymal stem cells (hMSCs). hMSCs are multipotent and can differentiate into the chondrogenic lineage. Originally MSCs were isolated from bone marrow, however nowadays they can be obtained from various tissue sources, like fetal tissues, placenta, umbilical cord blood and adipose tissue (35;50-54). In chapter 9 we investigated the chondrogenic potential of hMSCs originating from various tissues. Bone marrow derived MSCs appeared to have the best chondrogenic potential, with fetal bone marrow prevailing over adult bone marrow. A passage-dependent decrease in the capacity of cartilage formation was seen in line with previous results in adult MSCs (55).

In chapter 10 we studied in detail the cartilage forming capacity of fetal hMSCs in order to explore in more detail the molecular processes and interactions taking place during early phases of chondrogenesis, chondrocyte proliferation and chondrocyte differentiation. To determine which type of hyaline cartilage is formed by differentiating hMSCs, we compared the gene expression profile with previously established gene expression fingerprints of human articular and epiphyseal growth plate cartilage. As differentiation towards chondrocytes proceeded, hMSCs gradually

obtained a gene expression profile that was more overlapping with the fingerprint of epiphyseal growth plate cartilage than of articular cartilage. This study validates differentiating fetal bone marrow-derived hMSCs as an excellent model for the epiphyseal growth plate. This new human model now opens the opportunity to elucidate clinical conditions influencing chondrogenesis and cartilage homeostasis in more detail as well as the opportunity to develop strategies for new treatment options for cartilage disorders.

Final remarks and suggestions for future studies

Patients with growth disorders are frequently presented to pediatricians. The etiology can only be established in a minority of these patients and even in such cases a causal treatment is usually not available. A better understanding of the mechanisms by which longitudinal growth is regulated at the level of the epiphyseal plate is therefore needed. We focused in our studies on the effects of estrogen and growth plate maturation and found interesting new clues for further study in order to design new treatment options.

17 β -estradiol treatment is used from the mid-fifties to decrease final height, however there are several potential side-effects like an increased risk for breast and uterus cancer and decreased fertility (3). We showed a growth plate selective estrogenic effect in rats with 2-methoxyestradiol treatment. This could be a potential new treatment option, however more detailed studies on longitudinal bone growth and potential side-effects of 2-methoxyestradiol treatment in the human are needed.

Adult height is achieved at the end of puberty after the growth plate has fused and there is no longitudinal growth potential anymore. The process of epiphyseal fusion in the human is still largely unknown and modulation of this process could potentially lead to new treatment strategies. Delaying epiphyseal fusion is expected to result in an increase in adult height by allowing more time for growth supporting treatments. On the contrary, initiating epiphyseal fusion would help in the treatment of tall stature. In our studies we have shown that estrogen increases VEGF expression in growth plate chondrocytes and suggested that VEGF plays an important role in estrogen-induced growth plate fusion.

We showed that apoptosis is not likely to be involved in the end phase of growth plate fusion, however we did detect signs of hypoxia in the fusing growth plate. Therefore we present a new hypothesis in which hypoxia plays a more important role in growth plate maturation and epiphyseal fusion. Both our morphological and microarray experiments are in line with this assumption. We hypothesize that hypoxia increases during maturation of the growth plate. At the end of puberty a border of dense bone is formed that surrounds the growth plate functioning as a physical barrier for oxygen and nutrients resulting in more hypoxia and eventually cell death in a non-classical apoptotic way. Increasing levels of VEGF might be a result of this process as well, since many studies reported an increase in VEGF expression by hypoxia (56-58). This model needs further investigations. It would be interesting to study Hif-1 α and Hif-2 α protein expression in our human growth plate collection. Moreover it would be useful to extend our collection of growth plates for investigations regarding maturation of the growth plate and the proposed hypotheses in more detail. Our microarray results are promising and contain a great amount of data; however more samples are needed to validate our findings. With a larger collection, results could serve as a database and clarify multiple research questions involving the growth plate.

Without a large collection of human growth plates other methods and models are needed, like MSCs. We recommend using MSCs derived from human fetal bone marrow. These MSCs showed to

be a good model for the human growth plate and have the advantage that they can be genetically modified. Interesting experiments would be over-expression or down-silencing of certain growth factors and receptors like the estrogen-receptor. Ultimately this will help us in understanding in depth the molecular mechanisms that drive growth plate maturation and will help us to develop new strategies for the treatment of cartilage and growth disorders.

References

1. **Morishima A, Grumbach MM, Simpson ER, Fisher C, Qin K** 1995 Aromatase deficiency in male and female siblings caused by a novel mutation and the physiological role of estrogens. *J Clin Endocrinol Metab* 80:3689-3698
2. **Smith EP, Boyd J, Frank GR, Takahashi H, Cohen RM, Specker B, Williams TC, Lubahn DB, Korach KS** 1994 Estrogen resistance caused by a mutation in the estrogen-receptor gene in a man. *N Engl J Med* 331:1056-1061
3. **Venn A, Bruinsma F, Werther G, Pyett P, Baird D, Jones P, Rayner J, Lumley J** 2004 Oestrogen treatment to reduce the adult height of tall girls: long-term effects on fertility. *Lancet* 364:1513-1518
4. **Kennedy J, Baris C, Hoyland JA, Selby PL, Freemont AJ, Braidman IP** 1999 Immunofluorescent localization of estrogen receptor-alpha in growth plates of rabbits, but not in rats, at sexual maturity. *Bone* 24:9-16
5. **Kusec V, Virdi AS, Prince R, Triffitt JT** 1998 Localization of estrogen receptor-alpha in human and rabbit skeletal tissues. *J Clin Endocrinol Metab* 83:2421-2428
6. **Nilsson O, Chrysis D, Pajulo O, Boman A, Holst M, Rubinstein J, Martin RE, Savendahl L** 2003 Localization of estrogen receptors-alpha and -beta and androgen receptor in the human growth plate at different pubertal stages. *J Endocrinol* 177:319-326
7. **van der Eerden BC, Gevers EF, Lowik CW, Karperien M, Wit JM** 2002 Expression of estrogen receptor alpha and beta in the epiphyseal plate of the rat. *Bone* 30:478-485
8. **McDonnell DP** 1999 The Molecular Pharmacology of SERMs. *Trends Endocrinol Metab* 10:301-311
9. **Turner RT, Evans GL** 2000 2-Methoxyestradiol inhibits longitudinal bone growth in normal female rats. *Calcif Tissue Int* 66:465-469
10. **Sibonga JD, Sommer U, Turner RT** 2002 Evidence that 2-methoxyestradiol suppresses proliferation and accelerates apoptosis in normal rat growth plate chondrocytes. *J Cancer Res Clin Oncol* 128:477-483
11. **Batsi C, Markopoulou S, Kontargiris E, Charalambous C, Thomas C, Christoforidis S, Kanavaros P, Constantinou AI, Marcu KB, Kolettas E** 2009 Bcl-2 blocks 2-methoxyestradiol induced leukemia cell apoptosis by a p27(Kip1)-dependent G1/S cell cycle arrest in conjunction with NF-kappaB activation. *Biochem Pharmacol* 78:33-44
12. **Sutherland TE, Anderson RL, Hughes RA, Altmann E, Schuliga M, Ziogas J, Stewart AG** 2007 2-Methoxyestradiol--a unique blend of activities generating a new class of anti-tumour/anti-inflammatory agents. *Drug Discov Today* 12:577-584

13. **Karimian E, Chagin AS, Gjerde J, Heino T, Lien EA, Ohlsson C, Savendahl L** 2008 Tamoxifen impairs both longitudinal and cortical bone growth in young male rats. *J Bone Miner Res* 23:1267-1277
14. **Nilsson O, Falk J, Ritzen EM, Baron J, Savendahl L** 2003 Raloxifene acts as an estrogen agonist on the rabbit growth plate. *Endocrinology* 144:1481-1485
15. **Rey JR, Cervino EV, Rentero ML, Crespo EC, Alvaro AO, Casillas M** 2009 Raloxifene: mechanism of action, effects on bone tissue, and applicability in clinical traumatology practice. *Open Orthop J* 3:14-21
16. **Coutant R, de Casson FB, Rouleau S, Douay O, Mathieu E, Gatelais F, Bouhours-Nouet N, Voinot C, Audran M, Limal JM** 2004 Divergent effect of endogenous and exogenous sex steroids on the insulin-like growth factor I response to growth hormone in short normal adolescents. *J Clin Endocrinol Metab* 89:6185-6192
17. **Veldhuis JD, Keenan DM, Bailey JN, Adeniji A, Miles JM, Paulo R, Cosma M, Soares-Welch C** 2008 Estradiol supplementation in postmenopausal women attenuates suppression of pulsatile growth hormone secretion by recombinant human insulin-like growth factor type I. *J Clin Endocrinol Metab* 93:4471-4478
18. **Aronica SM, Katzenellenbogen BS** 1993 Stimulation of estrogen receptor-mediated transcription and alteration in the phosphorylation state of the rat uterine estrogen receptor by estrogen, cyclic adenosine monophosphate, and insulin-like growth factor-I. *Mol Endocrinol* 7:743-752
19. **Ignar-Trowbridge DM, Nelson KG, Bidwell MC, Curtis SW, Washburn TF, McLachlan JA, Korach KS** 1992 Coupling of dual signaling pathways: epidermal growth factor action involves the estrogen receptor. *Proc Natl Acad Sci U S A* 89:4658-4662
20. **Kazi AA, Jones JM, Koos RD** 2005 Chromatin immunoprecipitation analysis of gene expression in the rat uterus in vivo: estrogen-induced recruitment of both estrogen receptor alpha and hypoxia-inducible factor 1 to the vascular endothelial growth factor promoter. *Mol Endocrinol* 19:2006-2019
21. **Mekraldi S, Lafage-Proust MH, Bloomfield S, Alexandre C, Vico L** 2003 Changes in vasoactive factors associated with altered vessel morphology in the tibial metaphysis during ovariectomy-induced bone loss in rats. *Bone* 32:630-641
22. **Zelzer E, Mamluk R, Ferrara N, Johnson RS, Schipani E, Olsen BR** 2004 VEGFA is necessary for chondrocyte survival during bone development. *Development* 131:2161-2171
23. **Zelzer E, Olsen BR** 2005 Multiple roles of vascular endothelial growth factor (VEGF) in skeletal development, growth, and repair. *Curr Top Dev Biol* 65:169-187
24. **Dai J, Rabie AB** 2007 VEGF: an essential mediator of both angiogenesis and endochondral ossification. *J Dent Res* 86:937-950

25. **Gerber HP, Vu TH, Ryan AM, Kowalski J, Werb Z, Ferrara N** 1999 VEGF couples hypertrophic cartilage remodeling, ossification and angiogenesis during endochondral bone formation. *Nat Med* 5:623-628
26. **Weise M, De Levi S, Barnes KM, Gafni RI, Abad V, Baron J** 2001 Effects of estrogen on growth plate senescence and epiphyseal fusion. *Proc Natl Acad Sci U S A* 98:6871-6876
27. **Gafni RI, Weise M, Robrecht DT, Meyers JL, Barnes KM, De Levi S, Baron J** 2001 Catch-up growth is associated with delayed senescence of the growth plate in rabbits. *Pediatr Res* 50:618-623
28. **Drissi H, Hushka D, Aslam F, Nguyen Q, Buffone E, Koff A, van WA, Lian JB, Stein JL, Stein GS** 1999 The cell cycle regulator p27kip1 contributes to growth and differentiation of osteoblasts. *Cancer Res* 59:3705-3711
29. **Kiyokawa H, Kineman RD, Manova-Todorova KO, Soares VC, Hoffman ES, Ono M, Khanam D, Hayday AC, Frohman LA, Koff A** 1996 Enhanced growth of mice lacking the cyclin-dependent kinase inhibitor function of p27(Kip1). *Cell* 85:721-732
30. **Teixeira LT, Kiyokawa H, Peng XD, Christov KT, Frohman LA, Kineman RD** 2000 p27Kip1-deficient mice exhibit accelerated growth hormone-releasing hormone (GHRH)-induced somatotrope proliferation and adenoma formation. *Oncogene* 19:1875-1884
31. **Ballock RT, Zhou X, Mink LM, Chen DH, Mita BC, Stewart MC** 2000 Expression of cyclin-dependent kinase inhibitors in epiphyseal chondrocytes induced to terminally differentiate with thyroid hormone. *Endocrinology* 141:4552-4557
32. **Beier F, Taylor AC, LuValle P** 1999 The Raf-1/MEK/ERK pathway regulates the expression of the p21(Cip1/Waf1) gene in chondrocytes. *J Biol Chem* 274:30273-30279
33. **Lin J, la-Fera MA, Li C, Page K, Choi YH, Hartzell DL, Baile CA** 2003 P27 knockout mice: reduced myostatin in muscle and altered adipogenesis. *Biochem Biophys Res Commun* 300:938-942
34. **Boersma B, Wit JM** 1997 Catch-up growth. *Endocr Rev* 18:646-661
35. **Marino R, Hegde A, Barnes KM, Schrier L, Emons JA, Nilsson O, Baron J** 2008 Catch-up growth after hypothyroidism is caused by delayed growth plate senescence. *Endocrinology* 149:1820-1828
36. **Kember NF** 1973 Aspects of the maturation process in growth cartilage in the rat tibia. *Clin Orthop Relat Res* 288-294
37. **Weise M, De Levi S, Barnes KM, Gafni RI, Abad V, Baron J** 2001 Effects of estrogen on growth plate senescence and epiphyseal fusion. *Proc Natl Acad Sci U S A* 98:6871-6876

38. **Siepel A, Bejerano G, Pedersen JS, Hinrichs AS, Hou M, Rosenbloom K, Clawson H, Spieth J, Hillier LW, Richards S, Weinstock GM, Wilson RK, Gibbs RA, Kent WJ, Miller W, Haussler D** 2005 Evolutionarily conserved elements in vertebrate, insect, worm, and yeast genomes. *Genome Res* 15:1034-1050
39. **Schrier L, Ferns SP, Barnes KM, Emons JA, Newman EI, Nilsson O, Baron J** 2006 Depletion of resting zone chondrocytes during growth plate senescence. *J Endocrinol* 189:27-36
40. **Nilsson O, Mitchum RD, Jr., Schrier L, Ferns SP, Barnes KM, Troendle JF, Baron J** 2005 Growth plate senescence is associated with loss of DNA methylation. *J Endocrinol* 186:241-249
41. **Hunziker EB** 1994 Mechanism of longitudinal bone growth and its regulation by growth plate chondrocytes. *Microsc Res Tech* 28:505-519
42. **Kronenberg HM** 2003 Developmental regulation of the growth plate. *Nature* 423:332-336
43. **White JR, Wilsman NJ, Leiferman EM, Noonan KJ** 2008 Histomorphometric analysis of an adolescent distal tibial physis prior to growth plate closure. *J Child Orthop* 2:315-319
44. **Stewart AJ, Houston B, Farquharson C** 2006 Elevated expression of hypoxia inducible factor-2alpha in terminally differentiating growth plate chondrocytes. *J Cell Physiol* 206:435-440
45. **Scortegagna M, Ding K, Oktay Y, Gaur A, Thurmond F, Yan LJ, Marck BT, Matsumoto AM, Shelton JM, Richardson JA, Bennett MJ, Garcia JA** 2003 Multiple organ pathology, metabolic abnormalities and impaired homeostasis of reactive oxygen species in *Epas1*^{-/-} mice. *Nat Genet* 35:331-340
46. **Codogno P, Meijer AJ** 2006 *Atg5*: more than an autophagy factor. *Nat Cell Biol* 8:1045-1047
47. **Heath-Engel HM, Chang NC, Shore GC** 2008 The endoplasmic reticulum in apoptosis and autophagy: role of the BCL-2 protein family. *Oncogene* 27:6419-6433
48. **Nilsson O, Chrysis D, Pajulo O, Boman A, Holst M, Rubinstein J, Martin RE, Savendahl L** 2003 Localization of estrogen receptors-alpha and -beta and androgen receptor in the human growth plate at different pubertal stages. *J Endocrinol* 177:319-326
49. **van der Eerden BC, Gevers EF, Lowik CW, Karperien M, Wit JM** 2002 Expression of estrogen receptor alpha and beta in the epiphyseal plate of the rat. *Bone* 30:478-485
50. **Bieback K, Kern S, Kluter H, Eichler H** 2004 Critical parameters for the isolation of mesenchymal stem cells from umbilical cord blood. *Stem Cells* 22:625-634
51. **Friedenstein AJ** 1980 Stromal mechanisms of bone marrow: cloning in vitro and retransplantation in vivo. *Haematol Blood Transfus* 25:19-29

52. **Im GI, Shin YW, Lee KB** 2005 Do adipose tissue-derived mesenchymal stem cells have the same osteogenic and chondrogenic potential as bone marrow-derived cells? *Osteoarthritis Cartilage* 13:845-853
53. **in 't Anker PS, Noort WA, Scherjon SA, Kleijburg-van der Keur C, Kruisselbrink AB, van Bezooijen RL, Beekhuizen W, Willemze R, Kanhai HH, Fibbe WE** 2003 Mesenchymal stem cells in human second-trimester bone marrow, liver, lung, and spleen exhibit a similar immunophenotype but a heterogeneous multilineage differentiation potential. *Haematologica* 88:845-852
54. **in 't Anker PS, Scherjon SA, Kleijburg-van der Keur C, Groot-Swings GM, Claas FH, Fibbe WE, Kanhai HH** 2004 Isolation of mesenchymal stem cells of fetal or maternal origin from human placenta. *Stem Cells* 22:1338-1345
55. **Sekiya I, Colter DC, Prockop DJ** 2001 BMP-6 enhances chondrogenesis in a subpopulation of human marrow stromal cells. *Biochem Biophys Res Commun* 284:411-418
56. **Cramer T, Schipani E, Johnson RS, Swoboda B, Pfander D** 2004 Expression of VEGF isoforms by epiphyseal chondrocytes during low-oxygen tension is HIF-1 alpha dependent. *Osteoarthritis and Cartilage* 12:433-439
57. **Kim HK, Bian H, ya-Ay J, Garces A, Morgan EF, Gilbert SR** 2009 Hypoxia and HIF-1alpha expression in the epiphyseal cartilage following ischemic injury to the immature femoral head. *Bone*
58. **Nishida T, Kondo S, Maeda A, Kubota S, Lyons KM, Takigawa M** 2009 CCN family 2/ connective tissue growth factor (CCN2/CTGF) regulates the expression of Vegf through Hif-1alpha expression in a chondrocytic cell line, HCS-2/8, under hypoxic condition. *Bone* 44:24-31

12

SUMMARY

Summary

Longitudinal bone growth takes place in the epiphyseal growth plates of the long bones and comparable structures in the vertebrae. Regulatory mechanisms within this epiphyseal plate are complex. Only in a minority of children with a growth disorder the aetiology can be definitely established and even in such cases a causal treatment is usually not available.

During puberty longitudinal growth rate first increases, but finally as the growth plate further matures growth decreases and eventually ceases with epiphyseal fusion at the end of puberty. Epiphyseal fusion results in a complete arrest in longitudinal growth ruling out every possible non-surgical treatment option to increase longitudinal growth and thereby adult height. Therefore, modulation of timing of epiphyseal fusion might be beneficial in the treatment of growth disorders; e.g. extending epiphyseal fusion can potentially result in an increase in adult height by allowing more time for growth supporting treatments, while initiating epiphyseal fusion would benefit patients with tall stature. Little is known about the exact mechanisms underlying growth plate maturation and epiphyseal fusion. In this thesis we investigated growth plate maturation and epiphyseal fusion in more detail.

With puberty estrogen levels increase and this is known to play an important role in growth plate maturation and epiphyseal fusion. We detected both estrogen receptor alpha (ER α) and beta (ER β) in the rat growth plate, predominantly in late proliferating and early hypertrophic chondrocytes and observed a decrease in ER α and ER β staining with estrogen suppletion. We investigated the genomic and non-genomic pathway by which estrogen can exert its effects on ovariectomized rats with desoxyestrone administration, a synthetic compound that exclusively acts through the non-genomic pathway, and 17 β -estradiol administration. Treatment resulted in different degrees of growth inhibiting effects. We concluded that estrogenic effects on longitudinal growth are regulated both through genomic and nongenomic pathways with genomic signalling prevailing.

Estrogen treatment has potential side-effects, that can be circumvented with selective estrogen receptor modulators (SERMs). We investigated the effects of 2-methoxyestradiol and confirmed a tissue-selective effect in the growth plate of sexually immature male rats. However, we were not able to detect an effect on longitudinal growth.

Estrogen and its receptors interact with various growth factors in order to control longitudinal growth. In this thesis we demonstrated that Vascular Endothelial Growth Factor (VEGF) expression in rat chondrocytes was elevated by estrogen treatment *in vivo* and *in vitro*. Removal of estrogens by ovariectomy resulted in a decrease in VEGF expression. Moreover, pubertal human growth plate maturation resulted in an increase in VEGF expression, suggestive for a role of VEGF in the process of epiphyseal maturation as well as epiphyseal fusion.

Another effect of estrogen is acceleration of growth plate senescence, a term for structural changes like a decrease in height of different zones in the growth plate, but also for the decline in chondrocyte proliferation. We hypothesized that senescence might influence proliferation and the cell cycle of chondrocytes by orderly inactivation and activation of cyclin-dependent kinases and kinase inhibitors like p27Kip1 (p27). We did detect p27 mRNA in the growth plates of 5-wk-old mice by real-time PCR, but found no significant difference in p27 expression between the separate zones. In addition, we studied p27-deficient mice and found that p27 negatively modulates growth plate chondrocyte proliferation, but p27 was not required for the conditional regulation of chondrocyte proliferation as induced by dexamethasone in the growth plate of rats. In the human growth plate we did find a possible role for p27 in pubertal maturation of the growth plate, since microarray results showed an up-regulation in expression of the p27 gene with progression of puberty.

After a period of growth inhibition, the linear growth rate usually exceeds the normal range, which is known as catch-up growth. Evidence from animal studies suggests that catch-up growth is due, at least in large part, to a delay in growth plate senescence. We investigated catch-up growth in celiac patients and concluded that the pattern of catch-up growth in these patients is consistent with the hypothesis of delayed growth plate senescence.

Structural growth plate changes associated with senescence as described before in the rabbit and rat growth plate are in line with our data in a longitudinal study of two human growth plates obtained from one patient. Histological investigations showed a clear decrease in width of the total growth plate, more widely spaced columns with less cells and consequently more extracellular matrix in the more mature growth plate. Microarray results on human growth plates revealed for the first time the expression profile of human growth plate cartilage. Results from these experiments also confirmed our histological findings, since many genes and pathways related to the extracellular matrix significantly changed with maturation. In addition, progression of puberty affected many genes in the cell cycle pathway, hormonal pathways and programmed cell death. Moreover in this study we identified for the first time a set of 394 genes involved in growth plate maturation. The promoter regions of these genes contained transcription factor binding motifs for the Estrogen receptor, androgen receptor, STAT5B, ELK-1 and RUNX2. Particularly, ELK-1 and RUNX2 binding sites were enriched compared to controls suggesting a role for these transcription factors in pubertal maturation of the human growth plate. Overall changes in gene expression with pubertal maturation were small, indicating that there maturation is associated with small changes in multiple factors. This is in line with the senescence theory, suggesting that stem-like cells in the resting zone have a finite proliferative capacity, which is gradually exhausted resulting eventually in epiphyseal fusion.

The exact mechanism by which epiphyseal fusion occurs is not yet completely understood. We performed a detailed study on apoptosis in terminal hypertrophic chondrocytes in pubertal female growth plates and found no signs of classical apoptosis at the chondro-osseous junction. In addition, we studied a unique tissue specimen of a late pubertal human growth plate in the process of epiphyseal fusion and found clear evidence that apoptosis is not likely to be involved in the end phase of growth plate fusion. We did observe a dense border of thick bone surrounding the growth plate remnant and signs of hypoxia. We also found a significant increase in expression of the hypoxia-inducible factor 2 alpha gene from prepuberty to early and late stage puberty. Microarray results revealed that many genes of which the expression changed with pubertal maturation are involved in programmed cell death, e.g. proapoptotic and anti-apoptotic genes, but also genes involved in the regulation of autophagy. From these findings we speculate that growth plate fusion is a hypoxia related process eventually leading to a non-classical and perhaps intermediate mechanism of different types of cell death.

We investigated a promising and relatively new human model for the growth plate based on the use of human mesenchymal stem cells (hMSCs). hMSCs can differentiate into the chondrogenic lineage and bone marrow derived MSCs appeared to have the best chondrogenic potential, with fetal bone marrow prevailing over adult bone marrow. Fetal bone marrow-derived hMSCs showed to be an excellent model for the epiphyseal growth plate as during differentiation towards chondrocytes they gradually obtain a gene expression profile that was overlapping the fingerprint of epiphyseal growth plate cartilage. Many genes and pathways were identified as being important in different stages of chondrocyte differentiation. The hyaline cartilage formed by differentiating hMSCs resembled the profile of epiphyseal growth plate cartilage rather than of articular cartilage.

13

SAMENVATTING

Samenvatting

Lengtegroei vindt plaats in de epifysaire groeischijven die zich bevinden aan de uiteinden van de lange pijpbeenderen en in groeischijven in de wervelkolom. Deze groeischijven bevatten verschillende zones kraakbeencellen (chondrocyten) die zich in verschillende stadia van differentiatie bevinden. De mechanismen die een rol spelen in de regulatie van de groeischijf zijn complex en slechts in geringe mate bekend. Het is van belang om meer inzicht te krijgen in de mechanismen die de lengtegroei beïnvloeden, omdat bij kinderen met een groeistoornis slechts in een minderheid van de gevallen een onderliggende oorzaak kan worden gevonden. In de zeldzame gevallen dat er wel een oorzaak gevonden wordt is er dikwijls geen causale behandeling mogelijk. Gedurende de puberteit neemt de groeisnelheid eerst toe, een fenomeen dat bekend staat als de pubertaire groeispuurt, maar met voortgang van de puberteit neemt de groeisnelheid steeds verder af totdat de volwassen eindlengte is bereikt en de groeischijven sluiten. Nadat de groeischijven gesloten zijn, is het niet meer mogelijk om de groei medicamenteus te beïnvloeden. Voor de behandeling van groeistoornissen zou het daarom gunstig zijn als het proces van sluiting van de groeischijf zou kunnen worden beïnvloed. Bij kinderen met een kleine lengte zou bijvoorbeeld een verlenging van het proces van groeischijfsluiting kunnen leiden tot een grotere eindlengte, doordat meer tijd beschikbaar komt voor stimulering van de groei. Aan de andere kant zou het versnellen van de groeischijfsluiting een goede behandelingsmogelijkheid zijn voor patiënten met een te grote lengte. Het precieze mechanisme dat ten grondslag ligt aan de rijping en uiteindelijke sluiting van de groeischijf is grotendeels onopgehelderd. Meer kennis zou kunnen leiden tot het ontwikkelen van medicamenten die de timing van groeischijfsluiting beïnvloeden. In dit proefschrift is op verschillende niveaus en in diverse experimentele modellen de rijping van de groeischijf en het proces van groeischijfsluiting onderzocht.

In de puberteit neemt de concentratie van oestrogenen in het bloed toe. Oestrogenen spelen niet alleen een belangrijke rol in de ontwikkeling van secundaire geslachtskenmerken tijdens de puberteit van een meisje, maar zijn ook betrokken bij de rijping en sluiting van de groeischijf, zowel bij jongens als bij meisjes. In ons onderzoek toonden we aan dat zowel de oestrogeen-receptor alpha ($ER\alpha$) als de oestrogeen-receptor beta ($ER\beta$) tot expressie komen in de groeischijf van de rat, voornamelijk in de laat-prolifererende chondrocyten en de vroege hypertrofe chondrocyten. Als oestrogeen werd toegediend, nam de expressie van beide receptoren af. Na toediening van desoxyestrone, een synthetisch oestrogeen dat alleen via non-genomische signalering zijn werking uitoefent, aan ratten met een status post ovariectomie (het verwijderen van de eierstokken), resulteerde dit in minder groeivertraging dan werd waargenomen met 17β -estradiol. Hieruit concludeerden we dat oestrogenen een effect op de lengtegroei uitoefenen via de genomische en ook via de non-genomische route, waarbij de genomische route waarschijnlijk overheerst.

Behandeling met oestrogenen heeft naast een positieve werking ook mogelijke bijwerkingen, die vermeden kunnen worden met Selectieve Oestrogeen Receptor Modulators (SERMs). Wij onderzochten het effect van één van die SERMs, 2-methoxyoestradiol, op de lengtegroei en zagen inderdaad een weefsel-specifiek effect op de groeischijf van jonge ratten, maar geen meetbaar effect op de lengtegroei.

Oestrogeen en oestrogeen receptoren worden beïnvloed door verschillende groeifactoren en hormonen. In dit proefschrift onderzochten we de relatie tussen oestrogeen en de expressie van Vascular endothelial growth factor (VEGF) in de groeischijf. Ovariëctomie bij ratten resulteerde in een afname van de VEGF-expressie in de groeischijf, terwijl oestrogeensuppletie resulteerde in een toename van VEGF-expressie. In groeischijfpreparaten van meisjes zagen we op eiwit-niveau een toename in VEGF-expressie met het voortschrijden van de puberteit. Hieruit concludeerden

we dat VEGF-expressie beïnvloedt kan worden door oestrogenspiegels en dat VEGF mogelijk een rol speelt in het proces van groeischijfsluiting.

Van oestrogeen is ook bekend dat het de “senescence” (veroudering) van de groeischijf versnelt. Met deze term worden de structurele veranderingen in de groeischijf in de tijd aangeduid, zoals een afname in de hoogte van de groeischijfzones en een afname in proliferatie van de chondrocyten. In dit proefschrift onderzochten we de rol van een celcyclusremmer p27Kip1 (p27) op de proliferatie van chondrocyten en de lengtegroei in de muis. In de groeischijf van 5 weken oude muizen komt p27 op mRNA niveau in iedere zone van de groeischijf in ongeveer gelijke mate tot expressie. Muizen met een p27-deficiëntie (p27 knock-out) lieten een toename zien in de proliferatie van de chondrocyten. Er was echter geen duidelijk effect zichtbaar op de lengtegroei na 7 weken. Tevens bleek dat p27 niet nodig is voor het groeiremmende effect van dexamethason; p27 deficiënte muizen lieten namelijk een zelfde mate van vertraging zien als de “wild-type” muizen (muizen zonder de mutatie). In een ander experiment, waarin we de gen-expressie bestudeerden in de humane groeischijf, zagen we dat de gen-expressie van p27 steeg met het voortschrijden van de puberteit. Deze bevinding wijst op een mogelijke rol voor p27 in de afname van chondrocytenproliferatie en daarmee de afname in groeisnelheid aan het einde van de puberteit.

Als na een periode van groeivertraging, bijvoorbeeld door een ziekte of bepaalde medicamenten, de ziekte adequaat wordt behandeld of de medicamenten worden gestopt, gaat de groeisnelheid vaak aanzienlijk omhoog. Dit fenomeen staat bekend als “inhaalgroei” (catch-up growth). Het is onbekend wat het achterliggende mechanisme is, maar dierexperimentele studies hebben aanwijzingen gevonden dat inhaalgroei tenminste voor een belangrijk deel te verklaren is door een vertraging in de “senescence” van de groeischijf. Om de hypothese te toetsen dat dit fenomeen ook bij kinderen met inhaalgroei een rol speelt, onderzochten wij de groei van kinderen met coeliakie (gluten-allergie) die na de start van een glutenvrij dieet een inhaalgroei vertoonden. Het groeipatroon van deze kinderen kwam inderdaad overeen met het groeipatroon van jongere kinderen, zoals men zou verwachten bij vertraging van de “senescence” gedurende de fase van groeivertraging.

In een studie naar de veranderingen die optreden in de humane groeischijf over een periode van 1 jaar tijdens de puberteit, zagen we structurele veranderingen die leken op de veranderingen die werden waargenomen in het proces van “senescence” bij ratten en konijnen. We zagen een significante afname in de totale groeischijfdikte en een afname van de dikte van elke afzonderlijke zone. Daarnaast zagen we een toename in de ruimte tussen de kolommen van chondrocyten, en daarmee ook een toename van de extracellulaire matrix in de groeischijf in de loop van de puberteit. Voor het eerst hebben wij met zogenaamde “microarray” experimenten laten zien hoe het gen-expressie-profiel eruitziet van de humane groeischijf. De veranderingen in het gen-expressie-profiel kwamen overeen met de histologische veranderingen die we microscopisch hadden waargenomen; veel genen die geassocieerd zijn met de extracellulaire matrix lieten een toename zien in expressie naarmate de maturatie van de groeischijf voortschreed. Tevens veranderde de expressie van veel genen die te maken hebben met de celcyclus, met hormoonsystemen en met de zogenaamde “geprogrammeerde celdood”. In de groep genen waarvan de expressie veranderde gedurende de puberteit vonden we veel genen met transcriptiefactor-bindingsplaatsen voor de oestrogeen receptor, de androgeen receptor, STAT5B, ELK-1 en RUNX2 in hun promotor regio's die de expressie van het gen mogelijk reguleren. Met name de bindingsplaatsen voor de transcriptiefactoren ELK-1 en RUNX2 waren verrijkt ten opzichte van controles. Dit wijst op een rol van deze transcriptiefactoren in de maturatie van de groeischijf in de puberteit. In het algemeen was de verandering in gen-expressie gering, wat in overeenstemming is met de “senescence”

theorie, die suggereert dat stamcellen in de zogenaamde “reserve zone” een beperkte capaciteit hebben om zich te delen. Als het aantal stamcellen is uitgeput, zou dit volgens deze hypothese resulteren in sluiting van de groeischijf.

Het precieze mechanisme waardoor de groeischijf uiteindelijk sluit is nog grotendeels onbekend, maar men neemt aan dat “apoptose” (geprogrammeerde celdood) hierin een rol speelt. Wij hebben een gedetailleerde studie verricht naar apoptose in de terminale hypertrofe zone van groeischijven van meisjes in verschillende stadia van puberteit. We hadden ook de beschikking over een groeischijf die zich in het laatste stadium bevond van sluiting. In geen van de groeischijven waren typische kenmerken te zien van apoptose. Wel zagen we een dikke en compacte rand van bot om de fuserende groeischijf heen en daarnaast ook tekenen van hypoxie en van necrose. In een microarray studie van humane groeischijven zagen we tevens dat de expressie van het hypoxia-inducible factor 2 alpha gen (Hif-2 alpha) significant omhoog ging met het voortschrijden van de puberteit. Daarnaast veranderde ook de expressie van vele genen die geassocieerd zijn met geprogrammeerde celdood, zoals genen die betrokken zijn bij pro-apoptose, anti-apoptose en autophagie. Op basis van deze bevindingen veronderstellen wij dat hypoxie een rol speelt bij de sluiting van de groeischijf en dat chondrocyten uiteindelijk ten gronde gaan aan een specifiek type celdood.

In de laatste hoofdstukken van dit proefschrift bestudeerden we een relatief nieuw model voor de groeischijf, namelijk humane mesenchymale stamcellen (hMSCs) die kunnen differentiëren naar chondrocyten. Deze MSCs kunnen uit verschillende bronnen geïsoleerd worden. Wij concludeerden dat MSCs uit foetaal beenmerg het meest geschikt waren om tot chondrocyten te differentiëren. In een microarray studie zagen we dat het expressieprofiel van MSCs die differentiëerden naar chondrocyten beter overeenkwam met dat van chondrocyten uit de groeischijf dan met chondrocyten uit gewrichtskraakbeen. Daarnaast zagen we in het differentiatieproces veel genen en groepen genen veranderen waarvan reeds bekend was dat ze een rol spelen in processen in de groeischijf. Dit geeft aan dat uit MSCs gedifferentieerde chondrocyten een uitstekend model vormen om de groeischijf en het chondrogene differentiatie proces in meer detail op verschillende niveaus te kunnen bestuderen.

Curriculum Vitae

Curriculum vitae

Joyce Adriana Mathilde Emons was born on the 26th of February, 1977 in Berkel en Rodenrijs, the Netherlands. She attended secondary school at the "Sint Laurens College" in Rotterdam, where she passed her exam in 1995. In the same year she started her study Biology at the University of Leiden. In the academic years 1997- 2001 she specialized in Medical Biology. In 1998 she started a second study at the Faculty of Medicine of the Leiden University Medical Center. From May 2000 till February 2001 she carried out a research project at the Departments of Endocrinology & Metabolism and the Department of Pediatrics of the Leiden University Medical Center (supervisors Dr. B. van der Eerden and Dr. M. Karperien). In March 2001 she received her Medical Biology degree and two years later in March 2003 her medical degree, cum laude. From February 2003 till August 2004 she worked as a research fellow at the Growth and Development Department of the National Institutes of Health in Bethesda, Maryland, USA, subsidized by a grant of the Ter Meulen Foundation (Supervisor Dr. J. Baron). From August 2004 till June 2005 she continued her research project at the Department of Pediatrics of the Leiden University Medical Center (supervisors Prof. Dr. J.M. Wit and Dr. M. Karperien). After almost 2 years of research she started in June 2005 her AGIKO (AIOSKO) program, i.e. a combined residency in Pediatrics and PhD scholarship, in the Leiden University Medical Center. In March 2006 she was a research fellow in the Pediatric Endocrinology Unit of the Karoliska Institutet in Stockholm, Sweden, subsidized by an ESPE visiting scholarship. From March 2007 till September 2008 she worked as a resident in the "Reinier de Graaf Gasthuis" in Delft (head: Dr.N.van der Lely), followed by a research fellowship until September 2009, and a continuation of her pediatric residency in the Leiden University Medical Center (head: Prof.dr.H.A.Delemarre-van de Waal).

LIST OF PUBLICATIONS

List of publications

1. **van der Eerden BC, Emons J, Ahmed S, van Essen HW, Löwik CW, Wit JM, Karperien M** 2002 Evidence for genomic and non-genomic actions of estrogen in growth plate regulation in female and male rats at the onset of sexual maturation. *J Endocrinol* 175(2):277-288
2. **Emons JAM, Boersma B, Baron J, Wit JM** 2005 The pattern of catch-up growth in celiac disease is consistent with the hypothesis of delayed growth plate senescence. *Journal of Pediatrics* 147(6):843-6.
3. **Emons JAM, Marino R, Nilsson O, Barnes KM, Chatterjee NA, Karperien M, Wit JM, Baron J** 2006 The role of p27 kip1 in the regulation of growth plate chondrocytes Proliferation. *Pediatr Res.* 2006 Sep;60(3):288-93.
4. **Schrier L, Ferns SP, Barnes KM, Emons JAM, Newman E, Nilsson O, Baron J** 2006 Depletion of resting zone chondrocytes during growth plate senescence. *J Endocrinol.* Apr;189(1):27-36.
5. **Emons JAM, Phillip M, Wit JM, Savendahl L.** The Sixth ESPE Growth Plate Working Group Symposium (EUROGROP), June 30th, Rotterdam, the Netherlands, "a multidisciplinary approach to growth plate biology. *Pediatr Endocrinol Rev.* 2006 Dec-2007 Jan;4(2):153-9
6. **Bernardo ME, Emons JAM, Nauta AJ, Roelofs H, Karperien, Kleijburg C, Romeo S, Locatelli F, Willemze R, Fibbe WE** Human mesenchymal stem cells derived from bone marrow display a better chondrogenic differentiation compared with other sources. *Connect Tissue Res.* 2007;48(3):132-40.
7. **Marchini A, Häcker B, Marttila T, Hesse V, Emons J, Weiss B, Karperien M, Rappold G.** BNP is a transcriptional target of the short stature homeobox gene SHOX. *Hum Mol Genet.* 2007 Dec 15;16(24):3081-7. Epub 2007 Sep 19.
8. **Rose Marino, Anita Hegde, Kevin Barnes, Lenneke Schrier, Joyce Emons, Ola Nilsson, Jeffrey Baron** Evidence that catch-up growth after hypothyroidism is caused by delayed growth plate senescence. *Endocrinology.* 2008 Jan 3;
9. **Emons JAM, Chagin A, Hultenby K, Wit JM, Karperien M, Savendahl L** Epiphyseal fusion in the human growth plate does not involve classical apoptosis. *Pediatr Res.* 2009 Dec;66(6):654-9
10. **Emons JAM*, van Gool S*, Decker E, Yu X, van Houwelingen H, Kleijburg C, Scherjon S, Gretz N, Wit JM, Rappold G, Karperien M** Human mesenchymal stem cells as a model for chondrocyte differentiation. *Submitted. Matrix Biology.* * = equal authorschip
11. **Emons JAM, Chagin A, Malmhof T, Lekman M, Wit JM, Karperien M, Savendahl L** Estradiol stimulates growth plate expression of VEGF; a potential mechanism for estrogen-induced growth plate closure in humans. *Submitted. J. Endocrinology.*

- 12. Emons JAM, Decker E, Yu X, Pirzer H, van Gool S, Chagin A, Savendahl L, Gretz N, Wit JM, Rappold G, Karperien M** Genome wide screening of two human growth plates during pubertal development. *In preparation*

